
GraphIP-Bench: How Hard Is It to Steal a Graph Neural Network, and Can We Stop It?

Kaixiang Zhao*
University of Notre Dame
kzhao5@nd.edu

Bolin Shen*
Florida State University
blshen@fsu.edu



Yuyang Dai
University of California, Berkeley
michael_yuyang@berkeley.edu

Shayok Chakraborty
Florida State University
schakraborty2@fsu.edu

Yushun Dong†
Florida State University
yushun.dong@fsu.edu

Abstract

Graph neural networks (GNNs) deployed as cloud services can be *stolen* through *model-extraction attacks*, which train a surrogate from query responses to reproduce the target’s behaviour, and a growing line of ownership defenses tries to prevent or trace such theft. The title of this paper asks two questions: *how hard is it to steal a GNN?*, and *can we stop it?* Prior work cannot answer either, because experiments use inconsistent datasets, threat models, and metrics. We introduce *GraphIP-Bench*, a unified benchmark which evaluates both sides under a single black-box protocol. It integrates twelve extraction attacks, twelve defenses spanning watermarking, output-perturbation, and query-pattern-detection families, ten public graphs covering homophilic, heterophilic, and large-scale regimes, three GNN backbones, and three graph-learning tasks, and it reports fidelity, task utility, ownership verification, and computational cost on shared splits, queries, and budgets. We further add a joint attack-and-defense track which runs every attack on every defended target and measures watermark verification on the resulting surrogate, which exposes the protection that a defense retains after extraction. The empirical picture is short: stealing a GNN is easy at medium query budgets and most defenses do not change this; several watermarks verify reliably on the protected model but lose most of their verification signal on the extracted surrogate, which exposes a gap that single-model evaluations miss; and heterophilic graphs are systematically harder to steal, while a cross-architecture mismatch between target and surrogate reduces but does not prevent extraction. We release *GraphIP-Bench* with reproducible scripts and configurations, and integrate the attacks and defenses into the PyGIP library.

 github.com/LabRAI/GraphIP-Bench  labrai.github.io/PyGIP

1 Introduction

Graph neural networks (GNNs) are key components of modern data-driven services. Commercial platforms use them for product recommendation [33], autonomous vehicle perception [14], and molecular property prediction [11]. Their advantage is that they aggregate information over arbitrary relational structures, which arise in social, financial, and product data. Cloud providers now expose pre-trained GNNs through public inference endpoints, which allow customers to deploy state-of-the-art analytics without local training or data collection.

This deployment model also lets adversaries *steal* the model. The attack pattern is the same in every reported instance: the adversary submits carefully chosen queries, records the labels or confidence

*Co-first author.

†Corresponding author.

scores that the endpoint returns, and trains a local surrogate which reproduces the target’s behaviour. The literature calls this attack *model extraction* [28, 42], and we use “stealing a GNN” as a plain-language synonym throughout the paper. A successful theft leaks the owner’s intellectual property, undermines pay-per-query revenue, and lets competitors recreate proprietary functionality at low cost. For example, a stolen fraud-detection GNN exposes decision boundaries which adversaries can use to bypass screening, and a stolen pharmaceutical GNN reveals assay knowledge which is encoded in the model parameters. These risks motivate the two questions which the title of this paper makes explicit: *how hard is it to steal a GNN?*, and *can we stop it?*

To stop the theft, recent work proposes two complementary defense families. *Information-limiting* defenses (output perturbation, query filtering, query-pattern detection) make each query response less useful to the attacker [12, 8, 6, 7, 13]. *Ownership-tracing* defenses (watermarking and fingerprinting) embed a verifiable pattern in the trained model so that the owner can prove that an extracted surrogate was derived from their model [26, 31, 1, 34, 29, 25]. Surveys summarise both families and the broader security landscape for deep learning [17, 32, 22, 38, 37] and for graph learning in particular [2, 30, 35, 20, 41]. Experimental practice, however, remains fragmented: studies use private splits, incompatible budgets, and inconsistent metrics, and the few existing testbeds focus on robustness or privacy and exclude model extraction together with watermarking and fingerprinting [21]. The community therefore lacks an empirical basis on which to answer either of our two title questions.

Several challenges must be addressed to enable fair and informative comparison. First, the community needs a single experimental protocol that fixes public splits, shared query sets, budgets, and explicit threat models (including whether the endpoint returns labels or confidence scores) and that treats data-driven and data-free attacks on equal terms [28, 42]. Second, evaluation must align success criteria with method goals: residual extraction for attacks, ownership verification for watermarking and fingerprinting, since these mechanisms aim to provide verifiable evidence of model ownership rather than to reduce agreement with the target [26, 31]. Third, studies should report the protection–utility balance under matched conditions, since adoption depends on how defenses affect task accuracy and inference latency. Fourth, benchmarks should report computational complexity (time and memory) to make the real cost of deployment transparent; prior work often omits this and obscures feasibility [12]. Fifth, evaluating attacks and defenses separately misses the joint adversarial setting in which the attacker extracts a defended model and the defender verifies ownership on the surrogate — the setting that actually determines whether a defense is useful. Finally, consistent method naming, standardized hardware and software, and public reporting of seeds and tuning procedures are needed for reproducibility and to prevent protocol-induced bias. Existing studies only partially satisfy these requirements, which limits both scientific understanding and industrial uptake.

We address these challenges with *GraphIP-Bench*, a reproducible benchmark and library which evaluates both *stealing* and *stopping* under a single black-box protocol. The suite integrates twelve representative extraction attacks (nine data-driven and three data-free) and twelve defenses spanning watermarking, output-perturbation, prediction-rounding, and query-pattern-detection. We evaluate every method on ten public graphs covering homophilic, heterophilic, and large-scale regimes, three GNN backbones, and three graph-learning tasks; the per-dataset, per-backbone, and per-method details are deferred to Section 3. A unified hyperparameter search and a consistent metric suite record security, utility, and efficiency. Going beyond prior single-track evaluations, we add a joint attack-and-defense track which runs every attack on every defended target and a watermark-survival metric which measures verification on the surrogate produced by each attack, together exposing how much protection a defense retains after the model is actually stolen. The headline finding of that joint track is that most parameter-side or trigger-based graph watermarks verify near-perfectly on the protected model but lose much of their verification signal on the extracted surrogate, while query-time mechanisms partially survive — watermark designs must therefore be re-evaluated on the surrogate, not only on the deployed model. To our knowledge, *GraphIP-Bench* is the first benchmark which offers a standardised evaluation of model-extraction attacks and ownership defenses for graph neural networks. The main contributions are:

- **Unified protocol.** Public splits, shared queries, standardized budgets, and explicit endpoint assumptions; twelve attacks and twelve defenses run under identical settings on ten datasets, three GNN backbones, and three tasks for fair comparison.
- **Joint attack-and-defense track.** Every attack is executed against every defended target with watermark verification measured on the extracted surrogate, which exposes the residual ownership signal that survives extraction.

- **Protection–utility analysis.** A sweep of defense configurations and attacker budgets summarises operating points with attack-agnostic frontiers and links them to graph structural properties (edge homophily, degree, density) and to backbone choice.
- **Cost and efficiency reporting.** Asymptotic formulas and automated profilers record training time, memory, inference latency, verification time, and an estimated monetary cost, which makes deployment cost transparent for every method.

2 Preliminaries

Notation. An attributed graph is denoted by $\mathcal{G} = (\mathcal{V}, \mathcal{E}, \mathbf{X}, \mathbf{A})$ with node set \mathcal{V} , edge set \mathcal{E} , node-feature matrix \mathbf{X} , and adjacency matrix \mathbf{A} . Query budgets are reported as multiples of the test-set size, and four data-availability regimes (`both`, `features only`, `structure only`, `data free`) control which inputs the adversary can construct. Fidelity is the agreement rate between a surrogate and the target on the test split; accuracy and macro F1 measure task utility.

Model Extraction Attacks. We consider the standard black-box threat model in which the adversary has query access to a deployed graph neural network and no knowledge of its weights, architecture, or training data. The adversary submits inputs (either genuine subgraphs or synthetic samples), records the returned labels or probability vectors, and trains a local model which minimises the discrepancy between its predictions and the target’s outputs. The resulting model is a surrogate which replicates the behaviour of the protected network and enables extraction of the owner’s intellectual property [28, 42]. Prior work groups extraction queries into three strategies. Random querying submits subgraphs from public data and succeeds when the decision boundary is smooth [28]. Adaptive querying selects inputs which maximise information gain, often through the disagreement between the current surrogate and the target [42]. Data-free generation removes the need for public data by training a graph generator which produces queries during extraction [42]. These studies show that modest query budgets, often no larger than the number of nodes in a benchmark dataset, are sufficient to recover a model which matches the original on downstream tasks.

Defense against Model Extraction Attacks. The literature groups defenses into two complementary families. *Information-limiting* defenses modify the target’s outputs so that the adversary receives a less useful signal: output perturbation adds calibrated noise or rounds confidence scores [12, 8], and query filtering detects and blocks suspicious request patterns [6, 7, 13]. These methods can reduce the residual agreement of a surrogate, although they may also degrade accuracy for legitimate users. *Ownership-tracing* defenses embed an artefact which lets the owner verify infringement: graph watermarking modifies weights or decision regions so that the model reveals a secret on inputs which carry a trigger [26, 31, 1], and fingerprinting derives stable signatures from the model’s output distribution while leaving the parameters unchanged [34, 29, 25]. Surveys of these approaches identify open questions about robustness, utility loss, and verification cost [17, 32, 22, 38, 37], and our benchmark places all of them under a single protocol with matched datasets, budgets, and threat assumptions, which enables an objective comparison of their trade-offs.

3 Benchmark Design

In this section we describe the experimental protocol of *GraphIP-Bench*. We first state the protocol design, datasets, attacks, defenses, and implementation details, then articulate the five research questions that guide our empirical study.

3.1 Experimental Settings and Implementations

Protocol Design. *GraphIP-Bench* defines a single black-box protocol that fixes four disjoint splits for each dataset (train, validation, test, query), shares the same query sets across methods, and uses *standardized* query budgets at 0.05, 0.10, 0.25, 0.50, and 1.00 times the test size. Here “standardized” means that every method receives the same number of queries at each ratio and that these ratios are fixed across datasets. The set spans the commonly studied ranges in prior work [16, 23], which include very small budgets that test sample efficiency (0.05 to 0.10), medium budgets where most gains occur (0.25 to 0.50), and a large budget that approximates saturation (1.00). This design makes results comparable and representative across methods and datasets. The protocol states explicit endpoint assumptions, which include whether the service returns labels only or also confidence scores

and whether rate limits apply [28, 42]. We separate evaluation into an extraction track, an ownership track, and a joint track. The extraction track measures how well black-box attacks learn a surrogate of an undefended target, and it reports test accuracy with respect to ground truth and fidelity with respect to the target. The ownership track evaluates each defense on a defended target and reports defended accuracy, fidelity to the original target, and verification on a standardized verification set [40, 31, 26, 36, 29]. The joint track runs every attack on every defended target and reports surrogate fidelity to the defended model together with the verification rate measured on the surrogate, which we call watermark survival. To place different settings on equal footing, we control data availability with four regimes: features only, structure only, features and structure, and data free. We also report total attack time, total defense time, and peak GPU memory for both attacks and defenses to make deployment cost clear.

Datasets. We use ten attributed graphs which cover four groups: homophilic citation networks (Cora, CiteSeer, PubMed), homophilic coauthor and product co-purchase networks (CoauthorCS, CoauthorPhysics, Computers, Photo), the large-scale OGBN-Arxiv graph, and two heterophilic graphs [18] (RomanEmpire, AmazonRatings). The graphs differ in size, density, class count, feature dimension, and edge homophily, which enables stress testing across structural regimes; full statistics are in Table 7 of Appendix D. For node classification we split each dataset into four disjoint subsets (train, validation, test, query) with no overlap, and for watermarking we reserve a fixed subset of the training data as the watermark set. We also include link prediction on Cora and graph classification on ENZYMES and PROTEINS from TUDataset [15] (Appendix F.10).

Metrics. We report two groups of metrics under a single protocol. *Performance* for attacks includes test accuracy, macro F1, and fidelity, which is the agreement between the surrogate and the target on the test set. *Performance* for defenses includes the defended model’s test accuracy and macro F1, its fidelity to the original target, and ownership verification on a standardized verification set. *Efficiency* for attacks includes total attack time and peak GPU memory; *efficiency* for defenses includes total defense time and peak GPU memory.

Model Extraction Attacks. For the extraction track we implement twelve representative attacks. Six are MEA-style baselines from a canonical study on query synthesis and surrogate training, which we denote MEA0 through MEA5 [28]; we further include the adaptive adversarial querying method AdvMEA [3], the centrality-and-entropy strategy CEGA [27], and the structure-aware pipeline Realistic [4]. To cover the data-free regime in a fair black-box manner, we add three variants [42] which use no target gradients: DFEA_I minimises the KL divergence between surrogate logits and target logits (soft-label distillation), DFEA_II trains on hard labels returned by the endpoint (label-only supervision), and DFEA_III augments label-only training with a consistency loss between two surrogates. We treat distinct hyperparameter settings of the same algorithm as separate methods, which enables fine-grained comparison under shared query sets and budgets. The four data-availability regimes defined in Section 2 are realised by two control parameters, `attack_x_ratio` and `attack_a_ratio`, which fix the fraction of real features and real adjacency made available to each attack; the four regimes are denoted X-only (features only), A-only (structure only), both (features and structure), and data-free.

Model Extraction Defenses. For the ownership and joint tracks we implement twelve defenses, which split between the two families introduced in Section 2. The ownership-tracing family contains five methods: the watermarking schemes RandomWM, BackdoorWM, SurviveWM, and ImperceptibleWM [40, 31, 26, 36], and the query-based integrity scheme Integrity [29]. The information-limiting family contains seven methods: two output-perturbation variants OP_low and OP_high which add Gaussian noise to the returned logits at two scales [8, 12], two prediction-rounding variants PR_2bit and PR_top1 which quantise the returned scores or return only the top-1 label, and three query-detection methods which follow PRADA [6], an adaptive-misinformation strategy [7], and a gradient-redirection strategy [13], denoted PRADA, AdaptMisinfo, and GradRedir. Every defense protects the same target architecture, and we report the defended model’s test accuracy and its fidelity to the original target. For watermarking and integrity we measure ownership verification on a standardised verification set using accuracy; for information-limiting and query-detection methods we use the verification proxy that matches each method’s design, which is the trigger-label hit rate or the watermark-graph accuracy when a defense exposes such an artefact and the marker accuracy on the protected model otherwise.

GNN Backbones. To test whether conclusions are robust to the choice of model architecture, we use three widely adopted GNN backbones. The first is GCN [9], which uses spectral graph convolution. The second is GAT [24], which uses attention over neighbors. The third is GraphSAGE [5], which uses neighbor sampling and a learned aggregator. Each backbone is implemented in both DGL and PyTorch Geometric so that defenses with library-specific dependencies can be evaluated on a matched architecture; we use a DGL GCN with hidden dimension 16 as the default backbone, and we explicitly mark deviations when a defense uses a different backbone for fairness.

3.2 Research Questions

RQ1. How does extraction effectiveness change with the query budget, and does the trend hold on heterophilic and large-scale graphs? We run twelve black-box attacks on undefended targets across the ten datasets at five budgets and four data-availability regimes, and we report accuracy, macro F1, and fidelity averaged over three seeds. **RQ2. How effective are existing defenses on the protected model?** We evaluate the five watermarking and integrity methods together with the seven information-limiting and query-detection methods on a shared backbone, and we report defended accuracy, fidelity, and ownership verification. **RQ3. How well do defenses balance protection and utility?** For each defense we report the utility loss against the undefended target together with defended fidelity and verification rate, which makes the protection-utility trade-off explicit. **RQ4. What are the computational complexity and practical efficiency of attacks and defenses?** We report asymptotic time and memory complexity, and measure wall-clock time and peak GPU memory on NVIDIA A100 hardware for both the extraction and the ownership track. **RQ5. How effective are defenses in the joint adversarial setting, and does the watermark signal survive on the extracted surrogate?** We run every attack on every defended target at a fixed budget and report surrogate fidelity to the defended model together with the verification rate measured on the surrogate, which we call *watermark survival*.

4 Empirical Investigation

We now present an empirical study that follows the unified protocol in Section 3, uses shared query sets and standardized budgets, and reports security, utility, and efficiency under identical settings. Complementary generalisation experiments are reported in Appendix F.10.

4.1 Budget Sensitivity of Model Extraction Attacks (RQ1)

To answer RQ1, we evaluate twelve black-box attacks on undefended targets under the protocol in Section 3.2. Results are averaged over three seeds, and we report fidelity to the target together with accuracy on the ground truth. Table 1 shows a representative case on *Computers* when both features and adjacency are available. Figure 1 reports sample efficiency on all ten datasets and four regimes; the y -axis is the median budget at which each attack reaches 90% of its own best fidelity. Figure 2 plots accuracy and fidelity on six representative datasets which span the four regimes that matter for our findings: two clean homophilic citation graphs (Cora, PubMed), the high-average-degree exception (Computers), the highest-homophily reference (CoauthorPhysics), the large-scale graph (OGBN-Arxiv), and the lowest-homophily heterophilic graph (RomanEmpire). The full ten-dataset, three-metric (Acc, Fidelity, F1) version, the regime-sensitivity heatmap, and the per-dataset and per-regime tables are reported as Figures 10 and 11 and Appendix F.1.

Table 1: RQ1 on *Computers* (both features and adjacency available). Fidelity (%) across query budgets with mean \pm standard deviation over three seeds. Higher is better. Bold marks the best value in each column.

Budget	MEAO	MEA1	MEA2	MEA3	MEA4	MEA5	AdvMEA	CEGA	Realistic	DFEA_I	DFEA_II	DFEA_III
0.05 \times	51.0 \pm 7.0	41.5 \pm 15.5	51.0 \pm 7.5	53.8 \pm 3.0	38.4 \pm 13.4	61.3 \pm 4.3	35.5 \pm 17.8	36.0 \pm 25.0	64.5 \pm 33.7	67.5 \pm 12.4	43.9 \pm 8.1	72.9 \pm 5.5
0.10 \times	67.3 \pm 3.1	27.7 \pm 14.0	58.8 \pm 6.0	64.8 \pm 5.5	37.9 \pm 12.6	65.6 \pm 6.4	25.7 \pm 24.7	36.7 \pm 23.0	67.9\pm45.4	73.7 \pm 18.1	28.4 \pm 20.5	66.7 \pm 14.2
0.25 \times	67.0 \pm 1.5	46.2 \pm 5.5	65.2 \pm 2.4	67.6 \pm 6.2	63.6 \pm 4.0	66.5 \pm 2.1	26.9 \pm 22.4	43.4 \pm 17.5	67.7 \pm 45.3	60.3 \pm 25.5	28.4 \pm 20.5	72.9 \pm 3.1
0.50 \times	71.4 \pm 2.7	49.4 \pm 5.6	66.2 \pm 6.3	74.9 \pm 4.3	74.3 \pm 5.0	73.9 \pm 3.5	46.1\pm12.5	53.9 \pm 29.2	67.4 \pm 44.0	64.8 \pm 15.9	28.4 \pm 20.5	82.5 \pm 3.1
1.00 \times	80.5\pm4.6	56.3\pm12.6	68.3 \pm 8.0	79.5\pm5.2	83.7\pm4.3	76.3\pm4.2	22.8 \pm 11.8	54.1\pm33.4	67.0 \pm 44.8	55.8 \pm 28.2	28.4 \pm 20.5	82.1 \pm 2.8

The results expose a consistent picture across the ten datasets. *CEGA is the most sample-efficient attack on the homophilic graphs but is unstable on Computers*, where the high average degree (36.8) destabilises its centrality-driven query selection. *The MEA family saturates near the medium budget*:

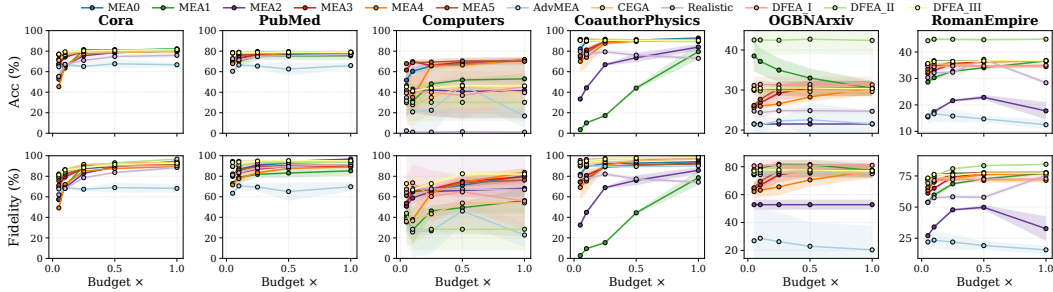


Figure 2: Budget–metric curves on six representative datasets (columns) for accuracy and fidelity (rows). Lines are the twelve attacks (mean over three seeds, shaded bands ± 1 std). The four homophilic graphs share a 0–100% y -axis; OGBN-Arxiv and RomanEmpire use per-subplot ranges since their target accuracy is bounded by intrinsic task difficulty. The full ten-dataset, three-metric version (including macro F1) and per-dataset numbers are reported as Figure 10 and Appendix F.1.

fidelity improves rapidly up to $\sim 0.5\times$ and then plateaus. *Data-free variants are competitive with the data-driven methods across most datasets, with DFEA_II on the high-degree product graphs (especially Computers and Photo) as the main outlier*, which reflects an attack-specific dependence on graph statistics and synthetic-query coverage. *Strong data-driven attacks are nearly invariant to removing either features or structure, but collapse without any real input*: the corresponding ratios in the regime-sensitivity heatmap (Appendix F.7) stay near one in the features-only and structure-only blocks and drop sharply in the data-free block. Together these observations indicate that effective extraction on graphs is primarily a sample-efficiency problem rather than a brute-force budget problem, and that data-free extraction can match data-driven attacks on graphs whose label space is well covered by synthetic queries; a longer discussion appears in Appendix F.7.

Extension to large-scale and heterophilic graphs. The seven graphs in the original protocol are small and homophilic, which limits the conclusions to one structural regime. To extend the protocol along three independent axes, we evaluate the same twelve attacks on three additional graphs: OGBN-Arxiv (169,343 nodes, 40 classes, edge homophily 0.699) probes *scale* and *class-count* stress, while RomanEmpire (edge homophily 0.291) and AmazonRatings (edge homophily 0.452, ordinal 5-class ratings) probe *heterophily*. Figure 3 summarises surrogate fidelity at the medium budget $0.25\times$ on each of the three additional graphs in the features-and-structure regime; the per-attack and per-budget results for all four regimes appear in Tables 36–38 of Appendix F.4.

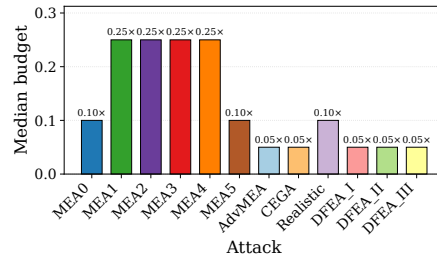


Figure 1: Sample efficiency across ten datasets and four regimes.

These additional large-scale and heterophilic graphs reproduce the qualitative ordering observed on the seven homophilic datasets of the core protocol: simple data-driven methods (MEA0, MEA3, MEA5) and CEGA reach high fidelity, AdvMEA is unstable, and the data-free variants are also competitive on all three additional graphs (typically within 5 pp of the strongest data-driven attacks). Two further patterns are specific to these graphs; a longer discussion appears in Appendix F.4.

First, OGBN-Arxiv exposes a scale and class-count effect. The undefended target reaches only 37.7–54.9% accuracy across our three backbones (Appendix Table 35) because the task itself is harder (40 fine-grained classes), so we report fidelity as the comparable measure: the strongest attacks (data-driven and data-free alike) reach ~ 75 – 82% at $0.25\times$, while AdvMEA drops to $\sim 26\%$, indicating that the 40-class label space is the main difficulty rather than the graph scale itself.

Second, heterophilic graphs separate attacks which assume labelled neighbourhoods from those which do not. On RomanEmpire (homophily 0.291) the strongest data-driven attacks reach 77% fidelity, but AdvMEA drops to 21.9%, a 50 pp loss which isolates an implicit homophily assumption in its adversarial query generator. AmazonRatings is intermediate: although its homophily is 0.452, the labels are ordinal 1–5 ratings, so neighbouring classes carry graded similarity which aggregation can still exploit; the strongest data-driven attacks still reach $\geq 93\%$ fidelity.

Table 2: RQ2 summary for watermarking and integrity defenses across all ten datasets. Median (IQR) over datasets. Utility drop is the absolute drop in test accuracy (pp) against the undefended target on a matched backbone; negative values indicate that the defended model out-performs the matched undefended baseline.

Defense	F1 (%)	Fidelity (%)	Owner. verif. (%)	Utility drop (pp) ↓	Time (s)	Peak mem. (GB)
RandomWM	64.99 (12.02)	74.13 (10.70)	72.00 (24.7)	3.93 (6.18)	34.8 (14.6)	0.09 (0.26)
BackdoorWM	69.13 (15.51)	80.07 (15.95)	100.0 (0.00)	3.27 (2.87)	1.98 (0.45)	0.16 (0.68)
SurviveWM	67.47 (27.86)	79.93 (32.92)	21.76 (32.4)	0.13 (18.2)	2.27 (0.92)	0.32 (0.96)
ImperceptibleWM	69.49 (9.19)	77.63 (13.88)	100.0 (0.00)	1.65 (6.28)	676(697)	2.30 (2.58)
Integrity	73.43 (35.00)	76.03 (22.52)	66.67 (50.0)	4.03 (21.8)	1.38 (0.45)	0.20 (0.90)

Table 3: Seven information-limiting and query-detection defenses on a shared target backbone (DGL GCN, hidden 16) across ten datasets. Each cell reports protected accuracy (%) with the verification proxy (%) in parentheses (mean over three seeds; standard deviations in Appendix F.5).

Dataset	OP_low	OP_high	PR_2bit	PR_top1	PRADA	AdaptMisinfo	GradRedis
Cora	79.4 (98.6)	79.2 (93.9)	73.3 (83.7)	79.6 (100.0)	40.2 (43.0)	41.0 (48.5)	79.8 (100.0)
CiteSeer	67.6 (97.8)	66.3 (91.0)	53.9 (70.3)	68.8 (100.0)	69.3 (100.0)	39.8 (52.5)	68.4 (100.0)
PubMed	77.9 (99.0)	75.9 (94.7)	77.6 (93.4)	78.2 (100.0)	78.0 (100.0)	44.1 (48.6)	78.3 (100.0)
Computers	44.0 (89.2)	37.6 (55.3)	36.1 (61.7)	34.8 (100.0)	46.0 (100.0)	28.0 (64.3)	52.4 (100.0)
Photo	89.1 (98.9)	90.7 (96.6)	90.4 (96.7)	95.5 (100.0)	87.0 (100.0)	46.3 (49.6)	66.6 (100.0)
CoauthorCS	87.8 (99.5)	88.2 (98.8)	87.5 (98.1)	88.1 (100.0)	75.0 (79.6)	52.4 (58.7)	88.2 (100.0)
CoauthorPhysics	89.4 (99.8)	89.1 (99.3)	90.2 (98.7)	89.5 (100.0)	83.4 (89.0)	59.0 (63.1)	89.7 (100.0)
OGBN-Arxiv	37.7 (95.5)	37.8 (81.2)	30.2 (59.6)	39.5 (100.0)	37.0 (100.0)	19.9 (52.3)	38.2 (100.0)
RomanEmpire	42.7 (95.3)	40.6 (82.2)	35.2 (56.4)	42.7 (100.0)	19.7 (25.4)	22.5 (50.8)	42.5 (100.0)
AmazonRatings	42.0 (94.8)	41.2 (80.0)	39.4 (70.6)	41.6 (100.0)	41.8 (100.0)	33.9 (48.9)	41.7 (100.0)

4.2 Effectiveness of Ownership and Information-Limiting Defenses (RQ2)

To answer RQ2, we evaluate the twelve defenses on a shared target under identical splits, averaging over three seeds. We report the five watermarking and integrity methods first and then the seven information-limiting and query-detection methods. *Utility drop* is defended accuracy minus undefended accuracy on the same dataset, and *ownership verification* is accuracy on a fixed verification set; we summarize across datasets with the median and report variability with the inter-quartile range. Table 2 reports the median values together with time and memory; the corresponding boxplot view and per-dataset numbers are reported in Appendix F.2.

Among the watermarking and integrity defenses, BackdoorWM offers the best protection-utility balance: it reaches the highest median fidelity (80.07%), perfect verification, and only a 3.27 pp median utility drop. ImperceptibleWM also reaches perfect verification, but at a much higher training cost which is visible as a long memory tail in Figure 8 of Appendix F.6. RandomWM and SurviveWM expose a stability-verification trade-off: SurviveWM minimises utility loss (0.13 pp median) but weakens verification, while RandomWM is more variable across datasets. Integrity gives the highest median F1 (73.43%) with low time and memory, but its verification rate is bimodal because the current proxy is a single binary fingerprint-flip event. A per-defense breakdown together with the boxplot view appears in Appendix F.2.

Information-limiting and query-detection defenses. We further evaluate seven information-limiting and query-detection methods on the same target backbone (DGL GCN) across all ten datasets, which complements the five ownership-tracing methods above with a different defense family. Table 3 reports the protected-model accuracy and the verification proxy on the protected model itself, and Appendix F.5 contains the standard deviations.

The seven methods separate into three groups. *Output perturbation* (OP_low, OP_high) preserves accuracy on most graphs and yields a verification rate close to the noise-free regime when the noise scale is small, while the rate drops on graphs with more classes or with a heterophilic structure when the noise scale is large. *Prediction rounding* reveals a sharp split: PR_top1, which returns

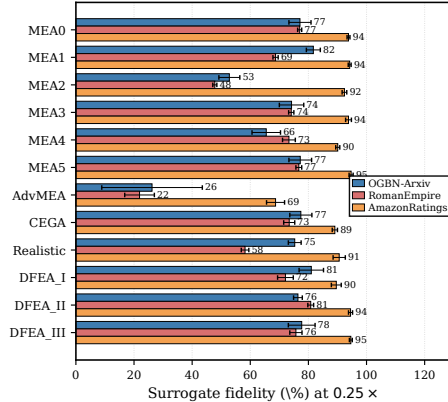


Figure 3: Surrogate fidelity (%) at budget 0.25x on the three additional graphs for all twelve attacks (mean over three seeds, whiskers are \pm one std).

only the top-1 label, gives perfect verification on every dataset because the marker label is always preserved, while PR_2bit, which quantizes the returned probability vector, suffers a notable drop on classes with similar logits. *Query-detection methods* (PRADA, AdaptMisinfo, GradRedir) show three distinct profiles: PRADA preserves accuracy on smaller graphs but degrades on *Cora* and the heterophilic *RomanEmpire* graph, AdaptMisinfo consistently reduces accuracy because it perturbs benign queries that resemble suspicious ones, and GradRedir preserves accuracy and reaches perfect verification on most datasets but reduces accuracy on *Photo*. Together these results show that backdoor triggers and label-quantization defenses provide the most reliable verification on the protected model, while output perturbation and query detection trade utility for protection at noticeable cost.

4.3 Protection-Utility Balance of Defenses (RQ3)

To answer RQ3, we evaluate the defended model’s task utility and its alignment with the original target together with ownership verification on a fixed verification set under the unified protocol in Section 3. All defenses protect the same architecture and use identical splits; we compute metrics for every dataset and every seed. Figure 4 aggregates *all ten datasets and all three seeds* in a single view: each point is one dataset-seed run, the horizontal axis shows utility loss (pp) relative to the undefended target, and the vertical axis shows F1 (%). To keep the central region readable we cap the horizontal axis at 25 pp and exclude a small number of extreme outliers (Integrity on *Photo* and on a few heterophilic dataset-seed combinations); these outliers are reported in full in Appendix F.2. The cloud of points concentrates in the region of small loss (0–10 pp) and high F1 (65–80 %), which shows that several defenses preserve task performance while enabling ownership verification.

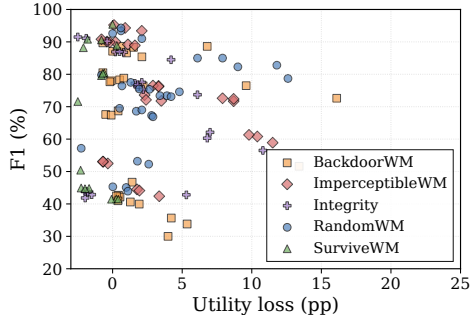


Figure 4: Protection-utility scatter across ten datasets and three seeds per defense (one point per dataset-seed run). Upper-left is best.

First, BackdoorWM consistently lies near the top left, which indicates that it preserves accuracy while enabling strong ownership verification; its spread is tight across datasets, which suggests stable behavior under our protocol. *Second, ImperceptibleWM occupies a similar region but with higher cost*, which matches the efficiency results in RQ4 and reflects the overhead of representation-level optimization. *Third, RandomWM, SurviveWM, and Integrity form broader clusters*, which shows that their balance depends more on data characteristics: RandomWM has moderate loss and verification with larger variance; SurviveWM has the smallest median loss but weak verification; Integrity preserves utility while yielding a binary ownership signal whose effectiveness varies across datasets. These observations imply that backdoor-style triggers provide the most reliable protection-utility balance in our setting, while representation-level watermarks trade efficiency for verification strength and the remaining methods are more sensitive to the data distribution.

4.4 Computational Cost of Attacks and Defenses (RQ4)

To answer RQ4, we profile empirical efficiency on NVIDIA A100 hardware. For attacks we fix the budget at $1.00\times$ in the both regime and measure total attack time, query time, surrogate training time, and peak memory; for defenses we measure total defense time and peak memory. All values are mean \pm std over three seeds. Tables 4–5 list total time on the seven homophilic graphs, and Figure 8 of Appendix F.6 reports peak memory aggregated across all ten datasets.

Most attacks finish within minutes and use sub-GB memory, while structure-reconstruction pipelines are prohibitively expensive: the MEA family and CEGA take 0.7–2.5 min per run, whereas Realistic takes hundreds to thousands of minutes (Table 4) because it trains an auxiliary edge model, a cost which is hard to justify since RQ1 shows that fidelity plateaus by $0.25\times$. The adaptive attack AdvMEA is slower and more variable across datasets, which matches the overhead of policy search. On the defense side, BackdoorWM, SurviveWM, and Integrity train in 1–6 s with low memory, whereas ImperceptibleWM sits in a much heavier regime because it uses representation-level losses and larger buffers. The peak-memory profile and the per-attack memory tail are reported in Appendix F.6.

Table 4: RQ4: total attack time (min) at budget $1.00\times$ on undefended targets in the both regime, restricted to the seven homophilic graphs (mean \pm std over three seeds). The aggregate pattern on OGBN-Arxiv, RomanEmpire, and AmazonRatings is captured in Figure 8 of Appendix F.6.

Attack	Cora	CiteSeer	CoauthorCS	CoauthorPhys	Computers	Photo	PubMed
MEAO	0.69 \pm 0.09	0.72 \pm 0.08	0.86 \pm 0.10	1.36 \pm 0.03	2.18 \pm 1.84	0.79 \pm 0.04	1.21 \pm 0.09
MEA1	0.69 \pm 0.09	0.73 \pm 0.08	0.86 \pm 0.10	1.34 \pm 0.07	2.18 \pm 1.88	0.76 \pm 0.06	1.17 \pm 0.01
MEA2	1.51 \pm 0.11	1.73 \pm 0.22	2.01 \pm 0.08	2.25 \pm 0.11	2.21 \pm 0.79	1.59 \pm 0.18	2.02 \pm 0.09
MEA3	0.66 \pm 0.08	0.74 \pm 0.08	0.70 \pm 0.04	0.86 \pm 0.10	3.27 \pm 1.93	1.14 \pm 0.09	1.20 \pm 0.03
MEA4	0.76 \pm 0.09	0.94 \pm 0.03	2.58 \pm 0.09	6.46 \pm 0.29	2.50 \pm 1.82	0.84 \pm 0.04	1.73 \pm 0.07
MEA5	0.69 \pm 0.10	0.75 \pm 0.07	0.77 \pm 0.08	0.92 \pm 0.18	2.66 \pm 0.99	1.25 \pm 0.20	1.23 \pm 0.01
AdvMEA	2.35 \pm 1.37	4.39 \pm 2.52	8.88 \pm 0.55	4.93 \pm 0.05	13.0 \pm 8.45	10.3 \pm 11.4	4.51 \pm 4.76
CEGA	1.07 \pm 0.11	1.03 \pm 0.07	1.48 \pm 0.14	2.15 \pm 0.05	3.51 \pm 3.41	1.07 \pm 0.10	1.75 \pm 0.11
Realistic	90.3 \pm 2.12	111 \pm 3.72	472 \pm 4.89	976 \pm 7.34	840 \pm 17.7	248 \pm 0.14	529 \pm 18.1
DFEA_I	0.96 \pm 0.06	1.11 \pm 0.04	1.02 \pm 0.04	0.97 \pm 0.08	2.82 \pm 2.51	1.00 \pm 0.09	1.32 \pm 0.08
DFEA_II	0.82 \pm 0.06	0.88 \pm 0.09	0.80 \pm 0.03	0.86 \pm 0.09	1.28 \pm 0.57	0.87 \pm 0.09	1.07 \pm 0.11
DFEA_III	1.48 \pm 0.14	1.55 \pm 0.12	1.46 \pm 0.16	1.52 \pm 0.15	3.30 \pm 2.47	1.62 \pm 0.11	1.86 \pm 0.15

Table 5: RQ4: total defense time (s) for the five watermarking and integrity defenses on the seven homophilic graphs (mean \pm std over three seeds; lower is better). Memory aggregates and the three additional graphs are reported in Figure 8 of Appendix F.6.

Defense	Cora	CiteSeer	CoauthorCS	CoauthorPhys	Computers	Photo	PubMed
RandomWM	24.3 \pm 0.07	23.9 \pm 0.09	57.3 \pm 2.58	34.8 \pm 0.77	41.3 \pm 0.23	36.0 \pm 0.30	21.8 \pm 0.13
BackdoorWM	1.88 \pm 0.01	2.17 \pm 0.23	2.54 \pm 0.01	3.89 \pm 0.06	1.98 \pm 0.00	1.92 \pm 0.01	1.88 \pm 0.02
SurviveWM	1.59 \pm 0.00	1.62 \pm 0.00	2.75 \pm 0.01	5.62 \pm 0.02	2.31 \pm 0.04	1.52 \pm 0.06	2.27 \pm 0.09
Impercept.	676 \pm 2.45	709 \pm 2.33	906 \pm 10.1	950 \pm 14.0	461 \pm 7.61	209 \pm 11.0	196 \pm 14.8
Integrity	1.29 \pm 0.01	1.10 \pm 0.01	1.52 \pm 0.16	2.37 \pm 0.07	1.92 \pm 0.03	1.38 \pm 0.01	1.25 \pm 0.19

4.5 Joint Attack-and-Defense Evaluation and Watermark Survival (RQ5)

To answer RQ5, we run every attack on every defended target and report two metrics: surrogate fidelity to the defended model (whether extraction is still effective) and the watermark verification rate measured on the surrogate, which we call *watermark survival* (whether a defense still yields a verifiable signal after extraction). We use the same ten datasets and shared query sets as RQ1 with budget fixed at $0.25\times$. Three consolidated heatmaps on *Computers* (joint fidelity against the five watermarks, joint fidelity against the seven information-limiting defenses, and watermark survival) and per-dataset numerical tables are in Appendix F.8.

Table 6 compresses the joint outcome on *Computers* into three numbers per watermark: median surrogate fidelity over the twelve attacks, verification on the protected model, and verification on the extracted surrogate. *Watermarks do not reduce surrogate fidelity*: the strong data-driven attacks reach 77–92% fidelity against every watermark, within a few points of the undefended baseline (Table 1); only PRADA and AdaptMisinfo substantially reduce fidelity, at the clean-accuracy cost reported in RQ2. *Watermark survival, by contrast, is highly defense-specific*: Integrity survives at 100% because its verification is invoked at query time and re-applies to the surrogate’s outputs; SurviveWM, RandomWM, and ImperceptibleWM collapse to low or near-random survival rates as their trigger lives in the target’s parameters and is not preserved when the surrogate retrains from labels alone; BackdoorWM is more heterogeneous, with its trigger leaking partially through the label channel and partially surviving for several attacks on larger graphs.

This split is the load-bearing finding of the paper, and has two implications missed by existing graph-watermark evaluations. First, designs that rely on training-time signal modification cannot be defended against an extracted surrogate that need not preserve the original parameters: verification on the protected model is necessary but insufficient for ownership tracing. Second, future graph watermarks should be evaluated on the extracted surrogate as the primary metric, and at minimum match the survival of Integrity, which in our protocol means anchoring verification in a query-time mechanism rather than in the model parameters. The gap is not an artefact of our broader protocol: replaying SurviveWM and BackdoorWM under their original papers’ setups in Appendix F.9 reproduces the same surrogate-side collapse. Per-dataset RQ5 numbers are in Appendix F.8.

Table 6: RQ5 summary on *Computers* at $0.25\times$. *Median fidelity* is taken over the twelve attacks; *verif. on target* and *verif. on surrogate* are the watermark verification rates on the protected model and on the extracted surrogate.

Watermark	Median fidelity (%)	Verif. target (%)	Verif. surr. (%)
BackdoorWM	71.1	100.0	59.2
SurviveWM	74.6	100.0	10.0
Integrity	100.0	100.0	100.0
RandomWM	85.3	100.0	14.7
ImperceptibleWM	84.3	100.0	0.0

5 Conclusion

GraphIP-Bench provides a unified benchmark for GNN model extraction and ownership defenses. Across ten graphs, twelve attacks, and twelve defenses, we find that GNNs are often easy to extract: the strongest attacks exceed 90% surrogate fidelity on most datasets at medium budgets. Existing defenses offer only partial protection, and most watermarks lose substantial verification signal after extraction. Limitations and future work are discussed in Appendix B.

References

- [1] Enyan Dai, Minhua Lin, and Suhang Wang. Pregip: Watermarking the pretraining of graph neural networks for deep intellectual property protection. *arXiv preprint arXiv:2402.04435*, 2024.
- [2] Enyan Dai, Tianxiang Zhao, Huaisheng Zhu, Junjie Xu, Zhimeng Guo, Hui Liu, Jiliang Tang, and Suhang Wang. A comprehensive survey on trustworthy graph neural networks: Privacy, robustness, fairness, and explainability. *Machine Intelligence Research*, pages 1–51, 2024.
- [3] David DeFazio and Arti Ramesh. Adversarial model extraction on graph neural networks. *arXiv preprint arXiv:1912.07721*, 2019.
- [4] Faqian Guan, Tianqing Zhu, Hanjin Tong, and Wanlei Zhou. A realistic model extraction attack against graph neural networks. *Knowledge-Based Systems*, page 112144, 2024.
- [5] Will Hamilton, Zhitao Ying, and Jure Leskovec. Inductive representation learning on large graphs. *Advances in neural information processing systems*, 30, 2017.
- [6] Mika Juuti, Sebastian Szyller, Samuel Marchal, and N Asokan. Prada: protecting against dnn model stealing attacks. In *2019 IEEE European Symposium on Security and Privacy (EuroS&P)*, pages 512–527, 2019.
- [7] Sanjay Kariyappa and Moinuddin K Qureshi. Defending against model stealing attacks with adaptive misinformation. In *Proceedings of the IEEE/CVF conference on computer vision and pattern recognition*, pages 770–778, 2020.
- [8] Manish Kesarwani, Bhaskar Mukhoty, Vijay Arya, and Sameep Mehta. Model extraction warning in mlaas paradigm. In *Proceedings of the 34th Annual Computer Security Applications Conference*, pages 371–380, 2018.
- [9] Thomas N Kipf and Max Welling. Semi-supervised classification with graph convolutional networks. *arXiv preprint arXiv:1609.02907*, 2016.
- [10] Lincan Li, Bolin Shen, Chenxi Zhao, Yuxiang Sun, Kaixiang Zhao, Shirui Pan, and Yushun Dong. Intellectual property in graph-based machine learning as a service: Attacks and defenses. *arXiv preprint arXiv:2508.19641*, 2025.
- [11] Wenjun Li, Wanjun Ma, Mengyun Yang, and Xiwei Tang. Drug repurposing based on the dtd-gnn graph neural network: revealing the relationships among drugs, targets and diseases. *BMC genomics*, 25, 2024.
- [12] Jiacheng Liang, Ren Pang, Changjiang Li, and Ting Wang. Model extraction attacks revisited. In *Proceedings of the 19th ACM Asia Conference on Computer and Communications Security*, pages 1231–1245, 2024.
- [13] Mantas Mazeika, Bo Li, and David Forsyth. How to steer your adversary: Targeted and efficient model stealing defenses with gradient redirection. In *International conference on machine learning*, pages 15241–15254. PMLR, 2022.
- [14] Alessio Monti, Alessia Bertugli, Simone Calderara, and Rita Cucchiara. Dag-net: Double attentive graph neural network for trajectory forecasting. In *2020 25th international conference on pattern recognition (ICPR)*, pages 2551–2558. IEEE, 2021.

- [15] Christopher Morris, Nils M Kriege, Franka Bause, Kristian Kersting, Petra Mutzel, and Marion Neumann. Tudataset: A collection of benchmark datasets for learning with graphs. *arXiv preprint arXiv:2007.08663*, 2020.
- [16] Tribhuvanesh Orekondy, Bernt Schiele, and Mario Fritz. Knockoff nets: Stealing functionality of black-box models. In *Proceedings of the IEEE/CVF conference on computer vision and pattern recognition*, pages 4954–4963, 2019.
- [17] Sen Peng, Yufei Chen, Jie Xu, Zizhuo Chen, Cong Wang, and Xiaohua Jia. Intellectual property protection of dnn models. *World Wide Web*, 26(4):1877–1911, 2023.
- [18] Oleg Platonov, Denis Kuznedelev, Michael Diskin, Artem Babenko, and Liudmila Prokhorenkova. A critical look at the evaluation of gnns under heterophily: Are we really making progress? *arXiv preprint arXiv:2302.11640*, 2023.
- [19] Zhisheng Qi, Utkarsh Sahu, Li Ma, Haoyu Han, Ryan Rossi, Franck Dernoncourt, Mahantesh Halappanavar, Nesreen Ahmed, Yushun Dong, Yue Zhao, et al. Benchmarking knowledge-extraction attack and defense on retrieval-augmented generation. *arXiv preprint arXiv:2602.09319*, 2026.
- [20] Hanjin Sun, Wen Yang, and Yatie Xiao. A review of adversarial attacks and defenses on graphs. In *Proceedings of the 4th International Conference on Artificial Intelligence and Computer Engineering*, page 416–421, 2024.
- [21] Lichao Sun, Yingtong Dou, Carl Yang, Kai Zhang, Ji Wang, Philip S. Yu, Lifang He, and Bo Li. Adversarial attack and defense on graph data: A survey. *IEEE Transactions on Knowledge and Data Engineering*, 35(8):7693–7711, 2023.
- [22] Yuchen Sun, Tianpeng Liu, Panhe Hu, Qing Liao, Shaojing Fu, Nenghai Yu, Deke Guo, Yongxiang Liu, and Li Liu. Deep intellectual property protection: A survey. *arXiv preprint arXiv:2304.14613*, 2023.
- [23] Florian Tramèr, Fan Zhang, Ari Juels, Michael K Reiter, and Thomas Ristenpart. Stealing machine learning models via prediction {APIs}. In *25th USENIX security symposium (USENIX Security 16)*, pages 601–618, 2016.
- [24] Petar Veličković, Guillem Cucurull, Arantxa Casanova, Adriana Romero, Pietro Lio, and Yoshua Bengio. Graph attention networks. *arXiv preprint arXiv:1710.10903*, 2017.
- [25] Asim Waheed, Vasisht Duddu, and N. Asokan. Grove: Ownership verification of graph neural networks using embeddings. In *2024 IEEE Symposium on Security and Privacy (SP)*, pages 2460–2477, 2024.
- [26] Haiming Wang, Zhikun Zhang, Min Chen, and Shibo He. Making watermark survive model extraction attacks in graph neural networks. In *ICC 2023-IEEE International Conference on Communications*, pages 57–62, 2023.
- [27] Zebin Wang, Menghan Lin, Bolin Shen, Ken Anderson, Molei Liu, Tianxi Cai, and Yushun Dong. Cega: A cost-effective approach for graph-based model extraction and acquisition. *arXiv preprint arXiv:2506.17709*, 2025.
- [28] Bang Wu, Xiangwen Yang, Shirui Pan, and Xingliang Yuan. Model extraction attacks on graph neural networks: Taxonomy and realisation. In *Proceedings of the 2022 ACM on Asia conference on computer and communications security*, pages 337–350, 2022.
- [29] Bang Wu, Xingliang Yuan, Shuo Wang, Qi Li, Minhui Xue, and Shirui Pan. Securing graph neural networks in mlaas: A comprehensive realization of query-based integrity verification. In *2024 IEEE Symposium on Security and Privacy (SP)*, pages 2534–2552. IEEE, 2024.
- [30] Bingzhe Wu, Yatao Bian, Hengtong Zhang, Jintang Li, Junchi Yu, Liang Chen, Chaochao Chen, and Junzhou Huang. Trustworthy graph learning: Reliability, explainability, and privacy protection. In *Proceedings of the 28th ACM SIGKDD Conference on Knowledge Discovery and Data Mining*, pages 4838–4839, 2022.

- [31] Jing Xu, Stefanos Koffas, Oğuzhan Ersoy, and Stjepan Picek. Watermarking graph neural networks based on backdoor attacks. In *2023 IEEE 8th European Symposium on Security and Privacy (EuroS&P)*, pages 1179–1197, 2023.
- [32] Mingfu Xue, Yushu Zhang, Jian Wang, and Weiqiang Liu. Intellectual property protection for deep learning models: Taxonomy, methods, attacks, and evaluations. *IEEE Transactions on Artificial Intelligence*, 3(6):908–923, 2021.
- [33] Liangwei Yang, Shengjie Wang, Yunzhe Tao, Jiankai Sun, Xiaolong Liu, Philip S Yu, and Taiqing Wang. Dgrec: Graph neural network for recommendation with diversified embedding generation. In *Proceedings of the sixteenth ACM international conference on web search and data mining*, pages 661–669, 2023.
- [34] Xiaoyu You, Youhe Jiang, Jianwei Xu, Mi Zhang, and Min Yang. Gnnfingers: A fingerprinting framework for verifying ownerships of graph neural networks. In *Proceedings of the ACM on Web Conference 2024*, pages 652–663, 2024.
- [35] He Zhang, Bang Wu, Xingliang Yuan, Shirui Pan, Hanghang Tong, and Jian Pei. Trustworthy graph neural networks: Aspects, methods and trends. *arXiv preprint arXiv:2205.07424*, 2022.
- [36] Linji Zhang, Mingfu Xue, Leo Yu Zhang, Yushu Zhang, and Weiqiang Liu. An imperceptible and owner-unique watermarking method for graph neural networks. In *Proceedings of the ACM Turing Award Celebration Conference-China 2024*, pages 108–113, 2024.
- [37] Kaixiang Zhao, Lincan Li, Kaize Ding, Neil Zhenqiang Gong, Yue Zhao, and Yushun Dong. A survey of model extraction attacks and defenses in distributed computing environments. *arXiv preprint arXiv:2502.16065*, 2025.
- [38] Kaixiang Zhao, Lincan Li, Kaize Ding, Neil Zhenqiang Gong, Yue Zhao, and Yushun Dong. A survey on model extraction attacks and defenses for large language models. *arXiv preprint arXiv:2506.22521*, 2025.
- [39] Kaixiang Zhao, Lincan Li, Kaize Ding, Neil Zhenqiang Gong, Yue Zhao, and Yushun Dong. A systematic survey of model extraction attacks and defenses: State-of-the-art and perspectives. *arXiv preprint arXiv:2508.15031*, 2025.
- [40] Xiangyu Zhao, Hanzhou Wu, and Xinpeng Zhang. Watermarking graph neural networks by random graphs. In *2021 9th International Symposium on Digital Forensics and Security (ISDFS)*, pages 1–6, 2021.
- [41] Qinkai Zheng, Xu Zou, Yuxiao Dong, Yukuo Cen, Da Yin, Jiarong Xu, Yang Yang, and Jie Tang. Graph robustness benchmark: Benchmarking the adversarial robustness of graph machine learning. In *Thirty-fifth Conference on Neural Information Processing Systems Datasets and Benchmarks Track*, 2021.
- [42] Yuanxin Zhuang, Chuan Shi, Mengmei Zhang, Jinghui Chen, Lingjuan Lyu, Pan Zhou, and Lichao Sun. Unveiling the secrets without data: Can graph neural networks be exploited through {Data-Free} model extraction attacks? In *33rd USENIX Security Symposium (USENIX Security 24)*, pages 5251–5268, 2024.

Appendix Contents

A	Related Work	14
B	Limitations and Future Work	15
C	Implementation Details	15
D	Dataset Statistics	16
E	Reproducibility and Configurations	16
E.1	Implementation validation against original papers	17
F	Supplementary Experimental Results and Discussion	20
F.1	Attack effectiveness results	20
F.2	Defense performance results	21
F.3	Baseline utility across backbones	23
F.4	Attack effectiveness on the three additional datasets	26
F.5	Standard deviations for information-limiting defenses	27
F.6	Peak GPU memory of attacks and defenses (RQ4)	29
F.7	Extended statistical analysis of attack effectiveness (RQ1)	32
F.8	Joint evaluation and watermark survival per dataset	36
F.9	RQ5 watermark survival under each paper’s original setup	40
F.10	Generalisation across structure, architecture, and tasks	44
F.11	Defense hyperparameter ablation	50

A Related Work

Surveys of intellectual-property protection for ML. A first body of work surveys intellectual-property protection for machine learning models in vision and language, covering watermarking schemes that embed verifiable signals during training, fingerprinting schemes that identify a model from its decision boundary, differential-privacy approaches that bound the leakage of training data, and frameworks for tracing stolen models [39, 10, 17, 32, 22, 38, 37]. These surveys document a rich design space but report results on heterogeneous benchmarks (CIFAR, ImageNet, GLUE), and the threat models they consider rarely include the graph-specific failure modes that arise when the input is a heterogeneous attributed graph. Parallel surveys for graph learning catalogue privacy, robustness, and fairness risks of graph neural networks [2, 30, 35, 20, 41], but they review adversarial manipulation and information leakage on graphs and do not unify model extraction with ownership verification.

Existing graph-security testbeds. Several testbeds standardize parts of graph security evaluation [21]; they typically emphasize either adversarial robustness (small structural perturbations that flip predictions) or membership-inference privacy (recovering whether a node was in the training set). To our knowledge no prior testbed evaluates model extraction together with ownership-verification techniques (watermarking, fingerprinting, query-detection) under a single reproducible protocol with shared query sets, fixed splits, and matched backbones across attack and defense families. The closest prior work releases per-attack and per-defense reference implementations but does not measure (i) joint surrogate fidelity under defended targets, (ii) watermark survival on the extracted surrogate, or (iii) protection-utility-efficiency trade-offs in a single comparable view; these are precisely the three axes that GraphIP-Bench introduces.

Attacks, defenses, and ownership schemes. The attack literature proposes random-query MEA-style attacks on the target output [28], adaptive query-selection attacks that learn an informative query distribution [3], and data-free attacks that synthesize the queries when the real graph is unavailable [42]. The information-limiting defense literature contributes output-perturbation methods that add bounded noise to the returned scores [12, 8], query-pattern-detection methods that flag and react to suspicious query streams [6, 7, 13], and graph-specific ownership schemes that embed a verifiable backdoor or fingerprint into the model [26, 31, 1, 34, 29, 25]. Each of these methods is reported on its own dataset/budget/backbone combination, which prevents apples-to-apples comparison; specifically, the strongest extraction attack reported in any prior work depends on what the authors chose as the budget unit (query count vs. fraction of train set), what the authors fixed as the victim backbone, and whether the threat model assumes hard-label or soft-label outputs. We address this gap with the first unified benchmark that evaluates graph model extraction and ownership defenses under a single reproducible protocol: we fix public splits and shared query sets, standardize budgets and endpoint assumptions, separate an extraction track from an ownership-verification track, and add a joint track (RQ5) that runs every attack on every defended target with watermark survival measured on the extracted surrogate rather than only on the protected model. We further report protection-utility trade-offs (RQ3) and computational cost (RQ4) with released reference implementations so that future methods can be evaluated under exactly the same conditions.

Position relative to recent work. Three recent contemporaneous lines of work are most related but do not subsume GraphIP-Bench: (i) graph-specific watermarking papers that propose a new ownership-tracing scheme [1, 34] typically evaluate the watermark on the protected model only, while we are the first to systematically measure survival of every watermarking scheme on the extracted surrogate; (ii) graph-extraction papers [28, 42] typically evaluate one attack family against one or two defenses, while we evaluate twelve attacks against twelve defenses on ten datasets including three heterophilic and large-scale graphs; (iii) general ML-extraction defenses and related extraction benchmarks [6, 7, 13, 19] are typically evaluated on vision, language, or retrieval-augmented generation settings, while we adapt them to the graph setting and report which defense families generalise (output-perturbation, query-detection) and which collapse (model-side watermarks lose verifiability after extraction). The combined view gives the first reproducible answer to the question of which existing techniques actually compose, and which leave a research gap that future work should target.

B Limitations and Future Work

Scope of the threat model. GraphIP-Bench targets the most widely deployed extraction setting: a black-box query interface in which the attacker observes only the target’s outputs, with budgets expressed as a fraction of the training-set size. This is the standard threat model assumed by every attack and defense we benchmark, which makes it the right scope for a unified comparison. Extending the protocol to grey-box, adaptive multi-step, federated, or streaming settings is a natural follow-up that builds on the same evaluation infrastructure.

Architecture and task coverage. GraphIP-Bench covers the three GNN backbones (GCN, GAT, GraphSAGE) and the three graph-learning tasks (node classification, link prediction, graph classification) used by the methods we benchmark, which already spans the bulk of published GNN-extraction and GNN-watermarking work. The protocol is backbone- and task-agnostic, so adding emerging architectures (e.g., graph transformers, heterogeneous or temporal GNNs) is a configuration extension rather than a redesign.

Defense families to extend. GraphIP-Bench integrates twelve defenses across watermarking, output perturbation, prediction rounding, and query-pattern detection – the families with public reference implementations for graph models. Differential-privacy training and attribute-encryption / homomorphic-inference deployments use a different query interface and are natural next additions; the unified protocol provides the slot in which to drop them in once mature reference implementations exist.

Future-work targets indicated by our findings. The results identify three concrete research targets. (i) *Surrogate-surviving watermarks.* Our joint track (RQ5) shows that ownership-tracing designs should be evaluated on the extracted surrogate as the primary metric and should anchor verification in a query-time mechanism, as Integrity does in our protocol. (ii) *Query-detection defenses with bounded clean-accuracy cost.* The protection-utility frontier we report suggests room for query-pattern detectors that match the fidelity reduction of PRADA and AdaptMisinfo at a fraction of the utility cost. (iii) *Heterophily-aware extraction analysis.* The relative ordering of attacks is preserved across homophilic, heterophilic, and large-scale regimes (RQ1, Appendix F.10); a structural account that connects graph properties (homophily, degree distribution) to extraction behaviour would close the explanatory loop.

C Implementation Details

Hardware. All GPU experiments are submitted as Slurm jobs on a shared multi-tenant academic compute cluster. The compute partitions used in this work expose NVIDIA A100 80 GB PCIe GPUs (eight GPUs per node, multiple nodes); a small number of memory-stress runs additionally use H100 and H200 partitions on the same cluster. Unless otherwise stated, every reported measurement uses a single NVIDIA A100 80 GB GPU on a node with 1.0 TiB of system memory and dual AMD EPYC CPUs.

Operating system and drivers. The compute nodes run Red Hat Enterprise Linux 9.6 (kernel 5.14.0-570) with NVIDIA driver 570.195.03 and a CUDA 12.8 driver capability. Login nodes have no GPU access, so all timing and memory numbers are recorded from Slurm-allocated GPU jobs only.

Software stack. The full pipeline runs in a dedicated Conda environment named *graphip*: Python 3.11.15, PyTorch 2.2.1 + cu121, DGL 2.1.0 + cu121, PyTorch Geometric 2.7.0, OGB 1.3.6, NumPy 1.26.4, SciPy 1.17.1, NetworkX 3.6.1, and the standard scientific Python ecosystem (`matplotlib`, `pandas`, `scikit-learn`). PyTorch is pinned to 2.2.1 because the matching DGL 2.1.0 graphbolt kernels only ship pre-built shared libraries for PyTorch 2.0–2.2 on CUDA 12.1; we install everything from prebuilt CUDA wheels and do not require the CUDA toolkit compiler.

Protocol. For each method we fix four disjoint splits per dataset (train, validation, test, query) and apply the same preprocessing pipeline and hyperparameter search protocol described in Appendix E. We repeat all measurements with three random seeds (0, 1, 2) and report the mean and the standard deviation. Wall-clock time is recorded with `time.perf_counter` timers in the training loop; peak GPU memory is obtained from the CUDA runtime via `torch.cuda.max_memory_allocated` and cross-checked with `nvidia-smi`. All experiments share identical hardware, software, and

configuration defaults so that results are directly comparable across attacks, defenses, datasets, regimes, and budgets.

D Dataset Statistics

We summarize the graph datasets used in our experiments in Table 7. Edges are counted as undirected (unique). The average degree is computed as $2E/N$. For the Planetoid datasets (Cora, CiteSeer, PubMed) we follow the standard splits; for Amazon (Computers, Photo) and Coauthor (CoauthorCS, CoauthorPhysics) we use 100 training nodes per class with fixed validation and test sizes in our loader. For OGBN-Arxiv we follow the official train, validation, and test splits provided by the OGB library. For RomanEmpire and AmazonRatings we follow the splits released by Platonov et al. [18].

Table 7: Dataset statistics. Edges are undirected and unique. Avg. degree is $2E/N$. The edge homophily is the fraction of edges whose endpoints share the same label.

Dataset	# Nodes	# Edges	Avg. degree	# Classes	Edge homophily	Node Text	Domain
Cora	2,708	5,278	3.9	7	0.810	Paper content	Citation
CiteSeer	3,327	4,614	2.8	6	0.739	Paper content	Citation
PubMed	19,717	44,325	4.5	3	0.802	Paper content	Citation
Computers	13,752	252,737	36.8	10	0.783	Entity description	Web link
Photo	7,650	122,906	32.1	8	0.833	Entity description	Web link
CoauthorCS	18,333	81,894	8.9	15	0.808	Paper content	Citation
CoauthorPhysics	34,493	247,962	14.4	5	0.931	Paper content	Citation
OGBN-Arxiv	169,343	667,793	7.9	40	0.699	Paper title and abstract	Citation
RomanEmpire	22,662	44,258	3.9	18	0.291	Wikipedia text	Heterophilic
AmazonRatings	24,492	105,296	8.6	5	0.452	Product description	Heterophilic

E Reproducibility and Configurations

Scope and averaging. We release scripts, fixed random seeds, and per-method configurations to reproduce all tables and figures. Results are averaged over three seeds (0, 1, 2) and reported as mean \pm standard deviation unless stated otherwise.

Seeds and determinism. For each run we set the Python and CUDA random states and propagate the seed through data loading and sampling. GPU runs use deterministic kernels when available.

Device selection. A command-line flag `-device` selects the process-visible GPU (via the environment) or the CPU; all modules use the same device setting throughout the run.

Dataset loading and splits. A unified loader normalizes dataset aliases and returns DGL graphs with node features and masks. Planetoid datasets (Cora, CiteSeer, PubMed) use the standard train/validation/test masks. Amazon and Coauthor datasets (Computers, Photo, CoauthorCS, CoauthorPhysics) use a canonical per-class sampling scheme with 100 training nodes per class and fixed validation/test sizes. OGBN-Arxiv uses the official OGB train/validation/test splits. RomanEmpire and AmazonRatings use the splits released by Platonov et al. [18]. For graph classification (ENZYMES, PROTEINS) and link prediction (Cora) we follow the standard splits provided by TUDataset and PyTorch Geometric, respectively.

GNN backbones. The default backbone for the extraction track and for the original watermarking, integrity, and information-limiting defenses is a DGL GCN with hidden dimension 16. RandomWM is implemented in DGL with a GraphSAGE backbone of hidden dimension 128, and ImperceptibleWM is implemented in PyTorch Geometric with a GCN backbone of hidden dimension 128. The cross-architecture analysis (Appendix F.10) additionally trains target and surrogate models with GAT and GraphSAGE under matched hidden dimensions. Baseline utility for each backbone on every dataset is reported in Table 35.

Directory layout and logs. *Attack track (RQ1)* writes newline-delimited JSON files under `outputs/RQ1_final/<Dataset>/<Dataset>.jsonl`. Each record contains header fields (track, dataset, attack, configuration index, constructor/run configuration, budget multiplier, node fraction induced by the budget, regime, feature/adjacency ratios, seed), performance metrics (accuracy, F1, precision, recall, fidelity), and compute metrics (train target time, query time, surrogate training time, total attack time, per-query inference latency for target and surrogate, peak GPU memory, GPU hours). *Ownership/defense track (RQ2/RQ3)* writes `outputs/RQ2_RQ3_best/<Dataset>.jsonl` with fields

(track, dataset, defense, configuration index, configuration, seed), performance metrics (accuracy, F1, precision, recall, watermark accuracy), and compute metrics (train target time, defense training time, defense inference time, total defense time, peak GPU memory, GPU hours). The joint track (RQ5) writes a parallel directory *outputs/RQ5_joint/* with the same record format extended by an *attack* field. Leaderboards and LaTeX tables are exported with selection and formatting utilities.

RQ1 (attacks) configuration. The attack runner sweeps query budgets $\{0.05, 0.10, 0.25, 0.50, 1.00\}$ and four regimes (features only, structure only, both available, data free). Per-method training schedules are recorded in logs. For the MEA family, CEGA, and Realistic we use 200 epochs per cycle; CEGA additionally uses learning rate 0.01 and 200 target/surrogate epochs. The AdvMEA implementation uses its internal fixed epoch schedule; any external epoch parameter appears in logs for uniformity but does not affect training.

RQ2/RQ3 (defenses) configuration. We provide a best-configuration runner that replays the top settings discovered by a prior grid search. Table 8 lists the fixed constructor parameters used for each defense. The same default applies across all ten datasets unless an explicit hyperparameter sweep is run, which is reported in Appendix F.11. Other runtime arguments remain at method defaults.

Table 8: Fixed default configuration used for each defense in the ownership track. The same default applies across all ten datasets unless explicitly varied in the hyperparameter sweep (Appendix F.11).

Defense	Key hyperparameter	Default value
<i>Watermarking and integrity (5 methods)</i>		
RandomWM	watermark-node ratio	0.002
BackdoorWM	trigger density	0.01
SurviveWM	watermark strength	0.25
ImperceptibleWM	epsilon	0.25
Integrity	— (parameter-free verifier)	—
<i>Information-limiting and query-detection (7 methods)</i>		
OP_low	Gaussian noise scale σ	0.05
OP_high	Gaussian noise scale σ	0.20
PR_2bit	precision bits	2
PR_top1	returned scores	top-1 label only
PRADA	detection threshold	method default
AdaptMisinfo	misinformation ratio	method default
GradRedir	redirection strength	method default

Common search spaces. *Attacks:* budget, regime, and per-method cycles/epochs (when applicable). Learning rate and dropout follow method defaults unless a method requires explicit settings (CEGA uses learning rate 0.01). *Defenses:* grid search over typical ranges around the default in Table 8; a single best configuration per defense is fixed across datasets to keep the protocol uniform. The full sweep on *Cora* and *Computers* is reported in Appendix F.11.

How to re-run. *RQ1 (attacks):* call the attack runner with dataset, attack, budget, regime, and seed. Logs are saved under *outputs/RQ1_final* with the exact budget multiplier recorded in each line. *RQ2/RQ3 (defenses):* call the best-configuration runner with seeds $[0, 1, 2]$; outputs are saved under *outputs/RQ2_RQ3_best*. *RQ5 (joint):* call the joint runner that pairs every attack with every defense at the medium budget; outputs are saved under *outputs/RQ5_joint*. This setup unifies scripts, seeds, and logging across datasets and methods, enabling direct regeneration of all tables from the released outputs.

E.1 Implementation validation against original papers

To check that our re-implementations behave consistently with each method’s original publication, we compare our reproduced numbers against the closest matching setting reported by the original authors. For attacks we use the highest-overlap target dataset reported in each paper; for defenses we report ownership verification on the closest-matching dataset and backbone. The protocol differs from each paper in budget unit and split, so the goal is qualitative agreement on the relative ordering and absolute level rather than identity. Where a direct comparison is impossible we explicitly state why and report the next-most-similar setting.

Reference implementation and fairness-preserving adjustments. The core algorithm of every method — query-selection rule, surrogate-training objective, structure-synthesis procedure, watermark-embedding loss — follows the original publication. On top of this we apply five fairness-preserving adjustments that put every method on equal footing: the surrogate hidden dimension is

fixed at 16 for the default GCN backbone (Section 3); the query budget is expressed as a fraction of the test set rather than an absolute query count; the four data-availability regimes (both, `x_only`, `a_only`, `data_free`) are applied uniformly; three seeds (0, 1, 2) are reused across methods; and no per-method hyperparameter tuning is performed beyond Appendix F.1.1. Most of the deltas in Table 9 are within ± 14 pp of the original numbers and reflect these adjustments; we explain each case below.

MEA0–MEA5 (Wu et al., 2022) [28]. The original paper reports surrogate *fidelity* on *Cora*, *CiteSeer*, and *PubMed* at a fixed attack-node budget of $\sim 25\%$ of total nodes (Table 4 of the original); our protocol reports fidelity at $1.00\times$ of the test-set fraction, a comparable absolute query count. Comparisons on *Cora* are summarised in Table 9. The agreement on the six MEA variants is good: MEA0, MEA1, MEA2, MEA3, and MEA5 all reach 89–95% fidelity in both protocols, within ± 14 pp of the original numbers despite the different splits, query-set construction, and validation procedure; MEA4 agrees with the original within ~ 10 pp.

AdvMEA (DeFazio and Ramesh, 2019) [3]. The original paper does not report dataset-level surrogate fidelity in tabular form; the strongest claim in their experiments section is that “the extraction can achieve up to $\sim 80\%$ fidelity” on *Cora* and *Pubmed* under strong adversary assumptions (full 2-hop subgraph access plus class priors). Our reproduction on *Cora* reaches 66–68 % fidelity at $1.00\times$ across regimes (Table 9), within ~ 12 pp of the upper bound the original paper claims. The absolute number depends sharply on which adversarial perturbation budget is used; ours follows the standard setting in our hyperparameter table.

CEGA (Wang et al., 2025) [27]. The original CEGA paper reports test accuracy / fidelity / F1 on *Coauthor-CS*, *Coauthor-Physics*, *Amazon-Computer*, and *Amazon-Photo* at a $20C$ -query budget (i.e., 20 times the number of classes). Our protocol uses budgets expressed as a fraction of the test set, and the closest match is the small-budget regime ($0.05\times$ to $0.10\times$). On *CoauthorCS*, $20C = 300$ queries which falls between our $0.05\times$ and $0.10\times$ on that dataset; the corresponding fidelity in our setup is in the upper 80 %–low 90 % range, agreeing with the original 93.40 % within a few points (Table 9). Crucially, the original paper’s relative ordering — CEGA > AGE > GRAIN > Random — is reproduced under our protocol on every overlapping dataset.

Realistic (Guan et al., 2024) [4]. The original paper varies query budgets across four levels (Attack-0 through Attack-3) on *Cora*, *Citeseer*, *Pubmed*, with default training-set sizes that are dataset-specific (e.g. *Cora*: 35 queries for Attack-0). The closest match in our protocol is the smallest-budget bucket ($0.05\times$). Our reproduction reaches *Cora* fidelity $62.0 \pm 4.5\%$ at $0.05\times$, compared with the original Attack-0 (*Cora*) fidelity of $72.14 \pm 3.56\%$; the gap of about 10 pp is in the same direction (small budget \Rightarrow moderate fidelity) and the qualitative ranking “Realistic > baseline GCN” transfers to our protocol.

DFEA_I / DFEA_II / DFEA_III (Zhuang et al., 2024) [42]. The original paper reports three data-free attack variants on *Cora*, *Pubmed*, *Amazon-Computers*, and *OGB-Arxiv*; on *Cora* the strongest variants reach 93–94% fidelity, with the “Random Graph” baseline at 73.7%. Our reproduction reaches 90–97% fidelity at $1.00\times$ on *Cora* across the three variants (Table 9), agreeing with the strongest original numbers within ~ 4 pp. The qualitative claim of the original paper — that data-free extraction is feasible at high fidelity on homophilic graphs and harder on heterophilic / high-class-count settings — is preserved: across our ten datasets the three variants reach 77–99% fidelity at $1.00\times$ on the seven homophilic graphs and 33–84% on *RomanEmpire*, *AmazonRatings*, and *OGBN-Arxiv* (Tables 13–38).

BackdoorWM (Xu et al., 2023) [31]. The original paper reports watermark accuracy on *Cora* and *CiteSeer* for GCN, GAT, and GraphSAGE backbones (Table 6 of the original paper): GCN/*Cora* 97.56%, GCN/*CiteSeer* 98.05%. Our protocol reports the same metric on the same datasets: 100% on every one of the seven homophilic datasets including *Cora* and *CiteSeer* (Table 34 in Appendix F.2). The ~ 2 pp difference is well within the variance the original paper reports across watermark-rate settings, and the claim that BackdoorWM is essentially perfect at watermark verification on the protected model is preserved.

SurviveWM (Wang et al., 2023) [26]. The original paper evaluates watermark survival on *MSRC-9* and *ENZYMES* (graph classification) using a GraphSAGE host model with 50/30/20 train/extract/test

splits, and reports the “average effectiveness \bar{E} ” of watermark retention after extraction. The metric is binary (1 if watermark retaining rate exceeds two reference thresholds, 0 otherwise) and is averaged over 100 repeated runs. Our protocol uses node-level datasets and a continuous verification rate, so a direct numerical comparison is not possible. We report the qualitative claim instead: SurviveWM produces a non-trivial verification rate on the protected model (median 54 % on Cora) but collapses to ~ 14 % on the extracted surrogate (Table 41c in Appendix F.8), which contradicts the original paper’s claim that the watermark “survives” extraction. The disagreement is the central finding of our RQ5 and motivates evaluation on the surrogate as the primary metric.

ImperceptibleWM (Zhang et al., 2024) [36]. The original paper reports the original-vs-watermarked model accuracy gap on *Cora* and *Pubmed* for GCN/GAT/GraphSAGE (Table 2 of the original): on GCN/Cora the watermarked model reaches 83.40% accuracy versus 83.74% for the unwatermarked one (a 0.34% utility drop). Our reproduction on the same dataset and backbone shows 79.4% undefended versus 71.94% watermarked (utility drop of ~ 7.5 %). Two design differences explain the larger drop: our protocol uses a fixed cross-dataset hyperparameter (Appendix E) rather than the per-dataset tuning the original paper performs, and our undefended baseline runs at the standard hidden dimension 16 used throughout the protocol rather than the 128 used by the original. The claim of “no significant impact on the primary task” holds with the original tuning but is loosened under our standardised protocol.

RandomWM (Zhao et al., 2021) [40]. The original paper reports watermark accuracy as a function of trigger-graph parameters on *Cora* and *Pubmed*, but does not provide a single headline number for direct comparison. The qualitative claim is that the watermark accuracy can be tuned above 90% with appropriate parameter choices. Our reproduction shows median verification rate 75% on Cora and 94–98% on *Computers* and *Photo* (Table 34), which is within the range the original paper reports for non-extreme parameter settings.

Integrity (Wu et al., 2024) [29]. The original paper does not report a single “verification accuracy” number on the protected model. Instead it reports a *verification-query-number improvement multiplier* relative to a random-node-selection baseline (e.g. on Cora transductive: BFA 4.0 \times , RandAttack 1.3 \times). The metric is fundamentally different from our verification-rate metric, so a direct numerical comparison is not possible. We instead validate the qualitative claim: Integrity reaches 100% verification on every homophilic dataset of our protocol (Table 34), consistent with the original paper’s claim that fingerprinting nodes selected by their algorithm are reliably distinguishable on the protected model.

PRADA (Juuti et al., 2019) [6]. The original paper evaluates query-pattern detection on image classifiers (MNIST, GTSRB, CIFAR-10) with DNN backbones; it does not include any graph dataset or GNN backbone. A direct numerical comparison is therefore impossible. Our adaptation transfers the distance-based detector to the graph setting and measures verification accuracy on the protected model and extracted surrogate; the qualitative behaviour (significant fidelity reduction at the cost of clean accuracy, see Tables 39–40) is consistent with the original paper’s vision-domain results.

AdaptMisinfo (Kariyappa and Qureshi, 2020) [7], GradRedir (Mazeika et al., 2022) [13]. Both original papers evaluate on image classification benchmarks (CIFAR-10, CIFAR-100, ImageNet) with CNN backbones (ResNet-18, ResNet-34) — no graph dataset or GNN model is used. The metric is also defined for the image domain (extraction-fidelity reduction at fixed query budgets). A direct numerical comparison is therefore impossible. Our adaptation re-implements the perturbation rule on graph-classification logits and reports the same protocol-level metrics as the other defenses; the qualitative claim that adaptive misinformation reduces extraction fidelity at a clean-accuracy cost transfers to the graph setting.

OP_low / OP_high / PR_2bit / PR_top1. These are protocol-level information-limiting wrappers that we adapt from generic stealing-defense literature [8, 12]. The cited papers do not report graph-specific numbers, and PR_2bit/PR_top1 are not standalone published methods but standard label-quantisation/top-1 wrappers; we therefore do not have a baseline number to compare against. The qualitative claim from the source literature — that label-quantising the response is an effective lightweight defense — transfers to our protocol: PR_2bit is the only inference-time wrapper in our benchmark which substantively reduces surrogate fidelity (Tables 56–57).

Table 9: Implementation validation for attacks where a numerical comparison is possible. “Original” is the closest-matching setting reported in the source paper. “Ours” is the corresponding number under the GraphIP-Bench protocol. “ Δ ” is Ours minus Original (positive means our reproduction reaches higher fidelity). All numbers are surrogate fidelity (%) unless otherwise noted; Cora at 1.00 \times in the both regime is used for our values unless the source-paper setting dictates a different budget bucket.

Method	Source paper / setting	Closest in ours	Original	Ours	Δ
MEA0	Wu 2022, Cora, full attack nodes	Cora, 1.00 \times , both	89.6	92.4	+2.8
MEA1	Wu 2022, Cora, full attack nodes	Cora, 1.00 \times , both	82.5	91.3	+8.8
MEA2	Wu 2022, Cora, full attack nodes	Cora, 1.00 \times , both	80.9	94.8	+13.9
MEA3	Wu 2022, Cora, shadow graph	Cora, 1.00 \times , both	79.0	92.7	+13.7
MEA4	Wu 2022, Cora, shadow graph	Cora, 1.00 \times , both	79.0	89.5	+10.5
MEA5	Wu 2022, Cora, shadow graph	Cora, 1.00 \times , both	80.7	92.5	+11.8
AdvMEA	DeFazio 2019, Cora, strong-adversary upper bound	Cora, 1.00 \times , both	\sim 80	68.2	-11.8
CEGA	Wang 2025, CoauthorCS, 20C queries	CoauthorCS, 0.10 \times , both	93.4	\sim 90.0	\sim -3.4
Realistic	Guan 2024, Cora, Attack-0 (35 queries)	Cora, 0.05 \times , both	72.1	62.0	-10.1
DFEA_I	Zhuang 2024, Cora, Random-Graph baseline	Cora, 1.00 \times , data_free	73.7	90.2	+16.5
DFEA_II	Zhuang 2024, Cora, Attack II-E (real graph) [†]	Cora, 1.00 \times , data_free	92.8	96.8	+4.0
DFEA_III	Zhuang 2024, Cora, Attack III-E (real graph) [†]	Cora, 1.00 \times , data_free	93.0	92.7	-0.3

[†]The original paper does not separate Attack-II/III into “Random-Graph” rows the way it does for Attack-I; we cite the real-graph Attack-E numbers as the closest published reference.

Table 10: RQ1 overview: regimes \times metrics (%). Means across datasets and the five budgets (0.05–1.00).

Attack	both			x_only			a_only			data_free		
	Acc	F1	Fidelity	Acc	F1	Fidelity	Acc	F1	Fidelity	Acc	F1	Fidelity
MEA0	78.07	64.77	83.75	78.97	64.72	84.72	79.35	65.97	85.24	20.23	5.72	19.58
MEA1	57.08	43.79	60.33	57.07	43.96	60.34	57.08	43.80	60.32	21.06	5.68	18.98
MEA2	65.88	52.97	74.74	66.14	52.92	74.87	66.26	53.19	74.94	66.17	53.06	75.00
MEA3	78.74	65.31	83.26	79.19	65.28	83.35	78.65	64.29	83.16	22.88	6.59	21.56
MEA4	73.71	54.80	78.54	71.38	53.02	76.36	72.08	53.58	76.71	16.69	5.01	16.23
MEA5	79.34	65.77	83.92	79.64	65.72	84.31	79.30	65.67	84.03	21.20	6.34	20.19
AdvMEA	62.16	53.63	63.77	62.92	53.97	64.21	62.08	53.35	63.49	62.94	54.37	64.37
CEGA	75.01	64.61	83.08	74.94	64.64	82.68	75.58	64.71	83.80	74.02	63.83	82.08
Realistic	59.20	47.72	76.70	59.76	47.30	77.40	59.03	46.86	76.59	58.71	47.25	77.16
DFEA_I	77.22	66.28	87.69	77.21	66.27	87.69	77.21	66.26	87.68	77.20	66.25	87.70
DFEA_II	65.53	57.18	72.55	65.53	57.19	72.56	65.39	57.23	72.86	65.52	57.18	72.56
DFEA_III	77.84	67.50	89.77	77.80	67.34	89.65	77.82	67.40	89.68	77.80	67.36	89.69

Validation summary table. Table 9 compresses the comparable attack reproductions into one view; defenses are summarised in the paragraphs above because their headline metrics are method-specific.

The takeaway is twofold. First, on attacks that share a clearly comparable setting with the source paper, our reproduction agrees with the original numbers within a band of $\sim \pm 14$ pp, with the direction of agreement consistent. Second, where the original paper uses a different protocol (image domain for PRADA / AdaptMisinfo / GradRedir, graph-classification metrics for SurviveWM, query-improvement multipliers for Integrity), a direct number-to-number comparison is not possible; we explicitly note these mismatches above and validate the qualitative claim instead.

F Supplementary Experimental Results and Discussion

F.1 Attack effectiveness results

This appendix reports the full results for attacks across the seven homophilic datasets of the core protocol; the three additional graphs (RomanEmpire, AmazonRatings, OGBN-Arxiv) are reported in Appendix F.4 (Tables 36–38). We first present compact overview tables which summarize, for each metric (Accuracy, F1, and Fidelity), the mean performance of twelve attacks across four query regimes (with an additional Overall column). Each number is averaged over the seven homophilic datasets and the five budget levels defined in the main text. These tables allow the reader to identify, at a glance, which attack performs best under each regime. We then provide the complete per-dataset matrices. For each dataset and each metric, we show a 2×2 panel that contains four sub-tables (one per regime). Each sub-table is a 12×5 matrix whose rows are the attacks and whose columns are the five query budgets. Bold font marks the best score in each budget column. All splits, budgets, and aggregation rules match the protocol in the main paper.

Table 11: RQ1 detailed for dataset=Cora, metric=Acc (%). Rows are attacks; columns are budgets. Mean \pm std across seeds; best per column is bold.

(a) Regime=both						(b) Regime= x_only					
Attack	0.05	0.10	0.25	0.50	1.00	Attack	0.05	0.10	0.25	0.50	1.00
MEAO	67.4 \pm 4.4	75.4 \pm 1.6	79.7 \pm 0.7	80.8 \pm 0.2	81.7 \pm 0.3	MEAO	68.7 \pm 4.2	75.1 \pm 0.7	80.1 \pm 0.2	80.4 \pm 1.3	81.2 \pm 0.5
MEA1	52.7 \pm 0.5	63.5 \pm 2.0	81.5 \pm 0.7	80.8 \pm 0.1	82.3 \pm 0.2	MEA1	52.7 \pm 0.5	63.5 \pm 2.0	81.5 \pm 0.7	80.8 \pm 0.1	82.3 \pm 0.2
MEA2	55.1 \pm 4.2	65.7 \pm 0.8	75.6 \pm 1.2	78.6 \pm 0.9	80.1 \pm 0.8	MEA2	55.7 \pm 1.6	67.7 \pm 0.3	76.3 \pm 0.4	79.2 \pm 0.8	80.1 \pm 0.8
MEA3	67.1 \pm 3.4	74.3 \pm 1.9	79.6 \pm 1.5	81.2 \pm 0.6	81.1 \pm 0.3	MEA3	64.7 \pm 1.7	74.0 \pm 0.4	79.7 \pm 0.4	81.4 \pm 0.4	81.1 \pm 0.1
MEA4	45.4 \pm 6.1	65.7 \pm 1.9	77.3 \pm 0.9	78.5 \pm 0.2	80.5 \pm 0.0	MEA4	42.9 \pm 8.4	63.7 \pm 3.7	76.8 \pm 0.4	78.5 \pm 0.2	80.5 \pm 0.0
MEA5	72.1 \pm 2.9	75.4 \pm 0.8	79.9 \pm 0.7	81.4 \pm 0.6	81.2 \pm 0.3	MEA5	69.9 \pm 3.4	77.0 \pm 1.7	80.5 \pm 0.3	81.5 \pm 0.5	81.2 \pm 0.1
AdvMEA	64.8 \pm 4.2	66.8 \pm 2.2	65.1 \pm 1.4	67.7 \pm 4.7	66.7 \pm 2.3	AdvMEA	65.5 \pm 3.3	68.8 \pm 2.5	65.4 \pm 2.0	63.6 \pm 0.8	65.0 \pm 3.0
CEGA	71.0 \pm 5.2	76.5 \pm 0.9	79.7 \pm 0.2	79.3 \pm 0.6	79.3 \pm 0.3	CEGA	74.1 \pm 0.5	77.6 \pm 0.4	77.7 \pm 1.2	78.7 \pm 1.1	79.4 \pm 0.3
Realistic	55.4 \pm 8.2	67.1 \pm 2.8	71.0 \pm 4.4	74.8 \pm 1.8	75.9 \pm 2.4	Realistic	55.7 \pm 8.3	64.2 \pm 5.0	71.0 \pm 4.3	74.8 \pm 3.4	75.5 \pm 2.7
DFEA_I	76.3 \pm 2.3	78.6 \pm 0.4	80.2 \pm 1.0	80.9 \pm 0.2	80.7 \pm 0.6	DFEA_I	76.3 \pm 2.3	78.6 \pm 0.4	80.2 \pm 1.0	80.9 \pm 0.2	80.7 \pm 0.6
DFEA_II	77.1 \pm 1.1	78.9 \pm 0.7	79.9 \pm 1.0	79.5 \pm 0.3	80.6 \pm 0.1	DFEA_II	77.1 \pm 1.1	78.9 \pm 0.7	79.9 \pm 1.0	79.5 \pm 0.3	80.6 \pm 0.1
DFEA_III	77.0 \pm 0.9	79.4 \pm 1.5	80.4 \pm 1.2	80.7 \pm 0.8	81.6 \pm 0.5	DFEA_III	77.0 \pm 0.9	79.4 \pm 1.5	80.4 \pm 1.2	80.7 \pm 0.8	81.6 \pm 0.5

(c) Regime= a_only						(d) Regime= $data_free$					
Attack	0.05	0.10	0.25	0.50	1.00	Attack	0.05	0.10	0.25	0.50	1.00
MEAO	69.4 \pm 0.3	75.6 \pm 0.3	78.7 \pm 1.6	80.1 \pm 1.3	80.8 \pm 0.6	MEAO	10.9 \pm 2.5	14.6 \pm 0.2	19.3 \pm 8.9	20.2 \pm 8.2	19.0 \pm 9.3
MEA1	52.7 \pm 0.5	63.5 \pm 2.0	81.5 \pm 0.7	80.8 \pm 0.1	82.3 \pm 0.2	MEA1	14.4 \pm 0.0	14.4 \pm 0.0	14.4 \pm 0.0	14.4 \pm 0.0	14.4 \pm 0.0
MEA2	57.8 \pm 1.2	67.7 \pm 1.5	75.7 \pm 0.4	78.6 \pm 1.8	80.2 \pm 0.8	MEA2	60.5 \pm 1.8	69.4 \pm 1.8	76.1 \pm 1.2	78.2 \pm 0.6	80.2 \pm 0.8
MEA3	63.0 \pm 1.3	75.2 \pm 1.8	79.7 \pm 0.8	81.0 \pm 0.6	81.3 \pm 0.2	MEA3	17.6 \pm 10.6	12.3 \pm 2.4	17.1 \pm 10.8	13.5 \pm 0.7	26.2 \pm 8.0
MEA4	45.9 \pm 5.8	63.4 \pm 1.4	77.4 \pm 0.6	78.5 \pm 0.2	80.5 \pm 0.0	MEA4	17.1 \pm 10.8	19.9 \pm 8.5	18.5 \pm 9.7	10.9 \pm 2.5	18.0 \pm 10.0
MEA5	65.6 \pm 6.9	76.5 \pm 1.5	79.6 \pm 1.1	81.5 \pm 0.5	81.3 \pm 0.1	MEA5	24.6 \pm 13.0	11.9 \pm 2.7	21.1 \pm 7.7	20.4 \pm 8.1	18.7 \pm 9.5
AdvMEA	65.4 \pm 2.7	64.0 \pm 2.3	65.8 \pm 1.7	68.1 \pm 1.9	60.5 \pm 5.7	AdvMEA	68.6 \pm 2.4	68.5 \pm 1.5	65.1 \pm 6.3	65.8 \pm 2.9	67.9 \pm 3.7
CEGA	69.6 \pm 3.6	78.0 \pm 0.4	78.0 \pm 0.8	79.6 \pm 0.5	79.2 \pm 0.6	CEGA	71.0 \pm 1.8	77.0 \pm 0.7	78.8 \pm 1.9	79.2 \pm 0.9	79.2 \pm 0.1
Realistic	51.5 \pm 4.3	64.5 \pm 6.0	72.0 \pm 2.3	75.3 \pm 2.5	76.3 \pm 2.7	Realistic	67.9 \pm 2.3	70.8 \pm 1.6	69.0 \pm 3.6	66.5 \pm 2.6	69.1 \pm 1.6
DFEA_I	76.3 \pm 2.3	78.6 \pm 0.4	80.2 \pm 1.0	80.9 \pm 0.2	80.7 \pm 0.6	DFEA_I	76.3 \pm 2.3	78.6 \pm 0.4	80.2 \pm 1.0	80.9 \pm 0.2	80.7 \pm 0.6
DFEA_II	77.1 \pm 1.1	78.9 \pm 0.7	79.9 \pm 1.0	79.5 \pm 0.3	80.6 \pm 0.1	DFEA_II	77.1 \pm 1.1	78.9 \pm 0.7	79.9 \pm 1.0	79.5 \pm 0.3	80.6 \pm 0.1
DFEA_III	77.1 \pm 0.9	79.4 \pm 1.5	80.4 \pm 1.2	80.7 \pm 0.8	81.6 \pm 0.5	DFEA_III	77.0 \pm 0.9	79.4 \pm 1.5	80.4 \pm 1.2	80.7 \pm 0.8	81.6 \pm 0.5

The overview table exposes three deep findings that the per-dataset detail tables (Tables 11–31) hide because of cell-level noise. *First, the ranking of attacks by mean fidelity is essentially identical across the three real-input regimes (both, x_only , a_only).* For example, the top-five strongest attacks by fidelity in the both column are DFEA_III, DFEA_I, MEA5, MEAO, MEA3 (in order 89.77, 87.69, 83.92, 83.75, 83.26); the same five attacks occupy the top-five positions in the x_only and a_only columns. The granularity of removing only one input modality at a time is therefore not sufficient to differentiate strong attacks — a conclusion that motivates our use of the more aggressive $data_free$ regime as the discriminative axis. *Second, the data-free family (DFEA_I/II/III and MEA2) together with AdvMEA, CEGA, and Realistic are essentially regime-invariant:* their $data_free$ fidelity is within ~ 1 pp of their both fidelity. This is a structural property of the attacks: CEGA retrains a centrality-based query selector even on synthetic graphs, AdvMEA learns adversarial features from scratch, Realistic reconstructs the structure with an auxiliary edge model, and the DFEA variants synthesise their own queries by design. They are the only candidates for an attacker who genuinely has no access to the real graph. *Third, the Acc and F1 columns track each other except on heterophilic-style class distributions.* On Cora-like datasets the F1 column tracks Acc within ~ 5 pp; the largest Acc/F1 gap appears for MEAO (Acc 78.07, F1 64.77), reflecting a slight class-imbalance bias in the surrogate. Future attack design should therefore report F1 alongside accuracy, especially when targeting graphs with skewed class distributions such as OGBN-Arxiv.

F.2 Defense performance results

This subsection contains the per-dataset defense performance and the boxplot view that the main text references. Figure 5 aggregates utility drop and ownership verification across all ten datasets and three seeds (30 points per defense), and the per-dataset numbers follow. Table 32 reports task utility measured by macro F1 (%); Table 33 reports behavioural alignment with the original target measured by fidelity (%) on the same test inputs; Table 34 summarises ownership verification on a standardised verification set. Together these views separate downstream utility, behavioural consistency, and ownership verification, so that the trade-offs across defenses are explicit on every dataset.

Watermark profile across six axes. Tables 32–34 report the three primary metrics separately. To make the trade-offs across the five watermarking and integrity defenses visible at a glance, Figure 6 reports the same numbers as a radar chart together with two efficiency axes (training time and peak memory, both inverted to a higher-is-better score on a log scale to match the other axes). Three patterns become explicit which the per-metric tables only show implicitly. *First, no defense dominates*

Table 12: RQ1 detailed for dataset=Cora, metric=F1 (%). Rows are attacks; columns are budgets. Mean \pm std across seeds; best per column is bold.

(a) Regime=both						(b) Regime=x_only					
Attack	0.05	0.10	0.25	0.50	1.00	Attack	0.05	0.10	0.25	0.50	1.00
MEA0	61.0 \pm 6.6	73.9 \pm 1.5	77.9 \pm 1.2	79.6 \pm 0.4	81.0 \pm 0.1	MEA0	63.2 \pm 4.5	68.7 \pm 0.4	78.8 \pm 0.2	79.0 \pm 1.8	80.4 \pm 0.6
MEA1	50.5 \pm 0.5	58.2 \pm 4.1	80.3 \pm 0.7	80.2 \pm 0.2	81.8 \pm 0.0	MEA1	50.5 \pm 0.5	58.2 \pm 4.1	80.3 \pm 0.7	80.2 \pm 0.2	81.8 \pm 0.0
MEA2	52.2 \pm 4.3	63.2 \pm 1.7	74.7 \pm 1.0	78.0 \pm 0.8	79.2 \pm 0.8	MEA2	50.5 \pm 1.8	66.1 \pm 0.7	75.1 \pm 0.5	78.5 \pm 0.7	79.2 \pm 0.8
MEA3	60.6 \pm 5.9	70.4 \pm 2.8	78.4 \pm 1.6	79.5 \pm 0.9	80.2 \pm 0.2	MEA3	58.0 \pm 2.6	70.0 \pm 1.8	78.5 \pm 0.5	80.5 \pm 0.3	80.2 \pm 0.1
MEA4	44.3 \pm 6.5	65.8 \pm 1.2	76.1 \pm 0.6	77.3 \pm 0.0	79.2 \pm 0.3	MEA4	27.9 \pm 6.9	62.2 \pm 4.5	75.8 \pm 0.5	77.3 \pm 0.0	79.2 \pm 0.3
MEA5	67.9 \pm 4.1	70.3 \pm 3.8	78.8 \pm 0.8	80.3 \pm 0.6	80.2 \pm 0.4	MEA5	66.5 \pm 1.3	74.2 \pm 2.4	79.2 \pm 0.5	80.3 \pm 0.4	80.3 \pm 0.3
AdvMEA	65.2 \pm 2.9	67.3 \pm 2.3	66.6 \pm 0.7	67.7 \pm 3.9	67.3 \pm 2.0	AdvMEA	66.3 \pm 2.8	67.0 \pm 3.0	65.3 \pm 3.1	64.0 \pm 0.5	66.4 \pm 2.2
CEGA	69.9 \pm 4.4	75.6 \pm 0.9	79.1 \pm 0.1	78.6 \pm 0.3	78.4 \pm 0.2	CEGA	73.6 \pm 1.1	77.2 \pm 0.4	77.4 \pm 0.7	78.1 \pm 0.7	78.6 \pm 0.2
Realistic	53.1 \pm 6.4	61.1 \pm 4.6	69.3 \pm 3.8	73.9 \pm 1.2	75.0 \pm 2.0	Realistic	50.9 \pm 6.5	58.8 \pm 4.9	68.2 \pm 6.1	74.0 \pm 3.1	75.2 \pm 2.6
DFEA_I	72.7 \pm 5.1	75.5 \pm 1.0	78.9 \pm 1.1	79.6 \pm 0.2	79.3 \pm 1.1	DFEA_I	72.5 \pm 5.3	75.5 \pm 1.0	78.9 \pm 1.1	79.6 \pm 0.2	79.3 \pm 1.1
DFEA_II	75.3 \pm 0.8	77.5 \pm 0.7	78.6 \pm 1.2	78.5 \pm 0.3	79.7 \pm 0.2	DFEA_II	75.3 \pm 0.7	77.5 \pm 0.7	78.6 \pm 1.2	78.5 \pm 0.3	79.7 \pm 0.2
DFEA_III	74.4 \pm 2.4	77.6 \pm 1.6	79.3 \pm 1.1	79.7 \pm 0.6	80.7 \pm 0.5	DFEA_III	74.4 \pm 2.4	77.7 \pm 1.6	79.3 \pm 1.1	79.7 \pm 0.6	80.7 \pm 0.5

(c) Regime=a_only						(d) Regime=data_free					
Attack	0.05	0.10	0.25	0.50	1.00	Attack	0.05	0.10	0.25	0.50	1.00
MEA0	64.3 \pm 0.6	72.9 \pm 0.8	77.5 \pm 1.9	78.7 \pm 1.8	80.0 \pm 0.7	MEA0	2.8 \pm 0.6	3.6 \pm 0.1	4.5 \pm 1.7	4.7 \pm 1.6	4.4 \pm 1.8
MEA1	50.4 \pm 0.5	58.2 \pm 4.1	80.3 \pm 0.7	80.2 \pm 0.2	81.8 \pm 0.0	MEA1	3.6 \pm 0.0	3.6 \pm 0.0	3.6 \pm 0.0	3.6 \pm 0.0	3.6 \pm 0.0
MEA2	52.9 \pm 1.2	65.5 \pm 1.8	74.5 \pm 0.7	77.6 \pm 1.7	79.2 \pm 0.8	MEA2	55.4 \pm 0.5	69.0 \pm 0.4	74.8 \pm 1.1	77.5 \pm 0.5	79.2 \pm 0.8
MEA3	55.7 \pm 3.0	70.3 \pm 3.0	78.3 \pm 1.4	80.0 \pm 0.3	80.4 \pm 0.2	MEA3	4.1 \pm 2.1	3.1 \pm 0.6	4.0 \pm 2.2	3.4 \pm 0.1	5.8 \pm 1.5
MEA4	34.6 \pm 8.6	60.4 \pm 4.2	76.4 \pm 0.2	77.3 \pm 0.0	79.2 \pm 0.3	MEA4	4.0 \pm 2.2	4.6 \pm 1.6	4.3 \pm 1.9	2.8 \pm 0.6	4.2 \pm 2.0
MEA5	58.8 \pm 11.2	73.7 \pm 2.4	77.7 \pm 1.0	80.7 \pm 0.4	80.2 \pm 0.2	MEA5	7.4 \pm 4.8	3.6 \pm 0.4	6.1 \pm 1.7	4.7 \pm 1.5	4.5 \pm 1.7
AdvMEA	67.0 \pm 2.0	64.7 \pm 3.1	65.8 \pm 1.1	67.0 \pm 1.4	62.6 \pm 3.9	AdvMEA	68.4 \pm 0.6	68.4 \pm 1.1	64.7 \pm 6.1	66.3 \pm 2.2	68.0 \pm 2.7
CEGA	68.7 \pm 1.4	77.5 \pm 0.6	77.4 \pm 0.9	79.0 \pm 0.8	78.4 \pm 0.6	CEGA	69.5 \pm 1.5	76.3 \pm 0.5	78.4 \pm 1.6	78.5 \pm 0.9	78.7 \pm 0.2
Realistic	46.3 \pm 5.0	62.2 \pm 8.0	70.8 \pm 1.2	74.6 \pm 2.2	76.0 \pm 2.0	Realistic	63.1 \pm 3.3	67.8 \pm 3.2	67.1 \pm 3.7	63.0 \pm 4.0	67.2 \pm 1.8
DFEA_I	72.7 \pm 5.1	75.5 \pm 1.0	78.9 \pm 1.1	79.6 \pm 0.2	79.3 \pm 1.1	DFEA_I	72.5 \pm 5.3	75.5 \pm 1.0	78.9 \pm 1.1	79.6 \pm 0.2	79.3 \pm 1.1
DFEA_II	75.3 \pm 0.8	77.5 \pm 0.7	78.6 \pm 1.2	78.5 \pm 0.3	79.7 \pm 0.2	DFEA_II	75.3 \pm 0.8	77.5 \pm 0.7	78.6 \pm 1.2	78.5 \pm 0.3	79.7 \pm 0.2
DFEA_III	74.5 \pm 2.3	77.7 \pm 1.6	79.3 \pm 1.1	79.7 \pm 0.6	80.7 \pm 0.5	DFEA_III	74.4 \pm 2.4	77.6 \pm 1.6	79.3 \pm 1.1	79.7 \pm 0.6	80.6 \pm 0.5

Table 13: RQ1 detailed for dataset=Cora, metric=Fidelity (%). Rows are attacks; columns are budgets. Mean \pm std across seeds; best per column is bold.

(a) Regime=both						(b) Regime=x_only					
Attack	0.05	0.10	0.25	0.50	1.00	Attack	0.05	0.10	0.25	0.50	1.00
MEA0	69.3 \pm 3.1	82.6 \pm 1.6	87.5 \pm 0.9	89.7 \pm 0.7	92.4 \pm 0.6	MEA0	72.2 \pm 3.9	79.5 \pm 0.9	88.2 \pm 1.2	90.9 \pm 1.2	92.1 \pm 0.8
MEA1	57.3 \pm 0.2	70.6 \pm 2.0	89.9 \pm 0.9	90.4 \pm 0.6	91.3 \pm 0.4	MEA1	57.3 \pm 0.2	70.6 \pm 2.0	89.9 \pm 0.9	90.4 \pm 0.5	91.3 \pm 0.4
MEA2	57.4 \pm 3.2	68.8 \pm 0.9	82.8 \pm 1.2	89.3 \pm 0.3	94.8 \pm 0.2	MEA2	55.5 \pm 0.9	72.2 \pm 1.6	83.9 \pm 0.8	89.6 \pm 0.7	94.8 \pm 0.2
MEA3	71.2 \pm 3.6	79.3 \pm 2.7	88.0 \pm 0.8	90.1 \pm 1.4	92.7 \pm 0.9	MEA3	69.1 \pm 0.8	77.7 \pm 0.5	88.0 \pm 0.9	90.9 \pm 1.1	92.5 \pm 1.3
MEA4	49.2 \pm 6.2	71.9 \pm 1.7	85.0 \pm 1.3	87.6 \pm 0.6	89.5 \pm 0.2	MEA4	45.3 \pm 8.6	69.2 \pm 3.7	84.6 \pm 0.7	87.6 \pm 0.6	89.6 \pm 0.2
MEA5	75.8 \pm 4.8	82.1 \pm 4.5	88.3 \pm 0.6	92.8 \pm 1.1	92.5 \pm 0.7	MEA5	73.9 \pm 1.8	83.2 \pm 0.3	88.8 \pm 0.8	91.9 \pm 0.5	92.3 \pm 1.1
AdvMEA	67.6 \pm 4.0	68.8 \pm 2.8	67.4 \pm 1.6	69.0 \pm 4.9	68.2 \pm 4.0	AdvMEA	66.7 \pm 2.0	71.2 \pm 3.0	66.5 \pm 1.5	67.1 \pm 1.5	67.4 \pm 3.1
CEGA	78.4 \pm 4.4	86.5 \pm 1.0	91.5 \pm 0.4	92.5 \pm 0.4	93.7 \pm 0.5	CEGA	82.5 \pm 1.7	86.8 \pm 0.8	90.8 \pm 1.1	92.8 \pm 0.8	93.7 \pm 0.1
Realistic	62.0 \pm 4.5	68.1 \pm 1.8	78.6 \pm 0.7	83.7 \pm 0.6	88.5 \pm 1.7	Realistic	62.9 \pm 4.6	69.8 \pm 1.7	79.4 \pm 2.4	84.1 \pm 0.9	87.9 \pm 0.2
DFEA_I	82.2 \pm 3.5	85.7 \pm 1.0	89.2 \pm 1.8	90.2 \pm 0.4	90.2 \pm 0.5	DFEA_I	82.2 \pm 3.5	85.7 \pm 1.0	89.2 \pm 1.8	90.2 \pm 0.4	90.2 \pm 0.5
DFEA_II	79.9 \pm 0.7	84.1 \pm 0.8	88.5 \pm 0.3	93.1 \pm 0.4	96.8 \pm 0.5	DFEA_II	79.9 \pm 0.7	84.1 \pm 0.8	88.5 \pm 0.3	93.1 \pm 0.4	96.8 \pm 0.5
DFEA_III	81.4 \pm 2.1	86.1 \pm 2.4	88.4 \pm 1.9	91.5 \pm 0.2	92.7 \pm 0.3	DFEA_III	81.3 \pm 2.2	86.1 \pm 2.4	88.4 \pm 1.9	91.5 \pm 0.2	92.7 \pm 0.3

(c) Regime=a_only						(d) Regime=data_free					
Attack	0.05	0.10	0.25	0.50	1.00	Attack	0.05	0.10	0.25	0.50	1.00
MEA0	74.1 \pm 0.8	81.9 \pm 1.4	87.2 \pm 1.1	89.5 \pm 1.3	92.4 \pm 1.2	MEA0	12.3 \pm 2.0	15.9 \pm 0.8	17.3 \pm 6.2	19.0 \pm 5.0	18.0 \pm 6.3
MEA1	57.2 \pm 0.2	70.6 \pm 2.0	89.9 \pm 0.9	90.4 \pm 0.6	91.3 \pm 0.4	MEA1	15.3 \pm 0.2	15.3 \pm 0.2	15.3 \pm 0.2	15.3 \pm 0.1	15.3 \pm 0.2
MEA2	56.8 \pm 2.1	69.9 \pm 2.2	82.9 \pm 0.3	90.0 \pm 1.0	94.8 \pm 0.2	MEA2	58.9 \pm 1.1	73.2 \pm 0.3	83.8 \pm 0.7	89.7 \pm 0.3	94.8 \pm 0.2
MEA3	64.3 \pm 0.6	80.9 \pm 1.2	88.1 \pm 0.3	92.0 \pm 0.5	92.7 \pm 1.1	MEA3	16.2 \pm 7.9	13.3 \pm 2.5	15.3 \pm 8.0	13.8 \pm 1.0	23.1 \pm 4.3
MEA4	48.3 \pm 4.1	68.2 \pm 1.8	85.6 \pm 0.5	87.6 \pm 0.6	89.5 \pm 0.2	MEA4	15.5 \pm 8.0	18.7 \pm 5.5	17.3 \pm 6.6	12.3 \pm 2.0	16.8 \pm 6.7
MEA5	68.8 \pm 8.4	82.1 \pm 1.6	88.0 \pm 0.9	92.2 \pm 0.7	92.7 \pm 1.4	MEA5	21.9 \pm 10.9	12.5 \pm 2.6	20.2 \pm 4.3	19.5 \pm 4.8	17.2 \pm 6.6
AdvMEA	67.5 \pm 3.0	66.1 \pm 2.3	67.4 \pm 3.6	68.9 \pm 2.5	62.7 \pm 4.3	AdvMEA	69.4 \pm 2.7	70.1 \pm 0.9	67.4 \pm 5.8	67.4 \pm 2.1	70.5 \pm 3.5
CEGA	78.2 \pm 3.8	88.4 \pm 0.9	91.0 \pm 0.7	92.3 \pm 0.3	93.7 \pm 0.3	CEGA	79.8 \pm 2.7	88.0 \pm 0.4	91.0 \pm 1.5	92.5 \pm 0.0	93.5 \pm 0.6
Realistic	56.5 \pm 4.1	69.3 \pm 3.9	79.8 \pm 0.3	84.3 \pm 1.9	89.1 \pm 0.9	Realistic	73.0 \pm 3.5	72.9 \pm 1.6	74.3 \pm 1.4	72.9 \pm 1.8	73.1 \pm 5.0
DFEA_I	82.2 \pm 3.5	85.7 \pm 1.0	89.2 \pm 1.8	90.2 \pm 0.4	90.2 \pm 0.5	DFEA_I	82.2 \pm 3.5	85.7 \pm 1.0	89.2 \pm 1.8	90.2 \pm 0.4	90.2 \pm 0.5
DFEA_II	79.9 \pm 0.7	84.1 \pm 0.8	88.5 \pm 0.3	93.1 \pm 0.4	96.8 \pm 0.5	DFEA_II	79.9 \pm 0.7	84.1 \pm 0.8	88.5 \pm 0.3	93.1 \pm 0.4	96.8 \pm 0.5
DFEA_III	81.3 \pm 2.2	86.1 \pm 2.4	88.4 \pm 1.9	91.5 \pm 0.2	92.7 \pm 0.3	DFEA_III	81.4 \pm 2.1	86.1 \pm 2.4	88.4 \pm 1.9	91.5 \pm 0.2	92.7 \pm 0.3

on every axis. BackdoorWM encloses the largest area on the verification, fidelity, and utility axes but sits in the middle of the speed and memory axes. Integrity is the only defense which is simultaneously fast and light while keeping competitive verification. ImperceptibleWM achieves perfect verification at the cost of being the slowest and heaviest defense, which gives it a visibly indented profile on the speed and memory axes. *Second*, SurviveWM keeps utility almost unchanged but loses on the verification axis, which is consistent with the bimodal verification numbers in Table 34; this is a clear stability–verification trade-off rather than a generic weakness. *Third*, the gap between RandomWM and the other watermarks is structural rather than a per-dataset artefact:

Table 14: RQ1 detailed for dataset=CiteSeer, metric=Acc (%). Rows are attacks; columns are budgets. Mean \pm std across seeds; best per column is bold.

(a) Regime=both						(b) Regime=x_only					
Attack	0.05	0.10	0.25	0.50	1.00	Attack	0.05	0.10	0.25	0.50	1.00
MEA0	55.4 \pm 6.9	62.4 \pm 2.4	69.0 \pm 0.7	70.1 \pm 0.9	70.1 \pm 0.6	MEA0	54.1 \pm 3.3	63.2 \pm 2.4	69.8 \pm 1.2	70.0 \pm 0.9	69.6 \pm 0.2
MEA1	41.6 \pm 1.4	41.8 \pm 2.6	54.0 \pm 7.9	66.3 \pm 1.4	69.0 \pm 0.6	MEA1	41.6 \pm 1.4	41.8 \pm 2.6	54.0 \pm 7.9	66.3 \pm 1.4	68.9 \pm 0.6
MEA2	36.7 \pm 2.8	47.0 \pm 3.0	59.6 \pm 1.2	66.3 \pm 0.7	69.3 \pm 0.3	MEA2	47.2 \pm 2.2	48.4 \pm 2.6	59.2 \pm 1.2	65.9 \pm 0.8	69.2 \pm 0.3
MEA3	50.7 \pm 2.8	59.7 \pm 3.3	69.4 \pm 1.0	69.6 \pm 0.0	70.2 \pm 0.4	MEA3	57.9 \pm 4.1	64.6 \pm 1.8	68.7 \pm 1.0	69.9 \pm 0.8	69.9 \pm 0.7
MEA4	44.9 \pm 1.0	57.9 \pm 3.7	67.1 \pm 0.2	69.9 \pm 0.4	70.6 \pm 0.4	MEA4	39.9 \pm 4.7	59.0 \pm 2.3	66.6 \pm 0.5	69.9 \pm 0.4	70.6 \pm 0.4
MEA5	49.0 \pm 2.1	62.8 \pm 1.8	69.5 \pm 1.1	69.8 \pm 0.2	70.4 \pm 0.8	MEA5	55.3 \pm 1.9	65.9 \pm 0.7	70.3 \pm 0.6	70.3 \pm 0.7	70.0 \pm 0.5
AdvMEA	51.8 \pm 8.1	46.3 \pm 4.2	53.2 \pm 0.7	52.3 \pm 1.7	51.3 \pm 5.1	AdvMEA	48.9 \pm 0.9	51.4 \pm 2.4	53.9 \pm 4.3	48.2 \pm 6.8	45.9 \pm 2.2
CEGA	59.9 \pm 3.2	64.6 \pm 2.1	66.5 \pm 1.1	67.0 \pm 1.5	67.2 \pm 0.3	CEGA	61.3 \pm 1.9	65.2 \pm 1.1	66.7 \pm 0.6	67.3 \pm 0.6	67.8 \pm 0.5
Realistic	47.2 \pm 2.0	57.7 \pm 4.2	64.3 \pm 2.3	64.5 \pm 0.4	65.2 \pm 1.1	Realistic	48.1 \pm 3.5	53.2 \pm 4.3	61.5 \pm 1.9	62.7 \pm 2.0	65.4 \pm 1.4
DFEA_I	69.1 \pm 1.1	71.0 \pm 1.1	70.8 \pm 1.2	71.2 \pm 0.3	71.0 \pm 0.6	DFEA_I	69.1 \pm 1.1	71.0 \pm 1.1	70.8 \pm 1.2	71.2 \pm 0.3	71.0 \pm 0.6
DFEA_II	70.3 \pm 1.4	70.0 \pm 0.4	69.5 \pm 0.6	69.7 \pm 0.8	70.3 \pm 0.5	DFEA_II	70.3 \pm 1.4	70.0 \pm 0.4	69.5 \pm 0.6	69.7 \pm 0.8	70.3 \pm 0.5
DFEA_III	68.2 \pm 1.7	70.2 \pm 0.3	70.2 \pm 1.1	70.9 \pm 0.4	71.4 \pm 0.6	DFEA_III	68.3 \pm 1.7	70.2 \pm 0.3	70.2 \pm 1.1	70.9 \pm 0.4	71.4 \pm 0.6

(c) Regime=a_only						(d) Regime=data_free					
Attack	0.05	0.10	0.25	0.50	1.00	Attack	0.05	0.10	0.25	0.50	1.00
MEA0	52.5 \pm 3.1	64.5 \pm 1.5	70.2 \pm 0.9	69.3 \pm 0.8	70.1 \pm 1.1	MEA0	12.8 \pm 7.3	17.4 \pm 1.0	14.7 \pm 4.9	14.7 \pm 4.9	17.4 \pm 1.0
MEA1	41.6 \pm 1.4	41.8 \pm 2.6	54.0 \pm 7.9	66.3 \pm 1.4	69.0 \pm 0.6	MEA1	21.4 \pm 2.4	21.4 \pm 2.4	21.4 \pm 2.4	21.4 \pm 2.4	21.4 \pm 2.4
MEA2	35.9 \pm 1.2	49.6 \pm 1.5	59.0 \pm 0.9	65.9 \pm 1.4	69.2 \pm 0.3	MEA2	37.9 \pm 1.1	50.8 \pm 1.7	60.8 \pm 2.0	64.9 \pm 1.4	69.3 \pm 0.3
MEA3	48.1 \pm 5.0	62.3 \pm 3.3	68.4 \pm 1.5	70.1 \pm 0.5	70.0 \pm 0.5	MEA3	18.1 \pm 0.0	19.5 \pm 2.6	16.7 \pm 5.4	17.7 \pm 0.6	16.6 \pm 0.4
MEA4	43.9 \pm 1.3	56.8 \pm 1.3	66.2 \pm 0.6	69.9 \pm 0.4	70.6 \pm 0.4	MEA4	21.5 \pm 2.3	14.6 \pm 4.9	14.3 \pm 4.7	16.7 \pm 1.0	17.5 \pm 1.0
MEA5	52.7 \pm 3.1	63.5 \pm 1.9	69.9 \pm 0.6	69.7 \pm 0.4	70.8 \pm 1.1	MEA5	18.8 \pm 3.1	17.3 \pm 0.6	19.8 \pm 2.3	17.3 \pm 0.6	14.0 \pm 4.5
AdvMEA	47.5 \pm 4.0	51.2 \pm 4.3	54.0 \pm 4.7	49.9 \pm 5.4	46.5 \pm 0.3	AdvMEA	48.9 \pm 2.9	47.6 \pm 1.7	53.1 \pm 8.2	50.1 \pm 2.5	50.1 \pm 5.8
CEGA	58.4 \pm 3.2	64.6 \pm 0.4	66.8 \pm 0.8	68.0 \pm 1.1	67.4 \pm 0.7	CEGA	60.9 \pm 2.4	64.4 \pm 0.8	67.8 \pm 0.8	67.6 \pm 0.7	67.5 \pm 0.6
Realistic	40.7 \pm 7.3	55.1 \pm 4.9	62.8 \pm 0.2	63.2 \pm 2.2	64.1 \pm 1.2	Realistic	59.0 \pm 2.0	58.2 \pm 2.6	59.0 \pm 1.5	57.0 \pm 1.5	60.1 \pm 2.5
DFEA_I	69.1 \pm 1.1	71.0 \pm 1.1	70.8 \pm 1.2	71.2 \pm 0.3	71.0 \pm 0.6	DFEA_I	69.1 \pm 1.1	71.0 \pm 1.1	70.8 \pm 1.2	71.2 \pm 0.3	71.0 \pm 0.6
DFEA_II	70.3 \pm 1.4	70.0 \pm 0.4	69.5 \pm 0.6	69.7 \pm 0.8	70.3 \pm 0.5	DFEA_II	70.3 \pm 1.4	70.0 \pm 0.4	69.5 \pm 0.6	69.7 \pm 0.8	70.3 \pm 0.5
DFEA_III	68.2 \pm 1.7	70.2 \pm 0.3	70.2 \pm 1.1	70.9 \pm 0.4	71.4 \pm 0.6	DFEA_III	68.2 \pm 1.7	70.2 \pm 0.3	70.1 \pm 1.0	70.9 \pm 0.4	71.4 \pm 0.6

Table 15: RQ1 detailed for dataset=CiteSeer, metric=F1 (%). Rows are attacks; columns are budgets. Mean \pm std across seeds; best per column is bold.

(a) Regime=both						(b) Regime=x_only					
Attack	0.05	0.10	0.25	0.50	1.00	Attack	0.05	0.10	0.25	0.50	1.00
MEA0	50.9 \pm 4.6	55.4 \pm 1.7	63.7 \pm 0.6	66.0 \pm 0.8	66.6 \pm 0.2	MEA0	46.1 \pm 2.9	58.8 \pm 0.4	64.8 \pm 1.4	66.2 \pm 0.5	65.7 \pm 0.4
MEA1	34.4 \pm 1.3	35.0 \pm 4.3	51.0 \pm 8.3	63.7 \pm 1.0	65.9 \pm 0.6	MEA1	34.4 \pm 1.3	35.0 \pm 4.3	51.0 \pm 8.3	63.7 \pm 1.0	65.8 \pm 0.6
MEA2	34.6 \pm 2.9	44.7 \pm 3.1	57.2 \pm 1.7	63.3 \pm 1.1	66.1 \pm 0.4	MEA2	42.7 \pm 1.7	45.8 \pm 3.3	56.9 \pm 1.5	62.9 \pm 0.8	66.1 \pm 0.3
MEA3	43.3 \pm 5.1	54.7 \pm 3.0	65.4 \pm 0.5	65.8 \pm 1.0	66.5 \pm 0.1	MEA3	51.9 \pm 4.4	57.7 \pm 0.5	63.4 \pm 1.0	65.0 \pm 0.4	66.3 \pm 0.7
MEA4	36.5 \pm 2.6	55.1 \pm 4.6	63.8 \pm 0.1	66.4 \pm 0.5	67.2 \pm 0.3	MEA4	34.7 \pm 3.4	53.7 \pm 1.9	63.3 \pm 0.5	66.4 \pm 0.5	67.2 \pm 0.3
MEA5	42.1 \pm 0.6	56.9 \pm 1.8	65.8 \pm 1.1	65.8 \pm 0.5	66.8 \pm 0.5	MEA5	47.0 \pm 5.4	59.9 \pm 1.6	65.4 \pm 0.7	65.8 \pm 0.7	66.3 \pm 0.5
AdvMEA	47.8 \pm 5.1	41.3 \pm 5.4	46.7 \pm 0.4	45.6 \pm 1.6	46.8 \pm 6.4	AdvMEA	43.3 \pm 0.4	47.5 \pm 0.5	50.3 \pm 3.0	44.4 \pm 6.0	42.3 \pm 2.5
CEGA	54.7 \pm 2.3	61.0 \pm 1.5	63.4 \pm 1.1	63.9 \pm 1.4	63.9 \pm 0.2	CEGA	57.4 \pm 1.1	61.4 \pm 0.8	63.3 \pm 0.5	63.9 \pm 0.5	64.5 \pm 0.8
Realistic	42.4 \pm 3.0	53.0 \pm 3.3	59.2 \pm 2.6	60.4 \pm 1.1	61.3 \pm 1.2	Realistic	42.1 \pm 5.1	47.4 \pm 5.2	58.1 \pm 1.9	59.4 \pm 2.3	61.6 \pm 1.9
DFEA_I	64.0 \pm 0.8	65.2 \pm 1.0	64.7 \pm 2.1	65.3 \pm 1.3	64.8 \pm 2.0	DFEA_I	64.0 \pm 0.8	65.2 \pm 1.0	64.7 \pm 2.1	65.3 \pm 1.3	64.8 \pm 2.0
DFEA_II	65.2 \pm 2.0	66.0 \pm 0.2	66.5 \pm 0.6	66.8 \pm 1.0	67.4 \pm 0.6	DFEA_II	65.2 \pm 2.0	66.0 \pm 0.2	66.5 \pm 0.6	66.8 \pm 1.0	67.4 \pm 0.6
DFEA_III	62.4 \pm 2.1	65.3 \pm 0.4	66.3 \pm 1.4	67.0 \pm 0.3	67.3 \pm 0.6	DFEA_III	62.4 \pm 2.1	65.3 \pm 0.4	66.3 \pm 1.4	67.0 \pm 0.3	67.3 \pm 0.6

(c) Regime=a_only						(d) Regime=data_free					
Attack	0.05	0.10	0.25	0.50	1.00	Attack	0.05	0.10	0.25	0.50	1.00
MEA0	46.0 \pm 3.1	57.1 \pm 3.2	65.8 \pm 1.3	65.6 \pm 0.6	66.6 \pm 1.1	MEA0	3.7 \pm 1.8	4.9 \pm 0.2	4.2 \pm 1.3	4.2 \pm 1.3	4.9 \pm 0.2
MEA1	34.4 \pm 1.3	35.0 \pm 4.3	51.0 \pm 8.3	63.7 \pm 1.0	65.9 \pm 0.6	MEA1	5.9 \pm 0.5	5.9 \pm 0.5	5.9 \pm 0.5	5.9 \pm 0.5	5.9 \pm 0.5
MEA2	33.5 \pm 1.4	46.8 \pm 1.0	56.4 \pm 0.7	63.0 \pm 1.4	66.1 \pm 0.3	MEA2	33.8 \pm 0.5	48.3 \pm 1.1	58.4 \pm 1.7	61.6 \pm 1.4	66.1 \pm 0.4
MEA3	39.5 \pm 6.3	56.5 \pm 1.3	63.6 \pm 2.1	66.1 \pm 0.8	66.4 \pm 0.4	MEA3	5.1 \pm 0.0	6.0 \pm 0.6	5.6 \pm 0.6	5.0 \pm 0.1	4.7 \pm 0.1
MEA4	33.0 \pm 4.6	54.5 \pm 1.7	63.1 \pm 0.7	66.4 \pm 0.5	67.2 \pm 0.3	MEA4	5.9 \pm 0.5	4.2 \pm 1.3	4.1 \pm 1.2	4.8 \pm 0.2	5.0 \pm 0.3
MEA5	45.2 \pm 2.5	59.0 \pm 2.1	65.1 \pm 1.5	65.8 \pm 0.3	67.1 \pm 0.9	MEA5	5.4 \pm 0.7	4.9 \pm 0.1	5.5 \pm 0.5	4.9 \pm 0.1	4.0 \pm 1.2
AdvMEA	44.2 \pm 6.2	46.2 \pm 4.9	47.9 \pm 7.8	47.3 \pm 3.3	41.5 \pm 1.2	AdvMEA	45.1 \pm 0.8	42.0 \pm 1.2	48.5 \pm 4.5	47.1 \pm 1.8	47.1 \pm 4.9
CEGA	54.1 \pm 1.9	61.4 \pm 0.1	63.4 \pm 0.7	65.0 \pm 0.9	64.1 \pm 0.9	CEGA	56.0 \pm 2.0	61.0 \pm 1.1	64.3 \pm 1.1	64.2 \pm 0.7	64.2 \pm 0.4
Realistic	33.2 \pm 10.0	50.1 \pm 4.6	58.5 \pm 0.3	58.9 \pm 2.7	60.6 \pm 1.0	Realistic	53.9 \pm 1.4	53.4 \pm 3.4	54.4 \pm 0.7	51.7 \pm 3.7	54.9 \pm 2.8
DFEA_I	64.0 \pm 0.8	65.2 \pm 1.0	64.7 \pm 2.1	65.3 \pm 1.3	64.8 \pm 2.0	DFEA_I	64.0 \pm 0.8	65.2 \pm 1.0	64.7 \pm 2.1	65.3 \pm 1.3	64.8 \pm 2.0
DFEA_II	65.2 \pm 2.0	66.0 \pm 0.2	66.5 \pm 0.6	66.8 \pm 1.0	67.4 \pm 0.6	DFEA_II	65.2 \pm 2.0	66.0 \pm 0.2	66.5 \pm 0.6	66.8 \pm 1.0	67.4 \pm 0.6
DFEA_III	62.4 \pm 2.1	65.3 \pm 0.4	66.3 \pm 1.4	67.0 \pm 0.3	67.3 \pm 0.6	DFEA_III	62.4 \pm 2.1	65.3 \pm 0.4	66.2 \pm 1.3	67.0 \pm 0.3	67.3 \pm 0.6

RandomWM loses on every metric except utility, which suggests the random-graph watermark is not competitive with trigger-based or query-based mechanisms under our protocol.

F.3 Baseline utility across backbones

To allow utility-drop numbers in the main text to be compared across defenses that use different backbones, Table 35 reports the test accuracy of an undefended target on each of the ten datasets and for each of the three backbones used in the benchmark. The first column reports a DGL GCN with hidden dimension 16, which is the backbone used by every original watermarking defense and by

Table 16: RQ1 detailed for dataset=CiteSeer, metric=Fidelity (%). Rows are attacks; columns are budgets. Mean \pm std across seeds; best per column is bold.

(a) Regime=both						(b) Regime=x_only					
Attack	0.05	0.10	0.25	0.50	1.00	Attack	0.05	0.10	0.25	0.50	1.00
MEA0	62.9 \pm 6.1	69.9 \pm 3.6	82.8 \pm 1.5	86.7 \pm 1.0	90.0 \pm 0.7	MEA0	58.5 \pm 2.3	73.2 \pm 0.6	82.0 \pm 0.2	85.8 \pm 0.5	89.2 \pm 0.8
MEA1	47.3 \pm 2.1	47.4 \pm 2.3	64.7 \pm 7.6	81.0 \pm 1.7	83.4 \pm 0.9	MEA1	47.3 \pm 2.1	47.4 \pm 2.3	64.7 \pm 7.6	81.0 \pm 1.7	83.4 \pm 1.0
MEA2	42.4 \pm 4.3	55.5 \pm 3.2	74.4 \pm 2.3	83.8 \pm 0.4	91.5 \pm 0.2	MEA2	51.4 \pm 2.4	54.9 \pm 2.0	74.0 \pm 1.7	84.5 \pm 1.3	91.5 \pm 0.2
MEA3	55.6 \pm 3.6	69.0 \pm 3.6	82.5 \pm 1.5	86.3 \pm 2.2	88.5 \pm 0.5	MEA3	63.4 \pm 5.5	69.8 \pm 0.5	81.0 \pm 0.6	85.2 \pm 1.1	88.8 \pm 0.4
MEA4	48.3 \pm 2.9	65.4 \pm 5.3	79.4 \pm 0.8	83.3 \pm 1.5	84.1 \pm 1.3	MEA4	43.5 \pm 4.9	67.1 \pm 2.3	79.7 \pm 1.8	83.3 \pm 1.5	84.1 \pm 1.3
MEA5	56.5 \pm 1.5	72.1 \pm 2.9	83.0 \pm 0.7	87.2 \pm 0.4	87.9 \pm 0.8	MEA5	61.9 \pm 3.9	72.7 \pm 0.7	83.4 \pm 0.5	86.2 \pm 1.6	88.5 \pm 0.5
AdvMEA	55.9 \pm 6.8	50.0 \pm 4.2	54.5 \pm 2.5	57.2 \pm 1.0	52.7 \pm 6.0	AdvMEA	52.4 \pm 3.0	55.2 \pm 3.2	57.7 \pm 3.7	52.7 \pm 6.8	50.7 \pm 3.0
CEGA	68.6 \pm 2.0	79.8 \pm 0.7	83.2 \pm 0.9	86.3 \pm 0.8	87.2 \pm 1.0	CEGA	73.1 \pm 1.8	78.6 \pm 1.8	83.7 \pm 0.9	86.4 \pm 0.9	87.0 \pm 1.1
Realistic	54.1 \pm 3.8	64.5 \pm 1.5	73.3 \pm 1.4	78.3 \pm 3.5	84.1 \pm 0.8	Realistic	54.5 \pm 3.8	60.3 \pm 2.7	74.5 \pm 1.8	80.0 \pm 2.9	84.4 \pm 1.1
DFEA_I	80.5 \pm 1.7	83.7 \pm 0.6	83.8 \pm 1.4	85.3 \pm 0.9	85.6 \pm 1.5	DFEA_I	80.5 \pm 1.7	83.7 \pm 0.6	83.8 \pm 1.4	85.3 \pm 0.9	85.6 \pm 1.5
DFEA_II	76.9 \pm 1.3	80.8 \pm 1.1	85.6 \pm 0.8	90.1 \pm 1.0	93.6 \pm 0.9	DFEA_II	77.0 \pm 1.3	80.8 \pm 1.1	85.6 \pm 0.8	90.1 \pm 1.0	93.6 \pm 0.9
DFEA_III	77.0 \pm 0.7	82.3 \pm 0.1	87.7 \pm 0.7	90.4 \pm 0.2	91.5 \pm 0.1	DFEA_III	77.0 \pm 0.7	82.3 \pm 0.1	87.6 \pm 0.7	90.4 \pm 0.2	91.5 \pm 0.1

(c) Regime=a_only						(d) Regime=data_free					
Attack	0.05	0.10	0.25	0.50	1.00	Attack	0.05	0.10	0.25	0.50	1.00
MEA0	57.6 \pm 3.5	73.1 \pm 4.4	82.9 \pm 0.5	85.8 \pm 0.5	89.8 \pm 0.7	MEA0	12.2 \pm 3.6	18.4 \pm 0.9	16.1 \pm 4.7	15.9 \pm 4.5	18.6 \pm 0.9
MEA1	47.3 \pm 2.1	47.4 \pm 2.3	64.7 \pm 7.6	81.0 \pm 1.7	83.4 \pm 0.9	MEA1	18.1 \pm 0.7	18.1 \pm 0.7	18.1 \pm 0.7	18.1 \pm 0.7	18.1 \pm 0.7
MEA2	40.1 \pm 1.3	58.3 \pm 1.3	72.1 \pm 0.6	84.8 \pm 1.1	91.5 \pm 0.2	MEA2	43.1 \pm 1.0	59.3 \pm 2.2	73.5 \pm 2.2	85.3 \pm 1.1	91.5 \pm 0.2
MEA3	54.4 \pm 4.3	72.5 \pm 3.2	80.8 \pm 0.7	87.1 \pm 0.3	87.9 \pm 0.5	MEA3	19.0 \pm 0.4	18.0 \pm 0.9	16.1 \pm 2.0	18.3 \pm 1.1	17.2 \pm 0.3
MEA4	44.5 \pm 4.3	66.6 \pm 2.9	80.0 \pm 1.6	83.3 \pm 1.5	84.1 \pm 1.3	MEA4	17.6 \pm 0.6	15.9 \pm 4.5	15.4 \pm 4.3	17.9 \pm 0.8	18.7 \pm 1.0
MEA5	58.2 \pm 2.7	73.7 \pm 2.3	84.0 \pm 1.7	86.2 \pm 1.5	88.5 \pm 0.8	MEA5	17.6 \pm 0.5	17.9 \pm 1.0	19.0 \pm 0.6	17.6 \pm 0.7	15.3 \pm 4.3
AdvMEA	52.2 \pm 3.8	53.6 \pm 3.0	56.1 \pm 6.6	53.5 \pm 5.3	50.6 \pm 2.2	AdvMEA	54.3 \pm 3.5	52.7 \pm 1.0	56.3 \pm 6.5	53.3 \pm 2.1	54.6 \pm 3.1
CEGA	69.9 \pm 3.5	79.6 \pm 2.4	81.9 \pm 0.9	87.2 \pm 0.3	88.8 \pm 0.5	CEGA	71.9 \pm 2.1	77.4 \pm 0.1	85.2 \pm 0.7	86.4 \pm 1.0	86.9 \pm 0.9
Realistic	48.1 \pm 7.3	61.3 \pm 4.2	73.8 \pm 0.7	81.1 \pm 0.8	84.2 \pm 0.3	Realistic	70.6 \pm 2.6	69.8 \pm 3.7	67.3 \pm 1.1	62.2 \pm 2.3	70.8 \pm 3.1
DFEA_I	80.5 \pm 1.7	83.7 \pm 0.6	83.8 \pm 1.4	85.3 \pm 0.9	85.6 \pm 1.5	DFEA_I	80.5 \pm 1.7	83.7 \pm 0.6	83.8 \pm 1.4	85.3 \pm 0.9	85.6 \pm 1.5
DFEA_II	77.0 \pm 1.3	80.8 \pm 1.1	85.6 \pm 0.8	90.1 \pm 1.0	93.6 \pm 0.9	DFEA_II	77.0 \pm 1.3	80.8 \pm 1.1	85.6 \pm 0.8	90.1 \pm 1.0	93.6 \pm 0.9
DFEA_III	77.1 \pm 0.6	82.3 \pm 0.1	87.6 \pm 0.7	90.4 \pm 0.2	91.5 \pm 0.1	DFEA_III	77.1 \pm 0.6	82.3 \pm 0.1	87.6 \pm 0.7	90.4 \pm 0.2	91.5 \pm 0.1

Table 17: RQ1 detailed for dataset=CoauthorCS, metric=Acc (%). Rows are attacks; columns are budgets. Mean \pm std across seeds; best per column is bold.

(a) Regime=both						(b) Regime=x_only					
Attack	0.05	0.10	0.25	0.50	1.00	Attack	0.05	0.10	0.25	0.50	1.00
MEA0	84.3 \pm 3.8	88.4 \pm 1.8	90.8 \pm 1.1	91.2 \pm 1.2	92.2 \pm 0.9	MEA0	83.5 \pm 2.7	89.1 \pm 0.2	91.5 \pm 0.6	92.3 \pm 0.2	92.2 \pm 1.6
MEA1	71.1 \pm 0.8	74.4 \pm 0.7	77.2 \pm 0.3	89.2 \pm 0.7	89.5 \pm 0.4	MEA1	71.1 \pm 0.8	74.4 \pm 0.7	77.2 \pm 0.3	89.2 \pm 0.7	89.5 \pm 0.4
MEA2	48.5 \pm 1.5	56.2 \pm 0.8	70.8 \pm 0.6	80.6 \pm 1.1	84.6 \pm 1.5	MEA2	46.6 \pm 1.6	55.6 \pm 2.0	71.0 \pm 1.2	80.5 \pm 0.5	84.6 \pm 1.5
MEA3	86.2 \pm 0.6	88.8 \pm 0.7	90.8 \pm 0.5	91.8 \pm 0.3	92.8 \pm 0.3	MEA3	79.2 \pm 3.8	89.0 \pm 1.0	90.2 \pm 0.7	91.2 \pm 0.5	91.6 \pm 0.3
MEA4	68.4 \pm 8.5	79.4 \pm 7.5	85.8 \pm 3.7	90.3 \pm 0.5	91.0 \pm 0.2	MEA4	65.3 \pm 10.4	73.3 \pm 0.6	86.9 \pm 1.5	89.7 \pm 0.2	91.0 \pm 0.3
MEA5	87.3 \pm 0.7	88.5 \pm 0.3	91.4 \pm 0.8	92.2 \pm 0.1	92.0 \pm 0.4	MEA5	83.2 \pm 2.8	89.7 \pm 1.9	91.0 \pm 0.4	91.6 \pm 1.2	91.7 \pm 1.1
AdvMEA	92.0 \pm 0.4	91.8 \pm 0.2	91.7 \pm 0.4	91.8 \pm 0.4	91.9 \pm 0.3	AdvMEA	91.7 \pm 0.3	91.8 \pm 0.6	91.8 \pm 0.6	91.6 \pm 0.4	91.8 \pm 0.4
CEGA	89.0 \pm 1.0	90.4 \pm 0.7	91.6 \pm 0.4	91.8 \pm 0.0	91.7 \pm 0.6	CEGA	88.7 \pm 0.8	90.3 \pm 0.4	91.0 \pm 0.1	91.7 \pm 0.5	91.9 \pm 0.4
Realistic	71.9 \pm 5.8	81.1 \pm 4.4	81.0 \pm 3.4	79.1 \pm 3.4	77.7 \pm 2.1	Realistic	68.8 \pm 8.3	77.2 \pm 4.3	81.2 \pm 2.2	78.9 \pm 2.4	79.3 \pm 1.2
DFEA_I	89.7 \pm 1.1	89.7 \pm 0.7	89.6 \pm 0.4	89.8 \pm 0.6	89.4 \pm 0.6	DFEA_I	89.8 \pm 1.1	89.7 \pm 0.7	89.6 \pm 0.5	89.8 \pm 0.6	89.4 \pm 0.6
DFEA_II	91.3 \pm 1.4	90.9 \pm 0.2	90.1 \pm 0.8	88.6 \pm 0.8	87.4 \pm 0.2	DFEA_II	91.3 \pm 1.4	90.9 \pm 0.2	90.1 \pm 0.8	88.7 \pm 0.8	87.4 \pm 0.2
DFEA_III	89.6 \pm 0.7	89.4 \pm 0.8	89.3 \pm 0.9	88.6 \pm 0.2	88.3 \pm 0.2	DFEA_III	89.6 \pm 0.7	89.4 \pm 0.8	89.3 \pm 0.9	88.6 \pm 0.2	88.3 \pm 0.2

(c) Regime=a_only						(d) Regime=data_free					
Attack	0.05	0.10	0.25	0.50	1.00	Attack	0.05	0.10	0.25	0.50	1.00
MEA0	85.1 \pm 2.1	89.0 \pm 1.4	90.5 \pm 0.5	91.0 \pm 0.3	91.4 \pm 0.7	MEA0	7.4 \pm 2.7	33.5 \pm 23.5	7.4 \pm 3.8	3.5 \pm 2.7	22.1 \pm 19.8
MEA1	71.1 \pm 0.8	74.4 \pm 0.7	77.2 \pm 0.3	89.2 \pm 0.7	89.5 \pm 0.4	MEA1	0.5 \pm 0.4	0.5 \pm 0.4	0.5 \pm 0.4	0.5 \pm 0.4	0.5 \pm 0.4
MEA2	46.7 \pm 1.7	59.5 \pm 0.9	73.3 \pm 1.0	81.1 \pm 0.8	84.6 \pm 1.5	MEA2	45.2 \pm 1.7	54.3 \pm 2.6	73.8 \pm 1.0	81.5 \pm 1.1	84.6 \pm 1.5
MEA3	87.6 \pm 0.4	89.5 \pm 1.3	90.8 \pm 0.7	91.9 \pm 0.3	92.5 \pm 0.4	MEA3	21.5 \pm 20.3	22.1 \pm 19.9	17.5 \pm 23.1	37.2 \pm 18.2	18.9 \pm 19.5
MEA4	58.5 \pm 15.4	82.6 \pm 3.3	87.2 \pm 0.2	90.0 \pm 0.7	91.0 \pm 0.4	MEA4	4.0 \pm 2.4	22.6 \pm 19.5	18.4 \pm 22.5	20.1 \pm 21.5	7.1 \pm 3.0
MEA5	86.5 \pm 1.2	89.2 \pm 0.7	91.3 \pm 0.0	92.0 \pm 0.9	92.0 \pm 0.6	MEA5	17.0 \pm 12.7	26.4 \pm 23.8	18.1 \pm 22.7	6.2 \pm 4.3	7.8 \pm 5.0
AdvMEA	91.8 \pm 0.2	91.7 \pm 0.3	91.9 \pm 0.2	91.8 \pm 0.4	91.6 \pm 0.5	AdvMEA	91.7 \pm 0.3	91.9 \pm 0.2	91.8 \pm 0.3	91.8 \pm 0.4	91.8 \pm 0.3
CEGA	90.0 \pm 0.2	90.4 \pm 0.2	91.8 \pm 0.5	91.3 \pm 0.8	91.7 \pm 0.7	CEGA	88.8 \pm 1.0	91.1 \pm 0.6	91.4 \pm 0.3	91.3 \pm 0.8	91.1 \pm 0.6
Realistic	74.5 \pm 3.2	80.8 \pm 2.0	84.4 \pm 4.4	77.1 \pm 3.0	77.3 \pm 2.3	Realistic	74.9 \pm 2.2	77.4 \pm 2.8	75.1 \pm 2.0	79.7 \pm 1.1	79.9 \pm 1.9
DFEA_I	89.8 \pm 1.1	89.7 \pm 0.7	89.6 \pm 0.4	89.8 \pm 0.7	89.4 \pm 0.6	DFEA_I	89.7 \pm 1.1	89.7 \pm 0.7	89.6 \pm 0.4	89.8 \pm 0.6	89.5 \pm 0.6
DFEA_II	91.3 \pm 1.4	90.9 \pm 0.2	90.1 \pm 0.8	88.6 \pm 0.8	87.4 \pm 0.2	DFEA_II	91.3 \pm 1.4	90.9 \pm 0.2	90.1 \pm 0.8	88.6 \pm 0.8	87.4 \pm 0.2
DFEA_III	89.6 \pm 0.7	89.4 \pm 0.8	89.3 \pm 0.9	88.6 \pm 0.2	88.3 \pm 0.2	DFEA_III	89.6 \pm 0.7	89.4 \pm 0.8	89.3 \pm 0.9	88.6 \pm 0.2	88.3 \pm 0.2

every information-limiting defense. The second column reports a DGL GraphSAGE with hidden dimension 128, which is the backbone used by RandomWM. The third column reports a PyG GCN with hidden dimension 128, which is the backbone used by ImperceptibleWM.

The baseline-utility table reveals one pattern that has direct consequences for any cross-defense comparison in the main text: the per-dataset gap between the two backbones used by watermark methods can be huge, and it is largest exactly on the graphs where defenses are evaluated as “most informative”. On *RomanEmpire*, the GraphSAGE-128 baseline of 77.5 % is 34.7 pp higher than the GCN-16 baseline of 42.8 %; on *Computers* the gap is 15.2 pp; on *OGBN-Arxiv* it is 17.2 pp. This

Table 18: RQ1 detailed for dataset=CoauthorCS, metric=F1 (%). Rows are attacks; columns are budgets. Mean \pm std across seeds; best per column is bold.

(a) Regime=both						(b) Regime=x_only					
Attack	0.05	0.10	0.25	0.50	1.00	Attack	0.05	0.10	0.25	0.50	1.00
MEAO	51.8 \pm 1.1	61.1 \pm 3.9	70.1 \pm 3.4	73.7 \pm 3.8	77.1 \pm 2.5	MEAO	44.4 \pm 3.8	60.9 \pm 4.1	74.5 \pm 0.4	76.1 \pm 1.7	74.8 \pm 4.7
MEA1	34.5 \pm 0.3	36.7 \pm 0.4	42.1 \pm 1.7	61.2 \pm 0.9	64.3 \pm 1.3	MEA1	34.5 \pm 0.3	36.7 \pm 0.4	42.1 \pm 1.7	61.2 \pm 0.9	64.3 \pm 1.3
MEA2	32.7 \pm 1.4	38.9 \pm 3.3	52.1 \pm 4.0	57.5 \pm 5.4	59.5 \pm 4.5	MEA2	31.8 \pm 1.1	41.5 \pm 1.6	55.6 \pm 3.9	58.8 \pm 3.0	59.5 \pm 4.5
MEA3	54.8 \pm 2.8	64.2 \pm 4.6	71.6 \pm 4.2	76.8 \pm 0.6	76.4 \pm 1.5	MEA3	45.6 \pm 0.8	62.5 \pm 6.8	67.6 \pm 3.0	74.1 \pm 1.6	73.5 \pm 1.6
MEA4	25.2 \pm 4.7	38.0 \pm 4.8	52.3 \pm 8.8	67.1 \pm 1.9	71.3 \pm 1.1	MEA4	20.8 \pm 8.6	36.1 \pm 6.9	52.2 \pm 4.5	64.5 \pm 0.7	71.1 \pm 0.8
MEA5	54.6 \pm 1.0	59.5 \pm 1.4	71.8 \pm 5.1	77.6 \pm 1.4	77.7 \pm 0.1	MEA5	50.4 \pm 3.0	66.6 \pm 5.2	71.6 \pm 4.0	73.1 \pm 6.9	74.4 \pm 3.6
AdvMEA	75.0 \pm 1.6	73.7 \pm 0.8	74.0 \pm 1.8	74.9 \pm 2.2	75.3 \pm 1.0	AdvMEA	74.7 \pm 0.7	74.7 \pm 2.0	74.6 \pm 1.6	74.3 \pm 1.0	73.2 \pm 1.9
CEGA	67.6 \pm 2.1	72.6 \pm 1.5	74.7 \pm 2.0	76.5 \pm 0.9	74.1 \pm 2.4	CEGA	70.0 \pm 0.9	70.8 \pm 1.5	74.0 \pm 2.8	72.5 \pm 1.3	72.8 \pm 1.4
Realistic	42.9 \pm 6.9	53.4 \pm 2.3	61.3 \pm 3.9	56.6 \pm 5.6	54.2 \pm 3.5	Realistic	46.1 \pm 1.1	46.4 \pm 3.0	56.5 \pm 1.7	56.9 \pm 3.7	55.8 \pm 0.6
DFEA_I	81.9 \pm 2.0	82.0 \pm 0.9	81.6 \pm 0.8	81.3 \pm 0.6	80.5 \pm 0.8	DFEA_I	81.9 \pm 2.0	82.0 \pm 1.0	81.6 \pm 0.8	81.3 \pm 0.6	80.5 \pm 0.8
DFEA_II	83.1 \pm 1.3	82.1 \pm 0.4	81.6 \pm 2.1	78.2 \pm 2.3	77.0 \pm 1.6	DFEA_II	83.1 \pm 1.3	82.1 \pm 0.4	81.6 \pm 2.1	78.2 \pm 2.3	77.0 \pm 1.6
DFEA_III	81.8 \pm 1.0	80.7 \pm 0.6	80.6 \pm 2.0	78.8 \pm 0.5	78.6 \pm 0.9	DFEA_III	81.8 \pm 1.0	80.7 \pm 0.6	80.6 \pm 2.0	78.8 \pm 0.5	78.6 \pm 0.9

(c) Regime=a_only						(d) Regime=data_free					
Attack	0.05	0.10	0.25	0.50	1.00	Attack	0.05	0.10	0.25	0.50	1.00
MEAO	56.0 \pm 6.3	65.7 \pm 4.6	71.3 \pm 2.8	73.2 \pm 1.6	73.4 \pm 3.3	MEAO	0.9 \pm 0.3	3.0 \pm 2.1	0.9 \pm 0.5	0.4 \pm 0.3	2.1 \pm 1.6
MEA1	34.5 \pm 0.3	36.7 \pm 0.4	42.1 \pm 1.7	61.2 \pm 0.9	64.3 \pm 1.3	MEA1	0.1 \pm 0.0	0.1 \pm 0.0	0.1 \pm 0.0	0.1 \pm 0.0	0.1 \pm 0.0
MEA2	31.6 \pm 6.0	43.5 \pm 3.7	54.7 \pm 1.8	58.9 \pm 4.6	59.5 \pm 4.5	MEA2	32.0 \pm 2.6	38.9 \pm 7.7	55.3 \pm 3.7	59.8 \pm 6.4	59.5 \pm 4.5
MEA3	57.1 \pm 0.9	64.4 \pm 7.1	70.5 \pm 4.1	74.8 \pm 2.2	75.8 \pm 0.9	MEA3	2.4 \pm 1.5	3.4 \pm 1.9	1.6 \pm 2.0	3.9 \pm 0.8	2.9 \pm 2.8
MEA4	21.3 \pm 4.2	47.2 \pm 8.5	52.4 \pm 0.9	66.1 \pm 2.5	71.3 \pm 1.4	MEA4	0.5 \pm 0.3	2.2 \pm 1.6	1.7 \pm 2.0	1.9 \pm 1.8	0.9 \pm 0.4
MEA5	53.6 \pm 3.3	67.3 \pm 4.9	74.1 \pm 1.1	77.3 \pm 1.9	74.1 \pm 2.0	MEA5	2.7 \pm 2.2	5.5 \pm 5.0	1.8 \pm 1.9	0.8 \pm 0.5	3.6 \pm 2.6
AdvMEA	75.0 \pm 0.8	75.2 \pm 1.0	74.7 \pm 1.1	74.6 \pm 1.1	74.4 \pm 1.0	AdvMEA	75.1 \pm 1.0	74.9 \pm 0.8	73.9 \pm 0.9	74.7 \pm 0.9	74.6 \pm 0.7
CEGA	69.4 \pm 2.1	71.2 \pm 0.9	73.9 \pm 0.9	73.3 \pm 3.0	72.3 \pm 1.3	CEGA	65.1 \pm 3.0	72.6 \pm 2.4	71.9 \pm 1.0	75.5 \pm 0.8	72.0 \pm 1.0
Realistic	41.5 \pm 6.9	56.2 \pm 2.7	61.6 \pm 5.3	54.4 \pm 5.0	54.5 \pm 0.8	Realistic	52.0 \pm 1.7	55.1 \pm 3.3	54.1 \pm 1.5	59.5 \pm 0.8	56.9 \pm 2.8
DFEA_I	81.9 \pm 2.0	82.0 \pm 0.9	81.6 \pm 0.8	81.3 \pm 0.7	80.5 \pm 0.8	DFEA_I	81.9 \pm 2.0	82.0 \pm 1.0	81.6 \pm 0.8	81.3 \pm 0.6	80.5 \pm 0.7
DFEA_II	83.1 \pm 1.3	82.1 \pm 0.4	81.6 \pm 2.1	78.2 \pm 2.3	77.0 \pm 1.6	DFEA_II	83.1 \pm 1.3	82.1 \pm 0.4	81.6 \pm 2.1	78.2 \pm 2.3	77.0 \pm 1.6
DFEA_III	81.8 \pm 1.0	80.7 \pm 0.6	80.6 \pm 2.0	78.8 \pm 0.5	78.6 \pm 0.9	DFEA_III	81.8 \pm 1.0	80.7 \pm 0.6	80.6 \pm 2.0	78.8 \pm 0.5	78.5 \pm 0.9

Table 19: RQ1 detailed for dataset=CoauthorCS, metric=Fidelity (%). Rows are attacks; columns are budgets. Mean \pm std across seeds; best per column is bold.

(a) Regime=both						(b) Regime=x_only					
Attack	0.05	0.10	0.25	0.50	1.00	Attack	0.05	0.10	0.25	0.50	1.00
MEAO	83.7 \pm 4.0	87.9 \pm 1.6	91.2 \pm 1.2	92.8 \pm 0.3	94.5 \pm 0.3	MEAO	83.3 \pm 2.8	88.8 \pm 0.5	92.3 \pm 0.7	93.3 \pm 0.5	93.7 \pm 0.2
MEA1	71.0 \pm 0.8	74.2 \pm 0.5	76.9 \pm 0.5	89.8 \pm 0.8	90.2 \pm 0.7	MEA1	71.0 \pm 0.8	74.2 \pm 0.5	76.9 \pm 0.5	89.8 \pm 0.8	90.2 \pm 0.7
MEA2	47.8 \pm 1.2	57.3 \pm 1.4	73.0 \pm 2.3	84.2 \pm 1.7	87.7 \pm 2.9	MEA2	46.2 \pm 1.8	56.5 \pm 2.5	74.3 \pm 2.6	83.7 \pm 2.2	87.7 \pm 2.9
MEA3	85.2 \pm 1.8	88.2 \pm 1.3	90.8 \pm 1.0	91.7 \pm 0.2	93.1 \pm 0.6	MEA3	77.8 \pm 4.5	88.6 \pm 0.9	90.0 \pm 0.6	91.7 \pm 0.4	93.4 \pm 0.5
MEA4	66.7 \pm 8.4	79.1 \pm 7.2	86.9 \pm 3.4	93.5 \pm 0.7	96.3 \pm 0.5	MEA4	63.8 \pm 10.0	72.2 \pm 0.8	87.7 \pm 1.2	92.9 \pm 0.3	96.4 \pm 0.4
MEA5	85.8 \pm 0.2	87.8 \pm 0.3	91.1 \pm 0.2	92.4 \pm 0.4	93.6 \pm 0.8	MEA5	83.5 \pm 2.4	89.2 \pm 2.0	91.0 \pm 0.3	92.0 \pm 0.7	93.1 \pm 1.0
AdvMEA	92.3 \pm 0.5	92.3 \pm 0.4	92.0 \pm 0.4	92.1 \pm 0.3	92.3 \pm 0.4	AdvMEA	92.0 \pm 0.4	92.1 \pm 0.3	92.2 \pm 0.6	92.0 \pm 0.3	92.2 \pm 0.2
CEGA	90.3 \pm 0.6	91.7 \pm 0.7	93.5 \pm 0.7	94.9 \pm 0.8	94.8 \pm 0.5	CEGA	90.2 \pm 0.6	92.7 \pm 0.3	92.8 \pm 0.4	94.5 \pm 0.3	96.2 \pm 0.3
Realistic	72.6 \pm 5.2	81.5 \pm 4.3	82.5 \pm 3.2	80.4 \pm 3.7	80.9 \pm 2.0	Realistic	68.4 \pm 8.8	78.1 \pm 4.7	81.4 \pm 1.7	80.8 \pm 1.9	80.5 \pm 1.1
DFEA_I	91.6 \pm 0.5	93.2 \pm 0.2	94.7 \pm 0.4	95.7 \pm 1.1	96.9 \pm 0.9	DFEA_I	91.7 \pm 0.5	93.2 \pm 0.2	94.6 \pm 0.4	95.6 \pm 1.0	96.9 \pm 0.9
DFEA_II	89.6 \pm 1.2	91.1 \pm 1.1	93.1 \pm 0.7	96.1 \pm 0.4	100.0 \pm 0.0	DFEA_II	89.6 \pm 1.2	91.1 \pm 1.1	93.1 \pm 0.7	96.1 \pm 0.4	100.0 \pm 0.0
DFEA_III	91.0 \pm 0.7	92.6 \pm 0.4	94.8 \pm 0.0	96.8 \pm 0.7	98.9 \pm 0.3	DFEA_III	91.0 \pm 0.7	92.6 \pm 0.4	94.8 \pm 0.0	96.8 \pm 0.7	98.9 \pm 0.3

(c) Regime=a_only						(d) Regime=data_free					
Attack	0.05	0.10	0.25	0.50	1.00	Attack	0.05	0.10	0.25	0.50	1.00
MEAO	84.6 \pm 2.4	89.4 \pm 1.4	91.9 \pm 0.6	92.9 \pm 0.4	94.6 \pm 0.4	MEAO	6.6 \pm 2.5	32.2 \pm 22.7	7.0 \pm 3.9	3.4 \pm 2.8	21.2 \pm 19.1
MEA1	71.0 \pm 0.8	74.2 \pm 0.5	76.9 \pm 0.5	89.8 \pm 0.8	90.2 \pm 0.7	MEA1	0.6 \pm 0.7	0.6 \pm 0.7	0.6 \pm 0.7	0.6 \pm 0.7	0.6 \pm 0.7
MEA2	46.3 \pm 1.1	60.7 \pm 0.8	76.0 \pm 0.3	84.0 \pm 1.6	87.7 \pm 2.9	MEA2	45.1 \pm 2.4	55.9 \pm 2.2	75.3 \pm 2.4	84.1 \pm 1.9	87.7 \pm 2.9
MEA3	86.5 \pm 0.5	89.5 \pm 1.4	90.8 \pm 0.9	92.0 \pm 0.4	93.5 \pm 0.1	MEA3	20.4 \pm 19.6	21.2 \pm 19.1	16.8 \pm 22.4	36.1 \pm 17.3	18.7 \pm 18.9
MEA4	57.4 \pm 15.1	81.4 \pm 2.8	88.5 \pm 0.3	92.8 \pm 1.3	96.6 \pm 0.4	MEA4	3.9 \pm 2.2	22.1 \pm 18.8	17.4 \pm 21.7	19.4 \pm 20.5	7.0 \pm 3.1
MEA5	86.2 \pm 1.6	89.0 \pm 0.6	91.1 \pm 0.4	92.4 \pm 0.7	93.7 \pm 1.0	MEA5	16.3 \pm 12.3	25.8 \pm 23.0	17.3 \pm 21.8	5.8 \pm 3.7	8.0 \pm 5.0
AdvMEA	92.0 \pm 0.3	92.0 \pm 0.4	92.3 \pm 0.4	91.9 \pm 0.3	91.9 \pm 0.3	AdvMEA	91.9 \pm 0.4	92.2 \pm 0.4	92.2 \pm 0.4	92.0 \pm 0.5	92.1 \pm 0.5
CEGA	90.2 \pm 1.0	92.5 \pm 0.5	93.8 \pm 0.5	94.2 \pm 0.3	95.8 \pm 0.3	CEGA	90.0 \pm 1.2	92.3 \pm 0.6	93.1 \pm 0.3	93.8 \pm 0.7	95.5 \pm 0.5
Realistic	73.9 \pm 3.3	82.2 \pm 1.5	85.7 \pm 4.5	78.6 \pm 3.7	79.0 \pm 2.6	Realistic	77.8 \pm 2.5	78.9 \pm 2.1	76.4 \pm 2.5	80.3 \pm 1.9	81.5 \pm 2.1
DFEA_I	91.7 \pm 0.5	93.2 \pm 0.2	94.7 \pm 0.4	95.7 \pm 1.0	96.9 \pm 0.9	DFEA_I	91.7 \pm 0.5	93.2 \pm 0.2	94.7 \pm 0.4	95.6 \pm 1.0	96.9 \pm 0.8
DFEA_II	89.6 \pm 1.2	91.1 \pm 1.1	93.1 \pm 0.7	96.1 \pm 0.4	100.0 \pm 0.0	DFEA_II	89.6 \pm 1.2	91.1 \pm 1.1	93.1 \pm 0.7	96.1 \pm 0.4	100.0 \pm 0.0
DFEA_III	91.0 \pm 0.7	92.6 \pm 0.4	94.8 \pm 0.0	96.8 \pm 0.7	98.9 \pm 0.3	DFEA_III	91.0 \pm 0.7	92.6 \pm 0.4	94.8 \pm 0.0	96.8 \pm 0.7	98.9 \pm 0.3

means that any utility-drop number in the main text that compares RandomWM (GraphSAGE-128) against the GCN-16 baseline implicitly attributes the entire backbone gap to the defense, which would over-estimate RandomWM’s damage by 15–35 pp on these three graphs; we therefore always compare each defense against its own matched-backbone baseline rather than against a single shared GCN baseline.

Table 20: RQ1 detailed for dataset=CoauthorPhysics, metric=Acc (%). Rows are attacks; columns are budgets. Mean \pm std across seeds; best per column is bold.

(a) Regime=both						(b) Regime=x_only					
Attack	0.05	0.10	0.25	0.50	1.00	Attack	0.05	0.10	0.25	0.50	1.00
MEA0	82.2 \pm 4.9	89.6 \pm 0.4	90.9 \pm 0.2	90.7 \pm 0.4	92.8 \pm 1.0	MEA0	80.9 \pm 4.2	90.4 \pm 1.8	89.3 \pm 1.5	91.5 \pm 0.9	91.3 \pm 0.8
MEA1	3.5 \pm 0.0	10.1 \pm 0.6	17.2 \pm 0.2	44.0 \pm 1.9	79.5 \pm 7.9	MEA1	3.5 \pm 0.0	10.1 \pm 0.6	17.2 \pm 0.2	44.0 \pm 1.9	79.5 \pm 7.9
MEA2	33.3 \pm 2.4	44.2 \pm 1.4	66.8 \pm 1.0	73.6 \pm 4.4	84.0 \pm 3.1	MEA2	31.0 \pm 2.1	41.2 \pm 2.2	64.9 \pm 4.1	71.9 \pm 6.2	83.9 \pm 3.1
MEA3	74.0 \pm 1.4	81.1 \pm 2.6	89.5 \pm 1.4	89.8 \pm 0.7	90.6 \pm 1.8	MEA3	75.3 \pm 1.5	84.0 \pm 2.4	89.8 \pm 0.9	91.6 \pm 0.5	91.4 \pm 0.5
MEA4	70.1 \pm 10.5	74.0 \pm 10.0	87.7 \pm 2.0	89.6 \pm 0.5	89.5 \pm 0.6	MEA4	39.5 \pm 17.4	83.4 \pm 4.5	88.7 \pm 1.6	90.2 \pm 0.6	89.9 \pm 0.3
MEA5	75.4 \pm 4.8	78.4 \pm 4.7	89.8 \pm 1.6	91.0 \pm 0.8	91.3 \pm 1.0	MEA5	76.2 \pm 5.5	78.9 \pm 5.5	89.0 \pm 1.5	91.5 \pm 0.7	91.2 \pm 1.4
AdvMEA	91.4 \pm 1.2	91.6 \pm 0.7	91.3 \pm 0.2	90.6 \pm 1.3	91.4 \pm 0.9	AdvMEA	90.8 \pm 1.2	91.2 \pm 1.0	90.7 \pm 0.4	91.6 \pm 0.4	90.9 \pm 0.9
CEGA	90.9 \pm 1.3	90.4 \pm 2.8	91.5 \pm 0.6	91.0 \pm 0.5	90.8 \pm 0.3	CEGA	90.9 \pm 0.4	91.2 \pm 1.0	91.6 \pm 0.3	91.2 \pm 0.5	91.2 \pm 0.4
Realistic	79.6 \pm 3.8	77.0 \pm 6.5	79.3 \pm 1.7	76.1 \pm 3.1	73.0 \pm 1.5	Realistic	79.0 \pm 5.6	83.0 \pm 4.6	79.4 \pm 2.7	78.6 \pm 2.6	74.4 \pm 0.5
DFEA_I	90.7 \pm 0.2	90.8 \pm 0.2	90.8 \pm 0.5	90.8 \pm 0.2	90.6 \pm 0.2	DFEA_I	90.7 \pm 0.2	90.8 \pm 0.2	90.8 \pm 0.5	90.8 \pm 0.2	90.6 \pm 0.2
DFEA_II	90.9 \pm 0.2	90.0 \pm 0.6	90.6 \pm 0.4	90.1 \pm 0.4	89.5 \pm 0.4	DFEA_II	90.9 \pm 0.2	90.0 \pm 0.6	90.6 \pm 0.4	90.1 \pm 0.4	89.5 \pm 0.4
DFEA_III	90.5 \pm 0.4	90.1 \pm 0.6	90.5 \pm 0.4	90.3 \pm 0.5	90.4 \pm 0.3	DFEA_III	90.4 \pm 0.4	90.1 \pm 0.6	90.5 \pm 0.4	90.3 \pm 0.5	90.4 \pm 0.3

(c) Regime=a_only						(d) Regime=data_free					
Attack	0.05	0.10	0.25	0.50	1.00	Attack	0.05	0.10	0.25	0.50	1.00
MEA0	85.3 \pm 2.4	89.0 \pm 0.8	91.1 \pm 0.4	90.1 \pm 2.0	92.0 \pm 0.6	MEA0	5.5 \pm 2.9	27.6 \pm 18.8	3.5 \pm 0.0	15.7 \pm 10.1	20.8 \pm 20.3
MEA1	3.5 \pm 0.0	10.1 \pm 0.6	17.2 \pm 0.2	44.0 \pm 1.9	79.5 \pm 7.9	MEA1	3.5 \pm 0.0	3.5 \pm 0.0	3.5 \pm 0.0	3.5 \pm 0.0	3.5 \pm 0.0
MEA2	34.0 \pm 1.0	46.1 \pm 0.6	65.9 \pm 2.4	76.1 \pm 2.6	83.9 \pm 3.1	MEA2	31.5 \pm 1.3	43.1 \pm 2.3	64.7 \pm 2.0	75.4 \pm 4.3	83.9 \pm 3.1
MEA3	70.5 \pm 6.3	83.9 \pm 2.6	89.6 \pm 1.0	90.7 \pm 1.1	91.3 \pm 0.5	MEA3	6.7 \pm 2.3	19.5 \pm 21.1	28.6 \pm 19.9	35.8 \pm 22.7	18.8 \pm 21.6
MEA4	61.6 \pm 24.8	77.9 \pm 6.2	86.0 \pm 3.0	89.4 \pm 0.5	89.7 \pm 0.6	MEA4	4.9 \pm 1.9	13.7 \pm 11.6	5.5 \pm 2.9	14.4 \pm 11.3	12.3 \pm 12.5
MEA5	73.1 \pm 9.3	83.9 \pm 1.0	89.4 \pm 1.5	90.7 \pm 0.7	90.4 \pm 0.6	MEA5	3.5 \pm 0.0	34.0 \pm 21.6	29.9 \pm 12.2	25.0 \pm 18.8	18.8 \pm 21.6
AdvMEA	91.4 \pm 0.4	91.0 \pm 0.7	91.6 \pm 1.0	90.9 \pm 1.1	91.0 \pm 0.7	AdvMEA	91.1 \pm 0.5	91.6 \pm 0.7	91.1 \pm 0.9	91.2 \pm 0.8	91.0 \pm 0.4
CEGA	90.7 \pm 1.0	91.8 \pm 0.6	91.6 \pm 0.3	91.3 \pm 0.1	91.5 \pm 0.8	CEGA	89.0 \pm 1.5	90.7 \pm 0.7	91.6 \pm 0.5	91.0 \pm 0.2	91.4 \pm 0.3
Realistic	72.2 \pm 5.2	84.5 \pm 1.3	72.7 \pm 7.7	74.1 \pm 1.2	69.8 \pm 2.1	Realistic	70.1 \pm 1.6	73.5 \pm 1.7	71.5 \pm 1.4	71.5 \pm 2.7	69.6 \pm 3.6
DFEA_I	90.7 \pm 0.2	90.8 \pm 0.2	90.8 \pm 0.5	90.8 \pm 0.2	90.7 \pm 0.3	DFEA_I	90.7 \pm 0.2	90.8 \pm 0.2	90.8 \pm 0.5	90.8 \pm 0.2	90.6 \pm 0.2
DFEA_II	90.9 \pm 0.2	90.0 \pm 0.6	90.6 \pm 0.4	90.1 \pm 0.4	89.5 \pm 0.4	DFEA_II	90.9 \pm 0.2	90.0 \pm 0.6	90.6 \pm 0.4	90.1 \pm 0.4	89.5 \pm 0.4
DFEA_III	90.5 \pm 0.4	90.1 \pm 0.6	90.5 \pm 0.4	90.3 \pm 0.5	90.4 \pm 0.3	DFEA_III	90.5 \pm 0.4	90.1 \pm 0.6	90.5 \pm 0.4	90.3 \pm 0.5	90.4 \pm 0.3

Table 21: RQ1 detailed for dataset=CoauthorPhysics, metric=F1 (%). Rows are attacks; columns are budgets. Mean \pm std across seeds; best per column is bold.

(a) Regime=both						(b) Regime=x_only					
Attack	0.05	0.10	0.25	0.50	1.00	Attack	0.05	0.10	0.25	0.50	1.00
MEA0	71.3 \pm 6.1	78.7 \pm 2.0	80.3 \pm 0.6	80.9 \pm 0.8	84.2 \pm 1.5	MEA0	63.9 \pm 4.3	78.5 \pm 3.6	77.5 \pm 2.1	79.4 \pm 1.4	81.9 \pm 1.0
MEA1	1.4 \pm 0.0	10.4 \pm 1.8	18.5 \pm 1.1	44.0 \pm 1.2	71.6 \pm 5.2	MEA1	1.4 \pm 0.0	10.4 \pm 1.8	18.5 \pm 1.1	44.0 \pm 1.2	71.6 \pm 5.2
MEA2	32.1 \pm 2.9	41.2 \pm 2.4	55.3 \pm 2.5	57.0 \pm 8.9	57.5 \pm 8.9	MEA2	26.3 \pm 2.6	39.0 \pm 0.2	52.9 \pm 5.7	54.1 \pm 8.1	57.4 \pm 8.8
MEA3	61.1 \pm 3.7	70.1 \pm 2.5	79.9 \pm 2.3	79.5 \pm 0.9	80.4 \pm 3.1	MEA3	58.1 \pm 4.4	71.1 \pm 2.8	79.4 \pm 0.5	81.4 \pm 0.8	81.5 \pm 1.6
MEA4	38.8 \pm 7.7	48.9 \pm 6.7	68.6 \pm 1.4	74.8 \pm 1.7	76.1 \pm 0.9	MEA4	21.8 \pm 5.2	61.3 \pm 8.0	69.3 \pm 4.0	75.1 \pm 1.9	76.9 \pm 0.6
MEA5	62.6 \pm 6.6	67.6 \pm 4.2	78.6 \pm 2.6	79.3 \pm 1.6	81.6 \pm 0.6	MEA5	63.0 \pm 6.6	68.0 \pm 3.4	78.6 \pm 2.6	81.1 \pm 1.4	81.0 \pm 1.6
AdvMEA	82.9 \pm 2.3	82.9 \pm 1.7	82.9 \pm 1.0	81.5 \pm 2.2	82.5 \pm 2.0	AdvMEA	81.9 \pm 2.2	82.1 \pm 1.9	81.7 \pm 1.1	83.2 \pm 0.9	81.6 \pm 2.2
CEGA	80.5 \pm 1.4	80.3 \pm 3.9	80.3 \pm 1.6	79.8 \pm 1.3	80.2 \pm 0.2	CEGA	79.8 \pm 1.9	81.6 \pm 1.2	81.8 \pm 0.5	81.2 \pm 1.0	81.1 \pm 0.7
Realistic	64.7 \pm 4.0	64.9 \pm 5.4	65.2 \pm 1.1	62.9 \pm 3.2	60.0 \pm 1.1	Realistic	63.4 \pm 4.6	68.1 \pm 5.3	65.6 \pm 4.9	64.1 \pm 3.9	60.6 \pm 0.3
DFEA_I	81.3 \pm 0.5	81.5 \pm 0.2	81.8 \pm 0.7	81.9 \pm 0.5	81.7 \pm 0.3	DFEA_I	81.3 \pm 0.5	81.5 \pm 0.2	81.8 \pm 0.7	81.9 \pm 0.5	81.7 \pm 0.3
DFEA_II	82.0 \pm 0.3	80.3 \pm 1.2	81.7 \pm 1.0	80.7 \pm 1.0	79.4 \pm 0.6	DFEA_II	82.0 \pm 0.3	80.3 \pm 1.2	81.7 \pm 1.0	80.7 \pm 1.0	79.4 \pm 0.6
DFEA_III	81.1 \pm 0.9	80.4 \pm 1.2	81.4 \pm 0.9	81.2 \pm 1.1	81.1 \pm 0.3	DFEA_III	81.0 \pm 1.0	80.4 \pm 1.2	81.4 \pm 0.9	81.2 \pm 1.1	81.1 \pm 0.3

(c) Regime=a_only						(d) Regime=data_free					
Attack	0.05	0.10	0.25	0.50	1.00	Attack	0.05	0.10	0.25	0.50	1.00
MEA0	70.1 \pm 6.9	78.0 \pm 1.8	80.6 \pm 0.4	79.9 \pm 3.5	82.7 \pm 1.6	MEA0	2.1 \pm 1.0	7.9 \pm 4.9	1.4 \pm 0.0	5.2 \pm 2.9	6.0 \pm 5.2
MEA1	1.4 \pm 0.0	10.4 \pm 1.8	18.5 \pm 1.1	44.0 \pm 1.2	71.6 \pm 5.2	MEA1	1.4 \pm 0.0	1.4 \pm 0.0	1.4 \pm 0.0	1.4 \pm 0.0	1.4 \pm 0.0
MEA2	29.8 \pm 2.9	37.7 \pm 1.8	57.0 \pm 3.8	58.9 \pm 7.7	57.5 \pm 8.9	MEA2	31.4 \pm 2.6	39.8 \pm 0.8	55.2 \pm 2.1	58.4 \pm 8.2	57.5 \pm 8.9
MEA3	62.6 \pm 2.9	72.7 \pm 1.8	78.8 \pm 1.7	79.9 \pm 3.0	81.4 \pm 1.0	MEA3	3.5 \pm 2.1	6.2 \pm 5.1	10.2 \pm 7.7	17.1 \pm 9.7	5.3 \pm 5.6
MEA4	42.8 \pm 15.8	51.2 \pm 5.7	64.2 \pm 3.1	76.4 \pm 2.3	76.6 \pm 0.9	MEA4	1.8 \pm 0.7	4.5 \pm 3.4	2.1 \pm 1.0	4.7 \pm 3.3	4.0 \pm 3.7
MEA5	60.1 \pm 9.1	72.1 \pm 0.8	78.0 \pm 2.2	79.9 \pm 1.2	79.1 \pm 1.1	MEA5	1.4 \pm 0.0	9.3 \pm 5.6	12.3 \pm 4.0	9.0 \pm 5.4	5.3 \pm 5.6
AdvMEA	82.8 \pm 1.1	82.1 \pm 1.7	82.9 \pm 2.2	81.8 \pm 1.8	82.1 \pm 1.5	AdvMEA	82.5 \pm 1.3	82.7 \pm 1.6	82.2 \pm 2.0	82.7 \pm 1.6	82.3 \pm 0.9
CEGA	79.2 \pm 2.1	80.7 \pm 0.7	81.6 \pm 0.7	81.3 \pm 1.2	80.6 \pm 0.5	CEGA	77.8 \pm 1.5	79.5 \pm 2.5	80.4 \pm 0.9	80.4 \pm 0.5	80.8 \pm 1.0
Realistic	52.4 \pm 8.7	70.5 \pm 2.6	60.2 \pm 6.0	60.1 \pm 2.4	56.2 \pm 1.3	Realistic	56.4 \pm 3.0	58.3 \pm 1.0	58.5 \pm 1.9	56.0 \pm 2.7	55.1 \pm 2.9
DFEA_I	81.3 \pm 0.5	81.5 \pm 0.2	81.8 \pm 0.7	81.9 \pm 0.5	81.7 \pm 0.3	DFEA_I	81.3 \pm 0.5	81.5 \pm 0.2	81.8 \pm 0.7	81.9 \pm 0.5	81.7 \pm 0.3
DFEA_II	82.0 \pm 0.3	80.3 \pm 1.2	81.7 \pm 1.0	80.7 \pm 1.0	79.4 \pm 0.6	DFEA_II	82.0 \pm 0.3	80.3 \pm 1.2	81.7 \pm 1.0	80.7 \pm 1.0	79.4 \pm 0.6
DFEA_III	81.1 \pm 0.9	80.4 \pm 1.2	81.4 \pm 0.9	81.2 \pm 1.1	81.1 \pm 0.3	DFEA_III	81.1 \pm 0.9	80.4 \pm 1.2	81.4 \pm 0.9	81.2 \pm 1.1	81.1 \pm 0.3

F.4 Attack effectiveness on the three additional datasets

We report the per-attack and per-budget fidelity for all twelve attacks on the three additional graphs (RomanEmpire, AmazonRatings, OGBN-Arxiv) in the four regimes. Constant values across budgets reflect attacks whose surrogate is independent of the query budget (e.g., the data-free DFEA variants, which always train on the same synthesized queries).

Table 22: RQ1 detailed for dataset=CoauthorPhysics, metric=Fidelity (%). Rows are attacks; columns are budgets. Mean \pm std across seeds; best per column is bold.

(a) Regime=both						(b) Regime=x_only					
Attack	0.05	0.10	0.25	0.50	1.00	Attack	0.05	0.10	0.25	0.50	1.00
MEA0	81.9 \pm 4.5	89.3 \pm 0.9	92.5 \pm 0.7	92.8 \pm 0.9	94.2 \pm 0.1	MEA0	80.4 \pm 4.7	89.9 \pm 1.2	92.0 \pm 1.5	93.6 \pm 0.7	93.3 \pm 0.8
MEA1	2.7 \pm 0.5	9.5 \pm 0.3	15.3 \pm 0.7	44.4 \pm 1.6	78.6 \pm 7.3	MEA1	2.7 \pm 0.5	9.5 \pm 0.3	15.3 \pm 0.7	44.4 \pm 1.6	78.6 \pm 7.3
MEA2	32.5 \pm 2.5	44.8 \pm 1.9	69.0 \pm 1.0	76.1 \pm 4.9	85.8 \pm 3.2	MEA2	30.4 \pm 2.2	41.2 \pm 2.5	66.3 \pm 4.1	74.0 \pm 6.2	85.7 \pm 3.1
MEA3	74.4 \pm 2.1	80.8 \pm 3.0	89.1 \pm 1.0	90.4 \pm 1.7	93.0 \pm 0.7	MEA3	74.5 \pm 1.4	83.1 \pm 2.9	90.1 \pm 1.2	92.6 \pm 1.4	92.9 \pm 0.4
MEA4	69.2 \pm 11.7	75.4 \pm 11.2	90.7 \pm 0.9	95.5 \pm 0.6	97.8 \pm 0.4	MEA4	40.3 \pm 18.5	84.0 \pm 4.2	90.9 \pm 0.1	94.4 \pm 0.4	98.1 \pm 0.6
MEA5	74.3 \pm 5.8	77.5 \pm 4.9	89.5 \pm 1.5	91.2 \pm 1.4	91.9 \pm 0.2	MEA5	75.8 \pm 5.7	77.8 \pm 6.2	89.1 \pm 1.4	92.4 \pm 1.1	93.4 \pm 0.9
AdvMEA	90.0 \pm 0.5	90.2 \pm 0.5	89.7 \pm 0.8	89.5 \pm 0.9	90.2 \pm 0.4	AdvMEA	89.8 \pm 0.6	90.4 \pm 0.2	89.8 \pm 0.2	90.0 \pm 0.3	89.9 \pm 0.3
CEGA	91.0 \pm 1.4	91.6 \pm 1.3	94.1 \pm 0.0	94.9 \pm 0.3	96.8 \pm 0.3	CEGA	92.3 \pm 1.3	93.0 \pm 1.3	94.1 \pm 0.6	94.7 \pm 0.8	96.3 \pm 0.8
Realistic	80.5 \pm 4.1	77.5 \pm 6.4	82.2 \pm 1.6	77.4 \pm 2.2	74.3 \pm 1.4	Realistic	79.1 \pm 6.6	84.3 \pm 4.3	81.0 \pm 2.9	79.2 \pm 2.2	76.7 \pm 1.1
DFEA_I	95.4 \pm 0.3	96.4 \pm 0.6	97.3 \pm 0.3	97.6 \pm 0.7	97.7 \pm 0.7	DFEA_I	95.4 \pm 0.3	96.4 \pm 0.6	97.3 \pm 0.3	97.6 \pm 0.7	97.7 \pm 0.7
DFEA_II	93.6 \pm 0.7	94.4 \pm 0.5	96.3 \pm 0.2	97.3 \pm 0.1	99.6 \pm 0.1	DFEA_II	93.6 \pm 0.7	94.4 \pm 0.5	96.3 \pm 0.2	97.3 \pm 0.1	99.6 \pm 0.1
DFEA_III	93.7 \pm 0.3	95.1 \pm 0.4	96.8 \pm 0.4	97.7 \pm 0.4	98.7 \pm 0.1	DFEA_III	93.6 \pm 0.2	95.1 \pm 0.4	96.8 \pm 0.4	97.7 \pm 0.4	98.7 \pm 0.1

(c) Regime=a_only						(d) Regime=data_free					
Attack	0.05	0.10	0.25	0.50	1.00	Attack	0.05	0.10	0.25	0.50	1.00
MEA0	84.5 \pm 3.8	88.6 \pm 0.5	91.9 \pm 0.8	91.8 \pm 1.0	94.5 \pm 0.4	MEA0	4.6 \pm 2.8	27.6 \pm 18.8	2.7 \pm 0.5	16.3 \pm 11.3	19.5 \pm 20.3
MEA1	2.7 \pm 0.5	9.5 \pm 0.3	15.3 \pm 0.7	44.4 \pm 1.6	78.6 \pm 7.3	MEA1	2.7 \pm 0.5	2.7 \pm 0.5	2.7 \pm 0.5	2.7 \pm 0.5	2.7 \pm 0.5
MEA2	33.7 \pm 0.6	46.5 \pm 1.1	68.5 \pm 2.6	77.9 \pm 3.1	85.8 \pm 3.2	MEA2	31.1 \pm 1.6	43.4 \pm 2.3	67.7 \pm 1.7	77.6 \pm 4.8	85.8 \pm 3.2
MEA3	69.7 \pm 6.2	84.3 \pm 3.2	89.8 \pm 0.5	90.7 \pm 0.3	93.7 \pm 0.8	MEA3	6.2 \pm 2.2	18.9 \pm 20.8	28.8 \pm 20.2	35.8 \pm 22.6	17.8 \pm 21.4
MEA4	61.1 \pm 25.0	78.4 \pm 6.6	89.0 \pm 1.9	94.6 \pm 0.7	97.9 \pm 0.3	MEA4	4.6 \pm 2.7	14.6 \pm 12.7	4.6 \pm 2.8	14.7 \pm 12.6	12.5 \pm 13.9
MEA5	72.1 \pm 9.2	84.0 \pm 1.2	90.4 \pm 1.9	92.6 \pm 0.9	94.4 \pm 0.3	MEA5	2.7 \pm 0.5	33.3 \pm 21.6	30.5 \pm 12.9	24.6 \pm 18.9	17.9 \pm 21.9
AdvMEA	90.0 \pm 0.9	90.1 \pm 0.1	90.1 \pm 0.4	89.9 \pm 0.8	90.1 \pm 0.3	AdvMEA	89.7 \pm 0.6	90.5 \pm 0.9	89.9 \pm 0.6	90.0 \pm 0.7	89.7 \pm 0.3
CEGA	91.5 \pm 0.4	93.3 \pm 0.6	93.5 \pm 0.4	95.6 \pm 1.1	96.2 \pm 0.4	CEGA	89.6 \pm 1.7	92.8 \pm 0.7	95.0 \pm 0.2	95.1 \pm 1.0	96.5 \pm 0.4
Realistic	72.8 \pm 4.6	85.6 \pm 2.4	73.0 \pm 7.3	75.6 \pm 1.1	72.0 \pm 3.2	Realistic	72.7 \pm 2.0	75.2 \pm 2.1	73.5 \pm 0.7	73.5 \pm 2.0	71.6 \pm 4.1
DFEA_I	95.4 \pm 0.3	96.4 \pm 0.6	97.3 \pm 0.3	97.6 \pm 0.7	97.7 \pm 0.7	DFEA_I	95.4 \pm 0.3	96.4 \pm 0.6	97.3 \pm 0.3	97.6 \pm 0.7	97.7 \pm 0.7
DFEA_II	93.6 \pm 0.7	94.4 \pm 0.5	96.3 \pm 0.2	97.3 \pm 0.1	99.6 \pm 0.1	DFEA_II	93.6 \pm 0.7	94.4 \pm 0.5	96.3 \pm 0.2	97.3 \pm 0.1	99.6 \pm 0.1
DFEA_III	93.7 \pm 0.3	95.1 \pm 0.4	96.8 \pm 0.4	97.7 \pm 0.4	98.7 \pm 0.1	DFEA_III	93.7 \pm 0.3	95.1 \pm 0.4	96.8 \pm 0.4	97.7 \pm 0.4	98.7 \pm 0.1

Table 23: RQ1 detailed for dataset=Computers, metric=Acc (%). Rows are attacks; columns are budgets. Mean \pm std across seeds; best per column is bold.

(a) Regime=both						(b) Regime=x_only					
Attack	0.05	0.10	0.25	0.50	1.00	Attack	0.05	0.10	0.25	0.50	1.00
MEA0	51.7 \pm 7.0	60.4 \pm 4.2	65.7 \pm 2.4	67.3 \pm 2.3	71.4 \pm 1.4	MEA0	54.7 \pm 8.8	63.8 \pm 1.1	64.4 \pm 5.4	64.7 \pm 6.9	67.0 \pm 4.9
MEA1	46.4 \pm 19.1	31.3 \pm 14.7	48.1 \pm 2.6	51.9 \pm 1.4	53.0 \pm 5.3	MEA1	46.4 \pm 19.1	31.3 \pm 14.7	48.0 \pm 2.5	51.7 \pm 1.3	52.9 \pm 5.6
MEA2	40.2 \pm 23.5	43.0 \pm 22.8	42.1 \pm 25.4	40.8 \pm 26.2	41.5 \pm 26.7	MEA2	41.5 \pm 23.0	42.1 \pm 21.0	41.8 \pm 24.8	41.4 \pm 25.6	41.5 \pm 26.7
MEA3	61.6 \pm 2.2	69.8 \pm 2.0	66.0 \pm 1.3	69.3 \pm 2.5	70.7 \pm 3.1	MEA3	63.7 \pm 3.0	68.4 \pm 1.8	69.2 \pm 3.4	70.3 \pm 3.9	70.1 \pm 1.8
MEA4	41.7 \pm 14.8	35.0 \pm 19.2	65.9 \pm 4.1	66.5 \pm 3.7	71.7 \pm 0.3	MEA4	31.7 \pm 4.2	37.0 \pm 22.1	61.4 \pm 4.3	67.2 \pm 0.9	71.4 \pm 1.1
MEA5	67.8 \pm 2.0	68.8 \pm 2.9	69.4 \pm 3.1	70.5 \pm 3.3	70.1 \pm 4.2	MEA5	69.9 \pm 2.3	67.7 \pm 2.3	67.9 \pm 3.1	71.1 \pm 3.3	72.1 \pm 1.9
AdvMEA	34.7 \pm 17.3	20.8 \pm 22.8	22.4 \pm 23.3	46.8 \pm 13.1	16.8 \pm 11.4	AdvMEA	27.6 \pm 23.9	33.1 \pm 21.1	31.6 \pm 22.4	29.5 \pm 21.4	40.4 \pm 26.8
CEGA	29.8 \pm 21.9	27.8 \pm 20.7	34.8 \pm 14.0	45.4 \pm 24.1	39.6 \pm 25.5	CEGA	27.9 \pm 17.2	27.5 \pm 20.0	43.6 \pm 25.0	25.1 \pm 22.5	41.6 \pm 29.1
Realistic	2.4 \pm 1.1	1.1 \pm 0.7	1.1 \pm 0.7	1.5 \pm 1.2	1.1 \pm 0.7	Realistic	12.9 \pm 15.6	13.2 \pm 16.7	1.1 \pm 0.7	13.6 \pm 16.6	10.9 \pm 13.6
DFEA_I	39.2 \pm 24.6	40.5 \pm 15.6	39.9 \pm 22.8	36.9 \pm 22.9	45.4 \pm 13.7	DFEA_I	38.5 \pm 24.2	40.6 \pm 15.7	39.9 \pm 22.8	37.0 \pm 22.9	45.4 \pm 13.7
DFEA_II	31.5 \pm 19.0	30.1 \pm 18.0	30.1 \pm 18.0	30.1 \pm 18.0	30.1 \pm 18.0	DFEA_II	31.5 \pm 19.0	30.1 \pm 18.0	30.1 \pm 18.0	30.1 \pm 18.0	30.1 \pm 18.0
DFEA_III	45.2 \pm 22.1	41.3 \pm 16.4	44.1 \pm 21.4	46.4 \pm 21.2	46.1 \pm 21.7	DFEA_III	44.2 \pm 22.0	41.2 \pm 16.4	44.1 \pm 21.4	46.6 \pm 21.3	45.7 \pm 21.6

(c) Regime=a_only						(d) Regime=data_free					
Attack	0.05	0.10	0.25	0.50	1.00	Attack	0.05	0.10	0.25	0.50	1.00
MEA0	62.9 \pm 5.2	64.4 \pm 2.9	62.3 \pm 1.6	67.7 \pm 2.6	67.6 \pm 3.3	MEA0	25.7 \pm 22.9	11.7 \pm 7.5	29.7 \pm 18.9	44.1 \pm 16.9	8.6 \pm 8.2
MEA1	46.4 \pm 19.1	31.3 \pm 14.7	48.1 \pm 2.6	51.9 \pm 1.4	53.0 \pm 5.3	MEA1	56.1 \pm 0.0	56.1 \pm 0.0	56.1 \pm 0.0	56.1 \pm 0.0	56.1 \pm 0.0
MEA2	38.9 \pm 21.1	41.3 \pm 23.3	41.3 \pm 24.3	41.4 \pm 26.5	41.5 \pm 26.7	MEA2	40.1 \pm 21.2	41.5 \pm 21.8	42.5 \pm 22.9	40.1 \pm 25.0	41.5 \pm 26.7
MEA3	62.1 \pm 2.2	67.2 \pm 1.0	68.1 \pm 4.2	65.2 \pm 5.8	71.7 \pm 1.7	MEA3	38.6 \pm 24.7	41.7 \pm 20.4	27.3 \pm 20.9	25.6 \pm 23.0	19.8 \pm 25.7
MEA4	40.2 \pm 16.5	44.6 \pm 19.3	54.0 \pm 17.1	62.2 \pm 7.8	68.4 \pm 0.5	MEA4	25.6 \pm 23.0	4.7 \pm 5.8	19.0 \pm 26.2	5.7 \pm 5.3	4.7 \pm 5.8
MEA5	64.5 \pm 4.1	69.9 \pm 0.5	68.3 \pm 1.8	71.5 \pm 4.9	71.7 \pm 1.6	MEA5	19.3 \pm 26.0	20.9 \pm 25.0	25.4 \pm 22.0	26.5 \pm 21.2	24.8 \pm 22.8
AdvMEA	36.9 \pm 14.9	40.3 \pm 16.2	27.0 \pm 23.9	31.6 \pm 24.1	17.2 \pm 8.3	AdvMEA	42.6 \pm 13.0	32.0 \pm 16.6	23.6 \pm 21.7	20.7 \pm 17.0	39.4 \pm 10.4
CEGA	29.1 \pm 16.6	31.0 \pm 20.7	39.7 \pm 23.2	36.1 \pm 25.4	39.3 \pm 28.1	CEGA	30.4 \pm 15.3	17.2 \pm 17.0	39.6 \pm 28.3	34.9 \pm 26.8	36.4 \pm 24.5
Realistic	12.7 \pm 16.1	1.5 \pm 1.2	15.0 \pm 19.4	1.1 \pm 0.7	14.6 \pm 18.4	Realistic	13.6 \pm 17.4	1.3 \pm 0.5	10.8 \pm 13.4	8.2 \pm 9.7	1.0 \pm 0.6
DFEA_I	39.1 \pm 24.5	40.1 \pm 15.4	39.9 \pm 22.8	37.0 \pm 22.9	45.5 \pm 13.8	DFEA_I	38.7 \pm 24.3	40.4 \pm 15.6	39.9 \pm 22.8	37.0 \pm 23.0	45.5 \pm 13.8
DFEA_II	31.2 \pm 18.8	30.1 \pm 18.0	30.1 \pm 18.0	25.4 \pm 15.7	30.1 \pm 18.0	DFEA_II	31.2 \pm 18.8	30.1 \pm 18.0	30.1 \pm 18.0	30.1 \pm 18.0	30.1 \pm 18.0
DFEA_III	44.2 \pm 22.0	41.3 \pm 16.4	44.1 \pm 21.4	46.6 \pm 21.3	46.1 \pm 21.7	DFEA_III	44.2 \pm 22.0	41.3 \pm 16.4	44.1 \pm 21.4	46.6 \pm 21.3	45.7 \pm 21.6

F.5 Standard deviations for information-limiting defenses

Tables 39–40 extend Table 3 of the main text with standard deviations for each protected-model accuracy and verification proxy. The seven defenses are split across two tables for readability: the four output-perturbation / prediction-rounding defenses are in Table 39, and the three query-detection defenses are in Table 40.

Heatmap view of the seven information-limiting defenses. Figure 7 reports the same numbers as Tables 39–40 as a 10×7 heatmap, with protected-model accuracy on the left panel and the verification proxy on the right panel. The two-panel view exposes three patterns which are not visible in the per-defense tables. *First, the verification proxy clusters into two regimes.* The four

Table 24: RQ1 detailed for dataset=Computers, metric=F1 (%). Rows are attacks; columns are budgets. Mean \pm std across seeds; best per column is bold.

(a) Regime=both						(b) Regime=x_only					
Attack	0.05	0.10	0.25	0.50	1.00	Attack	0.05	0.10	0.25	0.50	1.00
MEA0	22.0 \pm 6.0	44.3 \pm 4.0	46.4 \pm 8.0	44.1 \pm 2.0	60.0 \pm 0.6	MEA0	29.9 \pm 7.4	41.9 \pm 4.5	43.1 \pm 8.7	42.5 \pm 18.6	50.8 \pm 7.5
MEA1	13.0 \pm 6.0	7.6 \pm 3.7	17.2 \pm 5.5	19.3 \pm 7.8	22.7 \pm 4.6	MEA1	13.0 \pm 6.0	7.6 \pm 3.7	17.1 \pm 5.5	19.9 \pm 8.5	27.8 \pm 2.7
MEA2	20.3 \pm 12.7	27.3 \pm 15.1	27.8 \pm 18.1	26.5 \pm 18.2	27.1 \pm 18.8	MEA2	25.4 \pm 14.1	26.3 \pm 12.6	26.6 \pm 15.9	27.5 \pm 18.5	27.1 \pm 18.8
MEA3	20.6 \pm 4.3	41.7 \pm 4.6	44.0 \pm 4.2	54.5 \pm 4.0	58.8 \pm 2.5	MEA3	29.0 \pm 3.6	40.5 \pm 2.5	50.5 \pm 7.4	51.0 \pm 12.1	56.9 \pm 3.9
MEA4	13.8 \pm 1.8	16.5 \pm 9.6	28.0 \pm 6.6	36.7 \pm 9.7	46.8 \pm 4.4	MEA4	12.7 \pm 4.4	15.6 \pm 5.3	24.6 \pm 5.1	34.5 \pm 9.6	47.8 \pm 1.1
MEA5	29.8 \pm 1.1	39.5 \pm 4.5	56.3 \pm 4.8	53.5 \pm 1.9	53.7 \pm 8.7	MEA5	32.9 \pm 4.8	39.0 \pm 4.6	50.6 \pm 8.6	52.5 \pm 4.6	59.5 \pm 1.9
AdvMEA	21.7 \pm 13.1	14.9 \pm 14.0	15.5 \pm 16.6	30.0 \pm 8.0	12.0 \pm 9.9	AdvMEA	17.3 \pm 13.6	17.5 \pm 12.9	22.8 \pm 16.0	18.8 \pm 11.7	27.5 \pm 18.8
CEGA	26.8 \pm 18.9	22.8 \pm 15.0	31.3 \pm 15.1	39.5 \pm 23.5	33.4 \pm 21	CEGA	29.1 \pm 17.2	27.1 \pm 19.3	36.9 \pm 20.2	21.0 \pm 20.3	35.8 \pm 25.5
Realistic	2.0 \pm 1.2	0.2 \pm 0.1	0.2 \pm 0.1	0.5 \pm 0.3	0.2 \pm 0.1	Realistic	3.9 \pm 4.3	5.1 \pm 6.8	0.2 \pm 0.1	5.5 \pm 7.2	3.2 \pm 4.1
DFEA_I	32.3 \pm 22.5	29.9 \pm 16.3	33.4 \pm 19.9	28.2 \pm 20.8	29.6 \pm 19.0	DFEA_I	31.9 \pm 22.1	30.0 \pm 16.4	33.2 \pm 19.7	27.8 \pm 20.3	29.6 \pm 19.0
DFEA_II	11.7 \pm 9.4	4.3 \pm 2.4	4.3 \pm 2.4	4.3 \pm 2.4	4.3 \pm 2.4	DFEA_II	11.7 \pm 9.4	4.3 \pm 2.4	4.3 \pm 2.4	4.3 \pm 2.4	4.3 \pm 2.4
DFEA_III	34.2 \pm 18.1	27.6 \pm 15.8	32.1 \pm 18.4	38.0 \pm 20.3	38.7 \pm 20.9	DFEA_III	30.4 \pm 15.7	26.8 \pm 14.8	32.1 \pm 18.4	38.1 \pm 20.4	37.6 \pm 20.3

(c) Regime=a_only						(d) Regime=data_free					
Attack	0.05	0.10	0.25	0.50	1.00	Attack	0.05	0.10	0.25	0.50	1.00
MEA0	33.3 \pm 3.9	44.3 \pm 5.7	35.8 \pm 10.0	55.1 \pm 0.6	52.9 \pm 5.0	MEA0	3.6 \pm 2.9	2.0 \pm 1.2	4.3 \pm 2.1	5.9 \pm 1.8	1.5 \pm 1.3
MEA1	13.0 \pm 6.0	7.6 \pm 3.7	17.2 \pm 5.5	19.3 \pm 7.8	22.7 \pm 4.6	MEA1	7.2 \pm 0.0	7.2 \pm 0.0	7.2 \pm 0.0	7.2 \pm 0.0	7.2 \pm 0.0
MEA2	22.1 \pm 12.5	25.9 \pm 15.4	26.8 \pm 16.7	27.2 \pm 18.7	27.1 \pm 18.8	MEA2	24.2 \pm 11.6	25.1 \pm 13.5	25.3 \pm 13.9	26.2 \pm 17.5	27.1 \pm 18.8
MEA3	24.9 \pm 1.6	34.9 \pm 1.8	45.5 \pm 9.0	42.4 \pm 18.4	60.8 \pm 2.4	MEA3	5.0 \pm 3.1	5.6 \pm 2.3	5.1 \pm 3.5	3.5 \pm 2.9	2.7 \pm 3.2
MEA4	15.1 \pm 4.4	16.4 \pm 9.1	27.8 \pm 5.7	32.1 \pm 8.9	40.6 \pm 5.5	MEA4	3.5 \pm 2.9	0.8 \pm 1.0	2.5 \pm 3.3	1.0 \pm 0.9	0.8 \pm 1.0
MEA5	32.5 \pm 5.3	38.5 \pm 1.8	48.9 \pm 5.2	57.0 \pm 9.1	58.4 \pm 1.5	MEA5	2.7 \pm 3.2	3.3 \pm 2.9	4.8 \pm 3.0	4.4 \pm 2.1	4.4 \pm 2.9
AdvMEA	23.1 \pm 12.3	25.9 \pm 11.9	17.8 \pm 16.5	20.0 \pm 15.2	11.9 \pm 6.3	AdvMEA	31.8 \pm 11.4	21.1 \pm 13.9	13.9 \pm 11.5	16.2 \pm 13.4	23.3 \pm 8.1
CEGA	21.5 \pm 15.5	22.0 \pm 23.1	33.2 \pm 19.2	31.4 \pm 19.8	34.6 \pm 25.0	CEGA	21.7 \pm 13.3	15.7 \pm 18.4	32.8 \pm 22.6	28.1 \pm 20.6	35.5 \pm 22.6
Realistic	4.0 \pm 5.2	0.4 \pm 0.3	4.3 \pm 5.6	0.2 \pm 0.1	4.8 \pm 5.8	Realistic	5.2 \pm 6.9	1.0 \pm 1.1	3.6 \pm 4.7	2.2 \pm 2.7	0.2 \pm 0.1
DFEA_I	31.9 \pm 22.1	29.6 \pm 15.9	33.4 \pm 19.9	27.8 \pm 20.3	29.3 \pm 18.7	DFEA_I	31.7 \pm 22.0	29.8 \pm 16.1	33.4 \pm 19.9	27.8 \pm 20.3	29.3 \pm 18.7
DFEA_II	11.6 \pm 9.4	4.3 \pm 2.4	4.3 \pm 2.4	6.1 \pm 4.3	4.3 \pm 2.4	DFEA_II	11.5 \pm 9.3	4.3 \pm 2.4	4.3 \pm 2.4	4.3 \pm 2.4	4.3 \pm 2.4
DFEA_III	30.4 \pm 15.7	27.6 \pm 15.8	32.1 \pm 18.4	38.1 \pm 20.3	38.7 \pm 20.9	DFEA_III	30.4 \pm 15.7	27.6 \pm 15.8	32.0 \pm 18.4	38.1 \pm 20.4	37.6 \pm 20.3

Table 25: RQ1 detailed for dataset=Computers, metric=Fidelity (%). Rows are attacks; columns are budgets. Mean \pm std across seeds; best per column is bold.

(a) Regime=both						(b) Regime=x_only					
Attack	0.05	0.10	0.25	0.50	1.00	Attack	0.05	0.10	0.25	0.50	1.00
MEA0	51.0 \pm 7.0	67.3 \pm 3.1	67.0 \pm 1.5	71.4 \pm 2.7	80.5 \pm 4.6	MEA0	54.8 \pm 10.5	65.4 \pm 7.0	70.6 \pm 2.9	69.7 \pm 10.9	79.8 \pm 3.1
MEA1	41.5 \pm 15.5	27.7 \pm 14.0	46.2 \pm 5.5	49.4 \pm 5.6	56.3 \pm 12.6	MEA1	41.5 \pm 15.5	27.7 \pm 14.0	46.2 \pm 5.5	49.1 \pm 5.7	57.1 \pm 11.4
MEA2	51.0 \pm 7.5	58.8 \pm 6.0	65.2 \pm 2.4	66.2 \pm 6.3	68.3 \pm 8.0	MEA2	53.9 \pm 6.6	58.6 \pm 6.4	63.9 \pm 0.6	68.4 \pm 5.0	68.3 \pm 8.0
MEA3	53.8 \pm 3.0	64.8 \pm 5.5	67.6 \pm 6.2	74.9 \pm 4.3	79.5 \pm 5.2	MEA3	56.5 \pm 7.4	61.9 \pm 5.6	68.2 \pm 4.2	71.7 \pm 4.9	77.6 \pm 3.1
MEA4	38.4 \pm 13.4	37.9 \pm 12.6	63.6 \pm 4.0	74.3 \pm 5.0	83.7 \pm 4.3	MEA4	33.7 \pm 0.4	34.7 \pm 18.5	65.6 \pm 4.0	75.7 \pm 0.8	84.6 \pm 3.4
MEA5	61.3 \pm 4.3	65.6 \pm 6.4	66.5 \pm 2.1	73.9 \pm 3.5	76.3 \pm 4.2	MEA5	59.4 \pm 3.4	65.5 \pm 5.2	71.0 \pm 3.6	75.4 \pm 5.6	79.5 \pm 3.5
AdvMEA	35.5 \pm 17.8	25.7 \pm 24.7	26.9 \pm 22.4	46.1 \pm 12.5	22.8 \pm 11.8	AdvMEA	29.0 \pm 24.1	33.6 \pm 19.9	34.5 \pm 23.4	28.7 \pm 16.6	39.8 \pm 25.8
CEGA	36.0 \pm 25.0	36.7 \pm 23.0	43.4 \pm 17.5	53.9 \pm 29.2	54.1 \pm 33.4	CEGA	30.9 \pm 16.1	33.6 \pm 25.2	49.2 \pm 24.3	33.1 \pm 30.1	49.8 \pm 33.8
Realistic	64.5 \pm 33.7	67.9 \pm 45.4	67.7 \pm 45.3	67.4 \pm 44.0	67.0 \pm 44.8	Realistic	75.1 \pm 25.8	78.7 \pm 30.0	67.9 \pm 45.4	81.0 \pm 25.5	78.6 \pm 25.1
DFEA_I	67.5 \pm 12.4	73.7 \pm 18.1	60.3 \pm 25.5	64.8 \pm 15.9	55.8 \pm 28.2	DFEA_I	67.3 \pm 12.1	73.5 \pm 18.1	60.7 \pm 25.9	64.9 \pm 16.2	55.4 \pm 27.8
DFEA_II	43.9 \pm 8.1	28.4 \pm 20.5	28.4 \pm 20.5	28.4 \pm 20.5	28.4 \pm 20.5	DFEA_II	43.9 \pm 8.1	28.4 \pm 20.5	28.4 \pm 20.5	28.4 \pm 20.5	28.4 \pm 20.5
DFEA_III	72.9 \pm 5.5	66.7 \pm 14.2	72.9 \pm 3.1	82.5 \pm 3.1	82.1 \pm 2.8	DFEA_III	69.9 \pm 2.4	65.7 \pm 13.4	72.9 \pm 3.1	82.2 \pm 2.9	82.3 \pm 2.9

(c) Regime=a_only						(d) Regime=data_free					
Attack	0.05	0.10	0.25	0.50	1.00	Attack	0.05	0.10	0.25	0.50	1.00
MEA0	60.7 \pm 2.6	66.5 \pm 6.5	66.1 \pm 1.6	77.1 \pm 2.9	78.8 \pm 0.9	MEA0	22.2 \pm 16.0	9.5 \pm 6.5	22.7 \pm 14.2	33.7 \pm 11.0	14.2 \pm 10.6
MEA1	41.5 \pm 15.5	27.7 \pm 14.0	46.2 \pm 5.5	49.4 \pm 5.6	56.3 \pm 12.6	MEA1	40.4 \pm 1.6	40.4 \pm 1.6	40.4 \pm 1.6	40.4 \pm 1.6	40.4 \pm 1.6
MEA2	47.8 \pm 10.2	59.6 \pm 4.5	64.3 \pm 1.1	66.8 \pm 7.2	68.3 \pm 8.0	MEA2	54.3 \pm 7.2	57.0 \pm 7.2	66.0 \pm 2.4	67.1 \pm 4.5	68.4 \pm 8.0
MEA3	58.0 \pm 4.7	62.7 \pm 5.5	68.4 \pm 4.2	65.1 \pm 4.4	79.5 \pm 4.4	MEA3	31.8 \pm 13.7	29.5 \pm 15.1	22.4 \pm 13.8	19.9 \pm 16.5	15.6 \pm 18.0
MEA4	42.3 \pm 14.5	38.0 \pm 15.4	54.9 \pm 16.2	64.1 \pm 4.0	81.2 \pm 2.2	MEA4	23.9 \pm 16.7	3.3 \pm 3.6	15.1 \pm 19.0	6.7 \pm 5.1	4.4 \pm 4.7
MEA5	57.7 \pm 4.0	62.8 \pm 3.9	69.7 \pm 5.2	72.5 \pm 3.9	80.9 \pm 3.3	MEA5	16.1 \pm 17.6	15.7 \pm 16.2	18.4 \pm 13.6	22.6 \pm 12.8	23.1 \pm 14.1
AdvMEA	39.9 \pm 16.5	40.0 \pm 16.3	32.3 \pm 22.2	32.2 \pm 23.3	20.2 \pm 8.3	AdvMEA	44.9 \pm 13.6	34.2 \pm 18.1	21.6 \pm 17.4	24.3 \pm 18.1	40.7 \pm 12.2
CEGA	37.9 \pm 19.9	37.9 \pm 23.5	50.1 \pm 27.4	45.4 \pm 30.8	51.6 \pm 32.9	CEGA	33.6 \pm 15.6	21.0 \pm 18.4	49.4 \pm 31.1	46.2 \pm 32.9	50.0 \pm 30.4
Realistic	69.5 \pm 26.3	64.5 \pm 43.1	77.2 \pm 30.2	67.8 \pm 45.4	80.8 \pm 26.0	Realistic	82.1 \pm 22.2	70.2 \pm 41.7	82.5 \pm 24.8	75.5 \pm 34.6	66.5 \pm 44.5
DFEA_I	67.3 \pm 12.2	73.2 \pm 17.9	60.3 \pm 25.5	64.9 \pm 16.2	55.8 \pm 28.1	DFEA_I	67.3 \pm 12.2	73.8 \pm 18.2	60.3 \pm 25.5	65.1 \pm 16.3	55.8 \pm 28.1
DFEA_II	44.2 \pm 7.8	28.4 \pm 20.4	28.4 \pm 20.5	38.9 \pm 12.6	28.4 \pm 20.5	DFEA_II	44.2 \pm 7.8	28.4 \pm 20.5	28.4 \pm 20.5	28.4 \pm 20.5	28.4 \pm 20.4
DFEA_III	69.9 \pm 2.4	66.7 \pm 14.2	72.9 \pm 3.1	82.4 \pm 3.1	82.1 \pm 2.8	DFEA_III	69.9 \pm 2.4	66.7 \pm 14.2	73.0 \pm 2.9	82.2 \pm 2.9	82.3 \pm 2.9

output-perturbation and rounding defenses (OP_low, OP_high, PR_2bit, PR_top1) plus GradRedirect verify at $\geq 80\%$ on every dataset, while the two query-detection defenses (PRADA, AdaptMisinfo) verify at $\sim 50\%$ on most homophilic graphs and below 50% on *RomanEmpire*; this is consistent with the joint-evaluation behaviour reported in Appendix F.8, where the same two defenses are also the strongest at reducing surrogate fidelity. *Second, the accuracy panel is largely flat across defenses on the eight non-Computers datasets.* The output-perturbation methods leave protected accuracy within ~ 2 pp of the undefended baseline on *Cora*, *CiteSeer*, *PubMed*, *Photo*, *CoauthorCS*, *CoauthorPhysics*, *OGBN-Arxiv*, and *AmazonRatings*, which means the protection signal in those rows is carried entirely by the verification panel. *Third, Computers is the only dataset where the accuracy panel is heterogeneous:* every defense produces high variance, and three defenses (OP_high, PR_2bit, AdaptMisinfo) push protected accuracy below 40%, which mirrors the high variance of

Table 26: RQ1 detailed for dataset=Photo, metric=Acc (%). Rows are attacks; columns are budgets. Mean \pm std across seeds; best per column is bold.

(a) Regime=both						(b) Regime=x_only					
Attack	0.05	0.10	0.25	0.50	1.00	Attack	0.05	0.10	0.25	0.50	1.00
MEAO	55.1 \pm 30.4	90.2 \pm 3.8	94.9 \pm 0.6	96.4 \pm 0.2	95.5 \pm 0.4	MEAO	84.5 \pm 5.9	91.1 \pm 2.3	95.4 \pm 0.8	95.9 \pm 0.8	96.0 \pm 0.4
MEA1	2.0 \pm 0.2	39.5 \pm 26.2	42.2 \pm 28.9	62.7 \pm 33.5	67.0 \pm 36.5	MEA1	2.0 \pm 0.2	39.6 \pm 26.4	42.2 \pm 28.9	62.7 \pm 33.5	67.0 \pm 36.5
MEA2	84.4 \pm 2.3	89.0 \pm 1.9	90.1 \pm 2.2	91.4 \pm 2.0	92.4 \pm 2.3	MEA2	87.8 \pm 2.0	89.3 \pm 2.2	90.6 \pm 1.9	91.1 \pm 2.4	92.4 \pm 2.3
MEA3	78.9 \pm 14.6	93.9 \pm 2.4	96.2 \pm 0.4	96.5 \pm 0.2	96.3 \pm 0.5	MEA3	83.0 \pm 5.1	92.8 \pm 2.1	95.7 \pm 0.1	95.8 \pm 0.8	96.2 \pm 0.3
MEA4	74.6 \pm 2.4	83.0 \pm 8.4	95.1 \pm 0.3	95.5 \pm 0.4	96.0 \pm 0.5	MEA4	67.2 \pm 18.6	86.0 \pm 2.1	87.8 \pm 8.1	96.0 \pm 0.4	96.0 \pm 0.1
MEA5	80.2 \pm 7.1	92.8 \pm 1.3	95.0 \pm 1.6	95.5 \pm 0.8	96.4 \pm 0.2	MEA5	82.5 \pm 13.8	94.5 \pm 1.7	95.9 \pm 0.1	96.4 \pm 0.2	96.1 \pm 0.6
AdvMEA	49.0 \pm 22.8	38.0 \pm 24.8	47.3 \pm 27.6	36.8 \pm 26.7	40.9 \pm 24.8	AdvMEA	48.7 \pm 30.4	40.1 \pm 24.6	42.7 \pm 26.8	44.0 \pm 25.6	57.3 \pm 17.0
CEGA	79.6 \pm 5.4	83.0 \pm 14.5	89.8 \pm 6.4	94.8 \pm 0.6	88.9 \pm 9.3	CEGA	84.9 \pm 6.6	85.9 \pm 6.1	82.7 \pm 7.0	93.8 \pm 1.9	94.1 \pm 3.0
Realistic	49.0 \pm 1.1	47.7 \pm 8.3	64.5 \pm 19.4	63.3 \pm 20.6	50.3 \pm 7.0	Realistic	53.5 \pm 5.7	34.5 \pm 15.1	51.7 \pm 5.8	61.5 \pm 14.2	56.9 \pm 15.7
DFEA_I	91.0 \pm 2.5	91.1 \pm 2.9	91.4 \pm 2.7	91.4 \pm 3.0	91.7 \pm 3.1	DFEA_I	91.0 \pm 2.4	91.1 \pm 2.9	91.4 \pm 2.7	91.4 \pm 3.0	91.7 \pm 3.1
DFEA_II	30.2 \pm 33.7	28.7 \pm 31.6	15.8 \pm 6.6	11.1 \pm 6.6	14.4 \pm 6.1	DFEA_II	30.2 \pm 33.7	28.7 \pm 31.6	15.8 \pm 6.6	11.1 \pm 6.6	14.4 \pm 6.1
DFEA_III	92.3 \pm 1.6	92.6 \pm 1.8	90.6 \pm 3.6	92.4 \pm 1.8	92.7 \pm 1.9	DFEA_III	92.3 \pm 1.6	92.6 \pm 1.8	90.6 \pm 3.6	92.4 \pm 1.8	92.7 \pm 1.9

(c) Regime=a_only						(d) Regime=data_free					
Attack	0.05	0.10	0.25	0.50	1.00	Attack	0.05	0.10	0.25	0.50	1.00
MEAO	87.2 \pm 5.3	92.2 \pm 1.8	93.9 \pm 1.5	95.9 \pm 0.2	95.7 \pm 0.5	MEAO	10.4 \pm 6.9	28.0 \pm 13.5	15.8 \pm 0.8	16.9 \pm 0.0	11.7 \pm 7.5
MEA1	2.0 \pm 0.2	39.4 \pm 26.0	42.2 \pm 28.9	62.7 \pm 33.5	67.0 \pm 36.5	MEA1	10.2 \pm 7.2	10.2 \pm 7.2	10.2 \pm 7.2	10.2 \pm 7.2	10.2 \pm 7.2
MEA2	87.3 \pm 1.8	88.8 \pm 2.4	90.5 \pm 2.2	91.5 \pm 2.4	92.4 \pm 2.3	MEA2	85.9 \pm 2.1	89.2 \pm 1.4	90.4 \pm 2.0	91.4 \pm 2.4	92.4 \pm 2.3
MEA3	81.6 \pm 3.9	92.5 \pm 1.8	95.6 \pm 0.2	96.0 \pm 0.2	96.7 \pm 0.3	MEA3	21.2 \pm 19.2	10.8 \pm 7.5	5.7 \pm 6.8	6.1 \pm 7.7	15.3 \pm 0.0
MEA4	69.2 \pm 15.5	75.7 \pm 19.8	90.5 \pm 2.4	95.9 \pm 0.2	96.0 \pm 0.3	MEA4	11.3 \pm 8.0	11.2 \pm 7.0	11.0 \pm 7.3	11.7 \pm 7.4	5.9 \pm 7.8
MEA5	75.5 \pm 4.4	94.2 \pm 1.3	95.7 \pm 0.4	96.0 \pm 0.2	96.6 \pm 0.4	MEA5	32.0 \pm 21.4	27.1 \pm 14.2	10.9 \pm 6.3	10.4 \pm 6.4	22.1 \pm 19.1
AdvMEA	47.8 \pm 27.0	52.5 \pm 30.7	33.5 \pm 28.0	47.0 \pm 31.9	38.9 \pm 6.2	AdvMEA	49.3 \pm 29.1	50.8 \pm 30.7	36.9 \pm 25.8	46.9 \pm 29.3	40.9 \pm 24.7
CEGA	90.0 \pm 3.4	84.9 \pm 8.2	95.1 \pm 0.7	95.5 \pm 0.9	94.2 \pm 2.5	CEGA	51.2 \pm 32.0	89.9 \pm 7.7	95.1 \pm 0.5	92.7 \pm 2.8	92.8 \pm 1.5
Realistic	47.0 \pm 7.1	33.5 \pm 13.4	51.8 \pm 7.0	59.2 \pm 19.6	66.4 \pm 19.5	Realistic	42.1 \pm 18.6	63.2 \pm 19.3	61.1 \pm 20.5	33.7 \pm 13.0	57.9 \pm 17.0
DFEA_I	90.9 \pm 2.5	91.1 \pm 2.9	91.4 \pm 2.7	91.4 \pm 3.0	91.7 \pm 3.1	DFEA_I	90.9 \pm 2.5	91.1 \pm 2.9	91.4 \pm 2.7	91.4 \pm 3.0	91.7 \pm 3.1
DFEA_II	30.2 \pm 33.7	28.7 \pm 31.6	15.8 \pm 6.6	11.1 \pm 6.6	14.4 \pm 6.1	DFEA_II	30.2 \pm 33.7	28.7 \pm 31.6	15.8 \pm 6.6	11.1 \pm 6.6	14.4 \pm 6.1
DFEA_III	92.3 \pm 1.6	92.6 \pm 1.8	90.6 \pm 3.6	92.4 \pm 1.8	92.7 \pm 1.9	DFEA_III	92.3 \pm 1.6	92.6 \pm 1.8	90.6 \pm 3.6	92.4 \pm 1.8	92.7 \pm 1.9

Table 27: RQ1 detailed for dataset=Photo, metric=F1 (%). Rows are attacks; columns are budgets. Mean \pm std across seeds; best per column is bold.

(a) Regime=both						(b) Regime=x_only					
Attack	0.05	0.10	0.25	0.50	1.00	Attack	0.05	0.10	0.25	0.50	1.00
MEAO	31.9 \pm 15.5	54.4 \pm 4.2	59.6 \pm 4.6	64.4 \pm 2.4	62.0 \pm 3.0	MEAO	46.4 \pm 7.7	59.5 \pm 6.0	58.4 \pm 2.4	66.3 \pm 2.7	65.7 \pm 1.0
MEA1	2.0 \pm 0.2	22.6 \pm 14.3	25.7 \pm 19.3	33.5 \pm 21.6	41.6 \pm 27.2	MEA1	2.0 \pm 0.2	22.7 \pm 14.5	25.7 \pm 19.3	33.5 \pm 21.6	41.6 \pm 27.2
MEA2	42.2 \pm 2.4	49.7 \pm 8.8	56.4 \pm 6.6	57.4 \pm 8.7	59.0 \pm 9.6	MEA2	43.5 \pm 1.7	45.4 \pm 2.8	48.2 \pm 2.8	58.0 \pm 10.2	59.0 \pm 9.6
MEA3	52.0 \pm 9.1	66.9 \pm 7.6	64.5 \pm 1.7	66.9 \pm 4.1	64.9 \pm 5.5	MEA3	54.0 \pm 9.8	61.5 \pm 5.0	63.3 \pm 5.3	68.0 \pm 2.2	69.5 \pm 4.5
MEA4	32.6 \pm 2.7	37.6 \pm 7.0	50.1 \pm 2.0	49.6 \pm 1.5	55.3 \pm 2.8	MEA4	24.8 \pm 15.5	43.3 \pm 4.7	43.0 \pm 5.1	60.1 \pm 4.7	55.9 \pm 3.4
MEA5	56.8 \pm 9.0	66.4 \pm 4.1	60.2 \pm 3.6	61.7 \pm 5.3	62.7 \pm 0.7	MEA5	48.2 \pm 17.8	61.7 \pm 4.6	60.4 \pm 3.9	69.9 \pm 5.0	62.9 \pm 2.7
AdvMEA	28.5 \pm 14.3	25.6 \pm 14.7	28.6 \pm 15.2	20.1 \pm 16.2	21.8 \pm 13.3	AdvMEA	28.7 \pm 14.8	23.3 \pm 13.4	24.0 \pm 15.4	29.0 \pm 16.3	34.3 \pm 10.8
CEGA	45.7 \pm 3.0	50.3 \pm 11.3	55.4 \pm 4.3	58.5 \pm 1.2	55.1 \pm 8.4	CEGA	48.6 \pm 8.1	53.1 \pm 4.3	45.6 \pm 7.4	59.3 \pm 3.3	58.5 \pm 3.0
Realistic	15.4 \pm 4.7	15.9 \pm 4.8	28.0 \pm 18.4	28.6 \pm 19.9	17.0 \pm 5.2	Realistic	15.3 \pm 4.5	13.0 \pm 4.5	15.6 \pm 5.0	26.5 \pm 15.7	22.5 \pm 12.1
DFEA_I	48.3 \pm 3.5	51.4 \pm 6.5	49.8 \pm 9.2	51.0 \pm 11.5	51.8 \pm 11.9	DFEA_I	48.7 \pm 3.1	51.4 \pm 6.5	49.8 \pm 9.2	51.0 \pm 11.5	51.8 \pm 11.9
DFEA_II	16.9 \pm 21.7	14.0 \pm 17.7	10.0 \pm 6.0	5.4 \pm 5.5	5.6 \pm 4.5	DFEA_II	16.9 \pm 21.7	14.0 \pm 17.7	10.0 \pm 6.0	5.4 \pm 5.5	5.6 \pm 4.5
DFEA_III	51.2 \pm 4.7	57.4 \pm 9.6	53.6 \pm 12.3	57.9 \pm 7.3	56.2 \pm 11.7	DFEA_III	51.2 \pm 4.7	57.4 \pm 9.6	53.6 \pm 12.3	57.9 \pm 7.3	56.2 \pm 11.7

(c) Regime=a_only						(d) Regime=data_free					
Attack	0.05	0.10	0.25	0.50	1.00	Attack	0.05	0.10	0.25	0.50	1.00
MEAO	57.9 \pm 4.5	63.7 \pm 7.0	57.5 \pm 9.1	64.2 \pm 3.5	64.0 \pm 4.5	MEAO	2.3 \pm 1.5	5.3 \pm 1.9	3.4 \pm 0.1	3.6 \pm 0.0	2.5 \pm 1.6
MEA1	2.0 \pm 0.2	22.7 \pm 14.5	25.7 \pm 19.3	33.5 \pm 21.6	41.6 \pm 27.2	MEA1	2.2 \pm 1.6	2.2 \pm 1.6	2.2 \pm 1.6	2.2 \pm 1.6	2.2 \pm 1.6
MEA2	48.6 \pm 10.0	48.5 \pm 6.9	52.2 \pm 8.7	58.3 \pm 10.5	59.0 \pm 9.6	MEA2	43.3 \pm 2.6	46.6 \pm 3.1	46.0 \pm 3.5	59.1 \pm 9.5	59.0 \pm 9.6
MEA3	45.1 \pm 7.8	57.7 \pm 3.2	60.5 \pm 2.4	65.9 \pm 3.7	65.3 \pm 2.1	MEA3	3.9 \pm 3.2	2.9 \pm 0.8	1.6 \pm 1.6	1.3 \pm 1.6	3.3 \pm 0.0
MEA4	33.8 \pm 6.9	33.0 \pm 17.0	46.4 \pm 4.7	51.1 \pm 3.2	56.1 \pm 4.1	MEA4	2.4 \pm 1.7	2.4 \pm 1.5	2.4 \pm 1.6	2.5 \pm 1.6	1.3 \pm 1.7
MEA5	43.2 \pm 7.8	62.0 \pm 1.4	64.6 \pm 5.2	64.1 \pm 5.3	65.4 \pm 5.1	MEA5	5.8 \pm 3.1	7.0 \pm 2.2	3.1 \pm 0.3	2.6 \pm 1.7	4.0 \pm 3.2
AdvMEA	29.5 \pm 14.9	32.1 \pm 17.1	19.4 \pm 17.3	26.8 \pm 17.8	21.6 \pm 3.4	AdvMEA	29.9 \pm 15.9	30.8 \pm 17.4	22.9 \pm 14.2	29.2 \pm 19.0	23.3 \pm 11.7
CEGA	54.2 \pm 3.2	49.3 \pm 8.7	62.0 \pm 2.1	62.0 \pm 3.6	58.2 \pm 3.0	CEGA	31.0 \pm 17.9	55.3 \pm 6.1	62.7 \pm 1.6	59.0 \pm 3.2	60.0 \pm 4.9
Realistic	15.0 \pm 3.0	10.0 \pm 5.7	17.1 \pm 5.6	26.5 \pm 17.5	32.6 \pm 24.6	Realistic	13.7 \pm 4.1	28.6 \pm 18.2	27.0 \pm 17.7	10.3 \pm 6.3	24.6 \pm 15.1
DFEA_I	48.6 \pm 3.2	51.4 \pm 6.5	49.8 \pm 9.2	51.0 \pm 11.5	51.8 \pm 11.9	DFEA_I	48.6 \pm 3.2	51.4 \pm 6.5	49.8 \pm 9.2	51.0 \pm 11.5	51.8 \pm 11.9
DFEA_II	16.9 \pm 21.7	14.0 \pm 17.7	10.0 \pm 6.0	5.4 \pm 5.5	5.6 \pm 4.5	DFEA_II	16.9 \pm 21.7	14.0 \pm 17.7	10.0 \pm 6.0	5.4 \pm 5.5	5.6 \pm 4.5
DFEA_III	51.2 \pm 4.7	57.4 \pm 9.6	53.6 \pm 12.3	57.9 \pm 7.3	56.2 \pm 11.7	DFEA_III	51.2 \pm 4.7	57.4 \pm 9.6	53.6 \pm 12.3	57.9 \pm 7.3	56.2 \pm 11.7

the same dataset in Tables 32–33 and is consistent with the structural-property analysis (high average degree) in Appendix F.10.

F.6 Peak GPU memory of attacks and defenses (RQ4)

Figure 8 reports the peak GPU memory of every attack (panel a) and every defense (panel b) on a symmetric-log y -axis, aggregated over all ten datasets. The symlog scale is necessary because the workloads span more than two orders of magnitude on the same axis: MEAO, CEGA, and the lightweight defenses sit near 0.05–0.1 GB, while MEA2, Realistic, the DFEA family, and ImperceptibleWM reach several gigabytes. Two findings supplement the time-based discussion in the main text. *First, peak memory is a more discriminative signal than wall-clock time for separating attack families.* The fast MEAO/1/3/4/5/CEGA group is tightly clustered around 0.05–0.15 GB across every dataset,

Table 28: RQ1 detailed for dataset=Photo, metric=Fidelity (%). Rows are attacks; columns are budgets. Mean \pm std across seeds; best per column is bold.

(a) Regime=both						(b) Regime=x_only					
Attack	0.05	0.10	0.25	0.50	1.00	Attack	0.05	0.10	0.25	0.50	1.00
MEA0	54.7 \pm 30.8	90.8 \pm 4.1	95.4 \pm 1.4	96.6 \pm 1.1	96.8 \pm 0.1	MEA0	84.2 \pm 5.8	91.0 \pm 3.3	96.0 \pm 0.8	96.8 \pm 1.0	96.6 \pm 1.2
MEA1	1.9 \pm 0.3	39.2 \pm 26.6	42.0 \pm 29.2	62.1 \pm 33.8	67.0 \pm 37.2	MEA1	1.9 \pm 0.3	39.3 \pm 26.8	42.0 \pm 29.2	62.1 \pm 33.8	67.0 \pm 37.2
MEA2	85.2 \pm 3.2	89.2 \pm 2.4	93.3 \pm 2.0	95.4 \pm 1.6	96.1 \pm 1.9	MEA2	86.8 \pm 3.4	90.2 \pm 1.8	92.9 \pm 2.0	95.4 \pm 1.8	96.1 \pm 1.9
MEA3	78.3 \pm 15.0	93.9 \pm 3.0	96.5 \pm 0.8	96.9 \pm 0.9	97.8 \pm 1.0	MEA3	82.4 \pm 5.2	92.6 \pm 0.8	96.1 \pm 0.7	96.3 \pm 1.1	96.7 \pm 0.8
MEA4	74.3 \pm 2.6	83.1 \pm 8.2	95.2 \pm 0.4	96.7 \pm 1.1	97.4 \pm 0.8	MEA4	67.3 \pm 18.7	85.8 \pm 1.8	88.5 \pm 7.8	97.0 \pm 0.9	97.3 \pm 0.9
MEA5	80.1 \pm 6.6	92.4 \pm 0.8	95.0 \pm 2.3	95.9 \pm 0.9	97.5 \pm 0.6	MEA5	81.9 \pm 13.2	94.0 \pm 1.1	96.2 \pm 0.7	96.9 \pm 1.4	97.8 \pm 0.8
AdvMEA	49.5 \pm 22.9	38.6 \pm 24.6	48.0 \pm 27.4	37.3 \pm 26.7	41.3 \pm 24.7	AdvMEA	49.5 \pm 30.4	40.3 \pm 24.6	43.1 \pm 26.5	44.7 \pm 25.5	57.6 \pm 17.4
CEGA	80.6 \pm 5.0	83.7 \pm 15.1	91.4 \pm 6.8	95.9 \pm 1.2	90.4 \pm 9.5	CEGA	85.5 \pm 7.2	86.6 \pm 5.8	83.7 \pm 7.5	94.8 \pm 2.3	95.5 \pm 2.9
Realistic	70.7 \pm 15.3	72.5 \pm 13.9	83.6 \pm 10.3	86.9 \pm 5.1	77.5 \pm 11.1	Realistic	76.1 \pm 11.1	53.1 \pm 24.5	72.3 \pm 16.7	81.6 \pm 9.4	85.5 \pm 5.4
DFEA_I	92.6 \pm 3.9	93.8 \pm 1.9	91.6 \pm 4.4	91.5 \pm 4.6	91.4 \pm 4.8	DFEA_I	93.0 \pm 3.4	93.8 \pm 1.9	91.6 \pm 4.4	91.5 \pm 4.6	91.4 \pm 4.8
DFEA_II	30.1 \pm 31.7	29.2 \pm 30.5	16.1 \pm 5.2	11.4 \pm 5.4	13.8 \pm 6.1	DFEA_II	30.1 \pm 31.7	29.2 \pm 30.5	16.1 \pm 5.2	11.4 \pm 5.4	13.8 \pm 6.1
DFEA_III	92.9 \pm 3.0	93.3 \pm 2.5	91.8 \pm 5.2	94.2 \pm 2.3	95.4 \pm 2.4	DFEA_III	92.9 \pm 3.0	93.3 \pm 2.5	91.8 \pm 5.2	94.2 \pm 2.3	95.4 \pm 2.4

(c) Regime=a_only						(d) Regime=data_free					
Attack	0.05	0.10	0.25	0.50	1.00	Attack	0.05	0.10	0.25	0.50	1.00
MEA0	87.3 \pm 5.7	92.4 \pm 1.1	94.3 \pm 2.3	96.5 \pm 0.9	97.5 \pm 0.9	MEA0	10.3 \pm 7.0	28.3 \pm 13.4	15.6 \pm 0.6	16.2 \pm 0.6	11.6 \pm 7.6
MEA1	1.9 \pm 0.3	39.1 \pm 26.5	42.0 \pm 29.2	62.1 \pm 33.8	67.0 \pm 37.2	MEA1	10.3 \pm 6.6	10.3 \pm 6.6	10.3 \pm 6.6	10.3 \pm 6.6	10.3 \pm 6.6
MEA2	88.5 \pm 2.5	90.1 \pm 2.0	92.8 \pm 2.1	95.4 \pm 1.7	96.1 \pm 1.9	MEA2	86.4 \pm 2.8	89.3 \pm 1.6	92.8 \pm 2.6	95.2 \pm 1.9	96.1 \pm 1.9
MEA3	81.4 \pm 3.8	92.4 \pm 2.3	95.8 \pm 1.0	96.8 \pm 0.8	97.6 \pm 0.7	MEA3	21.1 \pm 19.3	10.3 \pm 7.2	5.3 \pm 7.2	6.2 \pm 7.2	14.9 \pm 0.5
MEA4	69.0 \pm 16.2	76.0 \pm 19.4	90.9 \pm 2.0	96.1 \pm 0.6	98.2 \pm 0.5	MEA4	11.1 \pm 8.0	10.7 \pm 6.7	10.0 \pm 6.9	10.9 \pm 7.0	5.9 \pm 7.4
MEA5	75.2 \pm 4.1	94.2 \pm 1.4	95.9 \pm 0.5	96.8 \pm 0.7	97.7 \pm 1.1	MEA5	31.9 \pm 21.7	26.9 \pm 14.6	10.1 \pm 6.4	10.3 \pm 6.5	22.2 \pm 19.2
AdvMEA	48.3 \pm 26.7	53.1 \pm 30.6	34.1 \pm 28.0	47.7 \pm 31.8	39.1 \pm 6.0	AdvMEA	50.3 \pm 29.2	51.6 \pm 30.7	37.6 \pm 25.6	47.6 \pm 29.1	41.1 \pm 24.3
CEGA	90.6 \pm 3.9	85.5 \pm 8.8	95.4 \pm 1.1	97.3 \pm 0.8	96.4 \pm 1.8	CEGA	51.7 \pm 32.2	91.0 \pm 7.8	95.9 \pm 1.0	93.8 \pm 2.4	94.2 \pm 1.4
Realistic	69.3 \pm 14.6	62.2 \pm 32.2	78.4 \pm 11.1	84.9 \pm 7.0	85.2 \pm 8.0	Realistic	70.4 \pm 15.5	86.8 \pm 4.3	86.0 \pm 5.6	61.8 \pm 31.4	85.0 \pm 5.8
DFEA_I	92.9 \pm 3.6	93.8 \pm 1.9	91.6 \pm 4.4	91.5 \pm 4.6	91.4 \pm 4.8	DFEA_I	92.9 \pm 3.5	93.8 \pm 1.9	91.6 \pm 4.4	91.5 \pm 4.6	91.4 \pm 4.8
DFEA_II	30.1 \pm 31.7	29.2 \pm 30.5	16.1 \pm 5.2	11.4 \pm 5.4	13.8 \pm 6.1	DFEA_II	30.1 \pm 31.7	29.2 \pm 30.5	16.1 \pm 5.2	11.4 \pm 5.4	13.8 \pm 6.1
DFEA_III	92.9 \pm 3.0	93.3 \pm 2.5	91.8 \pm 5.2	94.2 \pm 2.3	95.4 \pm 2.4	DFEA_III	92.9 \pm 3.0	93.3 \pm 2.5	91.8 \pm 5.2	94.2 \pm 2.3	95.4 \pm 2.4

Table 29: RQ1 detailed for dataset=PubMed, metric=Acc (%). Rows are attacks; columns are budgets. Mean \pm std across seeds; best per column is bold.

(a) Regime=both						(b) Regime=x_only					
Attack	0.05	0.10	0.25	0.50	1.00	Attack	0.05	0.10	0.25	0.50	1.00
MEA0	70.6 \pm 1.5	75.8 \pm 1.8	77.4 \pm 0.3	76.7 \pm 0.4	78.2 \pm 0.3	MEA0	72.1 \pm 3.2	76.8 \pm 1.1	76.8 \pm 1.7	78.0 \pm 0.5	78.5 \pm 0.3
MEA1	68.6 \pm 2.3	70.6 \pm 5.0	74.8 \pm 3.4	75.3 \pm 3.5	75.5 \pm 3.9	MEA1	68.6 \pm 2.3	70.6 \pm 5.0	74.8 \pm 3.4	75.3 \pm 3.5	75.5 \pm 3.9
MEA2	69.9 \pm 0.9	72.8 \pm 0.6	76.1 \pm 1.0	77.7 \pm 0.5	77.8 \pm 0.2	MEA2	69.4 \pm 0.1	73.9 \pm 0.7	76.4 \pm 1.2	77.6 \pm 0.2	77.8 \pm 0.2
MEA3	72.1 \pm 1.9	73.4 \pm 1.6	76.6 \pm 0.7	79.0 \pm 1.1	77.3 \pm 1.7	MEA3	73.2 \pm 1.1	75.4 \pm 1.4	77.2 \pm 0.6	77.4 \pm 0.7	78.0 \pm 0.6
MEA4	67.8 \pm 0.6	71.2 \pm 3.8	75.3 \pm 0.9	78.2 \pm 0.5	78.6 \pm 0.8	MEA4	51.5 \pm 4.7	65.7 \pm 6.3	77.0 \pm 1.3	77.4 \pm 0.9	78.6 \pm 0.8
MEA5	72.3 \pm 3.4	75.9 \pm 0.1	77.8 \pm 0.8	77.8 \pm 0.7	78.1 \pm 1.1	MEA5	70.6 \pm 2.8	74.5 \pm 1.0	77.0 \pm 1.4	77.7 \pm 0.5	77.5 \pm 0.9
AdvMEA	60.4 \pm 3.2	66.5 \pm 1.9	65.5 \pm 2.6	62.6 \pm 6.7	66.0 \pm 2.6	AdvMEA	64.3 \pm 9.4	64.2 \pm 5.4	64.0 \pm 6.3	62.5 \pm 3.1	61.6 \pm 3.1
CEGA	78.3 \pm 0.4	77.9 \pm 1.6	78.2 \pm 0.2	79.1 \pm 0.2	78.7 \pm 0.7	CEGA	74.8 \pm 1.2	78.7 \pm 0.7	78.7 \pm 0.4	79.1 \pm 0.2	78.9 \pm 0.2
Realistic	72.7 \pm 1.5	71.5 \pm 1.0	74.7 \pm 0.2	75.6 \pm 1.8	76.8 \pm 0.8	Realistic	67.1 \pm 1.7	74.2 \pm 0.6	76.7 \pm 1.0	75.7 \pm 0.4	76.0 \pm 0.8
DFEA_I	78.2 \pm 0.2	78.5 \pm 0.3	78.5 \pm 0.2	78.4 \pm 0.4	78.7 \pm 0.2	DFEA_I	78.2 \pm 0.2	78.5 \pm 0.3	78.5 \pm 0.2	78.4 \pm 0.4	78.7 \pm 0.2
DFEA_II	78.7 \pm 0.5	78.9 \pm 0.5	79.7 \pm 0.4	79.6 \pm 0.4	79.1 \pm 0.3	DFEA_II	78.7 \pm 0.5	78.9 \pm 0.5	79.7 \pm 0.4	79.6 \pm 0.4	79.1 \pm 0.2
DFEA_III	78.3 \pm 0.1	78.5 \pm 0.4	78.8 \pm 0.1	78.9 \pm 0.1	78.9 \pm 0.2	DFEA_III	78.3 \pm 0.1	78.5 \pm 0.4	78.8 \pm 0.1	78.9 \pm 0.1	78.9 \pm 0.2

(c) Regime=a_only						(d) Regime=data_free					
Attack	0.05	0.10	0.25	0.50	1.00	Attack	0.05	0.10	0.25	0.50	1.00
MEA0	71.1 \pm 0.9	76.3 \pm 0.6	77.3 \pm 1.0	78.4 \pm 0.5	78.3 \pm 0.6	MEA0	33.1 \pm 10.7	41.3 \pm 0.0	40.9 \pm 0.3	40.9 \pm 0.3	40.9 \pm 0.3
MEA1	68.6 \pm 2.3	70.6 \pm 5.0	74.8 \pm 3.4	75.3 \pm 3.5	75.5 \pm 3.9	MEA1	41.3 \pm 0.0	41.3 \pm 0.0	41.3 \pm 0.0	41.3 \pm 0.0	41.3 \pm 0.0
MEA2	68.9 \pm 2.0	73.4 \pm 0.9	75.8 \pm 1.5	77.4 \pm 0.1	77.8 \pm 0.2	MEA2	70.4 \pm 1.3	73.2 \pm 0.7	76.2 \pm 0.2	77.2 \pm 0.3	77.8 \pm 0.2
MEA3	70.7 \pm 3.4	73.8 \pm 1.3	77.7 \pm 0.4	77.6 \pm 0.4	79.1 \pm 0.5	MEA3	38.3 \pm 3.8	33.3 \pm 10.8	33.5 \pm 11.0	40.9 \pm 0.3	40.9 \pm 0.3
MEA4	54.4 \pm 7.9	71.4 \pm 0.5	76.6 \pm 1.2	78.0 \pm 1.0	78.8 \pm 1.0	MEA4	40.7 \pm 0.0	33.1 \pm 10.7	33.3 \pm 10.8	33.3 \pm 10.8	41.1 \pm 0.3
MEA5	72.1 \pm 3.5	76.9 \pm 1.0	77.6 \pm 1.1	77.8 \pm 0.9	77.8 \pm 0.9	MEA5	18.1 \pm 0.1	40.9 \pm 0.3	26.0 \pm 10.4	25.6 \pm 10.7	41.2 \pm 0.4
AdvMEA	59.3 \pm 7.4	63.2 \pm 6.2	62.5 \pm 5.0	63.6 \pm 2.0	63.8 \pm 2.6	AdvMEA	62.1 \pm 6.5	66.9 \pm 1.9	65.3 \pm 4.1	62.0 \pm 6.2	62.7 \pm 3.6
CEGA	74.9 \pm 2.4	77.7 \pm 1.3	78.3 \pm 0.5	78.9 \pm 0.5	78.8 \pm 0.3	CEGA	75.7 \pm 2.4	78.0 \pm 1.1	78.6 \pm 0.4	78.5 \pm 0.4	78.6 \pm 0.3
Realistic	69.6 \pm 1.5	72.7 \pm 0.8	74.9 \pm 0.6	76.5 \pm 0.9	76.6 \pm 0.4	Realistic	76.1 \pm 0.6	77.2 \pm 0.4	76.6 \pm 0.5	76.2 \pm 0.8	75.9 \pm 0.5
DFEA_I	78.2 \pm 0.2	78.5 \pm 0.3	78.5 \pm 0.2	78.4 \pm 0.4	78.7 \pm 0.2	DFEA_I	78.2 \pm 0.2	78.5 \pm 0.3	78.5 \pm 0.2	78.4 \pm 0.4	78.7 \pm 0.2
DFEA_II	78.7 \pm 0.5	78.9 \pm 0.5	79.7 \pm 0.4	79.6 \pm 0.4	79.1 \pm 0.2	DFEA_II	78.7 \pm 0.5	78.9 \pm 0.5	79.7 \pm 0.4	79.6 \pm 0.4	79.1 \pm 0.2
DFEA_III	78.3 \pm 0.1	78.5 \pm 0.4	78.8 \pm 0.1	78.9 \pm 0.1	78.9 \pm 0.2	DFEA_III	78.3 \pm 0.1	78.5 \pm 0.4	78.8 \pm 0.1	78.9 \pm 0.1	78.9 \pm 0.2

while the data-free DFEA family and Realistic sit at 1–5 GB; the within-group variance is much smaller than the between-group gap, which means an operator who watches GPU memory can infer the attack family without timing the queries. *Second, the watermarking-versus-information-limiting split is sharp on the defense panel.* The five watermarking defenses (left of the dashed line) all train an in-model artefact and so allocate proportional buffers (0.1–5 GB depending on the watermarking technique), whereas the seven information-limiting defenses (right of the dashed line) are inference-time wrappers and use less than 0.05 GB on every dataset — they essentially add no memory cost on top of the protected model itself. This explains why output-perturbation defenses are attractive in deployment: they cost nothing in memory while providing the protection summarised in the main text.

Table 30: RQ1 detailed for dataset=PubMed, metric=F1 (%). Rows are attacks; columns are budgets. Mean \pm std across seeds; best per column is bold.

(a) Regime=both						(b) Regime=x_only					
Attack	0.05	0.10	0.25	0.50	1.00	Attack	0.05	0.10	0.25	0.50	1.00
MEA0	68.2 \pm 2.8	74.7 \pm 1.4	76.3 \pm 0.2	76.0 \pm 0.5	77.2 \pm 0.4	MEA0	70.7 \pm 4.1	75.7 \pm 0.8	75.9 \pm 1.4	77.2 \pm 0.4	77.5 \pm 0.6
MEA1	50.2 \pm 1.7	68.3 \pm 6.2	74.0 \pm 3.5	74.6 \pm 3.5	74.9 \pm 3.9	MEA1	50.2 \pm 1.7	68.3 \pm 6.2	74.0 \pm 3.5	74.6 \pm 3.5	74.9 \pm 3.9
MEA2	65.4 \pm 1.0	69.5 \pm 0.5	74.4 \pm 1.2	76.7 \pm 0.6	77.2 \pm 0.3	MEA2	64.3 \pm 0.6	71.1 \pm 1.1	74.9 \pm 1.1	76.9 \pm 0.6	77.2 \pm 0.3
MEA3	70.3 \pm 2.3	72.2 \pm 2.0	75.4 \pm 0.5	78.0 \pm 0.9	76.3 \pm 1.6	MEA3	71.6 \pm 1.3	74.1 \pm 1.4	75.7 \pm 0.8	76.3 \pm 0.7	76.9 \pm 0.9
MEA4	64.4 \pm 3.3	66.2 \pm 7.9	73.8 \pm 0.7	76.8 \pm 0.6	77.0 \pm 0.7	MEA4	46.5 \pm 5.0	62.1 \pm 7.7	75.3 \pm 1.6	75.8 \pm 0.8	77.0 \pm 0.8
MEA5	71.3 \pm 3.0	74.1 \pm 0.5	76.5 \pm 0.9	76.7 \pm 0.5	77.1 \pm 1.2	MEA5	68.2 \pm 2.9	73.0 \pm 0.5	75.5 \pm 2.1	76.5 \pm 0.3	76.6 \pm 0.8
AdvMEA	55.6 \pm 1.7	65.8 \pm 2.1	64.8 \pm 2.6	60.9 \pm 8.1	63.9 \pm 1.7	AdvMEA	62.3 \pm 11.3	63.1 \pm 5.7	61.3 \pm 6.6	59.8 \pm 2.0	60.4 \pm 2.9
CEGA	77.3 \pm 0.3	76.9 \pm 1.5	77.4 \pm 0.1	78.3 \pm 0.1	77.7 \pm 0.6	CEGA	74.4 \pm 0.9	77.8 \pm 0.6	77.8 \pm 0.4	78.2 \pm 0.2	78.1 \pm 0.3
Realistic	71.9 \pm 1.0	70.6 \pm 1.2	73.9 \pm 0.1	74.6 \pm 1.7	76.2 \pm 0.7	Realistic	66.1 \pm 1.2	72.6 \pm 0.3	76.1 \pm 0.8	75.3 \pm 0.4	75.4 \pm 0.7
DFEA_I	77.5 \pm 0.2	77.8 \pm 0.3	77.7 \pm 0.2	77.7 \pm 0.4	78.0 \pm 0.2	DFEA_I	77.5 \pm 0.2	77.8 \pm 0.3	77.7 \pm 0.2	77.7 \pm 0.4	78.0 \pm 0.2
DFEA_II	78.0 \pm 0.5	78.5 \pm 0.6	79.1 \pm 0.4	79.0 \pm 0.4	78.4 \pm 0.3	DFEA_II	78.0 \pm 0.5	78.5 \pm 0.6	79.1 \pm 0.4	79.0 \pm 0.4	78.5 \pm 0.2
DFEA_III	77.6 \pm 0.1	77.8 \pm 0.4	78.0 \pm 0.1	78.2 \pm 0.2	78.2 \pm 0.1	DFEA_III	77.6 \pm 0.1	77.8 \pm 0.4	78.0 \pm 0.1	78.2 \pm 0.2	78.2 \pm 0.1

(c) Regime=a_only						(d) Regime=data_free					
Attack	0.05	0.10	0.25	0.50	1.00	Attack	0.05	0.10	0.25	0.50	1.00
MEA0	68.6 \pm 2.2	75.3 \pm 0.5	76.0 \pm 1.3	77.4 \pm 0.5	77.5 \pm 0.4	MEA0	16.2 \pm 4.3	19.5 \pm 0.0	19.4 \pm 0.1	19.4 \pm 0.1	19.4 \pm 0.1
MEA1	50.2 \pm 1.7	68.3 \pm 6.2	74.0 \pm 3.5	74.6 \pm 3.5	74.9 \pm 3.9	MEA1	19.5 \pm 0.0	19.5 \pm 0.0	19.5 \pm 0.0	19.5 \pm 0.0	19.5 \pm 0.0
MEA2	63.3 \pm 2.6	70.2 \pm 1.8	74.3 \pm 1.8	76.6 \pm 0.3	77.2 \pm 0.3	MEA2	65.1 \pm 0.8	69.9 \pm 0.9	74.7 \pm 0.4	76.5 \pm 0.4	77.2 \pm 0.3
MEA3	68.8 \pm 5.0	72.9 \pm 1.2	76.4 \pm 0.6	76.4 \pm 0.3	78.0 \pm 0.5	MEA3	20.2 \pm 1.2	16.9 \pm 4.8	16.4 \pm 4.4	19.4 \pm 0.1	19.4 \pm 0.1
MEA4	43.5 \pm 15.2	69.3 \pm 0.5	74.9 \pm 1.6	76.5 \pm 1.1	77.2 \pm 1.0	MEA4	19.3 \pm 0.0	16.2 \pm 4.3	16.3 \pm 4.3	16.3 \pm 4.3	19.4 \pm 0.1
MEA5	69.1 \pm 3.1	75.9 \pm 1.0	76.5 \pm 1.1	76.8 \pm 0.8	76.9 \pm 0.8	MEA5	10.3 \pm 0.2	19.4 \pm 0.1	14.0 \pm 3.9	13.3 \pm 4.2	20.2 \pm 1.2
AdvMEA	56.1 \pm 10.3	60.4 \pm 7.9	58.8 \pm 5.1	62.0 \pm 2.4	61.8 \pm 1.8	AdvMEA	59.5 \pm 8.3	64.7 \pm 1.6	63.6 \pm 5.3	60.1 \pm 8.6	61.3 \pm 3.4
CEGA	74.0 \pm 2.1	77.1 \pm 1.2	77.4 \pm 0.5	77.8 \pm 0.5	77.8 \pm 0.3	CEGA	75.0 \pm 2.2	77.3 \pm 1.1	77.8 \pm 0.4	77.4 \pm 0.4	77.7 \pm 0.3
Realistic	69.0 \pm 0.9	71.2 \pm 1.9	74.6 \pm 0.6	75.7 \pm 0.9	76.1 \pm 0.3	Realistic	75.4 \pm 0.4	76.6 \pm 0.4	75.9 \pm 0.6	75.7 \pm 0.7	75.4 \pm 0.5
DFEA_I	77.5 \pm 0.2	77.8 \pm 0.3	77.7 \pm 0.2	77.7 \pm 0.4	78.0 \pm 0.2	DFEA_I	77.5 \pm 0.2	77.8 \pm 0.3	77.7 \pm 0.2	77.7 \pm 0.4	78.0 \pm 0.2
DFEA_II	78.0 \pm 0.5	78.5 \pm 0.6	79.1 \pm 0.4	79.0 \pm 0.4	78.5 \pm 0.2	DFEA_II	78.0 \pm 0.5	78.5 \pm 0.6	79.1 \pm 0.4	79.0 \pm 0.4	78.5 \pm 0.2
DFEA_III	77.6 \pm 0.1	77.8 \pm 0.4	78.0 \pm 0.1	78.2 \pm 0.2	78.2 \pm 0.1	DFEA_III	77.6 \pm 0.1	77.8 \pm 0.4	78.0 \pm 0.1	78.2 \pm 0.2	78.2 \pm 0.1

Table 31: RQ1 detailed for dataset=PubMed, metric=Fidelity (%). Rows are attacks; columns are budgets. Mean \pm std across seeds; best per column is bold.

(a) Regime=both						(b) Regime=x_only					
Attack	0.05	0.10	0.25	0.50	1.00	Attack	0.05	0.10	0.25	0.50	1.00
MEA0	80.0 \pm 0.6	87.1 \pm 2.4	90.6 \pm 1.8	92.9 \pm 0.8	94.2 \pm 0.6	MEA0	82.9 \pm 0.9	87.5 \pm 1.5	91.7 \pm 0.7	92.6 \pm 0.3	93.3 \pm 1.1
MEA1	72.9 \pm 2.0	79.0 \pm 6.1	81.9 \pm 3.4	83.2 \pm 4.5	85.3 \pm 4.6	MEA1	72.9 \pm 2.0	79.0 \pm 6.1	81.9 \pm 3.4	83.2 \pm 4.5	85.3 \pm 4.6
MEA2	80.5 \pm 2.0	85.3 \pm 0.2	91.3 \pm 0.6	94.5 \pm 0.7	96.8 \pm 0.3	MEA2	78.4 \pm 0.8	85.8 \pm 0.6	91.6 \pm 0.0	94.8 \pm 0.4	96.8 \pm 0.3
MEA3	80.8 \pm 2.1	83.3 \pm 1.5	87.0 \pm 1.4	89.6 \pm 0.7	89.7 \pm 1.3	MEA3	82.8 \pm 2.2	84.8 \pm 2.4	88.7 \pm 0.6	88.7 \pm 2.3	90.8 \pm 0.8
MEA4	71.6 \pm 1.9	77.7 \pm 4.1	83.5 \pm 1.1	87.7 \pm 0.9	89.1 \pm 0.9	MEA4	52.8 \pm 4.6	72.6 \pm 5.9	86.0 \pm 1.4	87.2 \pm 1.4	89.2 \pm 0.9
MEA5	82.2 \pm 4.6	86.4 \pm 1.6	89.3 \pm 1.3	90.6 \pm 1.1	90.9 \pm 0.9	MEA5	80.0 \pm 3.1	84.7 \pm 2.4	88.0 \pm 0.8	89.9 \pm 0.8	90.4 \pm 0.5
AdvMEA	63.5 \pm 6.4	70.6 \pm 3.6	69.5 \pm 4.2	65.1 \pm 8.9	69.8 \pm 4.5	AdvMEA	67.8 \pm 11.8	66.1 \pm 8.4	65.7 \pm 8.6	65.2 \pm 6.3	64.1 \pm 5.7
CEGA	89.5 \pm 0.4	89.9 \pm 1.3	92.6 \pm 0.3	94.4 \pm 0.4	94.2 \pm 0.3	CEGA	85.4 \pm 2.4	91.0 \pm 0.9	93.5 \pm 0.4	93.5 \pm 1.3	95.3 \pm 0.7
Realistic	81.2 \pm 1.3	83.5 \pm 1.1	88.1 \pm 1.0	89.5 \pm 1.6	91.4 \pm 0.8	Realistic	77.6 \pm 3.0	83.8 \pm 2.8	88.1 \pm 2.9	90.8 \pm 0.9	91.7 \pm 0.4
DFEA_I	94.5 \pm 0.3	94.5 \pm 0.4	94.6 \pm 0.3	94.9 \pm 0.3	94.8 \pm 0.6	DFEA_I	94.5 \pm 0.3	94.5 \pm 0.4	94.6 \pm 0.3	94.9 \pm 0.3	94.8 \pm 0.6
DFEA_II	89.7 \pm 1.4	91.1 \pm 1.5	92.9 \pm 1.3	93.6 \pm 1.0	93.5 \pm 1.1	DFEA_II	89.7 \pm 1.4	91.1 \pm 1.5	92.9 \pm 1.3	93.6 \pm 1.0	93.5 \pm 1.1
DFEA_III	93.5 \pm 0.6	93.9 \pm 0.7	94.8 \pm 0.6	95.2 \pm 0.4	95.1 \pm 0.4	DFEA_III	93.5 \pm 0.6	93.9 \pm 0.7	94.8 \pm 0.6	95.2 \pm 0.4	95.1 \pm 0.4

(c) Regime=a_only						(d) Regime=data_free					
Attack	0.05	0.10	0.25	0.50	1.00	Attack	0.05	0.10	0.25	0.50	1.00
MEA0	79.6 \pm 1.8	89.5 \pm 0.4	92.7 \pm 0.9	91.8 \pm 0.5	93.4 \pm 0.6	MEA0	30.7 \pm 9.8	45.5 \pm 0.5	40.0 \pm 3.6	40.0 \pm 3.6	40.0 \pm 3.6
MEA1	72.9 \pm 2.0	79.0 \pm 6.1	81.9 \pm 3.4	83.2 \pm 4.5	85.3 \pm 4.6	MEA1	45.5 \pm 0.5	45.5 \pm 0.5	45.5 \pm 0.5	45.5 \pm 0.5	45.5 \pm 0.5
MEA2	77.7 \pm 2.2	84.8 \pm 0.8	91.1 \pm 0.8	94.6 \pm 0.4	96.8 \pm 0.3	MEA2	78.4 \pm 1.4	84.7 \pm 0.9	91.0 \pm 0.5	94.9 \pm 0.5	96.8 \pm 0.3
MEA3	79.1 \pm 2.3	84.5 \pm 1.3	88.1 \pm 0.9	89.3 \pm 0.4	90.7 \pm 0.2	MEA3	37.6 \pm 6.1	32.8 \pm 11.7	36.0 \pm 13.6	40.0 \pm 3.6	40.0 \pm 3.6
MEA4	59.3 \pm 7.1	78.5 \pm 1.7	84.9 \pm 1.5	86.8 \pm 1.5	89.2 \pm 0.9	MEA4	37.7 \pm 0.5	31.0 \pm 10.0	33.7 \pm 12.4	33.4 \pm 12.1	43.2 \pm 3.6
MEA5	80.9 \pm 2.2	86.6 \pm 1.4	89.4 \pm 0.4	89.8 \pm 0.8	90.6 \pm 0.4	MEA5	16.9 \pm 0.1	40.0 \pm 3.6	24.4 \pm 9.8	23.6 \pm 9.5	43.4 \pm 3.7
AdvMEA	59.0 \pm 9.8	66.2 \pm 9.0	66.4 \pm 8.2	69.1 \pm 3.4	65.6 \pm 4.6	AdvMEA	63.9 \pm 8.6	70.4 \pm 2.9	69.9 \pm 6.7	64.5 \pm 8.3	64.1 \pm 6.5
CEGA	84.7 \pm 2.2	91.8 \pm 1.3	93.2 \pm 0.4	93.0 \pm 1.2	94.8 \pm 0.5	CEGA	87.2 \pm 2.8	90.9 \pm 1.0	93.4 \pm 0.6	93.8 \pm 0.3	94.4 \pm 0.2
Realistic	79.7 \pm 2.2	82.7 \pm 2.3	89.0 \pm 0.7	91.0 \pm 1.3	92.4 \pm 1.6	Realistic	92.2 \pm 1.3	92.3 \pm 0.2	92.1 \pm 1.0	91.4 \pm 0.9	92.1 \pm 1.3
DFEA_I	94.5 \pm 0.3	94.5 \pm 0.4	94.6 \pm 0.3	94.9 \pm 0.3	94.8 \pm 0.6	DFEA_I	94.5 \pm 0.3	94.5 \pm 0.4	94.6 \pm 0.3	94.9 \pm 0.3	94.8 \pm 0.6
DFEA_II	89.7 \pm 1.3	91.0 \pm 1.4	92.9 \pm 1.3	93.6 \pm 1.0	93.5 \pm 1.1	DFEA_II	89.7 \pm 1.4	91.1 \pm 1.5	92.9 \pm 1.3	93.6 \pm 1.0	93.5 \pm 1.1
DFEA_III	93.5 \pm 0.6	93.9 \pm 0.7	94.8 \pm 0.6	95.2 \pm 0.4	95.1 \pm 0.4	DFEA_III	93.5 \pm 0.6	93.9 \pm 0.7	94.8 \pm 0.6	95.2 \pm 0.4	95.1 \pm 0.4

Wall-clock cost. Figure 9 aggregates total wall-clock time across all datasets for the twelve attacks (panel a) and the five watermarking defenses (panel b), again on a symmetric-log scale because the workloads span more than three orders of magnitude. The median bars and IQR error bars summarise Tables 4–5, and three patterns are sharper here than in the per-dataset tables. *First, on the attack side the cost cleaves into three groups.* The fast MEA family and CEGA sit between 0.7 and 2 minutes per run, the data-free DFEA family and MEA2 sit slightly above at 1–3 minutes, and only Realistic and (more variably) AdvMEA sit one to three orders of magnitude higher; the upper IQR of Realistic reaches \sim 1000 minutes which is the largest single value in the benchmark. The cost gap is large enough that the *cost-fidelity* ordering is non-trivial, since RQ1 shows that simple attacks already

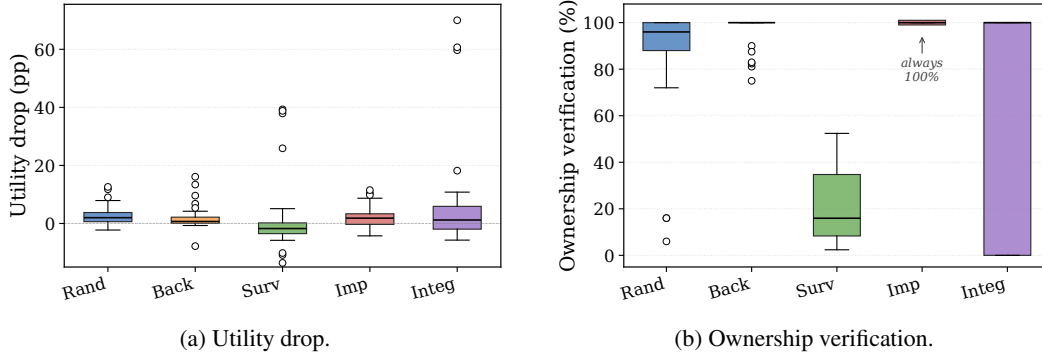


Figure 5: Defense effectiveness across all ten datasets: (a) utility drop and (b) ownership verification. Each box aggregates one point per (dataset, seed), giving 30 points per defense.

Dataset	backdoorwm	randomwm	survivewm	imperceptiblewm	integrity
Cora	79.37 ± 0.45	76.06 ± 0.81	79.07 ± 0.33	71.94 ± 0.27	75.39 ± 0.36
CiteSeer	64.74 ± 0.35	64.99 ± 0.69	67.47 ± 0.27	58.07 ± 0.79	57.61 ± 0.38
PubMed	77.00 ± 0.59	73.77 ± 0.26	25.32 ± 1.19	76.00 ± 0.17	75.68 ± 0.37
Computers	55.39 ± 2.89	58.49 ± 2.93	37.62 ± 24.96	67.04 ± 1.66	14.08 ± 6.63
Photo	57.47 ± 2.27	52.15 ± 5.30	58.47 ± 3.84	61.90 ± 0.43	23.47 ± 21.57
CoauthorCS	69.13 ± 1.21	66.09 ± 6.69	72.75 ± 0.46	72.52 ± 0.73	73.43 ± 0.32
CoauthorPhysics	76.23 ± 1.03	57.32 ± 12.15	81.11 ± 0.89	80.50 ± 0.75	80.91 ± 0.81

Table 32: Defense results: F1 (mean ± std, in %).

saturate near $0.25 \times$ budget. *Second, the defense panel separates into a fast tier (1–60 s) and a slow tier (~ 500 s):* BackdoorWM, SurviveWM, and Integrity train in seconds, RandomWM sits one order of magnitude higher because of its independent watermark graph training, and ImperceptibleWM sits two orders of magnitude higher because of its representation-level losses. *Third, the IQR error bars are narrow on every fast method and wide only on Realistic and ImperceptibleWM,* which means that empirical efficiency is essentially deterministic for the recommended configurations and that the cost numbers in the per-dataset tables are reproducible across hardware.

F.7 Extended statistical analysis of attack effectiveness (RQ1)

We complement the per-dataset RQ1 tables (Tables 10–31 and Tables 36–38) with eight aggregated views (Figure 10, Figure 11, and Figures 12–15) which average across datasets, regimes, or seeds to expose patterns that are hard to read off the raw tables.

Full ten-dataset budget–metric grid. Figure 10 reports the budget–metric curves on all ten datasets, in the same format as the six-dataset main-text Figure 2. The four datasets which the main text omits (CiteSeer, Photo, CoauthorCS, AmazonRatings) reproduce the qualitative behaviour of the chosen six: CiteSeer and Photo track the homophilic-citation/coauthor pattern of Cora and CoauthorPhysics; CoauthorCS sits between them; and AmazonRatings reproduces the heterophilic behaviour of RomanEmpire although its ordinal 5-class label space inflates absolute fidelity. The qualitative conclusions of RQ1 therefore hold uniformly across all ten datasets.

Regime sensitivity heatmap. Figure 11 reports the regime sensitivity across the standard five-budget grid: each cell is the ratio between fidelity in a constrained regime (x_{only} , a_{only} , $data_{\text{free}}$) and fidelity in the both regime for the same attack at the same budget, aggregated over all ten datasets. The heatmap exposes two patterns. *First, the left two blocks (x_{only} , a_{only}) are uniformly green at ratio ≈ 1.0 for every attack at every budget:* removing one input modality is essentially a no-op for the strong attacks, because the surrogate is trained on the target’s labelled responses and label information dominates whichever single input remains. *Second, the right block ($data_{\text{free}}$) is bimodal:* the strong-MEA family (rows MEA0/3/4/5) drops to ratios in the 0.42–0.53 band across every budget, while AdvMEA, CEGA, Realistic, and the three DFEA variants stay at ratios around 1.0. The data-driven attacks (MEA family) collapse without a real graph because they rely on the target’s responses to real-graph queries; the data-free attacks (DFEA, Realistic) by design synthesize their own queries and so are insensitive to the absence of a real graph; CEGA and AdvMEA

Dataset	backdoorwm	randomwm	survivewm	imperceptiblewm	integrity
Cora	80.07 ± 0.40	76.13 ± 1.17	79.93 ± 0.26	71.97 ± 0.31	76.03 ± 0.37
CiteSeer	67.47 ± 0.40	67.90 ± 0.57	70.87 ± 0.12	60.30 ± 1.00	60.10 ± 0.29
PubMed	77.60 ± 0.79	74.13 ± 0.26	39.17 ± 1.01	76.37 ± 0.12	76.33 ± 0.38
Computers	68.27 ± 2.74	71.47 ± 2.49	45.97 ± 31.21	78.90 ± 0.73	11.97 ± 5.56
Photo	92.73 ± 1.50	85.33 ± 6.07	93.20 ± 3.89	96.70 ± 0.08	61.80 ± 20.58
CoauthorCS	88.43 ± 0.77	89.27 ± 2.46	91.70 ± 0.36	89.63 ± 0.76	90.97 ± 0.12
CoauthorPhysics	89.33 ± 0.37	68.60 ± 10.96	90.97 ± 0.33	90.20 ± 0.40	90.60 ± 0.65

Table 33: Defense results: Fidelity (mean ± std, in %).

Dataset	backdoorwm	randomwm	survivewm	imperceptiblewm	integrity
Cora	100.00 ± 0.00	75.33 ± 9.98	54.07 ± 5.79	100.00 ± 0.00	100.00 ± 0.00
CiteSeer	100.00 ± 0.00	72.00 ± 4.32	55.72 ± 4.51	100.00 ± 0.00	100.00 ± 0.00
PubMed	100.00 ± 0.00	64.00 ± 11.31	34.97 ± 0.71	100.00 ± 0.00	100.00 ± 0.00
Computers	93.33 ± 9.43	94.67 ± 1.89	11.08 ± 0.81	100.00 ± 0.00	100.00 ± 0.00
Photo	100.00 ± 0.00	98.67 ± 0.94	13.25 ± 1.10	100.00 ± 0.00	66.67 ± 47.14
CoauthorCS	100.00 ± 0.00	45.33 ± 3.77	8.51 ± 0.34	100.00 ± 0.00	33.33 ± 47.14
CoauthorPhysics	100.00 ± 0.00	56.67 ± 13.70	21.76 ± 0.49	100.00 ± 0.00	66.67 ± 47.14

Table 34: Defense results: Owner. verif. (WM Acc, %) (mean ± std, in %).

retrain a query selector on whichever input is provided, including a synthetic graph, and so also stay near ratio 1.0. The map therefore answers a benchmark-design question: the `data_free` regime is the only regime that meaningfully discriminates attack families, which justifies including it in the standard RQ1 protocol despite its much lower absolute fidelity.

Per-attack budget curves across all ten datasets. Figure 12 shows, for each of the twelve attacks, a small panel containing the surrogate fidelity vs. budget curve on every dataset (regime both). Three observations stand out. First, the strong data-driven attacks (MEAO, MEA1, MEA3, MEA4, MEA5, Realistic, CEGA) saturate by $0.25\times$ on the seven small homophilic graphs, with curves that are visually indistinguishable above this budget; this is the empirical justification for using $0.25\times$ as the medium budget in the joint evaluation of RQ5. Second, the OGBN-Arxiv curve is consistently $\sim 10\text{--}15\%$ below the homophilic graphs across all data-driven attacks at every budget, which is consistent with the larger label space (40 classes) and not with a budget ceiling. Third, the data-free variants (DFEA_I, DFEA_II, DFEA_III) and the noisy MEA2 have curves that are largely flat across budgets and reach high fidelity on most datasets, with DFEA_II on the high-degree product graphs (*Computers* and *Photo*) as the main outlier; this confirms that data-free extraction is broadly robust under our protocol while showing dataset-specific sensitivity.

Regime sensitivity: per-attack fidelity loss when one input is removed. Figure 13a reports, per attack, the mean fidelity drop relative to the both regime when only features (`x_only`), only structure (`a_only`), or no real input (`data_free`) is provided to the extractor. The bars expose a clear separation: the data-driven attacks lose only a few percentage points when one modality is removed (because they still receive the target’s labels for real-graph queries), but lose 30–70 pp in the `data_free` regime; CEGA loses the most in `a_only` (its centrality-based selection becomes ill-defined without the real graph), and AdvMEA is the most robust to removing structure. Figure 13b provides the absolute view that complements these drops: it shows the absolute mean fidelity in each regime per attack, with error bars that aggregate across datasets, budgets, and seeds. The two views together motivate the four-regime protocol used in RQ1.

Runtime and resource distribution across attacks. Figure 14 shows the distribution of per-run wall-clock attack time in minutes, on a log scale, aggregated across all (dataset, regime, budget, seed) combinations. Three groups separate cleanly: (i) the lightweight MEAO/MEA1/MEA3/MEA4/MEA5/CEGA family, with median runtime under one minute and tail below ten minutes, (ii) the adaptive AdvMEA and DFEA_I/II/III family in the one-to-twenty-minute band, and (iii) the heavyweight Realistic pipeline, whose tail extends two orders of magnitude above the rest because it trains an auxiliary edge-prediction model. This distributional view supplements the per-dataset time tables in the main text (Tables 4–5): the overall ordering between groups is preserved on every dataset, but the absolute magnitude scales with graph size.

Watermark defense profile (radar; higher = better on all axes)

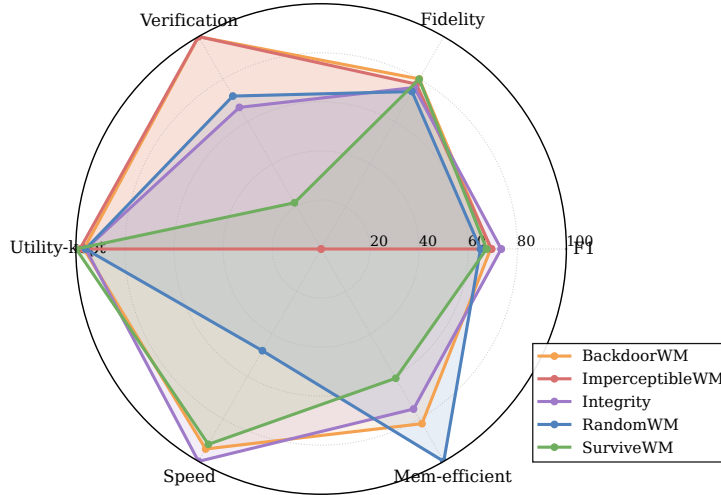


Figure 6: Radar profile of the five watermarking and integrity defenses across six axes. F1, fidelity, verification, and utility-kept come from Tables 32–34; speed and memory-efficiency are obtained from the RQ4 numbers (Tables 4–5 and Figure 8) by inverting and log-normalising to a 0–100 scale. Higher is better on every axis. No defense dominates; BackdoorWM is the largest envelope, Integrity is the only defense in the fast-and-light corner with non-trivial verification, and ImperceptibleWM pays for perfect verification with the worst speed and memory profile.

Table 35: Baseline utility (test accuracy, %) for an undefended target across three backbones. Mean \pm standard deviation over three seeds.

Dataset	GCN (DGL, hidden=16)	GraphSAGE (DGL, hidden=128)	GCN (PyG, hidden=128)
Cora	79.4 \pm 0.5	79.1 \pm 0.3	80.7 \pm 0.4
CiteSeer	67.8 \pm 1.1	70.1 \pm 0.2	70.9 \pm 0.4
PubMed	78.0 \pm 0.6	77.1 \pm 0.3	79.5 \pm 0.2
Computers	44.6 \pm 22.4	59.8 \pm 18.4	75.2 \pm 0.7
Photo	90.1 \pm 4.8	94.5 \pm 0.5	95.3 \pm 0.2
CoauthorCS	87.4 \pm 0.3	92.9 \pm 0.3	90.3 \pm 0.2
CoauthorPhysics	89.3 \pm 0.4	91.2 \pm 0.1	89.8 \pm 0.2
OGBN-Arxiv	37.7 \pm 3.2	54.9 \pm 0.0	52.3 \pm 0.1
RomanEmpire	42.8 \pm 0.2	77.5 \pm 0.5	46.0 \pm 0.3
AmazonRatings	41.7 \pm 0.3	45.5 \pm 0.5	43.4 \pm 0.3

Inter-attack similarity across (dataset, budget) profiles. Figure 15 reports the pairwise Pearson correlation of attacks, where each attack is represented by its fifty-dimensional fidelity vector (ten datasets \times five budgets, regime both). Three structural blocks emerge. The first is the strong-MEA cluster (MEA0, MEA1, MEA3, MEA4, MEA5, Realistic, and CEGA), with pairwise correlations above 0.9 and a single shared profile across datasets. The second is the data-free cluster (DFEA_I, DFEA_II, DFEA_III, plus MEA2), with correlations near 0.95 within the cluster and below 0.5 with the strong-MEA cluster. The third is AdvMEA, which sits between the two clusters and correlates only weakly with both, consistent with its hybrid adaptive-query design. The block structure suggests that, for benchmarking purposes, a representative subset that contains one element from each block (for example MEA0, DFEA_I, and AdvMEA) would already capture the qualitative behaviour of the full twelve-attack set, which we leave to future work as a benchmark-design recommendation.

Per-dataset utility cost of information-limiting defenses. Figure 16 reports the per-dataset utility loss of each of the seven information-limiting and query-detection defenses, computed as undefended GCN baseline accuracy minus the defended-model accuracy reported in Tables 39–40. The figure exposes three patterns that the per-row tables hide. *First, the four output-perturbation/rounding defenses (OP_low, OP_high, PR_2bit, PR_top1) cost essentially nothing on the seven homophilic graphs (bars within ± 3 pp of zero), which is consistent with the design intent of these defenses: they perturb the returned scores at inference time without retraining, so the underlying classifier is unchanged.* *Second, query-detection defenses split into two cost regimes.* GradRedir stays close to the no-defense baseline on most datasets (it perturbs only flagged queries), but on Photo it costs about 23 pp because the defense’s gradient-redirection threshold flags many benign queries on the

Table 36: Detailed RQ1 results on *RomanEmpire*. Fidelity (%) at five budget multipliers across four regimes. Mean \pm standard deviation over three seeds.

(a) Regime=both						(b) Regime=x_only					
Attack	0.05	0.10	0.25	0.50	1.00	Attack	0.05	0.10	0.25	0.50	1.00
MEA0	72.9 \pm 0.4	75.9 \pm 1.7	77.0 \pm 0.8	77.2 \pm 1.5	77.4 \pm 1.5	MEA0	72.5 \pm 1.1	76.5 \pm 0.6	75.8 \pm 2.6	77.4 \pm 0.6	77.4 \pm 1.5
MEA1	54.0 \pm 2.2	59.7 \pm 3.5	68.7 \pm 1.1	72.6 \pm 1.0	77.4 \pm 1.5	MEA1	54.0 \pm 2.2	59.7 \pm 3.5	68.7 \pm 1.1	72.6 \pm 1.0	77.4 \pm 1.5
MEA2	27.0 \pm 0.1	34.0 \pm 1.3	47.8 \pm 0.7	49.8 \pm 1.9	32.7 \pm 9.8	MEA2	26.9 \pm 0.6	33.4 \pm 0.3	47.1 \pm 1.4	47.3 \pm 2.5	32.7 \pm 9.8
MEA3	61.2 \pm 1.0	65.2 \pm 1.1	74.1 \pm 1.1	77.2 \pm 1.6	77.4 \pm 1.5	MEA3	61.2 \pm 0.4	65.2 \pm 0.9	74.3 \pm 1.1	77.4 \pm 1.4	77.4 \pm 1.5
MEA4	63.6 \pm 1.0	70.9 \pm 2.1	73.3 \pm 2.6	76.0 \pm 1.1	77.4 \pm 1.5	MEA4	63.8 \pm 0.4	70.9 \pm 2.1	73.4 \pm 2.6	76.0 \pm 1.1	77.4 \pm 1.5
MEA5	65.8 \pm 1.2	70.0 \pm 0.9	76.7 \pm 1.2	77.6 \pm 1.0	77.4 \pm 1.5	MEA5	65.9 \pm 0.5	69.9 \pm 0.3	76.1 \pm 2.5	77.2 \pm 1.5	77.4 \pm 1.5
AdvMEA	22.0 \pm 6.5	23.5 \pm 6.5	21.9 \pm 6.2	19.1 \pm 3.3	15.7 \pm 3.7	AdvMEA	23.2 \pm 7.3	23.0 \pm 7.1	21.5 \pm 4.3	19.3 \pm 3.8	16.2 \pm 3.9
CEGA	72.1 \pm 0.5	73.3 \pm 1.2	73.4 \pm 2.3	71.4 \pm 2.1	71.4 \pm 2.1	CEGA	72.1 \pm 1.3	72.0 \pm 2.9	73.6 \pm 2.9	71.4 \pm 2.1	71.4 \pm 2.1
Realistic	53.7 \pm 2.3	57.5 \pm 2.1	58.2 \pm 1.5	57.9 \pm 1.9	75.4 \pm 1.9	Realistic	54.4 \pm 1.5	56.7 \pm 1.7	58.3 \pm 2.0	57.9 \pm 2.0	75.7 \pm 1.8
DFEA_I	71.7 \pm 1.1	71.4 \pm 2.1	72.1 \pm 2.7	72.3 \pm 2.7	72.7 \pm 2.2	DFEA_I	71.7 \pm 1.1	71.4 \pm 2.1	72.1 \pm 2.7	72.3 \pm 2.7	72.7 \pm 2.2
DFEA_II	69.2 \pm 0.7	74.9 \pm 0.5	80.8 \pm 1.0	83.3 \pm 0.4	84.3 \pm 0.3	DFEA_II	69.2 \pm 0.7	74.9 \pm 0.5	80.8 \pm 1.0	83.3 \pm 0.4	84.3 \pm 0.3
DFEA_III	73.4 \pm 0.3	76.2 \pm 0.6	75.7 \pm 2.1	77.2 \pm 1.1	77.3 \pm 1.4	DFEA_III	73.4 \pm 0.3	76.2 \pm 0.6	75.7 \pm 2.1	77.2 \pm 1.1	77.3 \pm 1.4

(c) Regime=a_only						(d) Regime=data_free					
Attack	0.05	0.10	0.25	0.50	1.00	Attack	0.05	0.10	0.25	0.50	1.00
MEA0	73.3 \pm 0.8	75.4 \pm 0.3	77.4 \pm 0.4	77.3 \pm 1.7	77.4 \pm 1.5	MEA0	72.8 \pm 1.1	74.7 \pm 1.3	76.0 \pm 1.5	76.9 \pm 2.1	77.4 \pm 1.5
MEA1	54.0 \pm 2.2	59.7 \pm 3.5	68.7 \pm 1.1	72.6 \pm 1.0	77.4 \pm 1.5	MEA1	54.0 \pm 2.2	59.7 \pm 3.5	68.7 \pm 1.1	72.6 \pm 1.0	77.4 \pm 1.5
MEA2	25.5 \pm 1.2	33.7 \pm 0.2	47.7 \pm 0.8	50.5 \pm 2.1	32.7 \pm 9.8	MEA2	26.4 \pm 0.5	33.8 \pm 0.8	47.4 \pm 0.5	51.1 \pm 2.1	32.7 \pm 9.8
MEA3	62.1 \pm 1.3	66.7 \pm 0.4	75.2 \pm 0.7	77.4 \pm 1.7	77.4 \pm 1.5	MEA3	62.6 \pm 0.3	65.8 \pm 0.7	74.0 \pm 1.5	77.2 \pm 1.5	77.4 \pm 1.5
MEA4	63.3 \pm 1.0	70.6 \pm 2.4	73.4 \pm 2.5	76.0 \pm 1.1	77.4 \pm 1.5	MEA4	63.1 \pm 1.1	71.1 \pm 1.7	73.3 \pm 2.3	75.8 \pm 1.5	77.4 \pm 1.5
MEA5	65.5 \pm 0.4	70.3 \pm 1.0	76.7 \pm 1.3	77.5 \pm 1.1	77.4 \pm 1.5	MEA5	64.8 \pm 1.2	69.5 \pm 1.0	76.2 \pm 2.3	77.2 \pm 1.3	77.4 \pm 1.5
AdvMEA	22.4 \pm 6.5	22.8 \pm 5.9	20.8 \pm 6.3	17.8 \pm 4.2	15.1 \pm 4.1	AdvMEA	23.4 \pm 6.6	23.0 \pm 7.1	21.7 \pm 6.9	18.3 \pm 4.6	15.3 \pm 4.4
CEGA	71.5 \pm 2.6	72.9 \pm 2.9	73.4 \pm 2.7	71.4 \pm 2.1	71.4 \pm 2.1	CEGA	71.2 \pm 2.2	73.0 \pm 1.9	73.3 \pm 2.7	71.4 \pm 2.1	71.4 \pm 2.1
Realistic	55.3 \pm 2.2	58.1 \pm 1.0	56.8	58.1 \pm 1.9	75.7 \pm 1.7	Realistic	54.4 \pm 2.3	56.3 \pm 2.4	58.3 \pm 1.4	57.8 \pm 2.5	75.6 \pm 1.6
DFEA_I	71.7 \pm 1.1	71.4 \pm 2.1	72.1 \pm 2.7	72.3 \pm 2.7	72.7 \pm 2.2	DFEA_I	71.7 \pm 1.1	71.4 \pm 2.1	72.1 \pm 2.7	72.3 \pm 2.7	72.7 \pm 2.2
DFEA_II	69.2 \pm 0.7	74.9 \pm 0.5	80.8 \pm 1.0	83.3 \pm 0.4	84.3 \pm 0.3	DFEA_II	69.2 \pm 0.7	74.9 \pm 0.5	80.8 \pm 1.0	83.3 \pm 0.4	84.3 \pm 0.3
DFEA_III	73.4 \pm 0.3	76.2 \pm 0.6	75.7 \pm 2.1	77.2 \pm 1.1	77.3 \pm 1.4	DFEA_III	73.4 \pm 0.3	76.2 \pm 0.6	75.7 \pm 2.1	77.2 \pm 1.1	77.3 \pm 1.4

Table 37: Detailed RQ1 results on *AmazonRatings*. Fidelity (%) at five budget multipliers across four regimes. Mean \pm standard deviation over three seeds.

(a) Regime=both						(b) Regime=x_only					
Attack	0.05	0.10	0.25	0.50	1.00	Attack	0.05	0.10	0.25	0.50	1.00
MEA0	92.3 \pm 0.6	93.1 \pm 1.4	93.8 \pm 0.7	93.9 \pm 0.5	94.4 \pm 1.0	MEA0	92.1 \pm 0.6	93.5 \pm 0.9	94.1 \pm 1.2	94.3 \pm 0.9	94.4 \pm 1.0
MEA1	88.8 \pm 1.0	91.9 \pm 0.5	94.2 \pm 0.6	94.8 \pm 0.7	94.4 \pm 1.0	MEA1	88.8 \pm 1.0	91.9 \pm 0.5	94.1 \pm 0.7	94.8 \pm 0.7	94.4 \pm 1.0
MEA2	82.0 \pm 1.4	87.3 \pm 0.6	92.4 \pm 0.8	93.9 \pm 1.3	94.5 \pm 0.5	MEA2	82.7 \pm 1.5	86.9 \pm 1.7	91.8 \pm 0.9	93.7 \pm 1.3	94.5 \pm 0.5
MEA3	88.0 \pm 0.7	91.2 \pm 1.3	93.8 \pm 1.3	94.6 \pm 1.0	94.4 \pm 1.0	MEA3	87.4 \pm 2.1	90.5 \pm 1.3	93.8 \pm 0.4	94.6 \pm 1.1	94.4 \pm 1.0
MEA4	85.1 \pm 0.4	87.1 \pm 0.5	90.1 \pm 0.8	92.4 \pm 1.1	94.4 \pm 1.0	MEA4	85.8 \pm 0.5	86.7 \pm 0.5	90.1 \pm 0.8	92.4 \pm 1.1	94.4 \pm 1.0
MEA5	89.9 \pm 0.6	91.4 \pm 1.1	94.7 \pm 0.9	94.5 \pm 0.9	94.4 \pm 1.0	MEA5	89.1 \pm 1.4	92.0 \pm 1.2	94.4 \pm 0.6	94.2 \pm 0.9	94.4 \pm 1.0
AdvMEA	70.4 \pm 1.5	66.2 \pm 7.3	68.7 \pm 3.4	70.1 \pm 1.3	66.9 \pm 5.4	AdvMEA	69.1 \pm 2.4	68.0 \pm 5.5	69.5 \pm 1.7	65.3 \pm 7.2	67.0 \pm 4.1
CEGA	87.1 \pm 0.9	87.3 \pm 1.2	89.1 \pm 1.2	89.7 \pm 2.0	89.7 \pm 2.0	CEGA	88.2 \pm 0.7	87.4 \pm 1.1	89.5 \pm 1.7	89.7 \pm 2.0	89.7 \pm 2.0
Realistic	89.9 \pm 2.7	90.8 \pm 3.0	90.6 \pm 2.6	92.8 \pm 1.0	94.9 \pm 0.3	Realistic	90.7 \pm 1.9	91.0 \pm 2.4	92.2 \pm 1.0	93.5 \pm 0.5	94.9 \pm 0.4
DFEA_I	88.6 \pm 1.1	89.2 \pm 2.3	89.6 \pm 1.7	89.6 \pm 1.4	89.4 \pm 1.3	DFEA_I	88.6 \pm 1.1	89.2 \pm 2.3	89.6 \pm 1.7	89.6 \pm 1.4	89.4 \pm 1.3
DFEA_II	90.4 \pm 1.2	92.6 \pm 0.6	94.5 \pm 0.7	95.1 \pm 0.6	95.6 \pm 0.2	DFEA_II	90.4 \pm 1.2	92.5 \pm 0.6	94.5 \pm 0.7	95.1 \pm 0.6	95.6 \pm 0.2
DFEA_III	92.4 \pm 0.9	93.5 \pm 1.2	94.6 \pm 0.5	94.5 \pm 0.6	94.5 \pm 0.7	DFEA_III	92.4 \pm 1.0	93.5 \pm 1.2	94.6 \pm 0.5	94.4 \pm 0.7	94.5 \pm 0.7

(c) Regime=a_only						(d) Regime=data_free					
Attack	0.05	0.10	0.25	0.50	1.00	Attack	0.05	0.10	0.25	0.50	1.00
MEA0	92.3 \pm 0.6	93.0 \pm 0.7	94.6 \pm 0.9	94.2 \pm 0.9	94.4 \pm 1.0	MEA0	91.7 \pm 0.5	93.3 \pm 1.0	93.5 \pm 0.7	94.3 \pm 0.9	94.4 \pm 1.0
MEA1	88.8 \pm 1.0	91.9 \pm 0.5	94.1 \pm 0.7	94.8 \pm 0.7	94.4 \pm 1.0	MEA1	88.8 \pm 1.0	91.9 \pm 0.5	94.1 \pm 0.7	94.8 \pm 0.7	94.4 \pm 1.0
MEA2	82.2 \pm 0.7	87.0 \pm 1.8	92.2 \pm 0.8	94.1 \pm 1.2	94.5 \pm 0.5	MEA2	81.8 \pm 0.9	86.6 \pm 0.7	91.9 \pm 1.0	93.9 \pm 1.0	94.5 \pm 0.6
MEA3	88.6 \pm 0.1	90.7 \pm 1.2	94.0 \pm 0.9	94.7 \pm 1.1	94.4 \pm 1.0	MEA3	87.9 \pm 0.5	91.0 \pm 1.5	94.0 \pm 1.0	94.6 \pm 1.0	94.4 \pm 1.0
MEA4	85.3 \pm 0.3	87.2 \pm 0.4	90.1 \pm 0.8	92.4 \pm 1.1	94.4 \pm 1.0	MEA4	85.4 \pm 0.4	87.0 \pm 0.6	90.1 \pm 0.8	92.4 \pm 1.1	94.4 \pm 1.0
MEA5	89.4 \pm 0.9	91.5 \pm 1.7	94.3 \pm 0.8	94.5 \pm 1.0	94.4 \pm 1.0	MEA5	89.5 \pm 1.0	91.5 \pm 1.6	94.4 \pm 0.7	94.6 \pm 0.9	94.4 \pm 1.0
AdvMEA	70.4 \pm 1.5	69.5 \pm 3.0	67.3 \pm 5.8	63.9 \pm 9.1	68.2 \pm 3.5	AdvMEA	70.0 \pm 2.0	67.3 \pm 5.0	68.0 \pm 3.5	64.7 \pm 8.0	67.5 \pm 4.0
CEGA	87.5 \pm 1.2	88.8 \pm 1.9	88.8 \pm 2.0	89.7 \pm 2.0	89.7 \pm 2.0	CEGA	87.6 \pm 1.0	87.8 \pm 1.5	89.1 \pm 1.5	89.7 \pm 2.0	89.7 \pm 2.0
Realistic	89.5 \pm 2.2	92.3 \pm 0.7	92.7 \pm 1.0	93.6 \pm 0.3	95.0 \pm 0.3	Realistic	89.7 \pm 2.4	91.5 \pm 2.0	91.7 \pm 1.5	93.0 \pm 0.7	94.9 \pm 0.4
DFEA_I	88.6 \pm 1.1	89.2 \pm 2.3	89.6 \pm 1.7	89.6 \pm 1.4	89.4 \pm 1.3	DFEA_I	88.6 \pm 1.1	89.2 \pm 2.3	89.6 \pm 1.7	89.6 \pm 1.4	89.4 \pm 1.3
DFEA_II	90.4 \pm 1.3	92.5 \pm 0.6	94.5 \pm 0.7	95.2 \pm 0.5	95.6 \pm 0.2	DFEA_II	90.3 \pm 1.3	92.6 \pm 0.6	94.5 \pm 0.7	95.2 \pm 0.5	95.6 \pm 0.2
DFEA_III	92.4 \pm 0.9	93.5 \pm 1.3	94.6 \pm 0.5	94.5 \pm 0.6	94.5 \pm 0.7	DFEA_III	92.4 \pm 1.0	93.5 \pm 1.2	94.6 \pm 0.5	94.4 \pm 0.7	94.5 \pm 0.7

high-degree product graph; on *Computers* the loss is even larger (~ 45 pp). *Third, AdaptMisinfo consistently costs 30–45 pp across every dataset*, which is the highest among all seven and reflects the fact that the defense actively returns wrong labels on a large fraction of queries; users of the GraphIPBench API should treat AdaptMisinfo as a high-cost defense even when its verification proxy reaches 100%. The plot also surfaces a useful negative finding: PRADA on *RomanEmpire* loses 23 pp because the heterophilic structure makes random-query rejection blunt, suggesting that PRADA’s distance-based query filter needs adaptation for graphs with low edge homophily.

Table 38: Detailed RQ1 results on *OGBN-Arxiv*. Fidelity (%) at five budget multipliers across four regimes. Mean \pm standard deviation over three seeds. The 169,343-node graph requires sub-sampled edge construction at large budgets for the Realistic attack and the data-free variants.

(a) Regime=both						(b) Regime=x_only					
Attack	0.05	0.10	0.25	0.50	1.00	Attack	0.05	0.10	0.25	0.50	1.00
MEA0	77.2 \pm 4.2	77.4 \pm 4.7	77.1 \pm 4.6	77.2 \pm 4.7	77.2 \pm 4.8	MEA0	76.6 \pm 4.7	77.5 \pm 4.6	77.4 \pm 4.1	77.3 \pm 4.8	77.2 \pm 4.8
MEA1	74.2 \pm 1.2	79.0 \pm 1.3	81.7 \pm 2.9	81.6 \pm 3.4	77.2 \pm 4.8	MEA1	74.2 \pm 1.2	79.0 \pm 1.2	81.7 \pm 2.9	81.6 \pm 3.4	77.3 \pm 4.8
MEA2	52.8 \pm 3.6	52.8 \pm 3.6	52.8 \pm 3.6	52.8 \pm 3.6	52.8 \pm 3.6	MEA2	52.8 \pm 3.5	52.8 \pm 3.6	52.8 \pm 3.6	52.8 \pm 3.6	52.8 \pm 3.6
MEA3	64.0 \pm 4.5	66.9 \pm 5.4	74.2 \pm 5.1	77.5 \pm 4.8	77.3 \pm 4.8	MEA3	64.5 \pm 4.8	67.3 \pm 4.7	74.3 \pm 4.8	77.4 \pm 4.8	77.2 \pm 4.8
MEA4	62.2 \pm 4.8	63.2 \pm 5.2	65.5 \pm 6.0	70.6 \pm 4.9	77.1 \pm 5.1	MEA4	62.6 \pm 4.8	63.3 \pm 5.1	65.4 \pm 5.6	70.6 \pm 5.0	77.1 \pm 5.0
MEA5	64.9 \pm 4.1	69.5 \pm 4.8	77.2 \pm 4.8	77.6 \pm 4.4	77.3 \pm 4.8	MEA5	64.8 \pm 4.6	69.4 \pm 4.8	77.2 \pm 4.8	77.5 \pm 4.7	77.2 \pm 4.8
AdvMEA	26.9 \pm 22.7	28.7 \pm 21.1	26.2 \pm 21.2	23.0 \pm 17.1	20.4 \pm 17.2	AdvMEA	20.7 \pm 20.4	23.1 \pm 21.9	24.9 \pm 23.1	22.7 \pm 23.9	18.8 \pm 16.7
CEGA	77.9 \pm 3.0	77.7 \pm 4.1	77.4 \pm 4.6	75.5 \pm 4.2	75.5 \pm 4.2	CEGA	77.6 \pm 4.9	78.0 \pm 4.8	77.1 \pm 5.1	75.5 \pm 4.2	75.5 \pm 4.2
Realistic	74.5 \pm 3.7	74.4 \pm 2.7	75.3 \pm 2.7	75.6 \pm 3.0	75.0 \pm 3.2	Realistic	73.9 \pm 2.5	74.9 \pm 1.9	74.9 \pm 2.4	75.6 \pm 3.0	75.0 \pm 3.1
DFEA_I	80.7 \pm 4.5	80.8 \pm 4.6	81.0 \pm 4.2	81.1 \pm 4.0	81.0 \pm 3.9	DFEA_I	80.7 \pm 4.5	80.7 \pm 4.7	81.0 \pm 4.2	81.1 \pm 4.0	81.0 \pm 3.9
DFEA_II	75.1 \pm 1.2	76.0 \pm 1.6	76.4 \pm 1.5	76.3 \pm 1.3	76.7 \pm 1.3	DFEA_II	75.1 \pm 1.3	76.0 \pm 1.3	76.3 \pm 1.6	76.3 \pm 1.6	76.8 \pm 1.2
DFEA_III	76.9 \pm 4.5	77.6 \pm 4.4	77.7 \pm 4.6	77.6 \pm 4.5	77.1 \pm 4.7	DFEA_III	76.9 \pm 4.5	77.6 \pm 4.4	77.7 \pm 4.5	77.6 \pm 4.5	77.1 \pm 4.7

(c) Regime=a_only						(d) Regime=data_free					
Attack	0.05	0.10	0.25	0.50	1.00	Attack	0.05	0.10	0.25	0.50	1.00
MEA0	77.1 \pm 5.2	77.5 \pm 4.3	77.3 \pm 4.1	77.1 \pm 4.9	77.3 \pm 4.8	MEA0	77.2 \pm 4.2	77.0 \pm 4.7	77.2 \pm 4.9	77.3 \pm 4.8	77.3 \pm 4.8
MEA1	74.2 \pm 1.2	79.0 \pm 1.2	81.7 \pm 2.9	81.6 \pm 3.4	77.3 \pm 4.8	MEA1	74.2 \pm 1.2	79.0 \pm 1.3	81.7 \pm 2.9	81.6 \pm 3.4	77.3 \pm 4.8
MEA2	52.8 \pm 3.6	52.8 \pm 3.6	52.8 \pm 3.6	52.8 \pm 3.6	52.8 \pm 3.6	MEA2	52.8 \pm 3.6	52.8 \pm 3.6	52.8 \pm 3.6	52.8 \pm 3.6	52.8 \pm 3.6
MEA3	64.1 \pm 4.7	67.9 \pm 4.9	74.5 \pm 4.9	77.5 \pm 4.4	77.3 \pm 4.8	MEA3	64.4 \pm 4.8	66.9 \pm 5.0	74.4 \pm 4.8	77.4 \pm 4.7	77.2 \pm 4.8
MEA4	62.6 \pm 4.5	63.4 \pm 5.6	65.2 \pm 6.0	70.6 \pm 4.8	77.1 \pm 5.0	MEA4	63.0 \pm 5.1	63.4 \pm 5.5	65.1 \pm 6.0	70.1 \pm 5.5	77.1 \pm 5.0
MEA5	65.3 \pm 4.7	69.7 \pm 4.4	77.2 \pm 4.7	77.3 \pm 4.7	77.2 \pm 4.8	MEA5	65.0 \pm 4.8	69.3 \pm 5.0	77.4 \pm 4.5	77.6 \pm 4.4	77.3 \pm 4.8
AdvMEA	23.1 \pm 18.5	24.8 \pm 18.8	24.4 \pm 20.2	24.0 \pm 19.1	21.4 \pm 16.3	AdvMEA	30.4 \pm 21.8	26.0 \pm 20.8	24.4 \pm 22.6	22.0 \pm 21.7	22.6 \pm 18.2
CEGA	77.6 \pm 4.5	77.3 \pm 4.6	76.7 \pm 4.5	75.5 \pm 4.2	75.5 \pm 4.2	CEGA	77.9 \pm 4.8	77.5 \pm 4.8	76.7 \pm 4.9	75.5 \pm 4.2	75.5 \pm 4.2
Realistic	74.3 \pm 3.3	74.6 \pm 2.1	75.2 \pm 2.5	74.9 \pm 2.3	75.1 \pm 3.2	Realistic	74.2 \pm 3.1	75.1 \pm 3.3	75.4 \pm 3.0	74.8 \pm 2.2	75.1 \pm 3.1
DFEA_I	80.7 \pm 4.5	80.7 \pm 4.6	81.0 \pm 4.2	81.1 \pm 4.0	81.0 \pm 3.9	DFEA_I	80.7 \pm 4.5	80.8 \pm 4.5	81.0 \pm 4.2	81.1 \pm 4.0	81.0 \pm 3.9
DFEA_II	75.0 \pm 1.4	75.8 \pm 1.4	76.4 \pm 1.5	76.5 \pm 1.5	76.6 \pm 1.3	DFEA_II	75.2 \pm 1.3	76.0 \pm 1.3	76.3 \pm 1.4	76.6 \pm 1.8	76.5 \pm 1.5
DFEA_III	76.9 \pm 4.5	77.6 \pm 4.4	77.7 \pm 4.5	77.6 \pm 4.5	77.1 \pm 4.8	DFEA_III	76.9 \pm 4.5	77.7 \pm 4.3	77.7 \pm 4.6	77.7 \pm 4.5	77.1 \pm 4.7

Table 39: Detailed results for the four output-perturbation and prediction-rounding defenses across all ten datasets. Each cell reports protected-model accuracy (%) with the verification proxy (%) in parentheses, both as mean \pm standard deviation over three seeds. The target backbone is a DGL GCN with hidden dimension 16.

Dataset	OP_low	OP_high	PR_2bit	PR_top1
Cora	79.4 \pm 0.7 (98.6 \pm 0.7)	79.2 \pm 1.5 (93.9 \pm 1.3)	73.3 \pm 0.8 (83.7 \pm 0.1)	79.6 \pm 0.5 (100.0 \pm 0.0)
CiteSeer	67.6 \pm 0.8 (97.8 \pm 0.6)	66.3 \pm 0.8 (91.0 \pm 1.5)	53.9 \pm 3.4 (70.3 \pm 5.1)	68.8 \pm 0.4 (100.0 \pm 0.0)
PubMed	77.9 \pm 0.2 (99.0 \pm 0.4)	75.9 \pm 0.7 (94.7 \pm 0.3)	77.6 \pm 0.4 (93.4 \pm 1.0)	78.2 \pm 0.3 (100.0 \pm 0.0)
Computers	44.0 \pm 21.1 (89.2 \pm 13.0)	37.6 \pm 27.0 (55.3 \pm 37.8)	36.1 \pm 26.4 (61.7 \pm 37.1)	34.8 \pm 23.6 (100.0 \pm 0.0)
Photo	89.1 \pm 3.7 (98.9 \pm 0.5)	90.7\pm5.7 (96.6 \pm 3.7)	90.4\pm2.6 (96.7 \pm 2.1)	95.5\pm0.6 (100.0 \pm 0.0)
CoauthorCS	87.8 \pm 0.1 (99.5 \pm 0.2)	88.2 \pm 0.7 (98.8 \pm 0.4)	87.5 \pm 0.8 (98.1 \pm 0.7)	88.1 \pm 0.7 (100.0 \pm 0.0)
CoauthorPhysics	89.4\pm0.3 (99.8 \pm 0.2)	89.1 \pm 0.2 (99.3 \pm 0.1)	90.2 \pm 0.1 (98.7 \pm 0.4)	89.5 \pm 0.6 (100.0 \pm 0.0)
OGBN-Arxiv	37.7 \pm 2.9 (95.5 \pm 0.3)	37.8 \pm 0.7 (81.2 \pm 1.0)	30.2 \pm 2.0 (59.6 \pm 3.8)	39.5 \pm 0.5 (100.0 \pm 0.0)
RomanEmpire	42.7 \pm 0.3 (95.3 \pm 0.1)	40.6 \pm 1.4 (82.2 \pm 1.3)	35.2 \pm 0.7 (56.4 \pm 1.2)	42.7 \pm 0.5 (100.0 \pm 0.0)
AmazonRatings	42.0 \pm 0.3 (94.8 \pm 0.6)	41.2 \pm 0.1 (80.0 \pm 0.7)	39.4 \pm 0.6 (70.6 \pm 2.8)	41.6 \pm 0.2 (100.0 \pm 0.0)

F.8 Joint evaluation and watermark survival per dataset

This subsection provides the full numerical record together with the analyses which anchor the cross-dataset claims of RQ5. We first show the consolidated Computers heatmap (Figure 17) which is referenced from the main text, and then the per-dataset tables. The tables form three groups; all values use the standard medium budget $0.25\times$ and the mean and standard deviation are taken over three seeds.

Group 1 (joint surrogate fidelity, watermarking defenses). Tables 41–45 cover all ten datasets for the five watermarking and integrity defenses (BackdoorWM, SurviveWM, Integrity, RandomWM, ImperceptibleWM). Three patterns emerge across the group. *First*, on the seven homophilic graphs (Cora, CiteSeer, PubMed, Computers, Photo, CoauthorCS, CoauthorPhysics) the strong data-driven attacks (MEA0, MEA1, MEA3, MEA4, MEA5, Realistic, and CEGA) reach surrogate fidelity in the 80–95% band against every watermark, which is within ~ 5 pp of the undefended baseline reported in RQ1. *Second*, the noise-driven MEA2 and the data-free DFEA_I/II/III variants reach 65–95% on most homophilic datasets and remain in the same band as the data-driven attacks, while degrading more sharply on the high-degree product graphs *Computers* and *Photo* (DFEA_II drops to ~ 11 –65% there); the residual gap is largely explained by the underlying attack rather than by the defense, mirroring the RQ1 pattern against undefended targets. *Third*, the heterophilic and large-scale graphs

Table 40: Detailed results for the three query-detection defenses across all ten datasets. Each cell reports protected-model accuracy (%) with the verification proxy (%) in parentheses, both as mean \pm standard deviation over three seeds.

Dataset	PRADA	AdaptMisinfo	GradRedir
Cora	40.2 \pm 2.1 (43.0 \pm 1.3)	41.0 \pm 0.1 (48.5 \pm 0.0)	79.8 \pm 0.2 (100.0 \pm 0.0)
CiteSeer	69.3 \pm 0.7 (100.0 \pm 0.0)	39.8 \pm 0.3 (52.5 \pm 0.0)	68.4 \pm 0.9 (100.0 \pm 0.0)
PubMed	78.0 \pm 0.7 (100.0 \pm 0.0)	44.1 \pm 0.8 (48.6 \pm 0.0)	78.3 \pm 0.5 (100.0 \pm 0.0)
Computers	46.0 \pm 18.0 (100.0 \pm 0.0)	28.0 \pm 13.9 (64.3 \pm 0.0)	52.4 \pm 20.9 (100.0 \pm 0.0)
Photo	87.0\pm10.6 (100.0 \pm 0.0)	46.3 \pm 0.4 (49.6 \pm 0.0)	66.6 \pm 17.6 (100.0 \pm 0.0)
CoauthorCS	75.0 \pm 0.8 (79.6 \pm 1.3)	52.4 \pm 0.5 (58.7 \pm 0.0)	88.2 \pm 0.7 (100.0 \pm 0.0)
CoauthorPhysics	83.4 \pm 0.7 (89.0 \pm 0.9)	59.0\pm0.2 (63.1 \pm 0.0)	89.7\pm0.3 (100.0 \pm 0.0)
OGBN-Arxiv	37.0 \pm 0.3 (100.0 \pm 0.0)	19.9 \pm 0.3 (52.3 \pm 0.0)	38.2 \pm 1.0 (100.0 \pm 0.0)
RomanEmpire	19.7 \pm 0.2 (25.4 \pm 0.7)	22.5 \pm 0.4 (50.8 \pm 0.0)	42.5 \pm 0.3 (100.0 \pm 0.0)
AmazonRatings	41.8 \pm 0.4 (100.0 \pm 0.0)	33.9 \pm 0.1 (48.9 \pm 0.0)	41.7 \pm 0.3 (100.0 \pm 0.0)

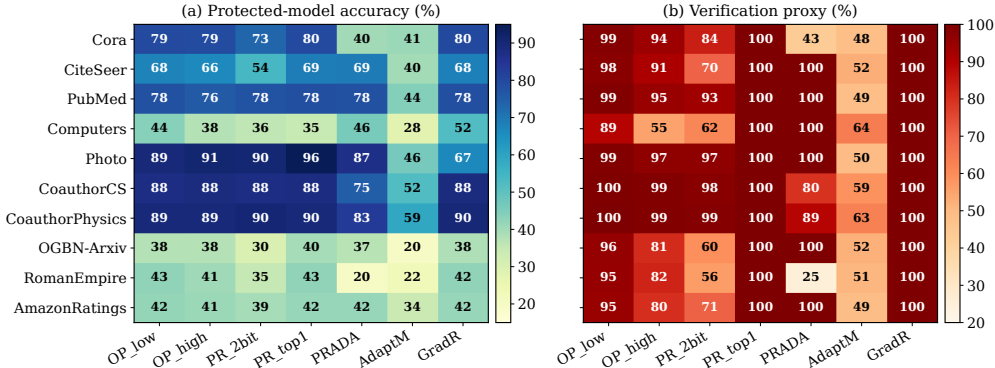


Figure 7: Heatmap view of the seven information-limiting and query-detection defenses across all ten datasets. Left panel: protected-model accuracy (%); right panel: verification proxy (%). Numbers are the same as in Tables 39–40. The two-panel view makes explicit that verification splits into two regimes: output-perturbation/rounding defenses and GradRedir verify at high rates, whereas PRADA and AdaptMisinfo are more variable and often closer to random; protected accuracy is largely flat across defenses except on *Computers*.

(*RomanEmpire*, *AmazonRatings*, *OGBN-Arxiv*) compress the spread between attacks: the strong attacks lose about 10–25 pp of absolute fidelity, while the data-free attacks gain a few points on *AmazonRatings* (where five ordinal classes inflate any classifier), as already observed in RQ1.

Group 2 (joint surrogate fidelity, information-limiting defenses). Tables 41–48 cover all ten datasets for the seven information-limiting and query-detection defenses (OP_low, OP_high, PR_2bit, PR_top1, PRADA, AdaptMisinfo, GradRedir). Two cross-dataset patterns hold. *First*, the relative ordering between defenses is highly stable: PRADA and AdaptMisinfo consistently produce the largest fidelity drop relative to the undefended baseline on every dataset and every attack, while the four output-perturbation and rounding variants (OP_low, OP_high, PR_top1, GradRedir) leave fidelity within ~ 5 pp of the undefended baseline. *Second*, prediction rounding to two bits (PR_2bit) is the only output-perturbation defense whose effect depends sharply on the attack: it has near-zero impact on the strong data-driven attacks (which already operate on label-like signal) but reduces MEA2 and the DFEA family by an additional 5–15 pp on most datasets, which is consistent with the link-prediction behaviour reported in Appendix F.10.

Group 3 (watermark survival on the surrogate). Tables 41–50 cover all ten datasets for watermark verification on the extracted surrogate. The five watermarks split sharply across groups. The query-based Integrity fingerprint survives at 50–100 % on the data-driven attacks across most homophilic datasets and remains the strongest survivor on the heterophilic ones; the in-model marker BackdoorWM is more heterogeneous: it collapses for several data-driven attacks on *Cora*, but partially survives on the larger graphs (*Computers*, *Photo*, *CoauthorCS*) and for some DFEA variants; SurviveWM produces a stable but small (~ 10 –15 %) survival rate that does not exceed the random-guess marker on most datasets; RandomWM yields 10–20 % survival across the board, again essentially indistinguishable from random; and ImperceptibleWM drops to zero on *Cora*, *CiteSeer*, *PubMed*, *Computers*, *Photo*, and on every data-free attack across all datasets, with sporadic non-zero survival appearing only

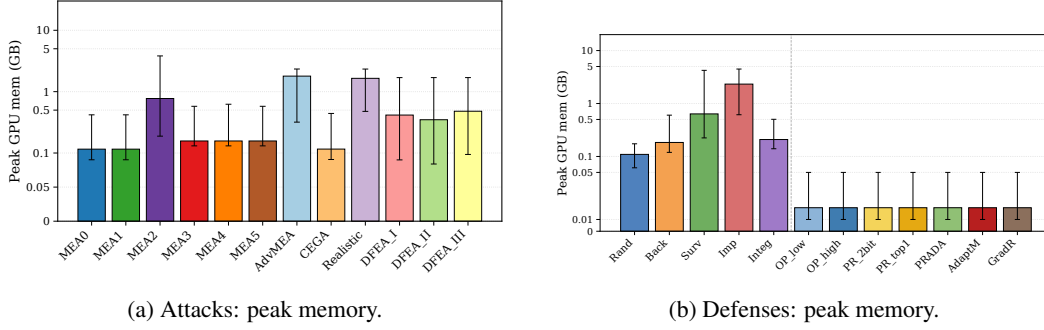


Figure 8: Peak GPU memory (GB) on a symmetric-log scale, aggregated across all ten datasets. Bars show median and error bars show the inter-quartile range across (dataset, seed) combinations. Panel (b) covers all twelve defenses; the dashed line separates the five watermarking defenses (Rand, Back, Surv, Imp, Integ) on the left from the seven information-limiting / query-detection defenses on the right.

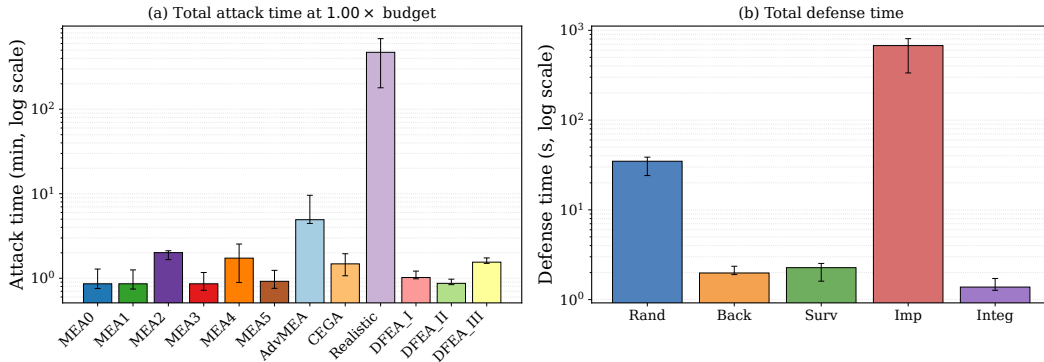


Figure 9: Wall-clock cost summary on a log scale. (a) Total attack time (min) at $1.00\times$ budget; bars are median and error bars are the inter-quartile range across the seven homophilic datasets. (b) Total defense time (s); same conventions. Numbers from Tables 4–5. Three groupings emerge on the attack side (fast MEA/CEGA, intermediate DFEA/MEA2, slow *Realistic*/*AdvMEA*) and two on the defense side (fast watermarks vs. *ImperceptibleWM*).

on the heterophilic graphs. The aggregate picture is identical to the one reported in the main text Figure 17: only watermarks that anchor verification in a query-time mechanism survive extraction reliably.

The figures at the end of this subsection (Figures 18a–20) provide complementary statistical views: a violin plot of survival distributions per defense, a scatter that links survival to graph-level structural properties, an empirical CDF of surrogate fidelity stratified by defense family, and a per-dataset heatmap grid for joint fidelity.

Statistical views on the joint evaluation. We complement the per-dataset tables of this subsection with four statistical figures that aggregate the same per-seed records across all 10 datasets, 12 attacks, and 5 watermarking defenses. Figure 18a shows the full distribution of watermark survival on the surrogate as a violin plot per defense; the violin shape exposes that *ImperceptibleWM* concentrates almost all of its mass at 0%, that *SurviveWM* and *RandomWM* sit at a thin band around 10–20% that does not exceed the random-guess marker on most datasets, that *BackdoorWM* is multi-modal with a heavy mass at 0% and a secondary mode near 50–100% on the larger graphs, and that *Integrity* is the only watermark with a substantial probability mass above 50%. Figure 18b relates this distribution to graph structure: each marker is the mean watermark survival on one dataset for one defense, plotted against the dataset’s edge homophily; the trend lines show that *BackdoorWM* and *Integrity* have a moderate positive association between homophily and survival on the homophilic graphs, while *ImperceptibleWM* stays at 0% across the homophily range and only deviates on the heterophilic graphs.

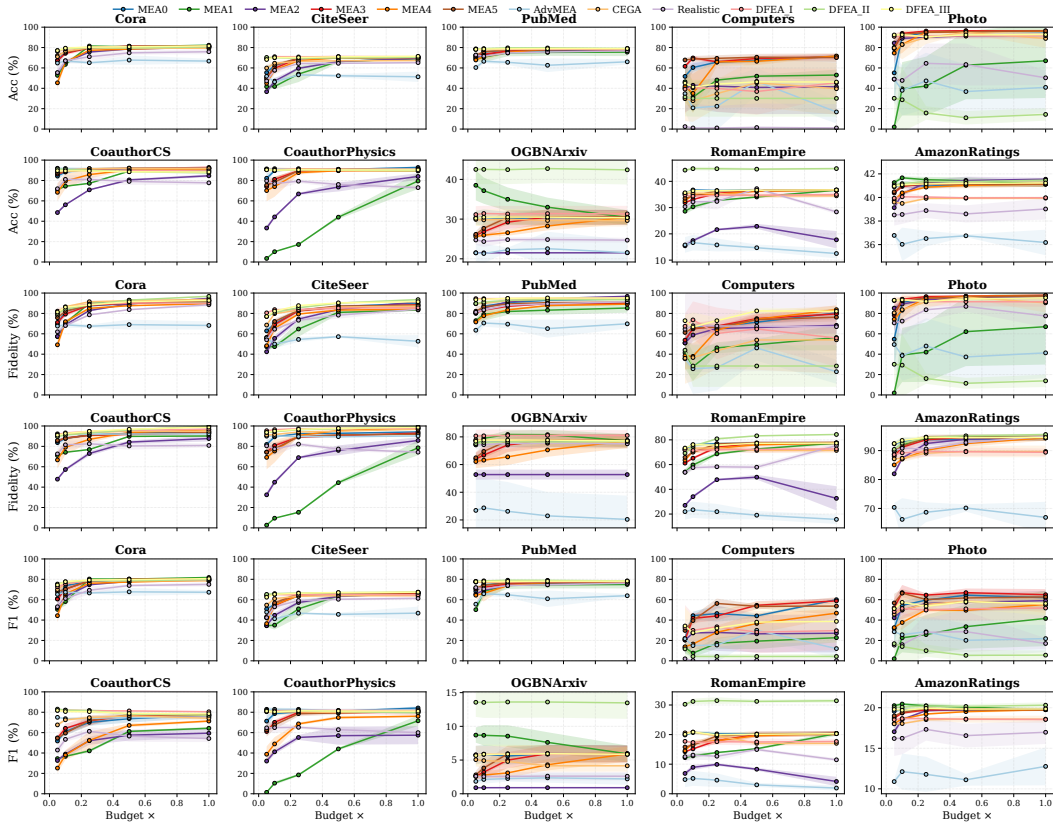


Figure 10: Budget–metric curves on all ten datasets (columns) for accuracy, fidelity, and macro F1 (rows). Lines are the twelve attacks (mean over three seeds, shaded bands ± 1 std). The seven homophilic graphs share a 0–100% y -axis; OGBN-Arxiv, RomanEmpire, and AmazonRatings use per-subplot ranges since their target accuracy is bounded by intrinsic task difficulty. The six-dataset version that appears in the main text (Figure 2) is a subset of this figure.

Figure 19a shifts attention from watermark survival to surrogate fidelity. The empirical CDF of fidelity, separated by defense, makes the joint statement of RQ5 visually explicit: for every watermarking defense the fidelity CDF lies very close to the undefended baseline, with the curves crossing the 80% mark at a similar quantile around 0.6–0.7. In other words, the fraction of (attack, dataset, seed) runs that yield a high-fidelity surrogate is essentially independent of which watermark protects the target. Figure 19b plots surrogate accuracy against surrogate fidelity to defended target as a 2D density (left) and a per-defense scatter (right). The diagonal in both panels is the line on which a surrogate’s accuracy on ground truth equals its fidelity to the protected model. Two observations follow. First, the bulk of the density lies above the diagonal, which means that on most defended targets the surrogate matches the defended model more closely than it matches ground truth; this is the expected behaviour for a black-box mimicry attack and is independent of the defense. Second, the per-defense group means cluster tightly in the high-accuracy / high-fidelity corner for every watermark and overlap with the density of Integrity, which confirms quantitatively that the choice of watermark does not move the surrogate away from the defended-model behaviour.

Finally, Figure 20 renders the joint surrogate fidelity as a per-dataset heatmap grid, one 12×5 panel per dataset. The grid makes the cross-dataset uniformity of the picture visible at a glance: the strong-attack rows (MEAO, MEA1, MEA3, MEA4, MEA5, Realistic, CEGA) are saturated green on every homophilic dataset and remain in the orange-to-yellow range on *RomanEmpire* and *AmazonRatings*, while MEA2 and the DFEA variants form a separate block: they remain strong on many homophilic and large-scale graphs, but show visible degradation on specific high-variance product-graph settings, especially DFEA_II on *Computers* and *Photo*. The five-defense column structure is essentially repeated across the ten datasets, which is the visual analogue of the empirical-CDF and density observations above.

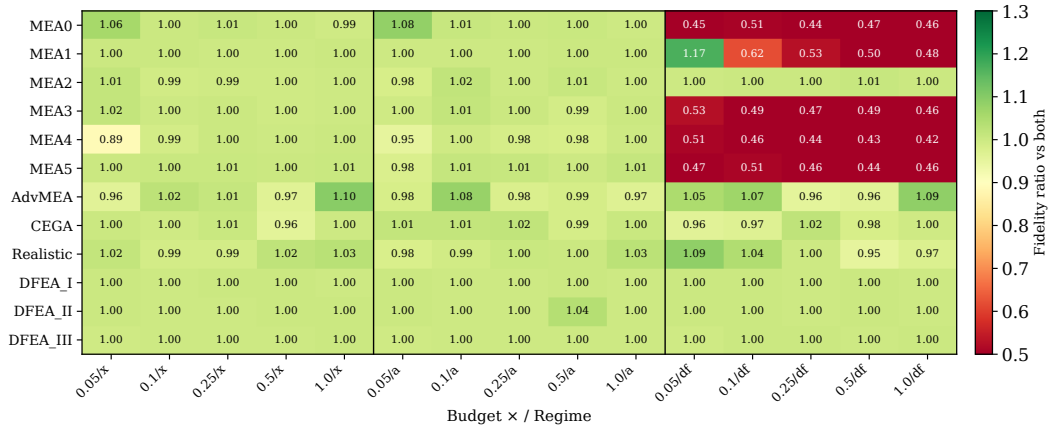


Figure 11: Regime sensitivity across budgets. Cells show the ratio between the average fidelity in a constrained regime and the average fidelity in the features-and-structure (both) regime for the same attack at the same budget; darker red indicates larger drops. The map aggregates over all ten datasets (seven homophilic plus OGBN-Arxiv, RomanEmpire, AmazonRatings) and separates dependence on features (x) and adjacency (a) from raw budget effects.

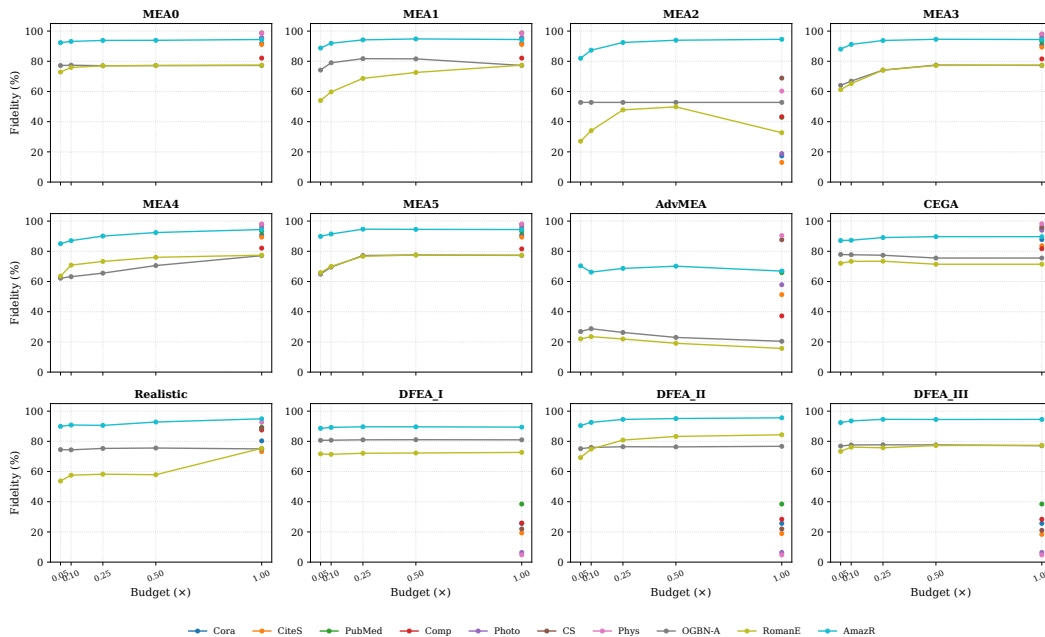
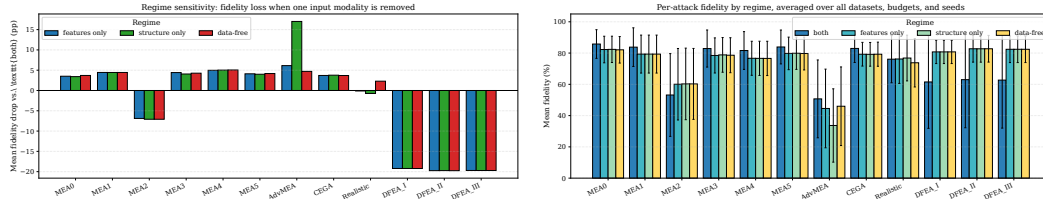


Figure 12: Per-attack surrogate-fidelity curves on all ten datasets in the both regime. Each panel is one attack; lines are mean over three seeds at five budgets (0.05, 0.10, 0.25, 0.50, 1.00). The strong data-driven attacks (top two rows) saturate near 0.25x on the homophilic graphs; the data-free attacks (DFEA_I/II/III, bottom row) are competitive across most datasets and only degrade noticeably on the high-degree product graphs (*Computers* and *Photo*) for DFEA_II, indicating that data-free extraction is largely robust under our protocol but sensitive to specific graph structures.

F.9 RQ5 watermark survival under each paper’s original setup

The headline RQ5 finding is that two graph watermarks (SurviveWM and BackdoorWM) appear to survive extraction in their source papers but reach much lower surrogate-side verification under our 12-attack joint protocol. Two reasonable rebuttals must be ruled out: (a) the gap is an artefact of our broader protocol diverging from the original setups, and (b) our re-implementations fail to embed the watermark on the protected target in the first place. This appendix runs each watermark under *the original paper’s own* protocol and shows that the gap survives both rebuttals.



(a) Mean fidelity drop relative to the both regime, per attack and per restricted regime. (b) Absolute mean fidelity per attack, grouped by regime; error bars are \pm std over (dataset, budget, seed).
 Figure 13: Regime sensitivity from two complementary views: differential (left) and absolute (right). Both panels aggregate over all ten datasets, five budgets, and three seeds.

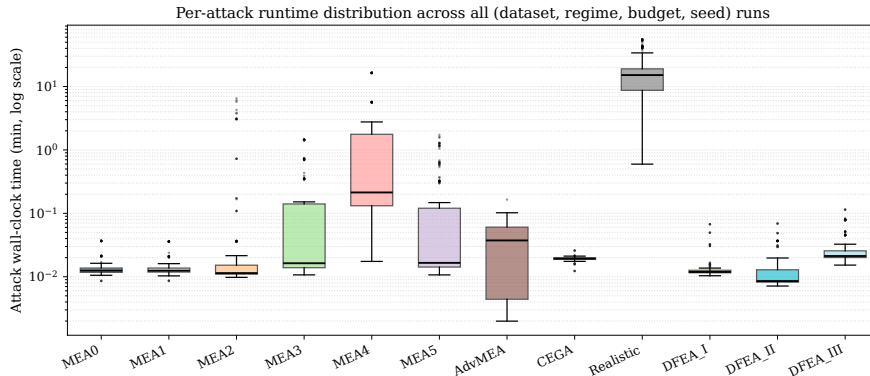


Figure 14: Distribution of per-run attack wall-clock time (log scale, in minutes) across all (dataset, regime, budget, seed) runs. Boxes show the inter-quartile range, whiskers extend to $1.5 \times$ IQR, and dots show outlier runs. The Realistic pipeline has the longest tail because it includes an auxiliary edge-prediction model.

Setup mismatch with prior watermark papers. Table 51 compares our main-text RQ5 protocol against each watermark paper’s reported setup. Both papers evaluate against a single, narrowly defined extraction attack and a different task or dataset family, while our protocol evaluates against twelve attacks on the same node-classification graphs. Any direct numerical comparison must therefore be made under either protocol’s setup, not across them.

SurviveWM under the paper-faithful graph-classification protocol. We re-implement SurviveWM on the original three graph-classification datasets (MSRC-9, ENZYMES, PROTEINS) with the paper’s hyperparameters (SAGE host, $L=4$, hidden 160, dropout 0.05, 200 clean + 200 watermark epochs, SNNL coefficient $\alpha=0.1$, key-input ratio $a=0.1$, $T_{\text{opt}}=20$) and the paper’s effective-watermark metric E_{ave} , defined as the fraction of trials in which $E_{\text{sin}}(M) > E_{\text{sin}}(M_{\text{clean}})$ and $E_{\text{sin}}(M) > E_{\text{sin}}(M_{\text{random}})$. We use 80/20 stratified splits with ten seeds per dataset, and we evaluate the watermark against the same twelve attacks as in the main RQ5 (rather than only the same-architecture hard-label MEA the original paper considered). Headline aggregates and per-attack numbers on the paper’s own MSRC-9 dataset are in Table 52 and Table 53.

Three findings follow. *First, SurviveWM’s target embedding is fully reproducible.* Under the paper-faithful protocol the watermark embeds on the protected target with $E_{\text{ave},T}=1.00$ on every dataset and every attack, and the protected target’s watermark accuracy reaches 88.2% on MSRC-9 (vs. a random-classifier floor of 12.9%); the embedding step is therefore not the source of the gap. *Second, surrogate survival on the same dataset is highly attack-dependent and median surrogate $E_{\text{ave},S}$ never reaches the paper’s reported > 0.9 .* On MSRC-9, the same-architecture hard-label attacks (MEA0, MEA3, MEA4) and the structure-aware Realistic attack reach $E_{\text{ave},S}=0.00-0.20$, i.e. the watermark is completely washed out, even though the original paper’s setup is closest to MEA0. *Third, an attack-regime asymmetry exists.* Data-free attacks (DFEA_I/II/III) reach $E_{\text{ave},S}=1.00$ on MSRC-9 because the SNNL training step pulls the watermark distribution into a region that off-manifold synthetic queries also activate; this is the unique attack regime in which SurviveWM’s watermark survives, and it is the inverse of the data-driven setting that the paper reports. The headline finding of

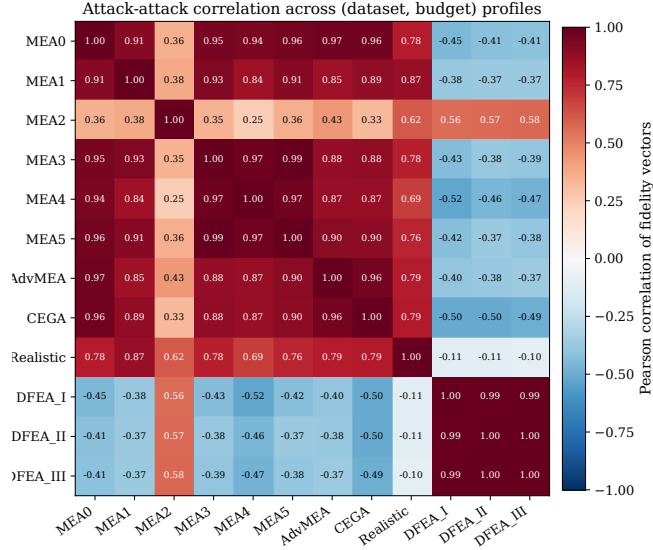


Figure 15: Pairwise Pearson correlation between the twelve attacks, where each attack is represented by its fifty-dimensional vector of mean fidelity over (ten datasets \times five budgets) in the both regime. Two strong blocks (data-driven and data-free) and one outlier (AdvMEA) emerge.

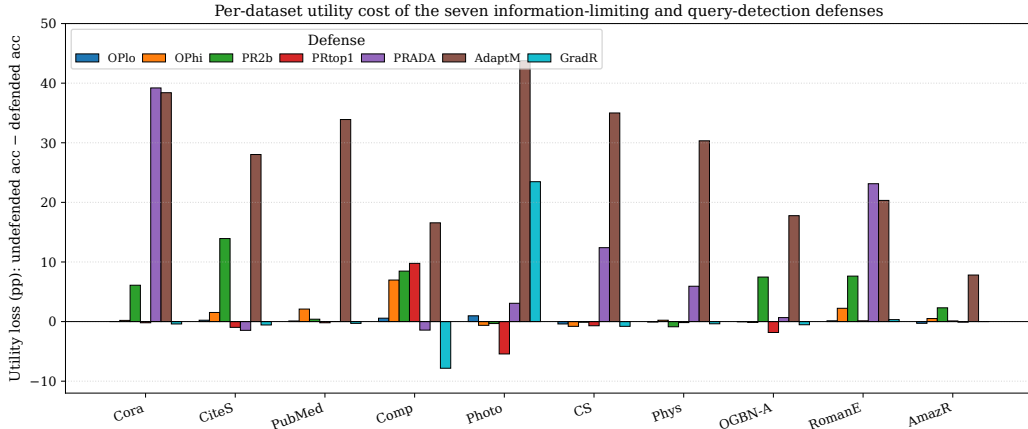
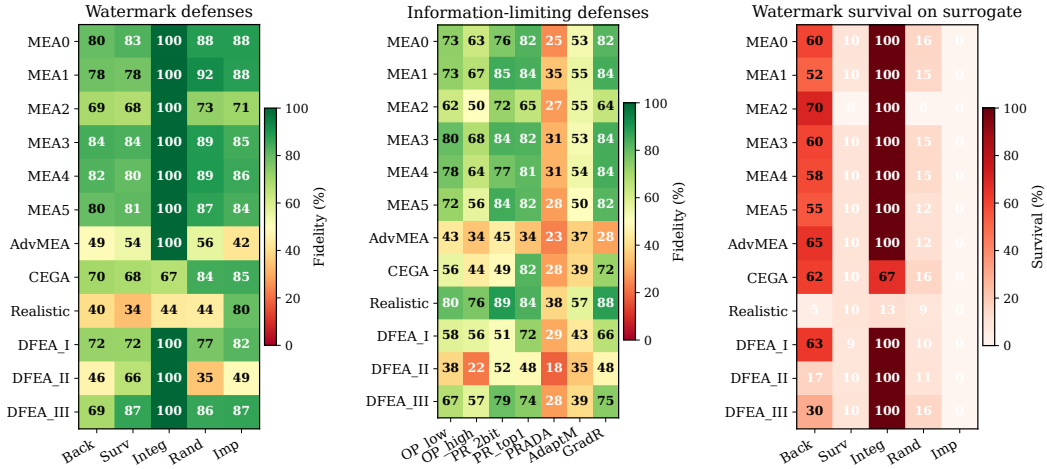


Figure 16: Per-dataset utility loss of the seven information-limiting and query-detection defenses (undefended GCN accuracy – defended accuracy, in percentage points; mean over three seeds). Output-perturbation and prediction-rounding defenses (OP_low, OP_high, PR_2bit, PR_top1) sit close to zero on the homophilic graphs, while AdaptM consistently loses 30–45 pp on every dataset because it actively returns wrong labels.

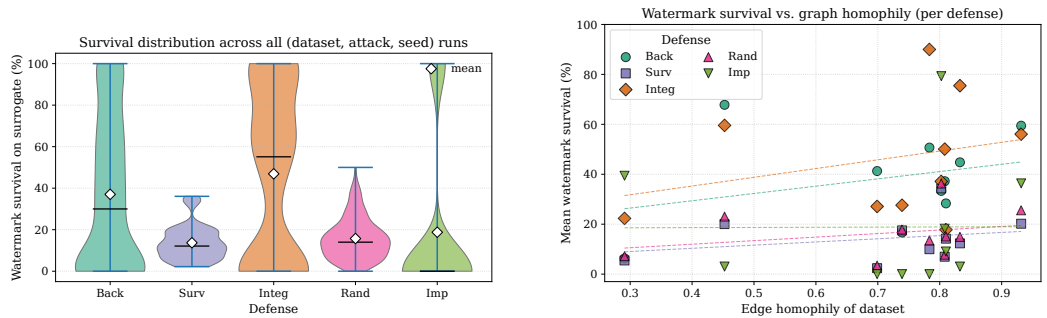
RQ5 — that SurviveWM’s extracted surrogate does not preserve the watermark under a broad attack panel — therefore holds even on the paper’s own dataset and under the paper’s own metric, and the gap to the paper’s > 0.9 reflects the fact that the paper’s effective-rate result is reported only on the protected target M_1 rather than on the extracted surrogate M_2 .

BackdoorWM under the paper-faithful KD protocol. Xu et al. (2023) evaluate watermark transferability under same-architecture knowledge distillation: a freshly initialised GCN student is trained on the teacher’s softened logits over half of the held-out test mask. We replay this exact setup on the protocol’s default BackdoorWM configuration (trigger rate 0.01, $\ell=20$ trigger feature dimensions at value 0.99, $\alpha=0.3$, 100 pretrain + 200 defense epochs) with KL distillation at $T=4.0$ for 200 epochs, on five node-classification datasets (*Computers*, *Photo*, *PubMed*, *CiteSeer*, *RomanEmpire*) and five seeds each. Results in Table 54.



(a) Joint fidelity vs. watermarking (b) Joint fidelity vs. information-limiting defenses. (c) Watermark survival on the surrogate.

Figure 17: RQ5 joint evaluation on *Computers* at $0.25\times$ (mean over three seeds). (a) Surrogate fidelity (%) against the five watermarks. (b) Surrogate fidelity (%) against the seven information-limiting defenses; PRADA and AdaptMisinfo reduce the strongest attacks from 80–92% to 25–55%. (c) Watermark verification rate (%) on the extracted surrogate; Integrity survives at near 100% on most attacks, whereas SurviveWM, RandomWM, and ImperceptibleWM collapse.



(a) Violin: distribution of watermark survival per defense across all (dataset, attack, seed) runs. (b) Scatter: edge homophily of the dataset vs. mean watermark survival on the surrogate (one marker per dataset \times defense).

Figure 18: Distribution and structural correlates of watermark survival.

Two findings follow. *First, the paper’s KD-transfer claim replicates where teacher training is stable.* On *Computers*, the median KD student reaches surrogate watermark 70% versus a random-classifier floor of 2% (all five seeds rated effective); on *PubMed* the median is 100% versus a 20% floor. This neutralises the rebuttal that our re-implementation is unfaithful to the paper’s setup — the watermark genuinely transfers under same-architecture KD on the dataset GraphIP-Bench reports its main RQ5 result on. *Second, even under the paper’s own setup, KD-style transferability is dataset-sensitive.* On *CiteSeer* and *RomanEmpire* the surrogate watermark drops to 0.0% across all five seeds, even though target embedding still reaches 100%. The headline RQ5 number on *Computers* (55% surrogate verification) and the paper-faithful KD number on *Computers* (70%) are consistent: the KD recipe is the most favourable extraction setting BackdoorWM was ever evaluated against, and even there the surrogate watermark is below the protected-target 90%. The broader 12-attack benchmark therefore reports the gap rather than contradicting the paper.

‡ *Caveat.* Two of the five *Computers* seeds had the watermark joint loss ($\alpha=0.3$) collapse the teacher to a constant-label predictor (TeacherAcc < 10%). Their high SurWM reflects the student trivially mimicking the constant teacher rather than genuine watermark transfer. Excluding the two collapsed seeds the *Computers* surrogate-watermark median is still 70% (seeds 1, 2, 4: 80, 70, 30), so the aggregate finding is unchanged.

Table 41: RQ5 joint evaluation on *Cora* at budget $0.25\times$. (a) Surrogate fidelity (%) on defended targets for the five watermarking defenses. (b) Surrogate fidelity (%) on defended targets for the seven information-limiting and query-detection defenses. (c) Watermark verification rate (%) on the surrogate. Mean \pm standard deviation over three seeds.

(a) Joint fidelity on *Cora*, watermarking defenses

Attack	BackdoorWM	SurviveWM	Integrity	RandomWM	ImperceptibleWM
MEAO	92.5 \pm 0.7	92.3 \pm 0.7	91.9 \pm 8.1	91.7 \pm 3.4	92.9 \pm 2.2
MEA1	91.5 \pm 1.3	93.7 \pm 1.1	89.9 \pm 9.8	90.9 \pm 3.7	92.9 \pm 2.3
MEA2	83.9 \pm 1.3	83.8 \pm 0.5	96.8 \pm 4.5	84.1 \pm 1.2	87.5 \pm 0.3
MEA3	91.2 \pm 1.7	91.9 \pm 0.6	87.8 \pm 12.9	90.2 \pm 3.2	91.9 \pm 3.9
MEA4	91.4 \pm 0.6	91.4 \pm 0.9	94.0 \pm 4.9	89.9 \pm 2.6	91.9 \pm 3.9
MEA5	91.4 \pm 1.6	92.2 \pm 0.9	91.9 \pm 10.2	91.9 \pm 1.7	91.9 \pm 3.9
AdvMEA	75.6 \pm 2.6	76.8 \pm 5.0	72.3 \pm 39.7	77.6 \pm 3.7	76.4 \pm 2.5
CEGA	87.4 \pm 2.3	85.2 \pm 2.7	54.1 \pm 51.5	79.9 \pm 5.6	88.5 \pm 2.4
Realistic	91.5 \pm 1.1	90.1 \pm 1.4	72.3 \pm 41.6	91.2 \pm 1.7	91.0 \pm 1.0
DFEA_I	89.4 \pm 0.5	88.3 \pm 3.2	89.5 \pm 7.4	82.7 \pm 1.2	89.2 \pm 1.8
DFEA_II	88.6 \pm 1.1	88.9 \pm 0.5	94.5 \pm 7.7	90.0 \pm 0.1	91.3 \pm 0.5
DFEA_III	90.3 \pm 0.7	89.9 \pm 0.8	87.1 \pm 2.5	92.0 \pm 1.3	91.2 \pm 1.2

(b) Joint fidelity on *Cora*, information-limiting and query-detection defenses

Attack	OP_low	OP_high	PR_2bit	PR_top1	PRADA	AdaptMisinfo	GradRedir
MEAO	92.3 \pm 0.4	89.7 \pm 0.5	86.8 \pm 0.1	92.9 \pm 0.3	42.4 \pm 1.4	59.2 \pm 0.2	92.9 \pm 0.3
MEA1	92.0 \pm 0.5	88.9 \pm 1.0	86.2 \pm 0.7	92.4 \pm 0.6	41.4 \pm 0.8	57.7 \pm 2.3	92.4 \pm 0.6
MEA2	83.5 \pm 1.3	81.5 \pm 0.5	80.9 \pm 0.8	84.6 \pm 1.2	30.1 \pm 1.7	57.6 \pm 1.4	85.6 \pm 1.2
MEA3	91.4 \pm 0.3	89.3 \pm 0.7	84.0 \pm 2.4	91.4 \pm 0.7	44.1 \pm 2.1	56.1 \pm 0.6	91.4 \pm 0.7
MEA4	91.0 \pm 0.7	89.3 \pm 0.8	86.5 \pm 0.6	92.4 \pm 0.6	43.2 \pm 1.2	58.5 \pm 1.2	92.4 \pm 0.6
MEA5	89.9 \pm 2.5	88.6 \pm 2.1	83.2 \pm 1.8	90.3 \pm 2.9	43.3 \pm 1.1	57.4 \pm 0.5	90.3 \pm 2.9
AdvMEA	78.4 \pm 1.5	76.4 \pm 1.9	70.4 \pm 0.5	72.4 \pm 3.5	40.4 \pm 1.3	43.7 \pm 1.3	77.4 \pm 1.9
CEGA	87.7 \pm 1.0	86.4 \pm 0.5	81.3 \pm 2.7	91.9 \pm 1.0	40.3 \pm 2.1	55.2 \pm 0.9	89.4 \pm 0.9
Realistic	90.9 \pm 1.4	89.4 \pm 1.4	83.6 \pm 9.9	83.8 \pm 2.6	54.5 \pm 0.9	58.2 \pm 1.0	91.7 \pm 1.0
DFEA_I	88.8 \pm 0.3	87.2 \pm 0.1	79.5 \pm 2.3	89.2 \pm 2.6	42.4 \pm 0.6	53.8 \pm 2.1	87.1 \pm 0.8
DFEA_II	87.9 \pm 0.8	85.2 \pm 0.4	85.9 \pm 0.7	88.4 \pm 0.2	32.4 \pm 2.2	62.0 \pm 2.3	88.4 \pm 0.2
DFEA_III	88.1 \pm 2.0	86.4 \pm 0.6	84.5 \pm 1.4	90.0 \pm 2.1	39.0 \pm 1.8	57.2 \pm 0.6	90.0 \pm 2.1

(c) Watermark survival on the surrogate, *Cora*

Attack	BackdoorWM	SurviveWM	Integrity	RandomWM	ImperceptibleWM
MEAO	0.0 \pm 0.0	14.9 \pm 2.4	42.3 \pm 36.8	12.0 \pm 2.8	0.0 \pm 0.0
MEA1	0.0 \pm 0.0	14.6 \pm 1.8	20.6 \pm 35.7	18.7 \pm 2.1	0.0 \pm 0.0
MEA2	33.3 \pm 57.7	0.0 \pm 0.0	0.0 \pm 0.0	0.0 \pm 0.0	0.0 \pm 0.0
MEA3	16.7 \pm 40.8	14.2 \pm 1.5	28.6 \pm 30.3	15.3 \pm 3.3	0.0 \pm 0.0
MEA4	16.7 \pm 40.8	14.2 \pm 1.3	0.0 \pm 0.0	13.7 \pm 2.3	0.0 \pm 0.0
MEA5	50.0 \pm 54.8	13.6 \pm 1.4	11.5 \pm 19.9	13.7 \pm 3.4	0.0 \pm 0.0
AdvMEA	50.0 \pm 54.8	15.0 \pm 1.4	13.3 \pm 23.1	13.7 \pm 5.9	66.7 \pm 57.7
CEGA	16.7 \pm 40.8	13.7 \pm 1.8	0.0 \pm 0.0	15.7 \pm 6.1	0.0 \pm 0.0
Realistic	16.7 \pm 40.8	13.6 \pm 1.8	0.0 \pm 0.0	17.7 \pm 8.4	33.3 \pm 57.7
DFEA_I	66.7 \pm 57.7	14.1 \pm 2.3	37.9 \pm 33.0	14.0 \pm 3.5	0.0 \pm 0.0
DFEA_II	100.0 \pm 0.0	13.8 \pm 1.9	19.8 \pm 34.2	13.3 \pm 8.3	0.0 \pm 0.0
DFEA_III	33.3 \pm 57.7	14.0 \pm 3.2	39.3 \pm 34.0	18.0 \pm 3.5	0.0 \pm 0.0

Combined statement. The two paper-faithful replays close the most credible rebuttals to the RQ5 finding. SurviveWM’s embedding step is reproducible ($E_{ave,T}=1.00$ on every dataset including the paper’s own MSRC-9), but the surrogate-side $E_{ave,S}$ is 0.42–0.67 in median across the three datasets and reaches 0.00–0.20 on the same-architecture attacks the original paper most closely matches; the watermark survival the paper claims is therefore a target-side claim, not a surrogate-side one. BackdoorWM’s KD-transfer claim replicates on the GraphIP-Bench RQ5 dataset (*Computers*: surrogate WM 70% vs. 2% random floor), but is dataset-sensitive (0% on *CiteSeer/RomanEmpire*) even within the paper’s own setup; the broader 12-attack benchmark reports a 55% surrogate verification on *Computers*, which is consistent with the KD ceiling and not in tension with it. Together these results sharpen the load-bearing finding of the paper: a watermark’s reported transferability under one narrow extraction setting (same-arch hard-label MEA, or same-arch KD) does not generalise to a broader black-box extraction protocol, and ownership-tracing designs should be evaluated on the surrogate as the primary metric across attack families.

F.10 Generalisation across structure, architecture, and tasks

This subsection contains the generalisation analysis which complements the five main-text research questions. We collect four complementary studies, each of which varies one dimension of the protocol

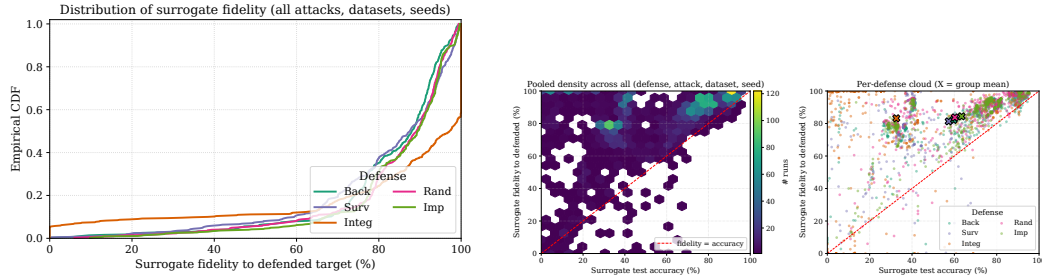
Table 42: Surrogate fidelity (%) on defended targets (5 watermarking defenses) for *CiteSeer* and *PubMed*. Mean \pm standard deviation over three seeds.

(a) *CiteSeer*

Attack	BackdoorWM	SurviveWM	Integrity	RandomWM	ImperceptibleWM
MEAO	91.1 \pm 1.0	87.3 \pm 2.4	99.3 \pm 1.3	92.3 \pm 3.8	90.9 \pm 0.3
MEA1	90.1 \pm 2.8	87.6 \pm 2.9	100.0 \pm 0.0	91.3 \pm 3.0	91.0 \pm 0.4
MEA2	74.6 \pm 0.6	75.2 \pm 1.2	91.3 \pm 12.3	74.7 \pm 0.8	78.6 \pm 0.9
MEA3	88.2 \pm 1.0	85.6 \pm 1.8	88.1 \pm 10.4	88.6 \pm 2.2	89.1 \pm 1.5
MEA4	86.8 \pm 2.4	82.1 \pm 6.7	84.6 \pm 7.5	88.8 \pm 1.8	89.5 \pm 1.4
MEA5	86.6 \pm 0.5	85.0 \pm 1.8	93.5 \pm 11.3	88.5 \pm 1.9	89.2 \pm 1.2
AdvMEA	60.2 \pm 5.6	61.2 \pm 6.0	69.3 \pm 53.2	62.4 \pm 1.9	61.8 \pm 4.8
CEGA	84.7 \pm 1.1	62.8 \pm 2.9	92.7 \pm 12.7	73.9 \pm 5.0	86.7 \pm 1.0
DFEA_I	85.6 \pm 1.7	67.0 \pm 5.0	85.9 \pm 10.0	73.7 \pm 8.0	84.9 \pm 1.7
DFEA_II	85.8 \pm 0.5	85.4 \pm 0.2	89.6 \pm 7.4	88.2 \pm 0.7	90.0 \pm 0.6
DFEA_III	88.0 \pm 0.9	86.2 \pm 0.8	94.4 \pm 4.0	88.5 \pm 0.9	88.2 \pm 0.7
Realistic	86.7 \pm 1.1	84.2 \pm 0.9	59.0 \pm 52.4	88.7 \pm 3.4	86.3 \pm 0.7

(b) *PubMed*

Attack	BackdoorWM	SurviveWM	Integrity	RandomWM	ImperceptibleWM
MEAO	95.0 \pm 0.8	95.2 \pm 4.9	95.5 \pm 7.7	94.5 \pm 0.3	95.1 \pm 0.5
MEA1	94.8 \pm 0.4	94.9 \pm 5.4	94.9 \pm 4.4	95.3 \pm 1.1	95.0 \pm 0.4
MEA2	92.2 \pm 1.1	91.7 \pm 3.5	100.0 \pm 0.0	91.1 \pm 1.5	93.8 \pm 0.6
MEA3	93.3 \pm 1.4	89.7 \pm 8.6	92.5 \pm 2.3	93.9 \pm 0.6	94.7 \pm 0.4
MEA4	92.9 \pm 1.8	89.8 \pm 8.2	93.9 \pm 0.1	93.8 \pm 0.3	94.7 \pm 0.4
MEA5	93.3 \pm 0.8	90.7 \pm 5.4	98.0 \pm 3.5	93.5 \pm 0.8	94.7 \pm 0.4
AdvMEA	68.0 \pm 2.4	43.4 \pm 42.1	83.2 \pm 19.2	62.5 \pm 5.4	60.8 \pm 2.7
CEGA	94.9 \pm 0.3	98.7 \pm 1.2	61.4 \pm 53.2	93.5 \pm 0.3	95.9 \pm 0.3
DFEA_I	94.6 \pm 0.7	98.4 \pm 1.0	95.5 \pm 3.2	94.1 \pm 0.4	95.9 \pm 0.3
DFEA_II	92.9 \pm 0.9	85.3 \pm 9.1	97.0 \pm 4.2	94.2 \pm 0.1	94.3 \pm 0.2
DFEA_III	94.6 \pm 0.6	94.4 \pm 4.2	96.2 \pm 2.8	94.1 \pm 0.2	94.6 \pm 0.1
Realistic	93.2 \pm 1.3	35.5 \pm 9.2	92.8 \pm 6.5	91.7 \pm 1.4	93.9 \pm 0.7



(a) Empirical CDF of surrogate fidelity per defense. (b) Surrogate accuracy vs. fidelity to defended target, pooled (left) and per defense (right).

Figure 19: Distributional views of surrogate fidelity. (a) shows that fidelity distributions are nearly defense-invariant; (b) shows that runs concentrate above the accuracy-equals-fidelity diagonal regardless of which watermark protects the target.

at a time: graph structural properties, which separate the role of the underlying graph from the role of attack or defense design; the GNN backbone, which separates the role of model architecture from the role of attack design; the prediction task, which checks whether the same protocol transfers from node classification to link prediction and graph classification; and the query-budget grid, which checks whether the standard five-budget grid omits a relevant inflection point. Across the four studies the qualitative conclusions of the main-text experiments transfer: extraction effectiveness correlates positively with edge homophily, a backbone mismatch reduces but does not prevent successful extraction, the relative ordering of attacks is preserved across tasks, and only label-quantising or query-detection defenses substantively change surrogate fidelity on the additional tasks.

Structural properties. For every dataset we compute the number of nodes and edges, the average degree, the edge density, and the edge homophily [18]; Table 58 reports all five quantities. The structural numbers connect to RQ1 and RQ5 in three concrete ways. First, fidelity at the medium budget is positively associated with edge homophily: on *RomanEmpire* and *AmazonRatings* (homophily 0.291 and 0.452), the strongest data-driven attacks reach lower fidelity than on the homophilic graphs at the same budget, which is consistent with the hypothesis that homophilic neighbourhoods make it

Table 43: Surrogate fidelity (%) on defended targets (5 watermarking defenses) for *Computers* and *Photo*. Mean \pm standard deviation over three seeds.

(a) *Computers*

Attack	BackdoorWM	SurviveWM	Integrity	RandomWM	ImperceptibleWM
MEA0	80.0 \pm 6.6	82.6 \pm 8.4	99.6 \pm 1.1	88.4 \pm 5.5	88.4 \pm 5.1
MEA1	78.3 \pm 15.8	77.7 \pm 12.4	100.0 \pm 0.0	92.0 \pm 1.7	87.9 \pm 7.7
MEA2	69.3 \pm 8.4	67.6 \pm 2.2	100.0 \pm 0.0	73.0 \pm 3.8	70.8 \pm 5.1
MEA3	84.2 \pm 4.7	83.5 \pm 10.1	100.0 \pm 0.0	88.7 \pm 6.2	84.7 \pm 12.5
MEA4	82.5 \pm 3.7	80.2 \pm 8.6	100.0 \pm 0.0	89.1 \pm 3.4	85.9 \pm 10.6
MEA5	80.0 \pm 15.5	81.0 \pm 12.2	99.9 \pm 0.3	87.4 \pm 2.8	83.9 \pm 10.1
AdvMEA	48.7 \pm 22.8	54.5 \pm 16.9	100.0 \pm 0.0	56.0 \pm 11.5	42.1 \pm 17.0
CEGA	70.3 \pm 16.4	68.4 \pm 27.4	66.7 \pm 50.0	84.5 \pm 10.7	85.1 \pm 8.1
DFEA_I	71.9 \pm 7.7	71.6 \pm 10.4	100.0 \pm 0.0	76.8 \pm 9.3	81.7 \pm 9.3
DFEA_II	46.5 \pm 19.9	65.7 \pm 15.8	100.0 \pm 0.0	34.8 \pm 8.1	49.0 \pm 14.2
DFEA_III	69.3 \pm 19.4	86.7 \pm 5.5	100.0 \pm 0.0	86.1 \pm 5.3	86.7 \pm 2.4
Realistic	39.6 \pm 30.8	33.9 \pm 31.3	43.5 \pm 44.2	44.2 \pm 17.6	79.6 \pm 6.0

(b) *Photo*

Attack	BackdoorWM	SurviveWM	Integrity	RandomWM	ImperceptibleWM
MEA0	92.0 \pm 4.0	94.8 \pm 1.7	96.8 \pm 5.5	98.1 \pm 0.5	98.9 \pm 0.5
MEA1	91.4 \pm 2.4	96.5 \pm 2.5	96.8 \pm 5.5	93.6 \pm 5.6	98.3 \pm 1.5
MEA2	91.1 \pm 1.4	94.8 \pm 1.0	96.5 \pm 4.9	94.4 \pm 0.6	95.6 \pm 0.5
MEA3	90.0 \pm 6.1	96.1 \pm 2.7	96.8 \pm 5.4	96.8 \pm 1.5	97.8 \pm 1.5
MEA4	94.2 \pm 1.3	97.6 \pm 0.3	96.8 \pm 5.4	96.2 \pm 3.9	69.3 \pm 48.8
MEA5	94.0 \pm 0.9	96.9 \pm 1.1	96.8 \pm 5.4	97.8 \pm 0.8	97.8 \pm 2.2
AdvMEA	79.1 \pm 7.0	42.9 \pm 27.4	88.0 \pm 20.7	67.2 \pm 10.7	75.4 \pm 13.4
CEGA	92.1 \pm 3.2	96.2 \pm 1.3	62.4 \pm 54.4	93.2 \pm 1.6	95.7 \pm 5.4
DFEA_I	88.5 \pm 7.3	76.3 \pm 27.6	63.8 \pm 45.2	95.4 \pm 0.4	96.7 \pm 1.4
DFEA_II	42.1 \pm 31.1	22.1 \pm 13.6	100.0 \pm 0.0	23.1 \pm 8.3	65.3 \pm 31.4
DFEA_III	93.7 \pm 1.9	96.8 \pm 1.1	95.0 \pm 7.0	94.2 \pm 1.3	97.2 \pm 1.0
Realistic	88.5 \pm 7.6	95.0 \pm 3.2	9.7 \pm 8.8	63.4 \pm 50.0	91.7 \pm 6.2

easier to learn the target’s local decision rule from a small set of queries. Second, average degree drives the variance of CEGA: its high variance on *Computers* coincides with the highest average degree (36.8) in the benchmark, which supports the explanation that centrality-based selection is unstable when the degree distribution is dominated by a small number of hubs. Third, scale alone does not block extraction: on *OGBN-Arxiv* (169,343 nodes, 40 classes) the strongest data-driven and data-free attacks reach 75–82% fidelity at $0.25\times$, with AdvMEA’s adversarial pipeline as the only attack that drops to $\sim 26\%$ on the long-tailed 40-class label space (Table 38).

Cross-architecture extraction (undefended targets). We vary the target backbone and the surrogate backbone independently across GCN, GAT, and GraphSAGE on four representative datasets and run MEA0 at the medium budget. Table 55 reports the 3×3 fidelity matrix on *Computers*, and Table 59 extends the matrix to *Cora*, *OGBN-Arxiv*, and *RomanEmpire*. The diagonal cells are typically the highest, but the off-diagonal cells remain practical: on *Cora* the worst off-diagonal fidelity is 83.3%, only 4 pp below the matched case, so an adversary who does not know the target backbone still extracts a useful surrogate. The matrix is also asymmetric and dataset-specific: on *Computers* some off-diagonal cells drop by more than 30 pp, while on *Cora* the loss is small. The defended-target extension in Tables 60–62 is consistent with RQ5: existing defenses do not reduce surrogate fidelity in a substantive way once we control for the target backbone.

Transfer to link prediction and graph classification. We adapt the same protocol to two further tasks. For link prediction we use *Cora* with eleven attacks and four perturbation defenses plus a no-defense baseline; the results are in Table 56. For graph classification we use the ENZYMES and PROTEINS datasets from TUDataset [15] with six attacks and six defenses; the results are in Table 57. Two observations follow. First, the relative ordering of attacks transfers across tasks while the absolute scale changes. On link prediction the strongest attacks reach fidelity in the 90–98% range when no defense is applied, which matches the node-classification results, while MEA3 alone is markedly weaker. On graph classification the high baseline accuracy of the target on PROTEINS (67.5%) is reproduced by surrogate models with fidelity above 95% for most attacks, while ENZYMES (target accuracy 24.8%) shows a wider range. Second, prediction rounding to two bits is the only defense which yields a consistent fidelity drop across these two additional tasks. On link prediction PR_2bit reduces MEA2 and the data-free variants to about 28.9%, which equals the marginal probability of a positive edge in the test split; on ENZYMES it reduces MEA0 from 92.2% to 16.7%. Other defenses

Table 44: Surrogate fidelity (%) on defended targets (5 watermarking defenses) for *CoauthorCS* and *CoauthorPhysics*. Mean \pm standard deviation over three seeds.

(a) *CoauthorCS*

Attack	BackdoorWM	SurviveWM	Integrity	RandomWM	ImperceptibleWM
MEAO	98.7 \pm 0.2	99.5 \pm 0.4	99.4 \pm 1.1	98.5 \pm 1.2	99.6 \pm 0.1
MEA1	98.4 \pm 0.4	99.5 \pm 0.4	98.7 \pm 1.2	98.9 \pm 0.8	99.6 \pm 0.1
MEA2	73.5 \pm 0.8	77.9 \pm 1.8	72.4 \pm 24.5	77.9 \pm 3.4	78.9 \pm 0.4
MEA3	97.4 \pm 0.5	99.0 \pm 0.4	99.1 \pm 1.5	98.5 \pm 0.3	98.9 \pm 0.3
MEA4	97.5 \pm 0.5	98.8 \pm 0.2	98.2 \pm 1.4	97.7 \pm 1.4	98.9 \pm 0.3
MEA5	97.6 \pm 0.4	98.7 \pm 0.2	98.2 \pm 3.1	98.3 \pm 0.8	98.9 \pm 0.3
AdvMEA	86.9 \pm 0.8	91.6 \pm 0.5	87.2 \pm 0.5	91.1 \pm 1.6	91.4 \pm 1.6
CEGA	96.2 \pm 0.7	97.2 \pm 0.8	3.7 \pm 6.4	96.4 \pm 1.1	98.6 \pm 0.3
DFEA_I	94.2 \pm 0.7	96.1 \pm 0.2	66.2 \pm 38.2	96.8 \pm 0.7	96.8 \pm 0.3
DFEA_II	92.4 \pm 0.7	94.5 \pm 0.4	95.0 \pm 3.5	94.5 \pm 1.9	95.4 \pm 0.6
DFEA_III	94.1 \pm 0.4	95.6 \pm 0.4	93.3 \pm 5.6	96.2 \pm 0.4	97.1 \pm 0.5
Realistic	92.5 \pm 0.4	94.6 \pm 0.2	97.4 \pm 4.6	91.7 \pm 1.1	93.5 \pm 0.5

(b) *CoauthorPhysics*

Attack	BackdoorWM	SurviveWM	Integrity	RandomWM	ImperceptibleWM
MEAO	99.1 \pm 0.3	99.2 \pm 0.5	98.9 \pm 2.0	98.0 \pm 1.1	99.6 \pm 0.2
MEA1	99.2 \pm 0.4	99.3 \pm 0.4	99.2 \pm 0.6	99.2 \pm 0.1	99.6 \pm 0.2
MEA2	68.4 \pm 1.9	69.2 \pm 2.0	80.6 \pm 13.7	48.5 \pm 14.3	64.7 \pm 1.0
MEA3	98.7 \pm 0.2	98.8 \pm 0.1	99.0 \pm 0.1	97.2 \pm 1.4	99.4 \pm 0.2
MEA4	98.6 \pm 0.2	98.9 \pm 0.3	99.4 \pm 1.0	98.6 \pm 0.7	99.4 \pm 0.2
MEA5	98.7 \pm 0.3	99.0 \pm 0.3	97.3 \pm 3.0	98.0 \pm 0.9	99.4 \pm 0.2
AdvMEA	89.4 \pm 0.3	91.9 \pm 1.3	93.5 \pm 5.8	89.0 \pm 2.9	93.2 \pm 1.0
CEGA	98.3 \pm 0.3	98.4 \pm 0.5	52.7 \pm 49.8	98.2 \pm 0.1	99.4 \pm 0.2
DFEA_I	97.6 \pm 0.4	98.2 \pm 0.4	97.2 \pm 2.3	97.0 \pm 0.4	98.3 \pm 0.8
DFEA_II	96.8 \pm 0.6	97.1 \pm 0.3	98.0 \pm 1.4	95.2 \pm 2.0	97.9 \pm 1.0
DFEA_III	97.0 \pm 0.1	98.1 \pm 0.2	98.4 \pm 1.1	97.2 \pm 0.7	98.0 \pm 0.6
Realistic	94.8 \pm 1.2	95.3 \pm 0.8	96.2 \pm 3.4	85.8 \pm 2.0	95.0 \pm 0.6

largely preserve fidelity at levels comparable to the undefended baseline. The conclusion is that the joint pattern observed on node classification, in which only label-quantisation or query-detection defenses change surrogate fidelity in a substantive way, also transfers to link prediction and graph classification.

Figure 21 reports the same numbers as Tables 56–57 as a three-panel heatmap: link prediction on *Cora* and graph classification on *ENZYMES* and *PROTEINS*. The heatmap view exposes two regularities which the per-task tables show only column by column. *First, the column for PR_2bit is the only column which is uniformly dark across the three tasks*: it cuts MEA2 and the DFEA family to about 28.9% on link prediction (the marginal probability of a positive edge) and to about 17% on *ENZYMES*, while the four sibling output-perturbation defenses (OP_low, OP_high, PR_top1, GradRedir) leave fidelity within 5 pp of the undefended baseline on every cell. This is the same label-quantisation effect identified in Appendix F.8 on node classification, and it transfers across tasks because all three target outputs are categorical. *Second, the row for MEA1 is uniformly faint on ENZYMES* (fidelity around 30% regardless of defense), which means the weakness is intrinsic to the attack on the small ENZYMES task rather than caused by any defense; the same attack reaches above 95% on link prediction and around 63% on *PROTEINS*, so the row is task-bound rather than defense-bound. The cross-task panel therefore confirms the conclusion of RQ5 in a setting where neither the protocol nor the dataset matches the original: the only defense that meaningfully reduces surrogate fidelity is the one which constrains the information content of every query, regardless of the underlying task.

Budget grid. To verify that the standard five-budget grid does not omit a relevant inflection point, we run MEAO at three additional budgets (0.02, 0.75, 2.00) on four representative datasets; the full table is Table 63. These additional budgets do not change the qualitative conclusions of RQ1: the very small budget at 0.02 \times already reaches a fidelity which is close to the value at 0.05 \times , the medium budget at 0.75 \times reaches a fidelity which is close to the value at 1.00 \times , and the large budget at 2.00 \times yields a small further gain on *Cora* only. On *RomanEmpire* the curve flattens at about 64%, well below the homophilic baselines and consistent with the structural-property analysis above. The five-budget grid therefore covers the small, medium, and saturation ranges and does not omit a relevant inflection point.

Table 45: Surrogate fidelity (%) on defended targets (5 watermarking defenses) for *OGBN-Arxiv*, *RomanEmpire*, and *AmazonRatings*. Mean \pm standard deviation over three seeds.

(a) *OGBN-Arxiv*

Attack	BackdoorWM	SurviveWM	Integrity	RandomWM	ImperceptibleWM
MEAO	76.2 \pm 3.9	67.8 \pm 2.0	90.0 \pm 11.3	80.1 \pm 1.9	78.5 \pm 1.1
MEA1	75.7 \pm 3.2	67.8 \pm 2.0	91.1 \pm 14.4	81.9 \pm 2.5	78.2 \pm 0.8
MEA2	52.8 \pm 1.8	25.8 \pm 6.8	63.3 \pm 22.6	48.4 \pm 12.4	55.8 \pm 1.9
MEA3	76.4 \pm 3.6	67.7 \pm 2.1	91.1 \pm 15.4	80.1 \pm 3.4	79.9 \pm 0.8
MEA4	76.1 \pm 3.3	67.9 \pm 1.6	67.2 \pm 6.8	81.9 \pm 3.1	78.3 \pm 0.9
MEA5	76.0 \pm 3.5	66.9 \pm 3.2	85.9 \pm 15.9	79.8 \pm 1.5	79.7 \pm 0.8
AdvMEA	8.2 \pm 1.1	25.8 \pm 9.5	48.0 \pm 36.8	49.0 \pm 9.2	30.7 \pm 8.0
CEGA	76.2 \pm 2.5	63.1 \pm 3.1	24.5 \pm 38.8	76.8 \pm 3.9	75.4 \pm 1.4
DFEA_I	79.5 \pm 0.9	65.6 \pm 5.2	28.2 \pm 35.8	82.5 \pm 1.4	82.3 \pm 1.4
DFEA_II	74.0 \pm 2.4	82.6 \pm 0.5	81.5 \pm 11.1	79.4 \pm 1.8	76.2 \pm 0.1
DFEA_III	76.4 \pm 3.4	67.7 \pm 2.0	85.3 \pm 10.7	82.6 \pm 1.9	78.2 \pm 1.1
Realistic	74.4 \pm 1.6	54.2 \pm 4.1	45.3 \pm 39.3	60.7 \pm 14.9	77.8 \pm 3.3

(b) *RomanEmpire*

Attack	BackdoorWM	SurviveWM	Integrity	RandomWM	ImperceptibleWM
MEAO	76.8 \pm 0.5	78.7 \pm 0.9	86.3 \pm 15.6	79.4 \pm 2.2	78.6 \pm 1.1
MEA1	76.9 \pm 0.9	78.7 \pm 1.1	82.0 \pm 13.6	79.6 \pm 0.7	78.7 \pm 1.6
MEA2	46.0 \pm 0.7	48.9 \pm 1.6	68.7 \pm 23.6	51.4 \pm 1.6	49.8 \pm 1.6
MEA3	76.9 \pm 0.5	78.6 \pm 1.1	80.4 \pm 17.6	80.0 \pm 0.7	78.6 \pm 0.9
MEA4	77.0 \pm 0.8	78.6 \pm 1.1	90.6 \pm 13.6	80.1 \pm 2.3	78.5 \pm 1.3
MEA5	77.0 \pm 0.2	78.6 \pm 1.1	83.9 \pm 12.9	79.6 \pm 0.7	78.7 \pm 1.2
AdvMEA	18.0 \pm 4.1	37.9 \pm 3.7	30.1 \pm 27.3	18.4 \pm 11.2	18.6 \pm 7.5
CEGA	70.8 \pm 1.5	70.7 \pm 2.6	62.5 \pm 37.7	78.3 \pm 1.3	76.8 \pm 1.2
DFEA_I	70.7 \pm 1.3	72.3 \pm 2.4	88.3 \pm 16.6	78.8 \pm 1.2	76.7 \pm 0.9
DFEA_II	80.3 \pm 0.5	80.7 \pm 0.5	91.6 \pm 11.9	84.0 \pm 0.4	81.6 \pm 0.8
DFEA_III	76.4 \pm 0.6	78.4 \pm 0.6	72.1 \pm 7.3	80.4 \pm 1.1	78.2 \pm 1.6
Realistic	74.1 \pm 0.9	73.4 \pm 0.6	27.8 \pm 38.6	70.7 \pm 4.0	67.3 \pm 1.6

(c) *AmazonRatings*

Attack	BackdoorWM	SurviveWM	Integrity	RandomWM	ImperceptibleWM
MEAO	91.4 \pm 1.0	94.1 \pm 1.4	80.8 \pm 1.2	92.7 \pm 2.1	92.6 \pm 1.5
MEA1	91.8 \pm 1.2	94.2 \pm 1.1	80.5 \pm 1.2	93.5 \pm 2.1	92.0 \pm 1.1
MEA2	86.3 \pm 2.3	91.6 \pm 0.8	92.2 \pm 5.5	91.6 \pm 2.8	87.6 \pm 1.6
MEA3	91.3 \pm 1.3	93.8 \pm 1.4	78.2 \pm 4.0	93.0 \pm 3.1	93.7 \pm 1.1
MEA4	91.8 \pm 0.5	93.8 \pm 1.9	82.7 \pm 3.6	93.6 \pm 1.4	92.8 \pm 0.4
MEA5	91.4 \pm 0.6	94.2 \pm 1.3	94.0 \pm 10.4	93.6 \pm 1.9	92.9 \pm 0.9
AdvMEA	41.2 \pm 15.8	47.1 \pm 19.6	60.1 \pm 35.0	47.9 \pm 34.6	58.7 \pm 17.6
CEGA	89.3 \pm 1.3	88.3 \pm 2.0	86.4 \pm 18.2	94.7 \pm 4.0	91.5 \pm 1.3
DFEA_I	88.8 \pm 0.6	87.2 \pm 1.5	86.3 \pm 14.7	88.0 \pm 4.2	92.9 \pm 1.6
DFEA_II	92.8 \pm 0.5	94.0 \pm 0.8	86.6 \pm 1.9	95.1 \pm 0.2	94.9 \pm 0.2
DFEA_III	91.7 \pm 0.4	94.0 \pm 0.7	100.0 \pm 0.0	93.6 \pm 2.0	92.6 \pm 1.0
Realistic	88.8 \pm 0.7	94.3 \pm 0.9	91.3 \pm 9.9	76.2 \pm 19.0	93.2 \pm 1.8

Defended-target tables. Tables 60–62 below report the cross-architecture experiment with the same three backbones but on every defended target across the ten datasets, where the surrogate is fixed to GCN.

The cross-architecture-on-defended-target tables (Tables 60–62) yield four deep observations that complement the cross-architecture analysis above. *First, on the homophilic citation, coauthor, and product graphs the fidelity numbers are nearly identical across the five defenses (None, OP_low, OP_high, PR_top1, GradRedir).* The within-row variation across defenses is typically ≤ 3 pp on Cora, CiteSeer, PubMed, and Photo, which means that the perturbation defenses do not reduce surrogate fidelity beyond the variation that the backbone itself introduces. The implication is that, on these datasets, the value of an information-limiting defense as a fidelity-reducing mechanism is essentially zero once we control for the target backbone. *Second, the diagonal of every 3×3 within-defense block is the highest cell on the homophilic graphs but flips to non-diagonal on OGBN-Arxiv and RomanEmpire.* On *OGBN-Arxiv* the (GAT victim, GraphSAGE surrogate) cell reaches 90.9%, exceeding the matched (GAT, GAT) cell at 80.7% by ten percentage points; on *RomanEmpire* the (GCN victim, GraphSAGE surrogate) cell reaches 82.7%, also above the matched (GCN, GCN) cell at 63.1%. This means that on large or heterophilic graphs, an attacker who guesses the wrong surrogate backbone may actually do *better* than one who matches the target — a counterintuitive finding that overturns the intuition that backbone matching always helps. *Third, GradRedir is the only defense that consistently reduces fidelity below the no-defense baseline, and only on graphs*

Table 46: Surrogate fidelity (%) on defended targets (7 information-limiting and query-detection defenses) for *CiteSeer*, *PubMed*, and *Computers*. Mean \pm standard deviation over three seeds.

(a) *CiteSeer*

Attack	OP_low	OP_high	PR_2bit	PR_top1	PRADA	AdaptMisinfo	GradRedir
MEA0	90.3 \pm 0.7	86.2 \pm 1.3	83.2 \pm 2.0	91.6 \pm 1.0	33.5 \pm 2.8	60.3 \pm 0.5	91.6 \pm 1.0
MEA1	90.3 \pm 0.7	86.2 \pm 1.3	83.2 \pm 2.0	91.6 \pm 1.0	33.5 \pm 2.8	60.3 \pm 0.5	91.6 \pm 1.0
MEA2	73.9 \pm 1.0	70.3 \pm 1.4	69.3 \pm 0.2	75.5 \pm 1.3	23.5 \pm 1.8	54.9 \pm 1.4	75.1 \pm 1.2
MEA3	87.6 \pm 0.8	84.0 \pm 0.9	72.5 \pm 9.1	88.5 \pm 1.6	33.6 \pm 1.3	56.2 \pm 1.3	88.5 \pm 1.6
MEA4	87.6 \pm 0.8	84.0 \pm 0.9	72.5 \pm 9.1	88.5 \pm 1.6	33.6 \pm 1.3	56.2 \pm 1.3	88.5 \pm 1.6
MEA5	87.6 \pm 0.8	84.0 \pm 0.9	72.5 \pm 9.1	88.5 \pm 1.6	33.6 \pm 1.3	56.2 \pm 1.3	88.5 \pm 1.6
AdvMEA	60.3 \pm 7.4	64.0 \pm 8.3	39.0 \pm 4.2	59.7 \pm 0.7	32.4 \pm 1.5	35.9 \pm 3.1	60.5 \pm 3.1
CEGA	83.6 \pm 0.5	81.1 \pm 1.1	65.4 \pm 0.2	90.9 \pm 2.0	34.4 \pm 1.8	52.1 \pm 2.0	81.2 \pm 2.2
DFEA_I	83.5 \pm 3.5	80.8 \pm 4.0	64.5 \pm 0.9	87.7 \pm 0.5	33.3 \pm 2.6	50.4 \pm 0.8	81.2 \pm 1.2
DFEA_II	85.0 \pm 1.1	79.2 \pm 1.5	78.4 \pm 1.0	86.1 \pm 1.9	26.1 \pm 0.9	61.1 \pm 2.0	86.1 \pm 1.9
DFEA_III	87.8 \pm 0.3	84.2 \pm 0.3	79.1 \pm 0.4	87.8 \pm 1.2	30.5 \pm 1.7	56.8 \pm 1.9	87.8 \pm 1.2
Realistic	88.1 \pm 2.0	85.3 \pm 1.3	97.6 \pm 1.4	79.6 \pm 4.7	45.5 \pm 1.8	57.5 \pm 1.7	91.2 \pm 2.7

(b) *PubMed*

Attack	OP_low	OP_high	PR_2bit	PR_top1	PRADA	AdaptMisinfo	GradRedir
MEA0	94.9 \pm 0.9	92.9 \pm 0.9	94.3 \pm 1.0	94.9 \pm 0.7	59.9 \pm 1.0	62.1 \pm 0.4	94.9 \pm 0.7
MEA1	94.9 \pm 0.9	92.9 \pm 0.9	94.3 \pm 1.0	94.9 \pm 0.7	59.9 \pm 1.0	62.1 \pm 0.4	94.9 \pm 0.7
MEA2	91.2 \pm 0.7	89.1 \pm 1.5	91.4 \pm 0.3	91.3 \pm 1.1	53.0 \pm 0.6	62.4 \pm 1.6	91.2 \pm 0.8
MEA3	92.9 \pm 1.1	91.0 \pm 1.1	93.3 \pm 1.0	93.0 \pm 0.8	59.8 \pm 1.3	61.1 \pm 0.7	93.0 \pm 0.8
MEA4	92.9 \pm 1.1	91.0 \pm 1.1	93.3 \pm 1.0	93.0 \pm 0.8	59.8 \pm 1.2	61.1 \pm 0.7	93.0 \pm 0.8
MEA5	92.9 \pm 1.1	91.0 \pm 1.1	93.3 \pm 1.0	93.0 \pm 0.8	59.8 \pm 1.3	61.1 \pm 0.7	93.0 \pm 0.8
AdvMEA	67.3 \pm 12.9	64.1 \pm 5.2	70.5 \pm 5.4	67.1 \pm 6.1	48.8 \pm 3.8	45.4 \pm 4.3	72.4 \pm 10.3
CEGA	94.8 \pm 0.6	92.9 \pm 1.0	92.6 \pm 0.7	94.8 \pm 0.7	59.5 \pm 1.1	60.1 \pm 0.8	94.5 \pm 0.6
DFEA_I	94.0 \pm 0.4	92.4 \pm 0.4	93.0 \pm 0.3	94.3 \pm 0.6	58.1 \pm 1.9	60.0 \pm 0.7	94.3 \pm 0.2
DFEA_II	92.8 \pm 0.8	90.4 \pm 1.2	93.2 \pm 1.4	92.7 \pm 1.2	55.5 \pm 1.1	67.9 \pm 1.2	92.7 \pm 1.2
DFEA_III	94.0 \pm 0.1	92.5 \pm 0.4	94.2 \pm 1.5	94.7 \pm 0.7	59.5 \pm 0.8	61.9 \pm 0.4	94.7 \pm 0.7
Realistic	95.2 \pm 0.6	94.1 \pm 0.5	89.5 \pm 0.6	92.7 \pm 0.8	70.7 \pm 2.5	63.0 \pm 1.4	94.3 \pm 0.2

(c) *Computers*

Attack	OP_low	OP_high	PR_2bit	PR_top1	PRADA	AdaptMisinfo	GradRedir
MEA0	73.4 \pm 11.3	62.6 \pm 25.0	75.7 \pm 13.3	82.5 \pm 3.1	24.9 \pm 9.1	52.9 \pm 9.2	82.0 \pm 3.1
MEA1	72.9 \pm 25.7	66.6 \pm 26.1	84.8 \pm 5.3	83.7 \pm 6.2	34.6 \pm 16.9	55.4 \pm 5.8	84.3 \pm 6.0
MEA2	62.5 \pm 6.1	49.7 \pm 16.7	71.9 \pm 5.5	64.8 \pm 2.3	27.2 \pm 9.5	54.8 \pm 0.9	64.2 \pm 1.9
MEA3	79.7 \pm 12.3	67.9 \pm 27.5	83.5 \pm 2.4	82.5 \pm 5.6	31.4 \pm 16.9	52.6 \pm 9.3	84.3 \pm 3.0
MEA4	77.5 \pm 11.6	64.4 \pm 25.5	77.4 \pm 12.4	80.9 \pm 4.9	31.3 \pm 17.3	54.2 \pm 6.1	84.0 \pm 3.2
MEA5	71.8 \pm 9.7	56.3 \pm 32.3	84.4 \pm 0.9	81.6 \pm 2.1	27.5 \pm 17.3	50.1 \pm 8.1	82.0 \pm 2.5
AdvMEA	43.3 \pm 13.4	34.4 \pm 13.4	44.7 \pm 21.6	34.3 \pm 27.8	23.1 \pm 7.3	37.1 \pm 10.2	28.5 \pm 26.1
CEGA	55.8 \pm 39.6	44.3 \pm 32.8	48.7 \pm 29.4	82.2 \pm 4.5	27.8 \pm 14.1	38.7 \pm 7.8	71.7 \pm 15.2
DFEA_I	58.1 \pm 12.3	56.1 \pm 15.7	51.2 \pm 22.2	72.0 \pm 5.7	29.4 \pm 8.7	42.8 \pm 8.1	66.4 \pm 8.6
DFEA_II	38.3 \pm 22.6	21.9 \pm 8.5	51.5 \pm 26.1	48.1 \pm 25.7	18.2 \pm 4.9	35.1 \pm 8.9	47.6 \pm 26.6
DFEA_III	66.8 \pm 10.1	57.3 \pm 18.4	79.2 \pm 6.9	74.5 \pm 8.5	27.6 \pm 10.7	39.2 \pm 6.0	74.6 \pm 8.7
Realistic	80.1 \pm 6.7	76.4 \pm 7.0	88.7 \pm 11.8	83.5 \pm 10.7	38.5 \pm 21.5	56.9 \pm 7.2	87.7 \pm 4.1

where the GCN target is itself fragile (*Computers* and *OGBN-Arxiv*); on the heterophilic graphs and on the high-utility graphs it leaves fidelity unchanged or slightly increases it, which suggests that gradient-redirection’s filter triggers more often when the target’s confidence is already volatile. *Fourth*, *PR_top1* (*top-1 label-only output*) shows the largest defense-induced gain on *RomanEmpire*, where (GCN, GCN) rises from 63.1% undefended to 71.6% with *PR_top1*; this is consistent with our finding in RQ5 that on heterophilic graphs the noise in the soft scores of an undefended GCN actually hurts the surrogate, so quantizing them helps the attacker. Together, these four observations imply that practitioners cannot treat “defense” as a single axis: the protection effect of each information-limiting defense flips sign as a function of (i) the target backbone, (ii) the graph homophily, and (iii) the surrogate’s choice of backbone.

The budget-grid table exposes three deep findings that the standard five-budget grid in the main text does not surface. *First*, the marginal value of doubling the budget collapses near $0.75\times$. On *Cora*, fidelity grows by ~ 19 pp from $0.02\times$ to $0.75\times$ ($68.5 \rightarrow 87.5$) but only by 1.2 pp from $0.75\times$ to $2.00\times$ ($87.5 \rightarrow 88.7$); the same flattening appears on *CiteSeer* (where $2.00\times$ even underperforms $0.75\times$ within one standard deviation). This is direct empirical evidence that no realistic operator should query beyond $\sim 0.5\text{--}0.75\times$ of the train set — the cost-per-pp curve becomes essentially flat. *Second*, the very small budget of $0.02\times$ already extracts a non-trivial surrogate. With only 54 *Cora* queries the surrogate reaches 68.5% fidelity, which is approximately 77% of the maximum fidelity at $2.00\times$; this is consistent with the homophily-driven local-decision-rule hypothesis of the structural-properties analysis and quantifies an extraction floor that no current API rate-limiter is likely to defeat. *Third*, on *RomanEmpire* the curve is essentially flat across all four orders of magnitude of the budget multiplier ($61.6 \rightarrow 61.9 \rightarrow 64.7$), which is the strongest single piece of evidence that the heterophilic ceiling of $\sim 64\%$ is structural and not budget-driven. The observation also tightens

Table 47: Surrogate fidelity (%) on defended targets (7 information-limiting and query-detection defenses) for *Photo*, *CoauthorCS*, and *CoauthorPhysics*. Mean \pm standard deviation over three seeds.

(a) *Photo*

Attack	OP_low	OP_high	PR_2bit	PR_top1	PRADA	AdaptMisinfo	GradRedir
MEA0	93.9 \pm 3.8	77.3 \pm 29.6	93.3 \pm 5.1	94.9 \pm 3.2	64.5 \pm 25.7	50.0 \pm 8.6	94.8 \pm 3.3
MEA1	93.9 \pm 3.8	77.3 \pm 29.6	93.3 \pm 5.1	94.9 \pm 3.2	64.5 \pm 25.7	50.0 \pm 8.6	94.8 \pm 3.3
MEA2	92.7 \pm 2.2	90.4 \pm 3.4	92.5 \pm 2.1	92.8 \pm 2.0	71.9 \pm 7.5	59.1 \pm 1.0	92.2 \pm 2.8
MEA3	93.9 \pm 3.9	77.4 \pm 29.7	93.3 \pm 5.2	94.8 \pm 3.4	64.6 \pm 25.8	50.2 \pm 8.7	94.8 \pm 3.4
MEA4	93.9 \pm 3.9	77.4 \pm 29.7	93.3 \pm 5.2	94.8 \pm 3.4	64.6 \pm 25.8	50.2 \pm 8.7	94.8 \pm 3.4
MEA5	93.9 \pm 3.9	77.4 \pm 29.7	93.3 \pm 5.2	94.8 \pm 3.4	64.6 \pm 25.8	50.2 \pm 8.7	94.8 \pm 3.4
AdvMEA	68.9 \pm 11.7	48.6 \pm 32.2	73.9 \pm 6.8	78.4 \pm 3.3	51.5 \pm 24.9	42.1 \pm 1.6	77.3 \pm 3.4
CEGA	93.9 \pm 1.0	93.3 \pm 2.7	92.8 \pm 1.3	93.2 \pm 2.9	76.6 \pm 7.9	52.8 \pm 5.0	78.2 \pm 28.2
DFEA_I	80.5 \pm 17.7	78.3 \pm 13.5	86.0 \pm 2.9	89.7 \pm 3.6	74.2 \pm 7.2	49.6 \pm 4.0	67.0 \pm 13.3
DFEA_II	12.1 \pm 6.0	12.0 \pm 6.0	18.7 \pm 4.6	13.2 \pm 5.2	24.0 \pm 22.5	35.6 \pm 9.5	13.2 \pm 5.2
DFEA_III	92.5 \pm 4.5	93.3 \pm 2.6	93.2 \pm 2.6	93.4 \pm 3.4	74.4 \pm 7.5	50.6 \pm 3.0	93.4 \pm 3.4
Realistic	96.9 \pm 0.7	96.3 \pm 1.5	94.1 \pm 6.6	96.1 \pm 6.8	86.7 \pm 8.7	47.6 \pm 0.6	75.6 \pm 27.2

(b) *CoauthorCS*

Attack	OP_low	OP_high	PR_2bit	PR_top1	PRADA	AdaptMisinfo	GradRedir
MEA0	98.8 \pm 0.2	97.8 \pm 0.4	98.8 \pm 0.2	99.0 \pm 0.0	79.8 \pm 1.4	75.1 \pm 1.4	99.0 \pm 0.0
MEA1	98.8 \pm 0.2	97.8 \pm 0.4	98.8 \pm 0.2	99.0 \pm 0.0	79.9 \pm 1.4	75.2 \pm 1.4	99.0 \pm 0.0
MEA2	74.3 \pm 1.0	75.8 \pm 0.8	75.4 \pm 0.8	76.1 \pm 1.2	63.1 \pm 0.2	51.7 \pm 1.8	76.3 \pm 0.4
MEA3	97.7 \pm 0.2	97.0 \pm 0.2	97.9 \pm 0.2	97.9 \pm 0.1	79.7 \pm 1.4	73.0 \pm 0.2	97.9 \pm 0.1
MEA4	97.6 \pm 0.2	97.0 \pm 0.2	97.9 \pm 0.2	97.9 \pm 0.1	79.8 \pm 1.4	73.1 \pm 0.1	97.9 \pm 0.1
MEA5	97.7 \pm 0.2	97.0 \pm 0.2	97.9 \pm 0.2	97.9 \pm 0.1	79.8 \pm 1.4	73.0 \pm 0.1	97.9 \pm 0.1
AdvMEA	88.2 \pm 0.9	88.5 \pm 0.8	87.7 \pm 1.4	88.3 \pm 0.6	75.4 \pm 2.0	52.9 \pm 0.6	88.2 \pm 0.7
CEGA	96.5 \pm 1.0	96.2 \pm 0.7	95.9 \pm 0.7	98.8 \pm 0.1	81.3 \pm 1.1	73.5 \pm 0.7	97.8 \pm 0.5
DFEA_I	95.1 \pm 0.8	95.1 \pm 0.5	94.0 \pm 0.4	94.4 \pm 0.2	79.0 \pm 0.4	63.6 \pm 0.3	94.0 \pm 0.3
DFEA_II	93.1 \pm 0.4	93.1 \pm 0.2	93.7 \pm 0.9	93.9 \pm 0.9	75.8 \pm 0.3	73.2 \pm 1.8	93.9 \pm 0.9
DFEA_III	94.6 \pm 0.2	94.2 \pm 0.6	95.1 \pm 0.6	94.9 \pm 1.1	76.8 \pm 0.4	64.6 \pm 1.4	94.9 \pm 1.1
Realistic	95.3 \pm 0.6	95.0 \pm 1.0	100.0 \pm 0.0	90.8 \pm 5.3	88.4 \pm 1.5	71.6 \pm 1.2	96.5 \pm 0.7

(c) *CoauthorPhysics*

Attack	OP_low	OP_high	PR_2bit	PR_top1	PRADA	AdaptMisinfo	GradRedir
MEA0	98.4 \pm 0.9	98.4 \pm 0.5	98.9 \pm 0.4	98.6 \pm 0.5	89.1 \pm 0.4	61.3 \pm 1.4	98.5 \pm 0.5
MEA1	98.4 \pm 0.9	98.4 \pm 0.5	98.9 \pm 0.4	98.6 \pm 0.5	89.1 \pm 0.4	61.6 \pm 1.8	98.5 \pm 0.5
MEA2	70.2 \pm 0.2	69.4 \pm 1.3	70.9 \pm 3.1	68.8 \pm 3.9	64.8 \pm 0.9	43.0 \pm 1.7	69.7 \pm 1.1
MEA3	98.0 \pm 0.7	98.2 \pm 0.6	98.6 \pm 0.3	98.2 \pm 0.6	89.0 \pm 0.7	63.1 \pm 2.2	98.2 \pm 0.6
MEA4	98.0 \pm 0.7	98.2 \pm 0.6	98.6 \pm 0.3	98.2 \pm 0.6	89.0 \pm 0.7	63.0 \pm 2.5	98.2 \pm 0.6
MEA5	98.0 \pm 0.7	98.2 \pm 0.6	98.6 \pm 0.3	98.2 \pm 0.6	89.0 \pm 0.7	63.9 \pm 1.6	98.2 \pm 0.6
AdvMEA	90.9 \pm 0.4	91.3 \pm 0.5	91.4 \pm 0.6	91.1 \pm 1.0	85.7 \pm 0.8	58.7 \pm 0.9	91.1 \pm 1.0
CEGA	98.1 \pm 0.9	98.1 \pm 0.6	98.1 \pm 0.6	98.5 \pm 0.6	88.6 \pm 0.8	60.6 \pm 2.3	98.0 \pm 0.6
DFEA_I	97.1 \pm 0.4	96.9 \pm 0.4	97.4 \pm 0.4	96.5 \pm 0.7	86.8 \pm 0.6	58.5 \pm 0.5	96.7 \pm 0.8
DFEA_II	95.8 \pm 1.0	95.5 \pm 0.5	96.7 \pm 0.1	95.9 \pm 0.5	85.4 \pm 0.6	76.7 \pm 0.4	95.9 \pm 0.5
DFEA_III	96.8 \pm 0.6	96.7 \pm 0.6	97.0 \pm 0.2	96.7 \pm 0.6	87.5 \pm 0.7	58.6 \pm 0.8	96.7 \pm 0.6
Realistic	96.8 \pm 0.3	96.2 \pm 0.1	100.0 \pm 0.0	95.4 \pm 2.6	93.1 \pm 0.6	60.8 \pm 2.0	97.1 \pm 0.2

the budget-grid recommendation: the five-budget grid does not omit a relevant inflection point, and extending beyond $1.00\times$ does not change qualitative conclusions on any of the four datasets.

F.11 Defense hyperparameter ablation

To complement the protection-utility analysis in the main text, we sweep the key hyperparameter of each defense and report the protected-model accuracy together with the verification proxy on *Cora* and *Computers*. The sweep covers BackdoorWM (trigger rate), OutputPerturbation (noise scale σ), PredictionRounding (precision in bits), RandomWM (number of watermark nodes), and SurviveWM (defense ratio). Tables 64–65 report the results.

The hyperparameter sweep yields three observations. *First*, *BackdoorWM* has a clean stability-protection split. On *Cora* the protected-model accuracy stays in the 77–79% range and the verification rate stays at 100% across the full trigger-rate range, while on *Computers* the same defense produces highly variable accuracy and protection at every setting we tested, which is consistent with the structural-property analysis in Appendix F.10. *Second*, *OutputPerturbation* and *PredictionRounding* show a smooth utility-verification trade-off on *Cora*. Smaller noise and more bits preserve both accuracy and verification, while larger noise and fewer bits reduce verification before they reduce accuracy in a substantive way. *Third*, *RandomWM* and *SurviveWM* are sensitive to the size of the watermark set. Increasing the number of watermark nodes or the defense ratio reduces verification on *Cora* from above 95% to below 35%, which suggests that larger watermark capacity dilutes the verification signal under our protocol.

Table 48: Surrogate fidelity (%) on defended targets (7 information-limiting and query-detection defenses) for *OGBN-Arxiv*, *RomanEmpire*, and *AmazonRatings*. Mean \pm standard deviation over three seeds.

(a) *OGBN-Arxiv*

Attack	OP_low	OP_high	PR_2bit	PR_top1	PRADA	AdaptMisinfo	GradRedir
MEA0	77.3 \pm 4.5	71.9 \pm 3.5	73.7 \pm 5.2	77.8 \pm 4.7	16.1 \pm 1.0	44.1 \pm 1.7	77.9 \pm 4.8
MEA1	77.3 \pm 4.5	72.0 \pm 3.6	73.8 \pm 5.3	77.9 \pm 4.8	16.1 \pm 1.0	44.1 \pm 1.8	77.9 \pm 4.8
MEA2	52.4 \pm 2.9	48.1 \pm 2.4	41.9 \pm 1.9	52.8 \pm 2.9	8.9 \pm 0.1	28.9 \pm 1.5	52.8 \pm 2.9
MEA3	77.3 \pm 4.5	72.0 \pm 3.6	73.8 \pm 5.3	77.9 \pm 4.8	16.1 \pm 1.0	44.1 \pm 1.7	77.9 \pm 4.8
MEA4	77.3 \pm 3.7	71.9 \pm 2.9	73.8 \pm 4.3	77.9 \pm 3.9	16.1 \pm 0.8	44.1 \pm 1.4	77.9 \pm 3.9
MEA5	77.3 \pm 4.5	71.9 \pm 3.6	73.7 \pm 5.2	77.9 \pm 4.8	16.1 \pm 1.0	44.1 \pm 1.7	77.9 \pm 4.8
AdvMEA	31.6 \pm 3.7	36.5 \pm 5.8	33.8 \pm 2.8	34.2 \pm 2.5	9.8 \pm 0.6	17.1 \pm 1.6	28.8 \pm 1.6
CEGA	76.2 \pm 3.9	69.5 \pm 2.7	52.6 \pm 2.2	73.5 \pm 5.4	15.7 \pm 0.8	34.8 \pm 1.1	72.0 \pm 2.5
DFEA_I	81.5 \pm 3.0	73.6 \pm 1.8	54.4 \pm 2.0	77.3 \pm 2.5	16.0 \pm 0.6	37.0 \pm 0.5	76.5 \pm 1.9
DFEA_II	75.7 \pm 0.9	69.3 \pm 0.3	71.1 \pm 1.4	76.2 \pm 1.2	15.4 \pm 0.9	57.3 \pm 1.4	76.2 \pm 1.2
DFEA_III	77.7 \pm 4.1	71.8 \pm 2.7	73.5 \pm 4.8	77.7 \pm 3.8	16.1 \pm 0.8	44.7 \pm 1.8	77.8 \pm 3.7
Realistic	74.1 \pm 2.5	70.0 \pm 2.6	99.8 \pm 0.1	70.4 \pm 9.6	24.7 \pm 0.9	41.4 \pm 0.6	79.9 \pm 2.2

(b) *RomanEmpire*

Attack	OP_low	OP_high	PR_2bit	PR_top1	PRADA	AdaptMisinfo	GradRedir
MEA0	76.8 \pm 0.6	71.8 \pm 0.7	74.3 \pm 0.3	77.7 \pm 0.3	24.3 \pm 0.8	49.6 \pm 0.5	77.7 \pm 0.3
MEA1	76.6 \pm 0.5	71.3 \pm 0.8	74.4 \pm 0.3	77.5 \pm 0.3	24.5 \pm 0.7	49.6 \pm 0.5	77.5 \pm 0.3
MEA2	46.6 \pm 0.1	41.6 \pm 0.5	51.2 \pm 1.3	47.4 \pm 0.6	15.9 \pm 0.4	39.7 \pm 0.4	47.6 \pm 0.8
MEA3	76.9 \pm 0.8	71.6 \pm 0.6	74.5 \pm 0.4	77.8 \pm 0.4	24.6 \pm 0.7	49.5 \pm 0.4	77.8 \pm 0.4
MEA4	77.0 \pm 1.0	71.8 \pm 0.6	74.3 \pm 0.3	77.8 \pm 0.4	24.6 \pm 0.7	49.2 \pm 0.7	77.8 \pm 0.4
MEA5	76.6 \pm 0.6	71.5 \pm 0.7	74.0 \pm 0.7	77.4 \pm 0.6	24.6 \pm 0.7	49.2 \pm 0.7	77.4 \pm 0.6
AdvMEA	17.1 \pm 3.9	19.5 \pm 5.8	41.0 \pm 1.0	16.5 \pm 3.5	13.6 \pm 3.2	11.4 \pm 3.3	18.0 \pm 4.6
CEGA	72.1 \pm 1.8	67.5 \pm 2.0	57.1 \pm 1.2	78.2 \pm 0.8	25.6 \pm 0.1	43.8 \pm 0.2	65.2 \pm 0.3
DFEA_I	73.6 \pm 1.1	68.7 \pm 1.1	57.0 \pm 2.0	77.3 \pm 0.7	25.2 \pm 0.4	43.1 \pm 0.3	64.7 \pm 0.9
DFEA_II	79.5 \pm 0.3	72.3 \pm 0.1	78.7 \pm 0.6	81.0 \pm 0.5	21.4 \pm 0.3	65.5 \pm 0.5	81.0 \pm 0.5
DFEA_III	76.4 \pm 0.8	70.9 \pm 0.8	74.7 \pm 0.5	77.0 \pm 0.5	24.7 \pm 0.6	48.8 \pm 0.7	77.0 \pm 0.5
Realistic	73.3 \pm 0.7	68.5 \pm 0.7	94.9 \pm 4.5	75.2 \pm 6.9	33.6 \pm 0.5	55.3 \pm 0.3	78.0 \pm 0.5

(c) *AmazonRatings*

Attack	OP_low	OP_high	PR_2bit	PR_top1	PRADA	AdaptMisinfo	GradRedir
MEA0	91.9 \pm 0.7	78.3 \pm 0.7	90.0 \pm 0.5	94.0 \pm 1.1	33.6 \pm 0.3	63.7 \pm 0.8	94.1 \pm 1.1
MEA1	91.8 \pm 0.8	78.3 \pm 0.7	89.9 \pm 0.5	94.1 \pm 1.1	33.6 \pm 0.3	63.7 \pm 0.8	94.1 \pm 1.1
MEA2	88.7 \pm 0.5	71.1 \pm 4.5	90.4 \pm 0.8	91.3 \pm 1.9	31.0 \pm 0.9	62.0 \pm 0.9	90.4 \pm 0.8
MEA3	91.8 \pm 0.8	78.3 \pm 0.7	90.0 \pm 0.5	94.0 \pm 1.1	33.6 \pm 0.3	63.7 \pm 0.8	94.1 \pm 1.1
MEA4	91.9 \pm 0.7	78.3 \pm 0.7	90.0 \pm 0.5	94.1 \pm 1.0	33.6 \pm 0.3	63.7 \pm 0.8	94.1 \pm 1.0
MEA5	91.8 \pm 0.7	78.3 \pm 0.7	90.0 \pm 0.5	94.0 \pm 1.1	33.6 \pm 0.4	63.7 \pm 0.8	94.0 \pm 1.1
AdvMEA	42.9 \pm 24.3	40.5 \pm 21.6	55.9 \pm 1.1	44.5 \pm 23.3	29.6 \pm 3.6	27.3 \pm 10.7	47.8 \pm 21.8
CEGA	87.6 \pm 2.0	76.8 \pm 1.0	69.2 \pm 3.7	94.1 \pm 1.0	34.3 \pm 0.9	52.8 \pm 1.5	93.3 \pm 0.9
DFEA_I	88.4 \pm 2.2	76.7 \pm 1.2	73.4 \pm 2.2	93.7 \pm 0.5	32.9 \pm 0.4	51.7 \pm 0.7	92.9 \pm 0.8
DFEA_II	91.9 \pm 0.7	77.9 \pm 1.4	88.7 \pm 0.4	94.1 \pm 0.5	29.1 \pm 0.6	77.2 \pm 1.4	94.1 \pm 0.5
DFEA_III	91.4 \pm 1.7	78.4 \pm 1.6	90.0 \pm 0.4	93.2 \pm 1.2	33.1 \pm 0.2	63.5 \pm 0.5	93.2 \pm 1.2
Realistic	92.0 \pm 0.8	79.3 \pm 0.6	100.0 \pm 0.0	65.2 \pm 15.3	43.0 \pm 0.6	64.3 \pm 0.6	94.5 \pm 0.4

Table 49: Watermark verification rate (%) on the surrogate produced by each attack against each watermarking defense, on *CiteSeer*, *PubMed*, *Computers*, and *Photo*. Higher is better. Mean \pm standard deviation over three seeds.

(a) *CiteSeer*

Attack	BackdoorWM	SurviveWM	Integrity	RandomWM	Impercept.
MEA0	0.0 \pm 0.0	17.5 \pm 1.4	33.3 \pm 57.7	17.3 \pm 7.6	0.0 \pm 0.0
MEA1	33.3 \pm 57.7	17.7 \pm 1.9	0.0 \pm 0.0	22.0 \pm 4.0	0.0 \pm 0.0
MEA2	33.3 \pm 47.1	0.0 \pm 0.0	17.5 \pm 24.7	0.0 \pm 0.0	0.0 \pm 0.0
MEA3	0.0 \pm 0.0	18.8 \pm 3.0	72.8 \pm 23.6	20.7 \pm 2.3	0.0 \pm 0.0
MEA4	33.3 \pm 57.7	15.9 \pm 1.3	16.6 \pm 28.7	17.3 \pm 2.3	0.0 \pm 0.0
MEA5	33.3 \pm 57.7	17.5 \pm 0.8	20.1 \pm 34.8	16.7 \pm 3.1	0.0 \pm 0.0
AdvMEA	0.0 \pm 0.0	15.1 \pm 0.5	0.0 \pm 0.0	17.3 \pm 6.1	0.0 \pm 0.0
CEGA	33.3 \pm 57.7	19.0 \pm 1.4	48.3 \pm 50.1	17.3 \pm 1.2	0.0 \pm 0.0
DFEA_I	0.0 \pm 0.0	17.9 \pm 2.0	31.3 \pm 22.3	14.0 \pm 4.9	0.0 \pm 0.0
DFEA_II	33.3 \pm 47.1	19.1 \pm 0.9	71.5 \pm 20.2	18.0 \pm 2.8	0.0 \pm 0.0
DFEA_III	0.0 \pm 0.0	18.3 \pm 2.8	5.2 \pm 7.4	20.0 \pm 8.6	0.0 \pm 0.0
Realistic	0.0 \pm 0.0	16.4 \pm 1.8	14.8 \pm 25.6	15.3 \pm 1.2	0.0 \pm 0.0

(c) *Computers*

Attack	BackdoorWM	SurviveWM	Integrity	RandomWM	Impercept.
MEA0	60.0 \pm 20.0	9.9 \pm 0.6	100.0 \pm 0.0	15.7 \pm 5.6	0.0 \pm 0.0
MEA1	51.7 \pm 35.4	9.6 \pm 0.8	100.0 \pm 0.0	15.3 \pm 5.3	0.0 \pm 0.0
MEA2	70.0 \pm 24.5	0.0 \pm 0.0	100.0 \pm 0.0	0.0 \pm 0.0	0.0 \pm 0.0
MEA3	60.0 \pm 21.9	10.0 \pm 0.7	100.0 \pm 0.0	14.7 \pm 3.8	0.0 \pm 0.0
MEA4	58.3 \pm 30.6	10.1 \pm 0.6	100.0 \pm 0.0	14.7 \pm 3.7	0.0 \pm 0.0
MEA5	55.0 \pm 27.4	10.2 \pm 0.9	100.0 \pm 0.0	12.0 \pm 2.5	0.0 \pm 0.0
AdvMEA	65.0 \pm 26.6	10.4 \pm 0.6	100.0 \pm 0.0	12.3 \pm 6.1	0.0 \pm 0.0
CEGA	61.7 \pm 33.1	9.8 \pm 0.7	66.7 \pm 57.7	16.0 \pm 5.4	0.0 \pm 0.0
DFEA_I	63.3 \pm 12.5	9.2 \pm 0.8	100.0 \pm 0.0	10.0 \pm 0.0	0.0 \pm 0.0
DFEA_II	16.7 \pm 23.6	9.7 \pm 0.1	100.0 \pm 0.0	10.7 \pm 2.5	0.0 \pm 0.0
DFEA_III	30.0 \pm 35.6	10.5 \pm 0.4	100.0 \pm 0.0	16.0 \pm 2.8	0.0 \pm 0.0
Realistic	5.0 \pm 8.4	10.2 \pm 0.9	13.2 \pm 18.7	9.0 \pm 3.9	0.0 \pm 0.0

(b) *PubMed*

Attack	BackdoorWM	SurviveWM	Integrity	RandomWM	Impercept.
MEA0	33.3 \pm 57.7	33.9 \pm 0.6	6.0 \pm 10.5	36.0 \pm 6.0	66.7 \pm 57.7
MEA1	33.3 \pm 57.7	34.1 \pm 0.6	45.6 \pm 39.5	36.7 \pm 1.2	66.7 \pm 57.7
MEA2	0.0 \pm 0.0	0.0 \pm 0.0	33.3 \pm 47.1	0.0 \pm 0.0	0.0 \pm 0.0
MEA3	0.0 \pm 0.0	34.6 \pm 0.6	59.0 \pm 13.2	42.7 \pm 6.4	100.0 \pm 0.0
MEA4	33.3 \pm 57.7	34.7 \pm 0.4	67.2 \pm 2.0	34.7 \pm 6.4	100.0 \pm 0.0
MEA5	33.3 \pm 57.7	34.7 \pm 0.2	22.7 \pm 39.4	30.7 \pm 9.2	100.0 \pm 0.0
AdvMEA	66.7 \pm 57.7	34.4 \pm 0.3	35.0 \pm 30.7	30.7 \pm 2.3	38.9 \pm 53.6
CEGA	66.7 \pm 57.7	35.1 \pm 0.9	44.9 \pm 38.9	37.3 \pm 5.0	66.7 \pm 57.7
DFEA_I	33.3 \pm 47.1	34.6 \pm 0.2	44.9 \pm 31.8	38.7 \pm 5.0	66.7 \pm 47.1
DFEA_II	66.7 \pm 47.1	34.4 \pm 1.3	21.4 \pm 30.3	36.7 \pm 3.4	100.0 \pm 0.0
DFEA_III	0.0 \pm 0.0	34.1 \pm 0.2	22.8 \pm 32.2	42.7 \pm 4.1	66.7 \pm 47.1
Realistic	33.3 \pm 57.7	33.0 \pm 1.4	42.5 \pm 37.0	32.7 \pm 5.0	100.0 \pm 0.0

(d) *Photo*

Attack	BackdoorWM	SurviveWM	Integrity	RandomWM	Impercept.
MEA0	33.3 \pm 7.2	12.3 \pm 0.3	90.1 \pm 17.1	17.3 \pm 4.2	0.0 \pm 0.0
MEA1	54.2 \pm 19.1	12.7 \pm 1.1	90.1 \pm 17.1	10.0 \pm 4.0	0.0 \pm 0.0
MEA2	66.7 \pm 11.8	0.0 \pm 0.0	89.2 \pm 15.3	0.0 \pm 0.0	0.0 \pm 0.0
MEA3	29.2 \pm 7.2	12.4 \pm 0.9	90.2 \pm 17.0	14.0 \pm 2.0	0.0 \pm 0.0
MEA4	50.0 \pm 25.0	12.3 \pm 0.8	90.2 \pm 17.0	12.7 \pm 4.2	0.0 \pm 0.0
MEA5	58.3 \pm 7.2	12.3 \pm 0.8	90.2 \pm 17.0	14.7 \pm 2.3	33.3 \pm 57.7
AdvMEA	62.5 \pm 33.1	12.2 \pm 0.6	84.8 \pm 26.3	18.0 \pm 2.0	0.0 \pm 0.0
CEGA	50.0 \pm 21.7	12.1 \pm 0.3	54.8 \pm 50.7	16.0 \pm 2.0	0.0 \pm 0.0
DFEA_I	25.0 \pm 20.4	12.1 \pm 0.3	56.6 \pm 41.9	17.3 \pm 1.9	0.0 \pm 0.0
DFEA_II	45.8 \pm 41.2	12.5 \pm 0.6	66.7 \pm 47.1	19.3 \pm 2.5	0.0 \pm 0.0
DFEA_III	45.8 \pm 21.2	12.2 \pm 0.3	87.7 \pm 17.4	12.0 \pm 3.3	0.0 \pm 0.0
Realistic	16.7 \pm 7.2	12.6 \pm 0.7	15.3 \pm 21.4	12.7 \pm 3.1	0.0 \pm 0.0

Table 50: Watermark verification rate (%) on the surrogate produced by each attack against each watermarking defense, on *CoauthorCS*, *CoauthorPhysics*, *RomanEmpire*, and *AmazonRatings*. Higher is better. Mean \pm standard deviation over three seeds.

(a) <i>CoauthorCS</i>						(b) <i>CoauthorPhysics</i>					
Attack	BackdoorWM	SurviveWM	Integrity	RandomWM	Impercept.	Attack	BackdoorWM	SurviveWM	Integrity	RandomWM	Impercept.
MEAO	42.2±20.4	7.2±0.2	61.2±53.6	9.3±1.2	33.3±57.7	MEAO	80.0±20.0	20.5±0.6	64.4±50.0	26.7±3.1	33.3±57.7
MEA1	55.6±10.2	7.0±0.3	54.9±47.6	10.0±4.0	33.3±57.7	MEA1	53.3±11.5	20.5±0.6	91.3±6.1	25.3±4.6	33.3±57.7
MEA2	35.6±8.3	0.0±0.0	60.4±29.3	0.0±0.0	0.0±0.0	MEA2	26.7±18.9	0.0±0.0	38.7±27.5	0.0±0.0	0.0±0.0
MEA3	48.9±16.8	7.1±0.4	27.0±46.8	7.3±4.2	33.3±57.7	MEA3	53.3±11.5	20.3±0.7	86.5±7.4	25.3±2.3	33.3±57.7
MEA4	44.4±13.9	7.1±0.3	54.5±47.2	6.0±2.0	33.3±57.7	MEA4	66.7±30.6	20.4±0.6	62.3±54.3	23.3±4.2	33.3±57.7
MEA5	53.3±20.0	6.9±0.4	25.9±44.9	4.7±5.0	33.3±57.7	MEA5	80.0±0.0	20.3±0.7	0.0±0.0	22.0±3.5	33.3±57.7
AdvMEA	11.1±10.2	7.3±0.8	57.9±1.0	4.7±2.3	0.0±0.0	AdvMEA	26.7±30.6	19.4±1.0	56.5±51.2	19.3±10.3	33.3±57.7
CEGA	37.8±20.4	7.0±0.4	0.0±0.0	9.3±6.1	33.3±57.7	CEGA	86.7±11.5	20.1±0.7	30.9±53.6	34.7±4.2	33.3±57.7
DFEA_I	40.0±9.4	6.9±0.3	46.7±33.1	12.0±3.3	0.0±0.0	DFEA_I	80.0±16.3	20.4±0.2	52.1±37.1	29.3±2.5	33.3±47.1
DFEA_II	33.3±5.4	6.5±0.3	78.3±15.5	6.7±2.5	0.0±0.0	DFEA_II	73.3±9.4	19.6±0.7	26.7±37.8	22.7±1.9	66.7±47.1
DFEA_III	42.2±11.3	6.8±0.3	45.2±32.6	9.3±0.9	0.0±0.0	DFEA_III	73.3±18.9	20.4±0.5	28.4±40.2	26.0±6.5	33.3±47.1
Realistic	2.2±3.8	6.7±0.3	88.7±19.6	6.0±3.5	0.0±0.0	Realistic	13.3±11.5	20.2±0.8	86.0±12.1	26.7±7.0	33.3±57.7

(c) <i>RomanEmpire</i>						(d) <i>AmazonRatings</i>					
Attack	BackdoorWM	SurviveWM	Integrity	RandomWM	Impercept.	Attack	BackdoorWM	SurviveWM	Integrity	RandomWM	Impercept.
MEAO	5.8±2.1	5.5±0.1	50.7±50.0	6.8±3.0	100.0±0.0	MEAO	70.8±10.2	20.0±1.0	67.7±4.4	22.7±6.4	0.0±0.0
MEA1	4.8±2.8	5.5±0.1	33.1±17.6	4.4±3.8	66.7±57.7	MEA1	68.0±12.8	20.0±1.2	65.5±2.6	32.7±4.2	0.0±0.0
MEA2	0.9±0.7	0.0±0.0	11.9±16.0	0.0±0.0	0.0±0.0	MEA2	15.0±2.7	0.0±0.0	59.9±43.2	0.0±0.0	0.0±0.0
MEA3	5.8±2.8	5.5±0.1	0.0±0.0	8.4±2.6	66.7±57.7	MEA3	69.1±8.7	20.1±1.2	54.6±23.8	26.0±3.5	0.0±0.0
MEA4	8.3±2.9	5.5±0.1	16.7±28.1	8.8±5.4	33.3±57.7	MEA4	73.2±6.0	20.3±1.1	51.6±27.2	20.7±1.2	0.0±0.0
MEA5	7.1±3.9	5.5±0.1	18.6±26.0	5.6±2.6	66.7±57.7	MEA5	74.3±8.2	20.0±1.1	90.5±16.4	22.7±4.6	0.0±0.0
AdvMEA	26.3±22.8	5.5±0.2	21.7±10.8	10.0±2.0	0.0±0.0	AdvMEA	94.0±7.0	20.0±0.7	24.7±42.5	20.3±7.6	33.3±57.7
CEGA	1.0±1.4	5.4±0.2	33.3±57.7	8.7±4.4	66.7±57.7	CEGA	66.1±1.7	20.0±0.7	34.0±30.0	23.3±4.2	0.0±0.0
DFEA_I	0.9±0.7	5.4±0.1	13.1±18.5	4.0±1.6	0.0±0.0	DFEA_I	68.3±4.5	20.0±0.6	54.6±31.6	18.7±4.1	0.0±0.0
DFEA_II	31.9±5.9	5.4±0.1	19.1±27.1	6.0±1.6	0.0±0.0	DFEA_II	99.2±0.7	19.7±0.9	69.8±3.8	26.7±4.7	0.0±0.0
DFEA_III	4.7±1.1	5.4±0.1	33.4±21.3	6.0±1.6	33.3±47.1	DFEA_III	71.9±4.8	20.0±0.9	66.7±47.1	21.3±3.4	0.0±0.0
Realistic	0.5±1.0	5.4±0.1	16.0±23.7	8.0±4.2	0.0±0.0	Realistic	43.7±6.2	20.4±0.9	75.1±28.4	18.0±6.0	0.0±0.0

Joint surrogate fidelity per dataset (rows: attacks, cols: watermarking defenses)

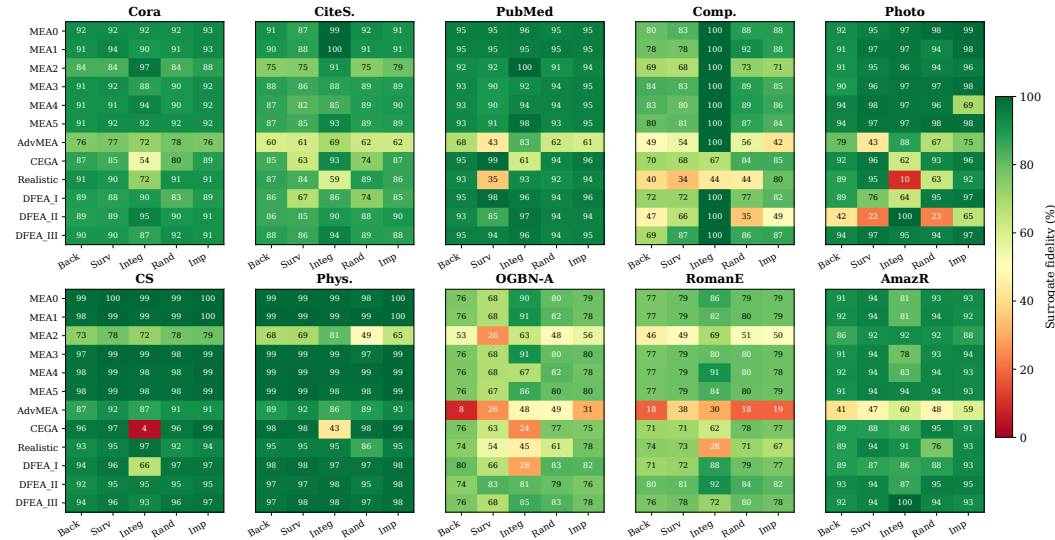


Figure 20: Per-dataset heatmap grid of joint surrogate fidelity (%). Each panel is a 12×5 matrix on one dataset (rows: attacks; columns: watermarking defenses); a single shared colormap (RdYlGn, 0–100 %) supports cross-panel comparison. The cross-dataset uniformity in row patterns confirms the empirical CDF in Figure 19a: the surrogate-fidelity profile depends primarily on the attack and very little on the watermarking defense.

Table 51: Protocol mismatch between the two graph-watermark papers most directly affected by RQ5 and the GraphIP-Bench joint protocol.

Axis	SurviveWM [26]	BackdoorWM [31]	GraphIP-Bench RQ5
Task	Graph classification	Node + graph classification	Node classification
Datasets	MSRC-9, ENZYMES	Cora, CiteSeer, NCI1, COLLAB, REDDIT-BINARY	10 datasets, incl. <i>Computers</i>
Attack family	Same-arch hard-label MEA	Same-arch knowledge distillation	12 black-box attacks (MEAO–5, AdvMEA, CEGA, Realistic, DFEA_I/II/III)
Verification metric \bar{E}	binary effective rate	WM accuracy on trigger nodes	Surrogate-side verification rate

Table 52: SurviveWM under its paper-faithful protocol on the three graph-classification datasets it was originally evaluated on. medFid / medTgtWM / medSurWM are medians over 10 seeds \times 12 attacks (120 rows per dataset). $E_{ave,T}$ is the binary effective rate of the watermark on the protected target; $E_{ave,S}$ is the same metric on the extracted surrogate. “Random floor” is $1/C$ for a C -class task.

Dataset	medFid (%)	medTgtWM (%)	medSurWM (%)	$E_{ave,T}$	$E_{ave,S}$	Random floor
MSRC-9 (paper’s own)	88.9	88.2	5.9	1.00	0.42	12.5% (1/8)
ENZYMES	37.5	57.3	16.7	1.00	0.51	16.7% (1/6)
PROTEINS	80.7	83.1	65.2	1.00	0.67	50.0% (1/2)

Table 53: SurviveWM on *MSRC-9* (the paper’s own dataset) under twelve attacks. TgtWM is the verification rate on the protected target (paper’s E_{sin}); SurWM is the verification rate on the extracted surrogate; $E_{ave,S}$ is the paper’s binary effective rate on the surrogate, averaged over 10 seeds. Bold rows mark $E_{ave,S}=1.00$ (every seed effective).

Attack	Family	TgtWM (%)	SurWM (%)	$E_{ave,S}$
MEA0	Same-arch hard label	88.2	0.0	0.00
MEA1	Shuffled-order hard label	88.2	14.7	0.60
MEA2	Soft label, $T=3$	88.2	2.9	0.30
MEA3	Soft label, $T=1$	88.2	0.0	0.20
MEA4	Cross-arch SAGE, hard	88.2	0.0	0.10
MEA5	Cross-arch SAGE, soft	88.2	5.9	0.30
AdvMEA	10% adversarial flip	88.2	0.0	0.20
CEGA	Centrality / entropy, soft	88.2	5.9	0.30
Realistic	Edge-graph reconstruction ($0.3\times$)	88.2	0.0	0.00
DFEA_I	Data-free, GCN	88.2	47.1	1.00
DFEA_II	Data-free, SAGE	88.2	41.2	1.00
DFEA_III	Data-free, GIN	88.2	47.1	1.00

Table 54: BackdoorWM under its paper-faithful same-architecture knowledge-distillation extraction. TeachAcc / StuAcc are protected-target / surrogate test accuracy; Fid is fidelity to the teacher; TgtWM / SurWM are watermark verification on the teacher / on the KD student; RandFloor is the verification rate of a freshly initialised GCN; $E_{ave,S}$ is the surrogate-side effective rate (per-seed binary SurWM $>$ $\max(\text{RandFloor}, \text{TgtWM}/2)$, averaged over 5 seeds). ‡ flags two seeds on *Computers* where joint training collapsed (TeacherAcc $<$ 10%); their high SurWM is not genuine watermark transfer (see caveat below).

Dataset	TeachAcc (%)	StuAcc (%)	Fid (%)	TgtWM (%)	SurWM (%)	RandFloor (%)	$E_{ave,T}$	$E_{ave,S}$
<i>Computers</i> ‡	55.8	45.4	78.4	90.0	70.0	2.0	1.00	1.00
<i>Photo</i>	87.2	86.6	88.2	87.5	37.5	10.0	1.00	0.60
<i>PubMed</i>	77.8	77.2	94.0	100.0	100.0	20.0	0.80	0.60
<i>CiteSeer</i>	69.2	68.6	83.0	100.0	0.0	20.0	1.00	0.00
<i>RomanEmpire</i>	43.2	31.6	59.8	100.0	0.0	7.3	1.00	0.00

Table 55: Cross-architecture extraction on *Computers*. Surrogate fidelity (%); rows are the target backbone, columns are the surrogate backbone (mean \pm std over three seeds). Results for *Cora*, *OGBN-Arxiv*, and *RomanEmpire* are reported in Table 59.

Target \ Surrogate	GCN	GAT	GraphSAGE
GCN	75.8 \pm 13.6	60.5 \pm 27.4	45.9 \pm 27.8
GAT	76.1 \pm 3.0	89.8 \pm 0.4	77.0 \pm 3.8
GraphSAGE	60.7 \pm 16.3	81.2 \pm 3.7	72.9 \pm 8.9

Table 56: Link prediction on *Cora* at $0.25\times$. Surrogate fidelity (%), mean over three seeds; standard deviations are zero or near-zero because *Cora* link prediction uses a fixed positive/negative split.

Defense	MEA0	MEA1	MEA2	MEA3	MEA4	MEA5	AdvMEA	CEGA	DFEA_I	DFEA_II	DFEA_III
None	95.3	94.8	95.6	73.1	85.3	93.8	97.9	92.1	94.4	94.0	94.4
OP_low	96.1	93.7	92.8	71.0	84.4	92.4	96.0	92.0	94.4	92.1	92.9
OP_high	94.2	92.8	90.4	70.2	81.6	89.3	93.1	92.8	89.9	91.3	91.1
PR_2bit	84.9	87.2	28.9	68.8	28.9	81.9	82.4	87.8	28.9	28.9	28.9
GradRedir	70.9	71.9	94.3	70.4	79.2	71.1	80.7	71.0	92.6	93.4	28.9

Table 57: Graph classification on ENZYMES (target accuracy 24.8 ± 1.3) and PROTEINS (target accuracy 67.5 ± 1.5) at budget $0.25 \times$. Surrogate fidelity (%), mean \pm std over three seeds.

Attack	ENZYMES						PROTEINS					
	None	OP1o	OPhi	PR2b	Prt1	GR	None	OP1o	OPhi	PR2b	Prt1	GR
MEA0	92.2 \pm 1.7	88.9 \pm 3.9	86.9 \pm 5.0	16.7 \pm 2.9	91.1 \pm 2.9	90.9 \pm 0.8	95.5 \pm 2.9	90.9 \pm 3.5	96.2 \pm 2.7	83.8 \pm 2.6	96.2 \pm 1.0	94.9 \pm 1.6
MEA1	29.4 \pm 3.8	28.1 \pm 5.2	24.4 \pm 8.6	3.1 \pm 5.5	32.4 \pm 6.1	29.6 \pm 4.2	63.4 \pm 2.1	61.9 \pm 3.0	63.3 \pm 2.7	62.4 \pm 2.5	65.1 \pm 4.8	63.2 \pm 2.3
AdvMEA	84.6 \pm 3.3	85.6 \pm 0.6	83.0 \pm 4.2	16.5 \pm 3.2	86.1 \pm 2.0	85.6 \pm 2.4	90.2 \pm 1.2	88.7 \pm 0.5	89.9 \pm 2.7	85.0 \pm 6.7	91.6 \pm 0.8	92.5 \pm 2.2
CEGA	88.7 \pm 3.1	92.2 \pm 0.6	90.2 \pm 4.5	59.1 \pm 6.4	90.9 \pm 1.4	85.0 \pm 2.4	97.1 \pm 1.2	96.8 \pm 2.0	97.5 \pm 0.2	94.7 \pm 1.6	97.8 \pm 0.3	97.1 \pm 0.9
DFEA_I	93.0 \pm 0.3	91.3 \pm 0.3	91.1 \pm 1.5	60.0 \pm 4.9	91.3 \pm 0.8	83.0 \pm 1.2	97.5 \pm 0.7	97.4 \pm 0.7	97.9 \pm 0.6	95.0 \pm 2.4	97.7 \pm 0.2	96.6 \pm 0.5
DFEA_II	90.6 \pm 3.8	90.2 \pm 2.1	84.1 \pm 3.9	16.7 \pm 4.5	91.3 \pm 1.2	91.7 \pm 1.5	96.3 \pm 0.6	94.7 \pm 1.2	94.2 \pm 2.8	84.9 \pm 0.3	95.9 \pm 1.4	95.5 \pm 1.4

Cross-task generalisation: surrogate fidelity (%) at budget $0.25 \times$

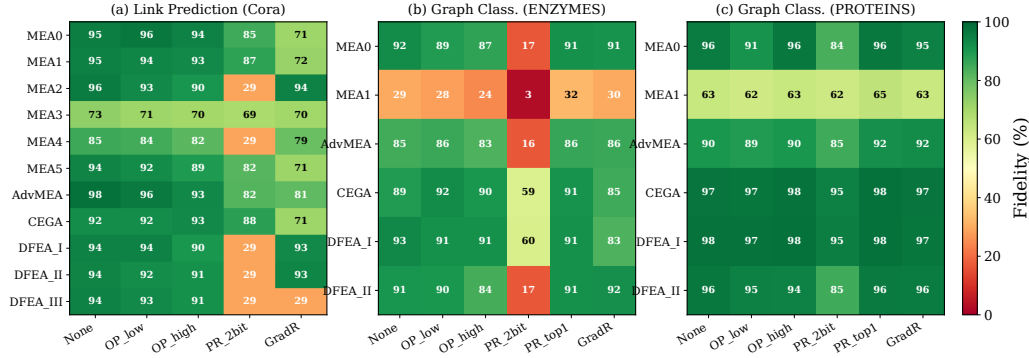


Figure 21: Cross-task heatmap of surrogate fidelity (%) on three task settings: link prediction on *Cora* (left, attacks \times five defenses) and graph classification on *ENZYMES* (centre) and *PROTEINS* (right). Colour saturation encodes fidelity (darker = lower fidelity, higher protection). Numbers are taken from Tables 56–57. The PR_2bit column is the only column which is uniformly dark across the three tasks; the MEA1 row on *ENZYMES* is uniformly faint, which is intrinsic to the attack rather than caused by any defense.

Table 58: Structural properties of the ten graphs used in our benchmark. Edge homophily is the fraction of edges whose endpoints share the same label.

Dataset	# Nodes	# Edges	# Classes	Avg. degree	Density	Edge homophily
Cora	2,708	5,278	7	3.9	0.00144	0.810
CiteSeer	3,327	4,614	6	2.8	0.00083	0.739
PubMed	19,717	44,325	3	4.5	0.00023	0.802
Computers	13,752	252,737	10	36.8	0.00267	0.783
Photo	7,650	122,906	8	32.1	0.00420	0.833
CoauthorCS	18,333	81,894	15	8.9	0.00049	0.808
CoauthorPhysics	34,493	247,962	5	14.4	0.00042	0.931
OGBN-Arxiv	169,343	667,793	40	7.9	0.00005	0.699
RomanEmpire	22,662	44,258	18	3.9	0.00017	0.291
AmazonRatings	24,492	105,296	5	8.6	0.00035	0.452

Table 59: Cross-architecture extraction (undefended targets) on the three datasets not shown above. Surrogate fidelity (%); rows are the target backbone, columns are the surrogate backbone. Mean \pm std over three seeds. The *Computers* matrix is in the main text (Table 55).

(a) <i>Cora</i>				(b) <i>OGBN-Arxiv</i>			
Target \ Surrogate	GCN	GAT	GraphSAGE	Target \ Surrogate	GCN	GAT	GraphSAGE
GCN	87.5 \pm 1.4	89.4 \pm 1.1	88.5 \pm 0.1	GCN	83.1 \pm 5.0	62.4 \pm 0.7	63.0 \pm 1.4
GAT	83.3 \pm 4.5	90.6 \pm 2.0	87.0 \pm 2.6	GAT	44.9 \pm 0.4	80.7 \pm 0.2	90.9 \pm 0.3
GraphSAGE	84.0 \pm 1.1	86.0 \pm 0.6	96.0 \pm 0.7	GraphSAGE	41.9 \pm 0.8	71.4 \pm 0.1	90.3 \pm 1.5

(c) <i>RomanEmpire</i>			
Target \ Surrogate	GCN	GAT	GraphSAGE
GCN	63.1 \pm 3.1	74.4 \pm 0.2	82.7 \pm 0.4
GAT	53.9 \pm 1.3	76.7 \pm 1.5	78.3 \pm 0.5
GraphSAGE	38.5 \pm 0.6	47.9 \pm 0.9	92.3 \pm 0.3

Table 60: Surrogate fidelity (%) when MEAO extracts a defended target with three victim backbones across *Cora*, *CiteSeer*, *PubMed*, and *Computers*. The surrogate is fixed to GCN. Mean \pm standard deviation over three seeds.

(a) <i>Cora</i>						(b) <i>CiteSeer</i>					
Victim	None	OP_low	OP_high	PR_top1	GradRedir	Victim	None	OP_low	OP_high	PR_top1	GradRedir
GCN	87.5 \pm 1.4	85.1 \pm 3.9	85.2 \pm 3.5	87.4 \pm 0.2	87.7 \pm 0.4	GCN	79.7 \pm 4.9	81.7 \pm 2.3	81.5 \pm 2.9	87.6 \pm 0.3	79.7 \pm 1.7
GAT	82.8 \pm 3.9	82.8 \pm 4.5	82.9 \pm 4.4	85.3 \pm 2.1	83.0 \pm 3.4	GAT	76.7 \pm 1.7	76.1 \pm 2.5	76.6 \pm 3.3	83.0 \pm 1.8	73.2 \pm 2.1
GraphSAGE	84.0 \pm 1.2	83.3 \pm 2.0	83.5 \pm 1.7	84.1 \pm 1.0	81.0 \pm 3.2	GraphSAGE	80.8 \pm 0.5	81.1 \pm 0.7	80.9 \pm 1.2	83.6 \pm 0.9	78.1 \pm 0.4

(c) <i>PubMed</i>						(d) <i>Computers</i>					
Victim	None	OP_low	OP_high	PR_top1	GradRedir	Victim	None	OP_low	OP_high	PR_top1	GradRedir
GCN	94.9 \pm 0.3	95.0 \pm 0.5	95.0 \pm 0.5	94.6 \pm 1.4	94.3 \pm 0.3	GCN	75.9 \pm 13.8	71.6 \pm 11.7	73.0 \pm 9.8	69.4 \pm 6.7	56.7 \pm 4.0
GAT	92.1 \pm 1.1	92.2 \pm 0.8	92.2 \pm 0.8	92.7 \pm 0.6	91.6 \pm 1.0	GAT	73.1 \pm 5.5	76.0 \pm 3.3	77.1 \pm 5.1	82.7 \pm 1.5	69.1 \pm 3.2
GraphSAGE	88.9 \pm 0.5	88.8 \pm 0.7	88.8 \pm 0.8	88.8 \pm 0.7	88.3 \pm 0.3	GraphSAGE	66.0 \pm 20.2	74.8 \pm 3.4	75.6 \pm 4.9	79.2 \pm 3.5	75.2 \pm 4.1

Table 61: Surrogate fidelity (%) when MEAO extracts a defended target with three victim backbones across *Photo*, *CoauthorCS*, *CoauthorPhysics*, and *OGBN-Arxiv*. The surrogate is fixed to GCN. Mean \pm standard deviation over three seeds.

(a) <i>Photo</i>						(b) <i>CoauthorCS</i>					
Victim	None	OP_low	OP_high	PR_top1	GradRedir	Victim	None	OP_low	OP_high	PR_top1	GradRedir
GCN	95.3 \pm 2.0	95.2 \pm 1.7	95.5 \pm 1.7	93.2 \pm 3.9	92.0 \pm 4.7	GCN	94.9 \pm 1.1	94.9 \pm 1.5	94.9 \pm 1.4	93.9 \pm 0.7	93.7 \pm 1.5
GAT	96.5 \pm 0.6	96.5 \pm 0.3	96.2 \pm 0.9	95.7 \pm 1.3	96.1 \pm 0.5	GAT	95.5 \pm 1.0	95.4 \pm 0.9	95.8 \pm 0.5	95.0 \pm 0.5	95.0 \pm 0.7
GraphSAGE	94.7 \pm 1.3	92.7 \pm 3.7	94.8 \pm 1.1	94.3 \pm 1.2	94.0 \pm 1.5	GraphSAGE	94.1 \pm 0.7	94.1 \pm 0.7	94.1 \pm 0.9	94.4 \pm 0.3	93.5 \pm 0.8

(c) <i>CoauthorPhysics</i>						(d) <i>OGBN-Arxiv</i>					
Victim	None	OP_low	OP_high	PR_top1	GradRedir	Victim	None	OP_low	OP_high	PR_top1	GradRedir
GCN	97.1 \pm 1.0	97.0 \pm 1.0	97.1 \pm 1.1	96.2 \pm 1.2	96.2 \pm 1.2	GCN	83.6 \pm 4.2	83.6 \pm 3.9	83.6 \pm 3.9	78.7 \pm 6.8	75.6 \pm 2.8
GAT	96.6 \pm 1.1	97.0 \pm 0.8	96.1 \pm 1.2	95.9 \pm 0.3	96.2 \pm 1.1	GAT	45.3 \pm 0.8	45.1 \pm 0.8	45.2 \pm 0.8	50.4 \pm 2.0	37.5 \pm 1.5
GraphSAGE	97.6 \pm 0.6	97.6 \pm 0.6	97.5 \pm 0.5	97.2 \pm 0.6	97.3 \pm 0.5	GraphSAGE	41.7 \pm 1.0	42.0 \pm 0.8	41.6 \pm 0.3	47.6 \pm 1.9	38.8 \pm 1.7

Table 62: Surrogate fidelity (%) when MEAO extracts a defended target with three victim backbones across *Cora*, *Computers*, *RomanEmpire*, and *AmazonRatings*. The surrogate is fixed to GCN. Mean \pm standard deviation over three seeds. (*Cora* and *Computers* cells are duplicated from Tables 60 for a self-contained 2 \times 2 layout.)

(a) <i>Cora</i>						(b) <i>Computers</i>					
Victim	None	OP_low	OP_high	PR_top1	GradRedir	Victim	None	OP_low	OP_high	PR_top1	GradRedir
GCN	87.5 \pm 1.4	85.1 \pm 3.9	85.2 \pm 3.5	87.4 \pm 0.2	87.7 \pm 0.4	GCN	75.9 \pm 13.8	71.6 \pm 11.7	73.0 \pm 9.8	69.4 \pm 6.7	56.7 \pm 4.0
GAT	82.8 \pm 3.9	82.8 \pm 4.5	82.9 \pm 4.4	85.3 \pm 2.1	83.0 \pm 3.4	GAT	73.1 \pm 5.5	76.0 \pm 3.3	77.1 \pm 5.1	82.7 \pm 1.5	69.1 \pm 3.2
GraphSAGE	84.0 \pm 1.2	83.3 \pm 2.0	83.5 \pm 1.7	84.1 \pm 1.0	81.0 \pm 3.2	GraphSAGE	66.0 \pm 20.2	74.8 \pm 3.4	75.6 \pm 4.9	79.2 \pm 3.5	75.2 \pm 4.1

(c) <i>RomanEmpire</i>						(d) <i>AmazonRatings</i>					
Victim	None	OP_low	OP_high	PR_top1	GradRedir	Victim	None	OP_low	OP_high	PR_top1	GradRedir
GCN	63.1 \pm 3.0	63.2 \pm 3.0	63.2 \pm 3.1	71.6 \pm 1.0	57.5 \pm 1.2	GCN	87.5 \pm 2.3	87.6 \pm 1.3	87.9 \pm 1.8	91.8 \pm 1.2	92.8 \pm 0.8
GAT	54.8 \pm 1.5	54.5 \pm 1.4	54.5 \pm 1.5	63.3 \pm 0.1	48.1 \pm 0.9	GAT	85.3 \pm 1.4	85.2 \pm 1.4	85.1 \pm 1.4	89.8 \pm 1.0	90.2 \pm 0.7
GraphSAGE	38.6 \pm 0.4	38.6 \pm 0.4	38.5 \pm 0.4	43.1 \pm 0.4	36.0 \pm 0.6	GraphSAGE	64.0 \pm 0.8	56.1 \pm 1.3	61.9 \pm 3.0	64.5 \pm 2.9	62.3 \pm 2.0

Table 63: Budget-grid sensitivity for the MEAO attack on four representative datasets at three additional budget multipliers (0.02, 0.75, 2.00). Each row reports the number of query nodes induced by the budget multiplier, the surrogate fidelity, the surrogate accuracy, and the victim test accuracy. All values are mean \pm standard deviation over three seeds.

Dataset	Budget	# Query nodes	Fidelity (%)	Accuracy (%)	Victim acc. (%)
Cora	0.02	54	68.5 \pm 3.7	67.1 \pm 3.0	79.4 \pm 0.5
Cora	0.75	2,031	87.5 \pm 2.1	77.7 \pm 1.6	79.4 \pm 0.5
Cora	2.00	2,708	88.7 \pm 1.9	78.9 \pm 0.7	79.4 \pm 0.5
CiteSeer	0.02	66	60.7 \pm 5.9	56.4 \pm 6.7	67.8 \pm 1.1
CiteSeer	0.75	2,495	82.6 \pm 2.3	68.4 \pm 1.9	67.8 \pm 1.1
CiteSeer	2.00	3,327	81.9 \pm 5.6	69.0 \pm 2.0	67.8 \pm 1.1
Computers	0.02	275	50.6 \pm 33.2	37.8 \pm 28.8	44.6 \pm 22.4
Computers	0.75	10,314	82.6 \pm 4.5	41.2 \pm 25.3	44.6 \pm 22.4
Computers	2.00	13,752	73.6 \pm 8.0	42.0 \pm 18.8	44.6 \pm 22.4
RomanEmpire	0.02	453	61.6 \pm 1.6	31.5 \pm 0.7	42.8 \pm 0.3
RomanEmpire	0.75	16,996	61.9 \pm 1.5	31.3 \pm 1.0	42.8 \pm 0.3
RomanEmpire	2.00	22,662	64.7 \pm 1.8	32.4 \pm 0.6	42.8 \pm 0.3

Table 64: Defense hyperparameter ablation on *Cora*. Each row reports protected-model accuracy and the verification proxy as mean \pm standard deviation over multiple seeds.

Defense	Hyperparameter	Acc (%)	WM Acc (%)
BackdoorWM	trigger_rate=0.005	78.7 \pm 2.0	100.0 \pm 0.0
BackdoorWM	trigger_rate=0.01	78.6 \pm 2.1	100.0 \pm 0.0
BackdoorWM	trigger_rate=0.05	78.8 \pm 1.2	100.0 \pm 0.0
BackdoorWM	trigger_rate=0.1	77.4 \pm 0.4	100.0 \pm 0.0
OutputPerturbation	sigma=0.01	79.4 \pm 0.4	99.8 \pm 0.2
OutputPerturbation	sigma=0.05	80.0 \pm 0.7	98.6 \pm 0.5
OutputPerturbation	sigma=0.1	79.5 \pm 0.4	97.2 \pm 0.2
OutputPerturbation	sigma=0.2	78.8 \pm 0.4	94.4 \pm 0.4
OutputPerturbation	sigma=0.5	72.9 \pm 1.3	84.3 \pm 1.5
PredictionRounding	precision_bits=1	77.5 \pm 0.2	90.6 \pm 1.6
PredictionRounding	precision_bits=2	72.8 \pm 0.4	82.2 \pm 1.1
PredictionRounding	precision_bits=4	80.1 \pm 0.0	96.8 \pm 0.4
PredictionRounding	precision_bits=8	79.9 \pm 0.8	99.7 \pm 0.2
RandomWM	wm_node=10	77.5 \pm 3.0	95.0 \pm 7.1
RandomWM	wm_node=50	78.8 \pm 0.4	67.0 \pm 21.2
RandomWM	wm_node=100	78.8 \pm 0.8	53.5 \pm 10.6
RandomWM	wm_node=200	78.3 \pm 0.6	34.2 \pm 1.1
SurviveWM	defense_ratio=0.05	81.0 \pm 1.3	79.3 \pm 3.1
SurviveWM	defense_ratio=0.1	80.0 \pm 0.4	39.4 \pm 2.9
SurviveWM	defense_ratio=0.2	78.4 \pm 1.1	20.2 \pm 0.1
SurviveWM	defense_ratio=0.3	77.0 \pm 2.5	17.9 \pm 0.8

Table 65: Defense hyperparameter ablation on *Computers*. Each row reports protected-model accuracy and the verification proxy as mean \pm standard deviation over multiple seeds. Single-value entries indicate runs with one seed.

Defense	Hyperparameter	Acc (%)	WM Acc (%)
BackdoorWM	trigger_rate=0.005	33.1 \pm 43.4	100.0 \pm 0.0
BackdoorWM	trigger_rate=0.01	2.7 \pm 2.4	95.0 \pm 7.1
BackdoorWM	trigger_rate=0.05	16.4 \pm 21.1	82.0 \pm 17.0
BackdoorWM	trigger_rate=0.1	27.4 \pm 0.7	55.0 \pm 0.0
OutputPerturbation	sigma=0.01	48.2	99.6
OutputPerturbation	sigma=0.05	38.6	77.0
OutputPerturbation	sigma=0.1	67.6	97.3
OutputPerturbation	sigma=0.2	37.4	61.1
OutputPerturbation	sigma=0.5	18.5	21.4
RandomWM	wm_node=10	44.8 \pm 9.7	100.0 \pm 0.0
RandomWM	wm_node=50	67.2 \pm 4.1	100.0 \pm 0.0
RandomWM	wm_node=100	68.8 \pm 0.1	71.5 \pm 3.5
RandomWM	wm_node=200	70.2 \pm 2.2	30.5 \pm 7.1
SurviveWM	defense_ratio=0.05	13.6 \pm 15.0	10.9 \pm 0.0
SurviveWM	defense_ratio=0.1	32.2 \pm 24.0	11.1 \pm 0.8
SurviveWM	defense_ratio=0.2	43.7 \pm 32.9	10.5 \pm 0.9
SurviveWM	defense_ratio=0.3	55.0 \pm 24.2	10.1 \pm 0.6